



**The author(s) shown below used Federal funding provided by the U.S. Department of Justice to prepare the following resource:**

**Document Title:** The Use of Gas Chromatography with Tandem Ultra Violet and Mass Spectrometric Detection for the Analysis of Emerging Drugs. Application to Synthetic Cathinones and Fentanyl Analogues

**Author(s):** Ira Saul Lurie, Ph.D.

**Document Number:** 253329

**Date Received:** August 2019

**Award Number:** 2017-R2-CX-0028

**This resource has not been published by the U.S. Department of Justice. This resource is being made publically available through the Office of Justice Programs' National Criminal Justice Reference Service.**

**Opinions or points of view expressed are those of the author(s) and do not necessarily reflect the official position or policies of the U.S. Department of Justice.**

Department of Justice, Office of Justice Programs, National Institute of Justice

Award Number: 2017-R2-CX-0028

The Use of Gas Chromatography with Tandem Ultra Violet and Mass Spectrometric Detection for the  
Analysis of Emerging Drugs. Application to Synthetic Cathinones and Fentanyl Analogues

Ira Saul Lurie

Research Professor



12/31/2018

The George Washington University

2121 Eye Street, NW, Washington D.C, 20052

Project Period 01/01/2018 to 03/31/2019

Final Research Report

Final Research Report, NIJ award 2017-R2-CX-0028

# The Use of Gas Chromatography with Tandem Ultra Violet and Mass Spectrometric Detection for the Analysis of Emerging Drugs. Application to Synthetic Cathinones and Fentanyl Analogues

## Purpose of Project

The purpose of this study is to establish gas chromatography with simultaneous vacuum ultraviolet and cold electron ionization mass spectrometric detection (GC-cold EI MS/VUV) as a viable technique for the analysis of emerging drugs. This methodology would not only greatly enhance the specificity of compound identification, both for screening and confirmation purposes, but also allow for significantly improved quantitation.

## Project Design

Experiments were designed to demonstrate the utility of GC-cold EI MS/VUV to increase the accuracy of the identification and quantification of emerging drugs, with significant savings in time over existing methodologies. Of particular interest was the ability to distinguish between positional isomers of emerging drugs. The study consists of three phases. For the first phase, separation and detection conditions were developed for twenty-four fentanyl analogues, including 7 sets of positional isomers (Table 1) and twenty-two synthetic cathinones, including 5 sets of positional isomers (Table 2). For the fentanyl analogues classical EI-MS spectra, cold EI MS spectra, and VUV spectra were obtained. For the synthetic cathinones, classical EI-MS spectra were compiled<sup>[1]</sup> and cold EI MS spectra, and VUV spectra were obtained. Experimental parameters were established, including restrictor id's, lengths to be added to a Y splitter and carrier gas flow rate, in order to obtain reasonable signals for simultaneous VUV and cold EI MS detection for the solute of interest. For the second phase, the utility of a combination of VUV spectra and cold EI MS spectra for

enhanced qualitative analysis of synthetic cathinone and fentanyl analogues were demonstrated by comparing cold EI MS spectra with classical EI MS spectra, and accessing the ability of both cold EI MS and VUV spectra to distinguish between similar compounds (particularly positional isomers). Repeatability of both VUV and cold EI MS spectra were accessed. Figures of merit were generated for VUV detection applicable to quantitative analysis including linearity range, linearity, and peak area and retention time precision. The last phase is the analysis of simulated samples of fentanyl analogues and synthetic cathinones.

## Methods

The GC-classical EI MS (GC-EI MS) system consisted of a Perkin Elmer Clarus 680 gas chromatograph coupled with a Perkin Elmer Clarus SQ 8C single quadrupole mass spectrometer (Shelton, CT, USA). Turbomass software was used to control the instrument as well as for data acquisition and processing.

The GC-cold EI MS system consisted of a Perkin Elmer Clarus 680 gas chromatograph coupled with a Perkin Elmer AxION iQT mass spectrometer (Shelton, CT, USA). MassIQ software was used to control the instrument, AxION iQT driver was used to monitor the MS parameters, and data analysis was performed using AxION iQT eCipher.

The GC-VUV system consisted of a Perkin Elmer Clarus 680 gas chromatograph coupled to a VUV Analytics VGA-101 VUV detector. For both the fentanyl analogues and the synthetic cathinones, the chromatographic conditions were identical to those employed for the GC-cold EI MS experiments. The GC was controlled by MassIQ software and VUVision was used to control the VUV detector as well as for data acquisition and processing.

For simultaneous cold EI MS and VUV detection the GC effluent was fed into a 0.25 mm MXT “Y”-Union Connector (Restek, Bellefonte, PA, USA). Approximately 1.5m Hydroguard Fused Silica Guard Column (0.15mm)(Restek, Bellefonte, PA, USA) was fastened into one side of the “Y”-Union Connector which went directly into the ionization source of the AxION IQT mass spectrometer. Approximately 0.5m of the same guard column was fastened into the other side of the “Y”-Union Connector which was fed into the VGA 101 transfer column.

An Eppendorf Vacufuge Plus (Hauppauge, NY, USA) was used for the evaporation of extracts. The instrumental setup is shown in Figure 1, the experimental conditions are described in Table 3, and the sample prep for the various instrumental procedures are shown in Table 4.

Seven fentanyl related samples were prepared. For this purpose sample solutions of target compounds were prepared by pipetting an appropriate amount from methanolic stock solutions of target compounds and benzyl fentanyl internal standard into a 1.6 mL plastic centrifuge tube; so that the resultant solution contained between 50  $\mu\text{g}$  and 150  $\mu\text{g}$  of each target component, up to 4.9X adulterant (ratio to target), and 100  $\mu\text{g}$  of the internal standard. After evaporation to dryness in an Eppendorf Vacuum Plus Centrifuge at 30°C, the resultant supernatant was reconstituted in 1mL of acetonitrile. Standard solutions of target compounds were similarly prepared so that the resultant solution contained 50  $\mu\text{g}$  of each component and 100  $\mu\text{g}$  of the internal standard.

### Data Analysis

GC-EI MS (Figure 2) and GC-cold EI MS (Figure 3) were performed on twenty-four fentanyl analogues including twenty-one controlled drugs and seven sets of positional isomers. Both techniques exhibited similar chromatographic profiles with the former technique exhibiting significantly higher signal-to-noise. A comparison of the EI MS and cold EI MS spectra for the fentanyl analogues are shown in Figure 4–Figure 51. For the fentanyl analogues GC-MS for the most part gave either no molecular ions or in a few instances very weak molecular ions (relative intensity to base peak  $\leq 1\%$ ). For those which gave no molecular ions by GC-EI MS, GC-cold EI MS for the most part gave small molecular ions ( $1\% \leq$  relative intensity to base peak  $\leq 2\%$ ). In those instances where very weak molecular ions were obtained by GC-EI MS large molecular ions were obtained by GC-cold EI MS ( $34\% \geq$  relative intensity to base peak  $\geq 100\%$ ).

The GC-cold EI MS spectra contained many of the same major ions, with different ratios, as obtained from GC-MS. The cold EI MS spectra for the positional isomers that were similar using EI-MS were also similar using cold EI MS. These included compounds A-C; H,I; K,L; M-O; Q-S; T-X (Table 1).

GC-VUV analysis was performed on the same twenty-four fentanyl analogues described above. GC-VUV exhibited similar chromatographic performance as GC-cold EI MS except for a small loss in peak resolution (Figure 3, Figure 52).

The VUV spectrum for the 24 fentanyl analogues is shown in Figure 53- Figure 59. All positional isomers which gave identical MS spectrum exhibited unique VUV spectrum. In fact each fentanyl related compound was successfully identified from a library containing hundreds of solutes of varying classes.

GC-cold EI MS was performed on twenty-two synthetic cathinones including a mixture of 10 controlled analytes and non-controlled isopentadrone Figure 60 and four sets of positional isomers (Figure 61- Figure 64).

A comparison of the EI MS<sup>[1]</sup> and cold EI MS spectra for the synthetic cathinones are shown in Figure 65- Figure 108. No molecular ions were obtained by GC-EI MS. In contrast using GC-cold EI MS, most of these solutes gave moderate to strong molecular ions (6% $\geq$  relative intensity to base peak  $\geq$ 100%), in agreement with a previous study<sup>[2]</sup>. Isopentadrone exhibited no molecular ion. The GC-cold EI MS spectra contained many of the same major ions, with different ratios, as obtained from GC-MS. The cold EI MS spectra for the positional isomers that were similar using EI-MS were also similar using cold EI MS. These included compounds C-E; F-H; K, P; L-O; Q, R; S-U (Table 2).

Overall poorer chromatographic performance GC-VUV was performed on a mixture of controlled synthetic cathinones and positional isomers employing either direct injections, sodium bicarbonate extracts<sup>[3]</sup> or pH 12.5 methylene chloride extracts (Figure 109- Figure 114), and five sets of positional isomers are shown in Figure 109- Figure 114.

The VUV spectrum for each of the twenty-two synthetic cathinones is shown in Figure 115- Figure 119. In contrast to previous studies<sup>2</sup>, the upper wavelength is extended from 240 nm to 310 nm, which provides for more spectral points of comparison. All positional isomers which gave identical MS spectrum exhibited unique VUV spectrum. Each synthetic cathinone related compound was successfully identified from a library containing hundreds of solutes of varying classes.

In order to accomplish both cold EI MS and VUV detection subsequent to GC separation, various restrictor id's and lengths were investigated to add to a Y splitter. For a test analyte (fentanyl analogue FIBF) reasonable signals were obtained for simultaneous cold EI MS and VUV detection subsequent to GC separation using the conditions described in the methods section. A comparison of the separation of a mixture of 24 fentanyl analogues using dual detection is shown in Figure 120. Although overall peak resolution decreased for both detectors with the use of a Y splitter, less loss in resolution was obtained for the MS detector. The greater loss in resolution for the VUV detector is due to the connection between the interface of the oven and the 250  $\mu\text{m}$  connecting tubing to the VUV detector. The greater loss of resolution of the VUV detector is not of concern due to its deconvolution capability as shown in Figure 121 for co-eluting compounds (B, and C Table 1). It should be noted that all co-eluting compounds, including positional isomers (compounds J, L and M, K Table 1), which could not be distinguished by retention time, gave unique cold EI MS spectra (Figure 23, Figures 29-Figure 31). However, it is highly likely that positional isomers exist for fentanyl analogues that give undistinguishable retention times and cold EI MS spectra, which could be distinguished by their VUV spectra. For GC-cold EI MS/ VUV linearity studies was performed using VUV detection for all fentanyl related compounds over a concentration range of 390 PPB to 200 PPM. For quantitation UV (VUV) detection would be preferred over MS detection, since for the former technique deuterated standards would not be required, and UV (VUV) detection is highly linear. As shown in Table 5 most solutes exhibited excellent linearity ( $R^2 \geq 0.999$ ) over at least two orders of magnitude via VUV detection. VUV detection typically offered two three times lower limits of detection than cold EI MS detection. For the fentanyl analogues limits of detection (LOD)  $260 \leq \text{LOD}(\text{PPB})$

$\leq 585$  were obtained for VUV detection. For cold EI MS detection  $LOD\ 334 \leq LOD\ (PPB) \leq 1040$ .

Day-to-day repeatability ( $n = 6$ ) of VUV spectra and the ability of VUV spectroscopy to distinguish between positional isomers is shown in Table 6. Excellent matches for the comparison of VUV spectra with library entries ( $R^2_{av} \geq 0.9993$  with  $\%RSD\ n=5 \leq 0.020$ ) were obtained on a given day and from day-to-day ( $R^2_{av} \geq 0.9995$  with  $\%RSD\ n=5 \leq 0.015$ ) with each fentanyl related compound in all instances, except one, identified as the top choice from the VUV library.

Run-to-run repeatability of VUV spectra for high, medium, and low concentrations (within linearity range) was measured for all twenty-four fentanyl analogues. As shown in Table 7 excellent matches and repeatability were obtained for the comparison of VUV spectra with library entries ( $R^2_{av} \geq 0.999$  and  $\%RSD \geq 0.1037$ ) were obtained for most solutes at the 50 and 100 ppm level. For these solutes at both levels the correct compound was identified as a top choice from the library search. Most solutes exhibited decent matches and repeatability ( $R^2_{av} \geq 0.994$  and  $\%RSD \geq 0.2411$ ) at the 3.12 ppm level. For the most part at the lower concentration level the correct compound was identified as one of the top candidates. As shown in Figure 122 even at 3.12 ppm a discernible VUV spectrum is still obtained.

Run-to-run repeatability of retention times for fentanyl related compounds was measured at 3.12 ppm, 50 ppm and 100 ppm. For these concentrations excellent repeatability was obtained ( $0.01 \leq \%RSD \leq 0.14$ ) were obtained (Table 8). Run-to-run repeatability of peak areas (relative to an internal standard) at 3.12 ppm, 50 ppm and 100 ppm is shown in Table 9. For the two higher concentrations, most of the solutes exhibited excellent repeatability

( $0.4 \leq \%RSD \leq 3.0$ ). Significantly higher repeatability was obtained for the fentanyl analogues at 3.12 ppm ( $2.4 \leq \%RSD \leq 10.1$ )

Day-to-day comparisons of cold EI MS spectra of selected fentanyl analogs were measured on 6 different days over an eleven day period (Table 10). Less favorable matches than obtainable with VUV detection was obtained with good precision ( $R^2_{av} \geq 0.99$ ,  $\%RSD \leq 1.2$ ) on a given day and from day-to-day for most solutes. For the individual solutes the molecular ions were discernible during all the runs. Run-to-run comparisons of cold EI MS spectra for high, medium and low concentrations (within linearity range) was measured for all twenty four fentanyl analogues (Table 11). For the most part  $R^2_{av} \geq 0.99$  ( $\%RSD \leq 3.59$ ) was obtained for most solutes at the 50 and 100 ppm level. At the 3.12 ppm level all solutes exhibited matches of  $R^2_{av} \geq 0.95$  ( $\%RSD \leq 4.76$ ). For all three concentration levels the molecular ions were discernible.

Exhibits analyzed by forensic chemists can contain besides a fentanyl related compounds, various adulterants, including heroin, as well as heroin synthesis impurities and by-products. GC-classical EI MS and GC-cold EI MS/ VUV data (chromatograms, MS and VUV spectra) for selected adulterants, heroin by-products and heroin impurities are shown in Figure 123- Figure 167. No peaks were exhibited for acetaminophen and morphine. Relative retention times (RRT) of fentanyl related compounds, selected adulterants, heroin by-products, and heroin impurities relative to benzyl fentanyl are shown in Table 12. Most of the non-fentanyl compounds showed enhanced molecular ions and gave unique VUV spectra. Seven synthetic fentanyl samples were analyzed. For the target fentanyl compounds (Table 12)  $91.2 \leq \% \text{recovery} \leq 115$  (average 103%) was obtained for the individual samples. The less than optimum recovery for certain samples could be attributed to the evaporation and

reconstitution step. This was necessary since heroin is not stable in methanol. Typically forensic samples would contain powders which can be analyzed by dilute and shoot into an appropriate solvent.

In addition to a refurbished VUV detector a new capillary column was added. Good chromatographic performance was now obtained for synthetic cathinones using both detectors using the previously published sodium bicarbonate sample prep method <sup>[3]</sup> (Figure 168-Figure 178). It should be noted that all co-eluting compounds, including positional isomers (compounds D, G; L, P and U,V Table 2), which could not be distinguished by retention time, gave unique cold EI MS spectra (Figure 76, Figure 79, Figure 92, Figure 96, Figure 107, Figure 108). However, it is highly likely that positional isomers exist for synthetic cathinones that give undistinguishable retention times and cold EI MS spectra, which could be distinguished by their VUV spectra. Due to their UV extinction coefficients, and MS performance, a significantly higher signal-to-noise was obtained for VUV over cold EI MS detection. The lower signal-to-noise for the cold EI MS chromatogram was due to the necessity of split injection to minimize solute decomposition. Significantly higher signal-to-noise was obtained for the molecular ion and base peak using extracted ion monitoring, which is useful for drug screening purposes, which is not possible in most cases using conventional GC-MS. It is possible by changing the length and/or the diameter of the connecting tubing in the splitter to obtain improved signal-to-noise of the cold EI MS detector, while maintaining good signal-to-noise for the VUV detector. This is easily obtained using automated Swafer technology, which is not available on our system. The spectral data obtained with both detectors connected in parallel was comparable to what earlier obtained with each detector used individually.

### Scholarly Products Produced or in Process

Buchalter, S.; Marginean, I.; Yohannan, J.; Lurie, I.S.\* Gas Chromatography with Tandem Cold Electron Ionization Mass Spectrometric and Vacuum Ultraviolet Detection for the Comprehensive Analysis of Fentanyl Analogues, Journal of Chromatography A, 2019 in press.

### Implications for Criminal Justice Policy and Practice in the United States

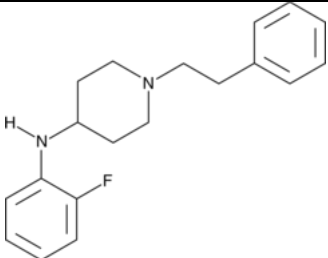
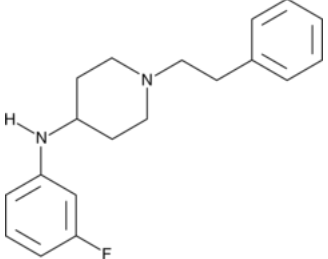
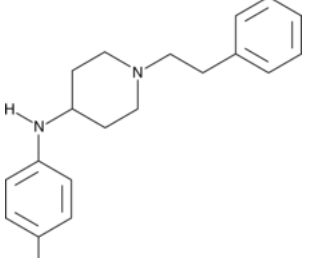
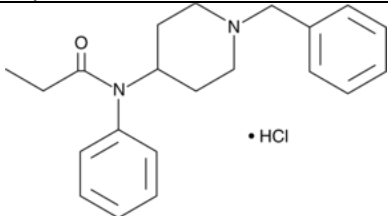
The use of GC-cold EI MS/ VUV would have a significant impact on the criminal justice system by providing streamlined analysis, which would increase the likelihood of a correct identification of a seized drug, and provide simultaneous quantitative analysis. The acquisition of retention time, diagnostic mass fragments, including molecular ion, and a complementary VUV spectrum will greatly decrease the likelihood of a false identification. The highly specific VUV spectra are particularly valuable for distinguishing between positional isomers, for which MS analysis can be lacking. VUV detection is an essential alternative to flame ionization detection for screening and quantitation, since it not only provides qualitative information but provides precise and accurate quantitation. The aforementioned technology is particularly useful for the analysis of emerging drugs for which exists a wide range of similar drugs. GC with simultaneous cold EI MS and VUV detection would positively affect the backlog, by facilitating the simultaneous screening and/or identification and quantitation of emerging drugs, for which the use of multiple instruments has been the norm.

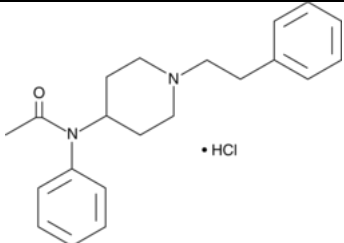
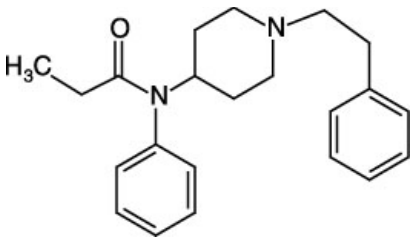
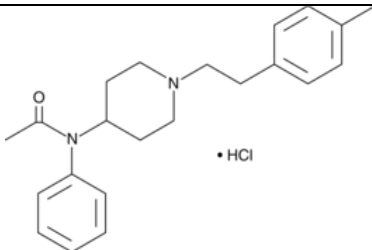
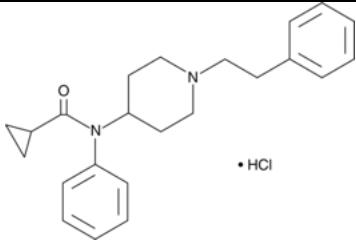
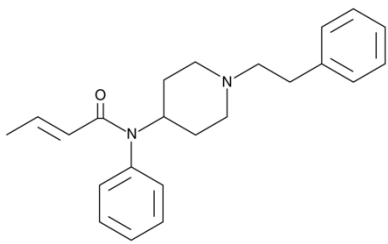
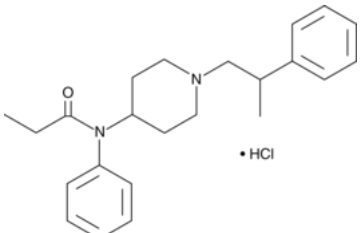
## Appendix

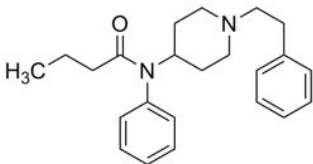
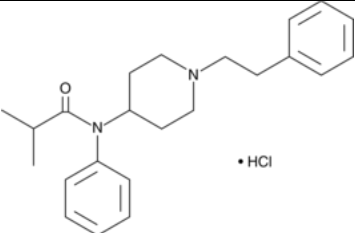
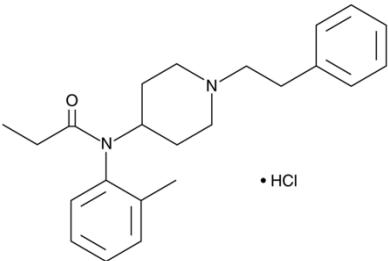
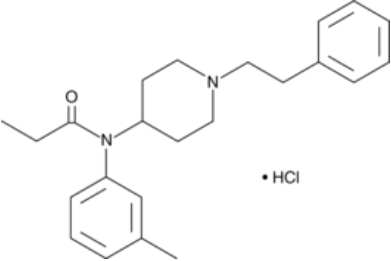
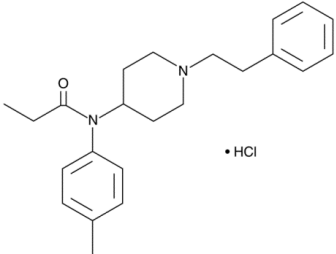
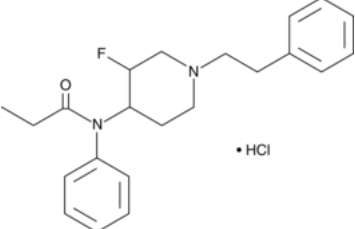
### References

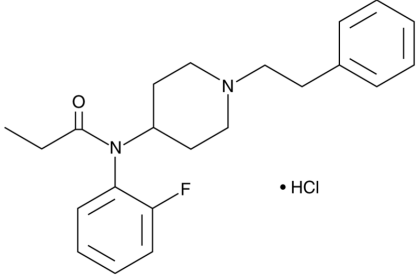
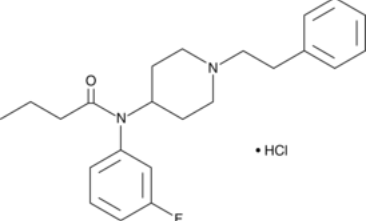
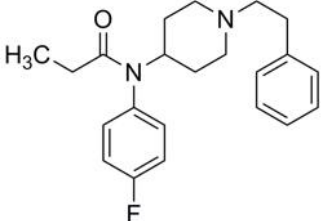
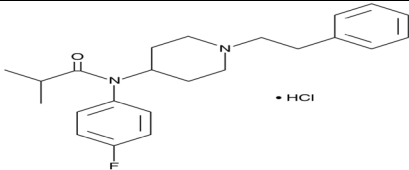
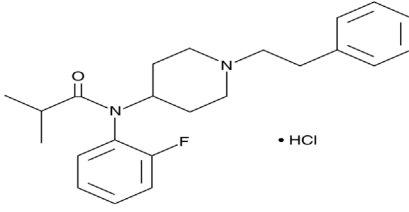
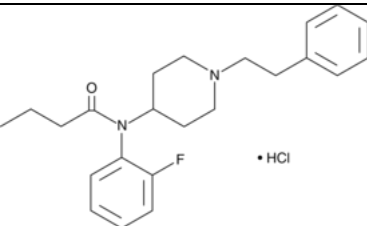
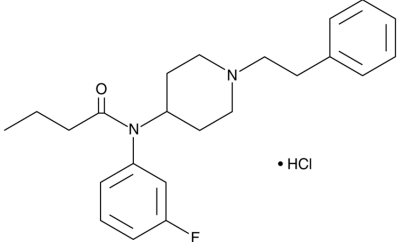
1. <https://www.caymanchem.com/>
2. M.P. Levitas, E. Andrews, I. Lurie, I. Marginean, *Forensic Sci. Int.* **288**, 107-114 (2018).
3. L. Skultety, P. Frycak, C. Qiu, J. Smuts, L. Shear-Laude, K. Lemr, J.X. Mao, P. Kroll, K.A. Schug, K.A., A. Szewczak, C. Vaught, I. Lurie, I., V. Havilicek, *Anal. Chim. Acta* **971**, 55-57 (2017).

Table 1: Fentanyl analogues included in NIJ study

<u>Name</u>	<u>Structure</u>	<u>Mass</u>	<u>Empirical Formula</u>	<u>Letter Representation</u>
Despropionyl ortho-fluorofentanyl		298	C <sub>19</sub> H <sub>23</sub> FN <sub>2</sub>	A
Despropionyl meta-fluorofentanyl		298	C <sub>19</sub> H <sub>23</sub> FN <sub>2</sub>	B
Despropionyl para-fluorofentanyl		298	C <sub>19</sub> H <sub>23</sub> FN <sub>2</sub>	C
Benzyl fentanyl		322	C <sub>21</sub> H <sub>26</sub> N <sub>2</sub> O	D

Acetyl fentanyl		322	$C_{21}H_{26}N_2O$	E
Fentanyl		336	$C_{22}H_{28}N_2O$	F
Acetyl fentanyl 4-methylphenethyl analogue		336	$C_{22}H_{28}N_2O$	G
Cyclopropyl		348	$C_{23}H_{28}N_2O$	H
Crotonyl		348	$C_{23}H_{28}N_2O$	I
$\beta$ -methyl fentanyl		350	$C_{23}H_{30}N_2O$	J

Butyryl fentanyl		350	$C_{23}H_{30}N_2O$	K
Isobutyryl fentanyl		350	$C_{23}H_{30}N_2O$	L
Ortho-methylfentanyl		350	$C_{23}H_{30}N_2O$	M
Meta-methylfentanyl		350	$C_{23}H_{30}N_2O$	N
Para-methylfentanyl		350	$C_{23}H_{30}N_2O$	O
3-fluorofentanyl		354	$C_{23}H_{30}N_2O$	P

Ortho-fluorofentanyl		354	$C_{22}H_{27}FN_2O$	Q
Meta-fluorofentanyl		354	$C_{22}H_{27}FN_2O$	R
Para-fluorofentanyl		354	$C_{22}H_{27}FN_2O$	S
4-Fluoroisobutyryl fentanyl (FIBF)		368	$C_{23}H_{29}FN_2O$	T
Ortho-fluoroisobutyryl fentanyl (2-FIBF)		368	$C_{23}H_{29}FN_2O$	U
Ortho-fluorobutyryl fentanyl		368	$C_{23}H_{29}FN_2O$	V
Meta-fluorobutyryl fentanyl		368	$C_{23}H_{29}FN_2O$	W

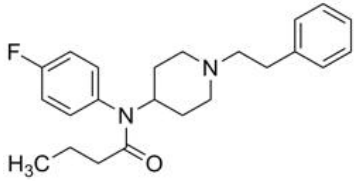
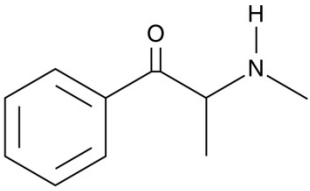
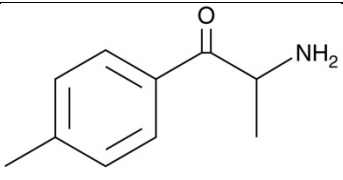
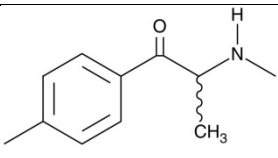
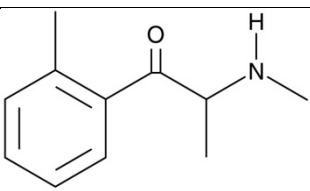
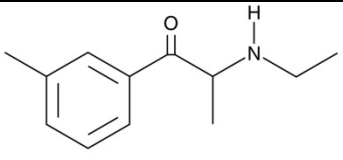
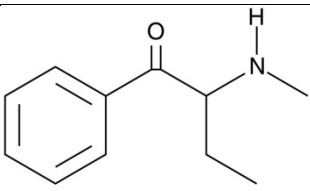
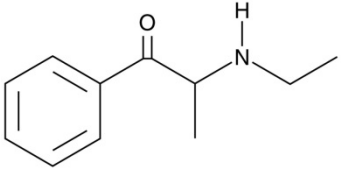
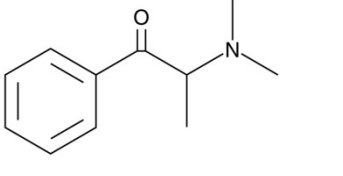
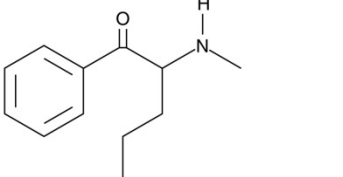
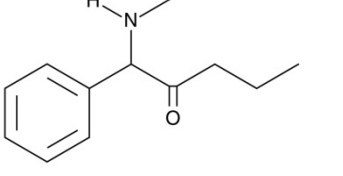
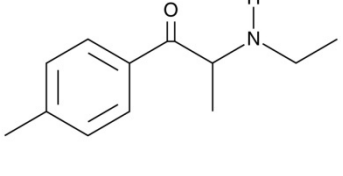
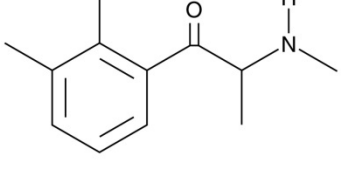
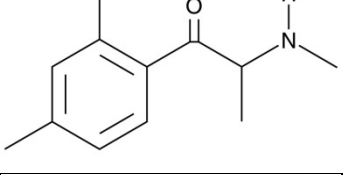
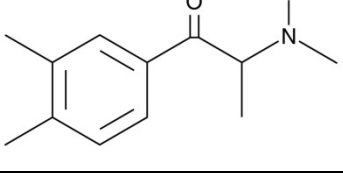
Para-fluorobutyryl fentanyl		368	C <sub>23</sub> H <sub>29</sub> FN <sub>2</sub> O	X
-----------------------------	---	-----	---	---

Table 2: Synthetic cathinones Included in NIJ Study

<u>Name</u>	<u>Structure</u>	<u>Mass</u>	<u>Empirical Formula</u>	<u>Letter Representation</u>
Methcathinone		163.2	C <sub>10</sub> H <sub>13</sub> NO	A
Nor-mephedrone		163.2	C <sub>10</sub> H <sub>13</sub> NO	B
Mephedrone		177.2	C <sub>11</sub> H <sub>15</sub> NO	C
2-methylmethcathinone		177.2	C <sub>11</sub> H <sub>15</sub> NO	D
3-methylmethcathinone		177.2	C <sub>11</sub> H <sub>15</sub> NO	E
Buphedrone		177.2	C <sub>11</sub> H <sub>15</sub> NO	F

Ethcathinone		177.2	C <sub>11</sub> H <sub>15</sub> NO	G
N,N-dimethylcathinone		177.2	C <sub>11</sub> H <sub>15</sub> NO	H
Pentedrone		191.2	C <sub>12</sub> H <sub>17</sub> NO	I
Isopentedrone		191.2	C <sub>12</sub> H <sub>17</sub> NO	J
4-methylethcathinone		191.2	C <sub>12</sub> H <sub>17</sub> NO	K
2,3-dimethylmethcathinone		191.2	C <sub>12</sub> H <sub>17</sub> NO	L
2,4-dimethylmethcathinone		191.2	C <sub>12</sub> H <sub>17</sub> NO	M
3,4-dimethylmethcathinone		191.2	C <sub>12</sub> H <sub>17</sub> NO	N

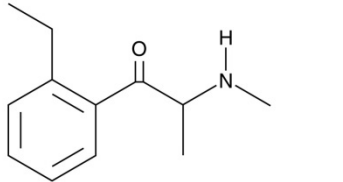
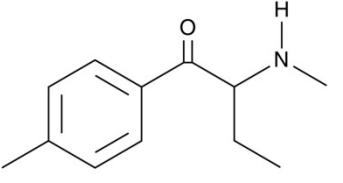
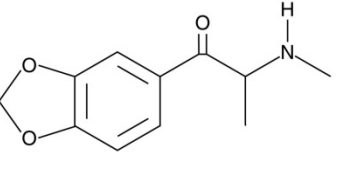
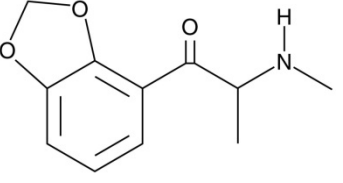
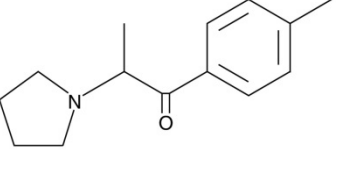
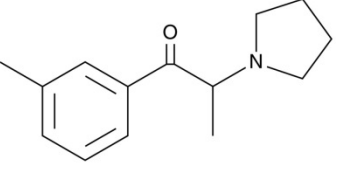
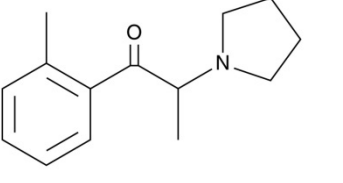
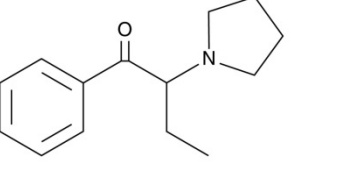
2-ethylmethcathinone		191.2	C <sub>12</sub> H <sub>17</sub> NO	O
4-methylbuphedrone		191.2	C <sub>12</sub> H <sub>17</sub> NO	P
Methylone		207.2	C <sub>11</sub> H <sub>13</sub> NO <sub>3</sub>	Q
2,3-methylenedioxy-methcathinone		207.2	C <sub>11</sub> H <sub>13</sub> NO <sub>3</sub>	R
4'-MePPP		217.3	C <sub>14</sub> H <sub>19</sub> NO	S
3-MePPP		217.3	C <sub>14</sub> H <sub>19</sub> NO	T
2-MePPP		217.3	C <sub>14</sub> H <sub>19</sub> NO	U
α-PBP		217.3	C <sub>14</sub> H <sub>19</sub> NO	V

Table 3: Instrumental conditions employed in NIJ study. All separations were carried out using a Perkin Elmer Elite-5MS column (30m x 0.25mm, 0.25  $\mu$ m)

Drug Type	Instrument Configuration	GC conditions	MS and VUV conditions
<b>Fentanyl Analogue</b>	GC-MS classical	helium flow 1.0 mL/min, a splitless injection with a 1.0 $\mu$ L injection volume; injection temperature 280°C;; oven program: 100°C initial temperature for 1.0 minute, increase to 300°C at a rate of 20°C/min, hold final temperature for 8 minutes; The carrier gas used was helium with a flow rate of 1 mL/min.	transfer line heater 250°C; ion source temperature 200°C; EI ionization energy 70 eV; MS data was acquired in the scan mode from 40 to 550 amu at a speed of 1.5 scans/sec with a solvent delay of 2 min.
<b>Synthetic Cathinone</b>	GC-MS classical	helium flow 1.0 mL/min, a split injection with a split ratio of 10 and an injection volume of 3.0 $\mu$ L; injection temperature 230°C;; oven program: 80°C initial temperature for 1.0 minute, increase to 300°C at a rate of 20°C/min, hold final temperature for 1.5 minutes.	transfer line heater 250°C; ion source temperature 200°C; EI ionization energy 70 eV; MS data was acquired in the scan mode from 40 to 250 amu at a speed of 1.0 scans/sec with a solvent delay of 2.50 min.
<b>Fentanyl Analogue</b>	GC-MS cold EI	same as the GC-MS experiments except for an injection volume of 3 $\mu$ L and a 9 minute hold for final temperature	same as GC-MS except MS data was acquired in the scan mode for 40 to 400 amu at a speed of 2 scan per second

<b>Synthetic Cathinone</b>	GC-MS cold EI	helium flow 1.0 mL/min, a split injection with a split ratio of 10 and an injection volume 3.0 $\mu$ L; injection temperature 230°C oven program: 80°C initial temperature for 1.5 minute, increase to 300°C at a rate of 20°C/min, hold final temperature for 1.5 minutes.	same as GC-MS except MS data was acquired in the scan mode for 20 to 300 amu at a speed of 2 scan per second
<b>Fentanyl Analogue</b>	GC-VUV	Same as for GC-MS cold EI	transfer line and the flow cell were 330°C; The nitrogen make-up gas pressure was set to 0.35 psi. The VUV detector was operated at 4.0 Hz data acquisition rate.
<b>Synthetic Cathinone</b>	GC-VUV	Same as for GC-MS cold EI	same as fentanyl analogues except transfer line temperature and flow cell temperature at 320°C
<b>Fentanyl Analogue</b>	GC-cold EI MS/VUV	Same as for GC-cold EI MS and VUV except helium flow 2.8 mL/min	Same as for GC-cold EI MS and VUV except cold EI MS had as solvent delay of 2.20 min
<b>Synthetic Cathinone</b>	GC-cold EI MS/VUV	Same as for GC-cold EI MS and VUV except helium flow 2.8 mL/min	Same as for GC-cold EI MS and VUV except cold EI MS had as solvent delay of 2.20 min

Table 4: Sample Prep employed in NIJ study

<b>Drug Type</b>	<b>Instrument Configuration</b>	<b>Concentration Stock Solutions</b>	<b>Sample Prep</b>
<b>Fentanyl Analogue</b>	GC-MS classical	50-2000 ppm methanol	aliquots of stock solutions of these solutes were diluted in methanol
<b>Fentanyl Analogue</b>	GC-MS cold EI	50-2000 ppm methanol	aliquots of stock solutions of these solutes were diluted in methanol
<b>Synthetic Cathinone</b>	GC-MS cold EI	1000 or 5000 ppm methanol	aliquots of stock solutions of these solutes were diluted in methanol
<b>Fentanyl Analogue</b>	GC-VUV	50-2000 ppm methanol	aliquots of stock solutions of these solutes were evaporated to dryness and reconstituted in acetonitrile
<b>Synthetic Cathinone</b>	GC-VUV	1000 or 5000 ppm methanol	aliquots of stock solutions were added to equal amounts of a pH 12.46 buffer and methylene chloride, followed by centrifugation at 10000 ppm for 1 minute, prior to removing the methylene chloride layer for analysis
<b>Fentanyl Analogue</b>	GC-cold EI MS/VUV	50-2000 ppm methanol	aliquots of stock solutions of these solutes were evaporated to dryness and reconstituted in acetonitrile
<b>Synthetic Cathinone</b>	GC-cold EI MS/VUV	1000 or 5000 ppm methanol	aliquots of stock solutions of these solutes were diluted in methanol to which was added 2 mg of sodium bicarbonate
<b>Fentanyl Analogue</b>	GC-cold EI MS/VUV (linearity)	50-2000 ppm aliquots were evaporated to dryness and reconstituted in acetonitrile to a final concentration of 200 ppm	aliquots of stock solutions of these solutes were serially diluted 1:2 in acetonitrile

Table 5: Linearity and Limits of Detection (LOD) for fentanyl analogues

<u>Solute</u>	<u>Concentration range</u>	<u>R<sup>2</sup></u>	<u>VUV LOD</u>	<u>Cold EI MS LOD</u>
<b>Despropionyl ortho-fluorofentanyl</b>	1.56 ppm - 200 ppm	0.9996	334 ppb	585 ppb
<b>Despropionyl meta-fluorofentanyl</b>	1.56 ppm - 200 ppm	0.9999	390 ppb	936 ppb
<b>Despropionyl para-fluorofentanyl</b>	1.56 ppm - 200 ppm	0.9999	260 ppb	669 ppb
<b>Benzyl fentanyl</b>	1.56 ppm - 200 ppm	0.9999	292 ppb	468 ppb
<b>Acetyl fentanyl</b>	1.56 ppm - 200 ppm	1	260 ppb	585 ppb
<b>Fentanyl</b>	1.56 ppm - 200 ppm	1	260 ppb	936 ppb
<b>Acetyl fentanyl 4-methylphenethyl analog</b>	1.56 ppm - 200 ppm	0.9996	390 ppb	936 ppb
<b>Cyclopropyl fentanyl</b>	1.56 ppm - 100 ppm	0.9995	292 ppb	936 ppb
<b>Crotonyl fentanyl</b>	1.56 ppm - 100 ppm	0.9999	390 ppb	936 ppb
<b>Beta-methyl fentanyl</b>	1.56 ppm - 200 ppm	0.9992	292 ppb	520 ppb
<b>Butyryl fentanyl</b>	1.56 ppm - 200 ppm	0.9979	390 ppb	585 ppb
<b>Isobutyryl fentanyl</b>	1.56 ppm - 100 ppm	0.9992	260 ppb	334 ppb
<b>Ortho-methylfentanyl</b>	1.56 ppm - 200 ppm	0.9993	334 ppb	936 ppb
<b>Meta-methylfentanyl</b>	1.56 ppm - 200 ppm	0.9999	334 ppb	936 ppb
<b>Para-methylfentanyl</b>	1.56 ppm - 100 ppm	0.9995	292 ppb	520 ppb
<b>3-fluorofentanyl</b>	1.56 ppm - 200 ppm	0.9967	292 ppb	585 ppb
<b>Ortho-fluorofentanyl</b>	1.56 ppm - 200 ppm	0.9999	260 ppb	585 ppb
<b>Meta-fluorofentanyl</b>	1.56 ppm - 200 ppm	1	260 ppb	780 ppb
<b>Para-fluorofentanyl</b>	3.12 ppm - 200 ppm	0.9996	585 ppb	1040 ppb
<b>4-Fluoroisobutyryl fentanyl</b>	1.56 ppm - 200 ppm	0.9999	292 ppb	790 ppb
<b>Ortho-fluoroisobutyryl fentanyl</b>	1.56 ppm - 200 ppm	0.9998	292 ppb	585 ppb
<b>Ortho-fluorobutyryl fentanyl</b>	1.56 ppm - 200 ppm	0.9991	390 ppb	585 ppb
<b>Meta-fluorobutyryl fentanyl</b>	1.56 ppm - 200 ppm	0.9999	260 ppb	936 ppb
<b>Para-fluorobutyryl fentanyl</b>	1.56 ppm - 200 ppm	0.9965	334 ppb	520 ppb

Limits of detection for cold EI MS and VUV were determined from 3 S/N measurements obtained from chromatographic runs at low concentration levels of the linearity determination. Benzyl fentanyl used as an internal standard at 100 ppm in most instances except for benzyl fentanyl linearity which employed fentanyl as an internal standard.

Table 6: Day-to-day VUV library searches for fentanyl positional isomers

Solute <sup>a</sup>	Day 1 R <sup>2</sup> <sub>av</sub> <sup>b</sup>	Day 2 R <sup>2</sup> <sub>av</sub> <sup>b</sup>	Day 3 R <sup>2</sup> <sub>av</sub> <sup>b</sup>	Day 4 R <sup>2</sup> <sub>av</sub> <sup>b</sup>	Day 5 R <sup>2</sup> <sub>av</sub> <sup>b</sup>	Day 6 R <sup>2</sup> <sub>av</sub> <sup>b</sup>	Day to day <sup>c</sup> R <sup>2</sup> <sub>av</sub>
<b>DFFF (ortho)</b>	1.0000	1.0000	0.9999	0.9999	0.9999	0.9999	0.9999
<b>DFFF (meta)</b>	0.9956	0.9956	0.9956	0.9956	0.9955	0.9955	0.9956
<b>DFFF (para)</b>	0.9889	0.9889	0.9888	0.9889	0.9888	0.9888	0.9889
<b>Cyclopropyl-fentanyl</b>	0.9999	0.9999	0.9999	0.9999	0.9999	0.9999	0.9999
<b>Crotonyl-fentanyl</b>	0.9685	0.9685	0.9688	0.9691	0.9686	0.9687	0.9687
<b>Isobutyryl-fentanyl</b>	0.9997	0.9998	0.9994	0.9995	0.9994	0.9993	0.9995
<b>Butyryl-fentanyl</b>	0.9993	0.9993	0.9988	0.9990	0.9989	0.9980	0.9990
<b>MF (para)</b>	1.000	1.0000	1.0000	1.0000	1.0000	1.0000	1.0000
<b>MF (ortho)</b>	0.9987	0.9987	0.9987	0.9987	0.9987	0.9987	0.9987
<b>MF (meta)</b>	0.9973	0.9973	0.9974	0.9973	0.9973	0.9973	0.9973
<b>FBF (ortho)</b>	0.9999	0.9999	0.9999	0.9999	0.9999	0.9999	0.9999
<b>FIBF (ortho)</b>	0.9998	0.9998	0.9998	0.9998	0.9999	0.9998	0.9998
<b>FBF (meta)</b>	0.9996	0.9996	0.9996	0.9996	0.9996	0.9996	0.9996
<b>FBF (para)</b>	0.9989	0.9990	0.9990	0.9990	0.9990	0.9990	0.9990
<b>FIBF (para)</b>	0.9987	0.9987	0.9987	0.9987	0.9987	0.9987	0.9987

With one exception (FBF (ortho) target compounds (solutes in red) were uniquely identified from a library search from a library of hundreds of compounds.

DFFF (Despropionyl fluorofentanyl), MF(methyl fentanyl), FBF (fluorobutyryl fentanyl), FIBF (fluoroisobutyryl fentanyl) <sup>a</sup>50ppm <sup>b</sup>n=5 <sup>c</sup> eleven day period

Table 7: Run-to-run repeatability<sup>#</sup> of comparison of VUV spectra with library entries for fentanyl analogues

Compound	<u>3.12 ppm</u>	<u>50 ppm</u>	<u>100 ppm</u>
	$R^2_{av}$ %RSD <sup>#</sup>	$R^2_{av}$ %RSD <sup>#</sup>	$R^2_{av}$ %RSD <sup>#</sup>
Despropionyl ortho-fluorofentanyl	0.9977	0.9999	0.9999
	0.1757	0.0000	0.0045
Despropionyl meta-fluorofentanyl	0.9982	1.0000	1.0000
	0.1082	0.0055	0.0000
4-Fluoroisobutyryl fentanyl	0.9990	1.0000	0.9999
	0.0643	0.0055	0.0045
Ortho-fluoroisobutyryl fentanyl	0.9985	0.9999	0.9999
	0.0556	0.0045	0.0045
Isobutyryl fentanyl	0.9991	0.9998	0.9991
	0.0433	0.0055	0.0288
3-fluorofentanyl	0.9800	0.9999	0.9999
	2.0348	0.0000	0.0000
Para-fluorobutyryl fentanyl	0.9980	1.0000	1.0000
	0.1389	0.0000	0.0045
Ortho-fluorobutyryl fentanyl	0.9984	0.9999	0.9999
	0.1173	0.0000	0.0000
Butyryl fentanyl	0.9982	1.0000	0.9999
	0.0978	0.0045	0.0045
Para-methylfentanyl	0.9987	1.0000	1.0000
	0.1067	0.0000	0.0000
Cyclopropyl fentanyl	0.9990	0.9999	0.9998
	0.0749	0.0055	0.0000
Despropionyl para-fluorofentanyl	0.9996	0.9999	1.0000
	0.1754	0.0000	0.0000
Meta-fluorofentanyl	0.9989	0.9992	0.9987
	0.1081	0.0000	0.0000
Para-fluorofentanyl	0.9978	0.9999	0.9998
	0.0643	0.1037	0.0123
Fentanyl	0.9989	1.0000	1.0000
	0.0556	0.0081	0.0055
Acetyl fentanyl 4-methylphenethyl analogue	0.9975	1.0000	1.0000
	0.0434	0.0055	0.0045
Crotonyl fentanyl	0.9964	0.9968	0.9983
	0.2411	0.0045	0.0045
Acetyl fentanyl	0.9992	0.9999	1.0000
	0.0321	0.0045	0.0055
Ortho-fluorofentanyl	0.9945	0.9992	0.9987
	0.1777	0.0623	0.0518

<b>Meta-fluorobutyryl fentanyl</b>	0.9944 0.0749	0.9999 0.0055	0.9998 0.0055
<b>Meta-methylfentanyl</b>	0.9982 0.0962	1.0000 0.0000	1.0000 0.0000
<b>Beta-methyl fentanyl</b>	0.9583 2.2502	0.9968 0.3436	0.9983 0.0945
<b>Ortho-methylfentanyl</b>	0.9989 0.0444	1.0000 0.0045	1.0000 0.0000
<b>Benzyl fentanyl</b>	0.9990 0.0483	0.9999 0.0045	1.0000 0.0045

#n=5

Table 8: Run-to-run repeatability# of retention time (RT) via VUV detection for fentanyl analogues

<b>Compound</b>	<b>3.12 ppm</b>	<b>50 ppm</b>	<b>100 ppm</b>
	<b>% RSD RT</b>	<b>% RSD RT</b>	<b>% RSD RT</b>
<b>Despropionyl ortho-fluorofentanyl</b>	0.08	0.03	0.02
<b>Despropionyl meta-fluorofentanyl</b>	0.07	0.03	0.02
<b>4-Fluoroisobutyryl fentanyl</b>	0.11	0.05	0.02
<b>Ortho-fluoroisobutyryl fentanyl</b>	0.10	0.05	0.02
<b>Isobutyryl fentanyl</b>	0.02	0.05	0.03
<b>3-fluorofentanyl</b>	0.03	0.05	0.03
<b>Para-fluorobutyryl fentanyl</b>	0.13	0.05	0.04
<b>Ortho-fluorobutyryl fentanyl</b>	0.11	0.05	0.04
<b>Butyryl fentanyl</b>	0.12	0.05	0.04
<b>Para-methylfentanyl</b>	0.13	0.06	0.04
<b>Cyclopropyl fentanyl</b>	0.13	0.06	0.04
<b>Despropionyl para-fluorofentanyl</b>	0.02	0.04	0.03
<b>Meta-fluorofentanyl</b>	0.01	0.02	0.03
<b>Para-fluorofentanyl</b>	0.03	0.03	0.03
<b>Fentanyl</b>	0.02	0.02	0.03
<b>Acetyl fentanyl 4-methylphenethyl analogue</b>	0.03	0.03	0.03
<b>Crotonyl fentanyl</b>	0.03	0.01	0.03
<b>Acetyl fentanyl</b>	0.01	0.05	0.09
<b>Ortho-fluorofentanyl</b>	0.02	0.06	0.11
<b>Meta-fluorobutyryl fentanyl</b>	0.01	0.07	0.10
<b>Meta-methylfentanyl</b>	0.02	0.06	0.10
<b>Beta-methyl fentanyl</b>	0.07	0.14	0.05
<b>Ortho-methylfentanyl</b>	0.09	0.04	0.06
<b>Benzyl fentanyl</b>	0.02	0.02	0.03

#n= 5

Table 9: Run-to-run repeatability# of peak area& via VUV detection for fentanyl analogues

<b>Compound</b>	<b>3.12ppm</b>	<b>50 ppm</b>	<b>100 ppm</b>
	% RSD Peak Area	% RSD Peak Area	% RSD Peak Area
<b>Despropionyl ortho-fluorofentanyl</b>	8.0	2.4	2.5
<b>Despropionyl meta-fluorofentanyl</b>	10.1	0.4	2.5
<b>4-Fluoroisobutyryl fentanyl</b>	4.0	2.1	1.4
<b>Ortho-fluoroisobutyryl fentanyl</b>	6.0	1.7	2.1
<b>Isobutyryl fentanyl</b>	4.6	3.1	1.9
<b>3-fluorofentanyl</b>	5.3	1.8	1.1
<b>Para-fluorobutyryl fentanyl</b>	5.4	3.8	2.9
<b>Ortho-fluorobutyryl fentanyl</b>	2.4	2.5	2.5
<b>Butyryl fentanyl</b>	4.0	0.7	2.4
<b>Para-methylfentanyl</b>	7.0	1.2	3.0
<b>Cyclopropyl fentanyl</b>	4.5	3.6	3.0
<b>Despropionyl para-fluorofentanyl</b>	5.0	0.7	0.7
<b>Meta-fluorofentanyl</b>	2.9	1.0	0.8
<b>Para-fluorofentanyl</b>	5.3	2.0	2.1
<b>Fentanyl</b>	8.5	1.7	0.9
<b>Acetyl fentanyl 4-methylphenethyl analogue</b>	5.9	3.1	1.6
<b>Crotonyl fentanyl</b>	8.9	1.0	2.4
<b>Acetyl fentanyl</b>	4.2	2.6	1.9
<b>Ortho-fluorofentanyl</b>	6.8	2.5	3.0
<b>Meta-fluorobutyryl fentanyl</b>	8.6	2.2	2.4
<b>Meta-methylfentanyl</b>	7.7	3.5	2.5
<b>Beta-methyl fentanyl</b>	9.4	2.6	1.7
<b>Ortho-methylfentanyl</b>	5.3	1.0	3.2
<b>Benzyl fentanyl</b>	3.8	0.5	1.4

#N=5 & area/ area internal standard (benzyl fentanyl (fentanyl internal standard for benzyl fentanyl))

Table 10: Day-to-day repeatability of the comparison of cold EI MS spectra with day 1 run#1 spectra for selected fentanyl analogues (50 PPM)

<b>Compound</b>	<b>Day 1</b> $R^2_{av}$ %RSD <sup>§</sup>	<b>Day 2</b> $R^2_{av}$ %RSD <sup>#</sup>	<b>Day 3</b> $R^2_{av}$ %RSD <sup>#</sup>	<b>Day 4</b> $R^2_{av}$ %RSD <sup>#</sup>	<b>Day 5</b> $R^2_{av}$ %RSD <sup>#</sup>	<b>Day 6</b> $R^2_{av}$ %RSD <sup>#</sup>	<b>Day –to-day</b> $R^2_{av}$ %RSD
<b>Despropionyl ortho-flouro fentanyl</b>	0.9968 0.3442	0.9940 0.1632	0.9951 0.4044	0.9964 0.2143	0.9987 0.1629	0.9980 0.1701	0.9965 0.1819
<b>Despropionyl meta-flouro fentanyl</b>	0.9963 0.5448	0.9986 0.0925	0.9960 0.2289	0.9995 0.0665	0.9992 0.0751	0.9991 0.1138	0.9981 0.1408
<b>4-Fluoroisobutyryl fentanyl</b>	0.9978 0.3097	0.9984 0.2156	0.9986 0.0765	0.9986 0.1062	0.9905 0.3678	0.9888 0.8332	0.9954 0.4616
<b>Ortho-fluoroisobutyryl fentanyl</b>	0.9986 0.0409	0.9989 0.1993	0.9988 0.1056	0.9989 0.1745	0.9980 0.1332	0.9881 0.3885	0.9952 0.5591
<b>Isobutyryl fentanyl</b>	0.9969 0.0716	0.9976 0.2284	0.9957 0.2571	0.9948 0.4371	0.9945 0.5294	0.9961 0.2577	0.9959 0.1331
<b>Para-fluorobutyryl fentanyl</b>	0.9991 0.1148	0.9957 0.3282	0.9979 0.0856	0.9968 0.2003	0.9867 0.8726	0.9933 0.3655	0.9949 0.4552
<b>Ortho-fluorobutyryl fentanyl</b>	0.9985 0.1903	0.9965 0.2530	0.9938 0.4038	0.9915 0.5582	0.9943 0.3598	0.9974 0.1104	0.9953 0.2684
<b>Butyryl fentanyl</b>	0.9989 0.0788	0.9982 0.0989	0.9991 0.0754	0.9989 0.1346	0.9790 0.6839	0.9948 0.3936	0.9948 0.7974
<b>Para-methylfentanyl</b>	0.9943 0.3778	0.9956 0.2528	0.9952 0.1814	0.9956 0.3264	0.9840 1.2161	0.9906 0.5669	0.9926 0.4731
<b>Cyclopropyl fentanyl</b>	0.9986 0.0656	0.9968 0.3078	0.9978 0.2998	0.9988 0.0577	0.9880 0.3936	0.9887 0.9057	0.9948 0.5104

<sup>§</sup>n=4    <sup>#</sup>n=5

Table 11: Run-to-run repeatability of the comparison of cold EI MS spectra with run#1 50 ppm spectra for selected fentanyl analogues

Compound	<u>3.12 ppm</u>	<u>50 ppm</u>	<u>100 ppm</u>
	$R^2_{av}$ %RSD <sup>#</sup>	$R^2_{av}$ %RSD <sup>s</sup>	$R^2_{av}$ %RSD <sup>#</sup>
<b>Despropionyl ortho-fluorofentanyl</b>	0.9857	0.9991	0.9989
	1.4464	0.0871	1.5468
<b>Despropionyl meta-fluorofentanyl</b>	0.9908	0.9992	0.9992
	1.2348	0.0403	1.1823
<b>4-Fluoroisobutyryl fentanyl</b>	0.9748	0.9968	0.9947
	3.6944	0.2391	1.2833
<b>Ortho-fluoroisobutyryl fentanyl</b>	0.9621	0.9994	0.9965
	0.0556	0.0378	2.9682
<b>Isobutyryl fentanyl</b>	0.9991	0.9993	0.9965
	4.7601	0.0245	1.3809
<b>3-fluorofentanyl</b>	0.9793	0.9994	0.9994
	1.6062	0.0469	3.5890
<b>Para-fluorobutyryl fentanyl</b>	0.9627	0.9964	0.9927
	3.3286	0.2316	3.5449
<b>Ortho-fluorobutyryl fentanyl</b>	0.9816	0.9951	0.9955
	1.7759	0.4006	0.6123
<b>Butyryl fentanyl</b>	0.9783	0.9983	0.9993
	1.4300	0.0395	1.6152
<b>Para-methylfentanyl</b>	0.9461	0.9954	0.9912
	3.4988	0.4635	1.8345
<b>Cyclopropyl fentanyl</b>	0.9686	0.9976	0.9954
	2.3433	0.1709	0.9936
<b>Despropionyl para-fluorofentanyl</b>	0.9916	0.9980	0.9920
	1.3273	0.1935	1.3494
<b>Meta-fluorofentanyl</b>	0.9779	0.9977	0.9923
	2.2533	0.0716	0.7255
<b>Para-fluorofentanyl</b>	0.9573	0.9793	0.9825
	2.8880	0.6783	3.1715
<b>Fentanyl</b>	0.9845	0.9977	0.9873
	1.4039	0.3284	1.6452
<b>Acetyl fentanyl 4-methylphenethyl analogue</b>	0.9776	0.9991	0.9844
	1.3834	0.0771	1.7144
<b>Crotonyl fentanyl</b>	0.9605	0.9979	0.9691
	3.3496	0.1705	4.0156
<b>Acetyl fentanyl</b>	0.9865	0.9978	0.9886

	1.1282	0.2263	1.2974
<b>Ortho-fluorofentanyl</b>	0.9873	0.9981	0.9980
	1.0719	0.1010	0.7456
<b>Meta-fluorobutyryl fentanyl</b>	0.9627	0.9979	0.9983
	3.3286	0.1464	2.5385
<b>Meta-methylfentanyl</b>	0.9614	0.9908	0.9926
	1.2193	0.2832	2.2412
<b>Beta-methyl fentanyl</b>	0.9779	0.9983	0.9837
	2.2977	0.0863	2.5282
<b>Ortho-methylfentanyl</b>	0.9702	0.9965	0.9855
	2.7674	0.2414	1.7519
<b>Benzyl fentanyl</b>	0.9758	0.9902	0.9857
	1.9758	0.6470	1.9025

#<sub>n=5</sub>      §<sub>n=4</sub>

Table 12: Relative retention times (relative to benzyl fentanyl) for fentanyl analogues, heroin

Solute	RRT
Caffeine	0.7012
Diphenhydramine	0.7079
Lidocaine	0.7127
Procaine	0.7880
Cocaine	0.8485
Codeine	0.9250
Despropionyl ortho-fluorofentanyl	0.9247
Despropionyl para-fluorofentanyl	0.9446
Despropionyl meta-fluorofentanyl	0.9483
6-acetylcodeine	0.9630
3-acetylmorphine	0.9713
6-acetylmorphine	0.9758
Benzyl fentanyl	1.000
Heroin	1.011
4-Fluoroisobutyryl fentanyl	1.021
Meta-fluorofentanyl	1.026
Acetyl fentanyl	1.026
Para-fluorofentanyl	1.030
Ortho-fluoroisobutyryl fentanyl	1.032
Ortho-fluorofentanyl	1.036
Beta-methyl fentanyl	1.037
Isobutyryl fentanyl	1.039
Fentanyl	1.047
3-fluorofentanyl	1.047
Meta-fluorobutyryl fentanyl	1.049
Para-fluorobutyryl fentanyl	1.057
Ortho-fluorobutyryl fentanyl	1.065
Meta-methylfentanyl	1.067
Acetyl fentanyl 4-methylphenethyl analog	1.070
Ortho-methylfentanyl	1.074
Butyryl fentanyl	1.077
Para-methylfentanyl	1.087
Cyclopropyl fentanyl	1.104
Papaverine	1.106
Crotonyl fentanyl	1.110
Quinine	1.125
Noscapine	1.378

by-products and heroin impurities

Table 13: Results of simulated samples

Sample number	Target Compound	Target Concentration (ppm)	VUV Calculation	Adulterant	Ratio of Adulterant to Target
1	isobutyl fentanyl	100	102	none	N/A
2	para-fluorobutyl fentanyl	150	156	none	N/A
3	meta-fluorofentanyl	150	156	caffeine diphenhydramine lidocaine	1.7 4.5 1.5X
4	para-methylfentanyl	50	51.5	acetaminophen caffeine	5.0 4.9
5	meta-fluorofentanyl	50	49.7	quinine diphenhydramine	2.4 2.5
6	despropionyl ortho-fluorofentanyl	50	45.6	none	N/A
7	fentanyl	50	57.5	heroin acetylcodeine O6-monoacetylmorphine morphine papaverine caffeine diphenhydramine lidocaine	2.0 0.2 0.06 0.02 0.02 1.32 1.0 1.0

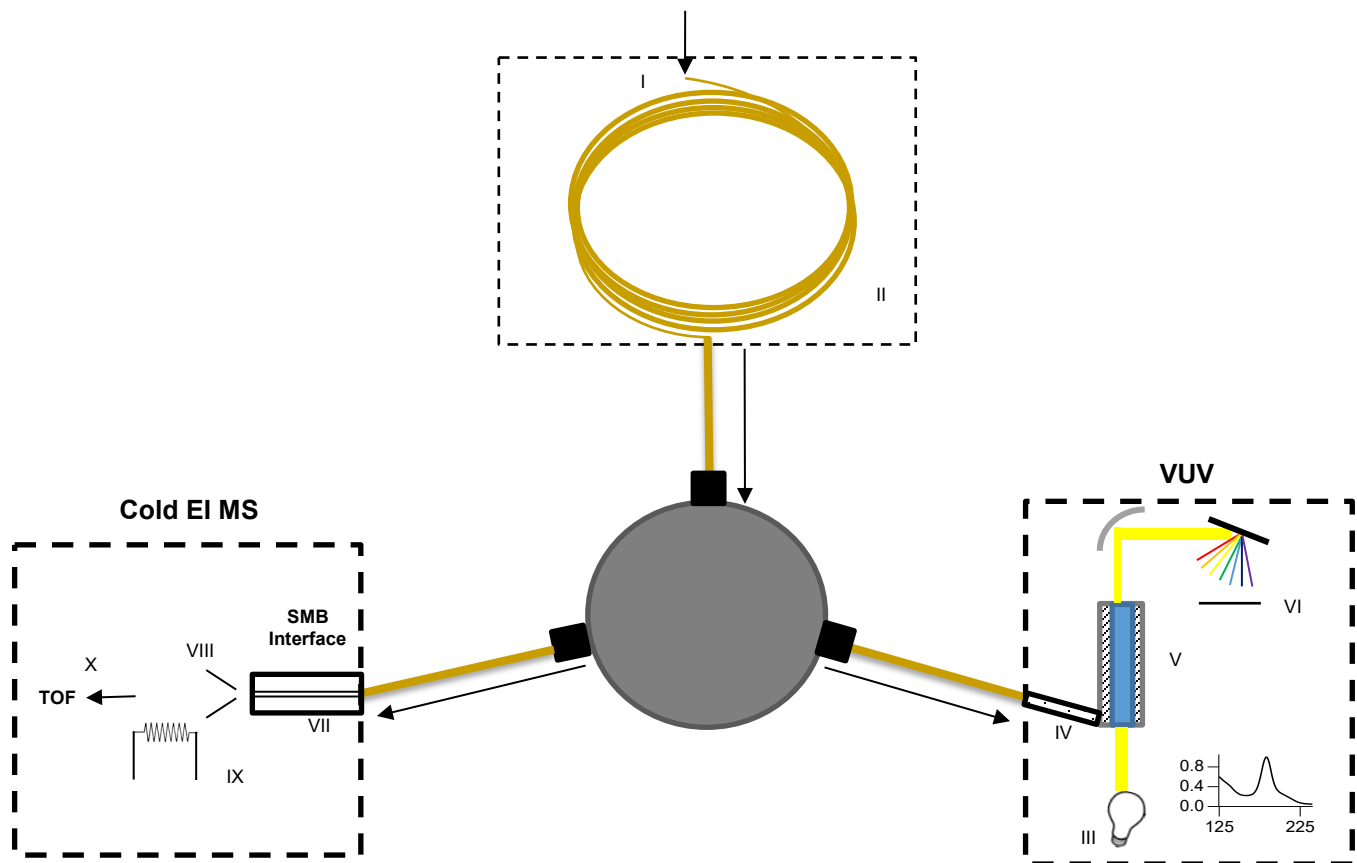


Figure 1: Instrumental setup for NIJ study. Schematic of the parallel GC-cold EI MS/VUV system (not drawn to scale). (I) GC injection port, (II) GC column and oven, (III) VUV transfer arm, (IV) VUV deuterium lamp, (V) VUV flow cell, (VI) VUV detector, (VII) Supersonic Molecular Beam (SMB) interface, (VIII) Skimmer, (IX) Ion source filament, and (X) MS detector.

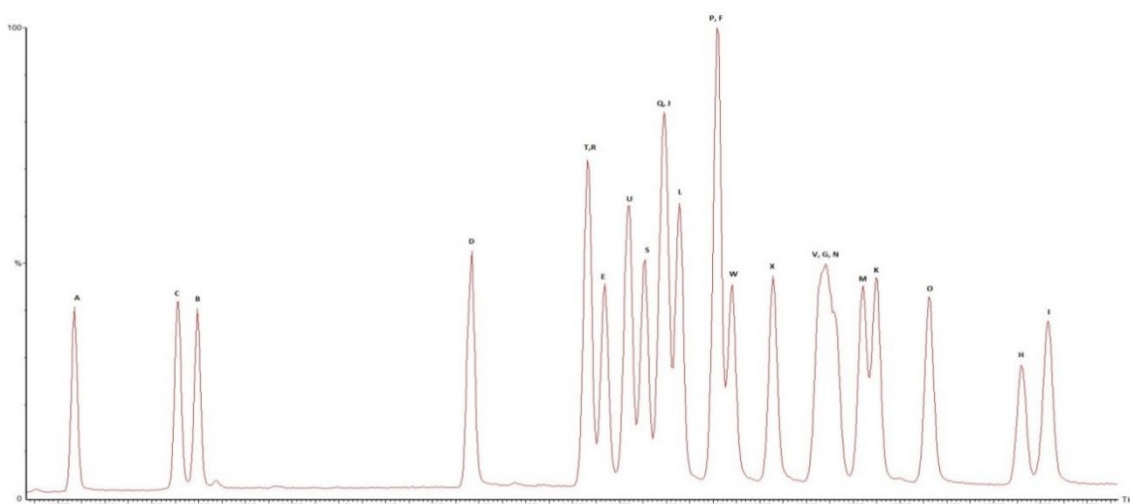


Figure 2: GC-MS chromatogram of controlled fentanyl analogues and the despropionyl non-controlled positional isomers (10 ppm). 10 PPM each compound, see Table 1 for compound identification.

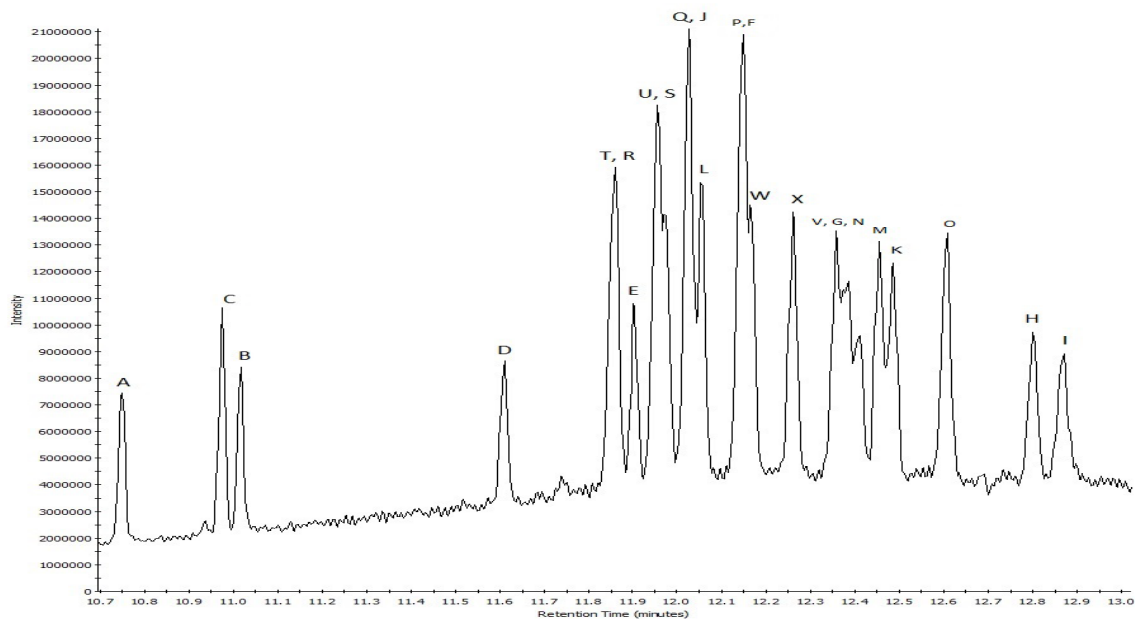


Figure 3: GC-cold EI MS chromatogram of controlled fentanyl analogues and the despropionyl non- controlled positional isomers (10 ppm). See Table 1 for compound identification.

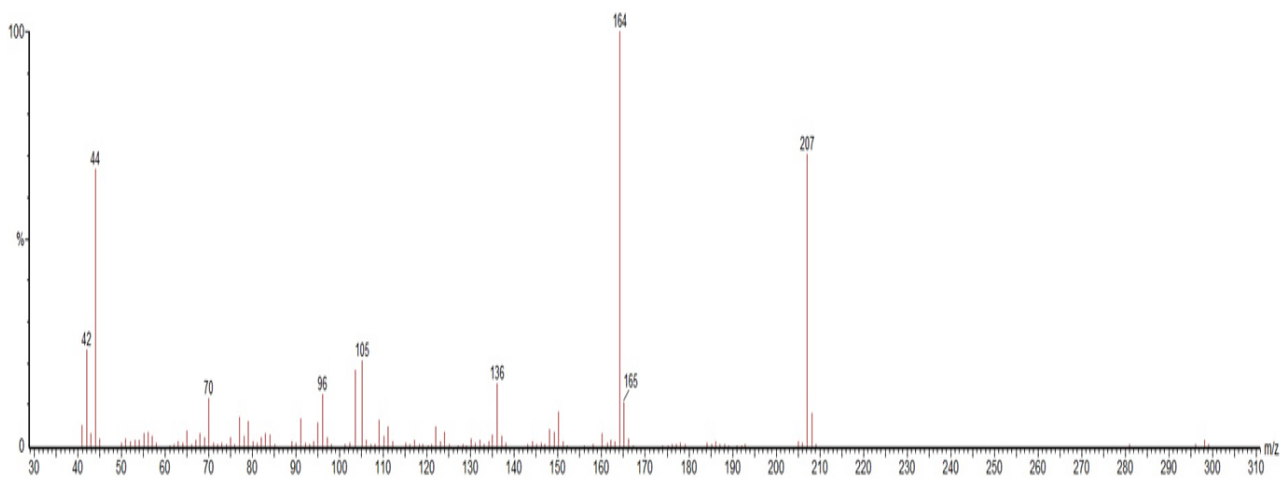


Figure 4: GC-EI MS spectrum for 10 PPM despropionyl ortho-fluorofentanyl mass 298.

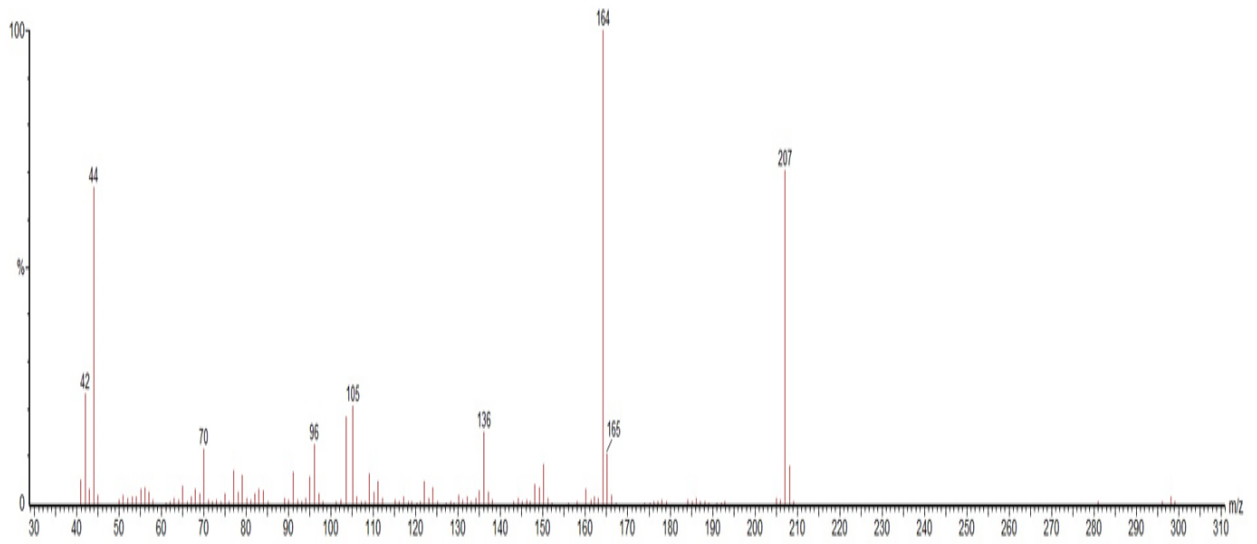


Figure 5: GC-EI MS spectrum for 10 PPM despropionyl para-fluorofentanyl mass 298.

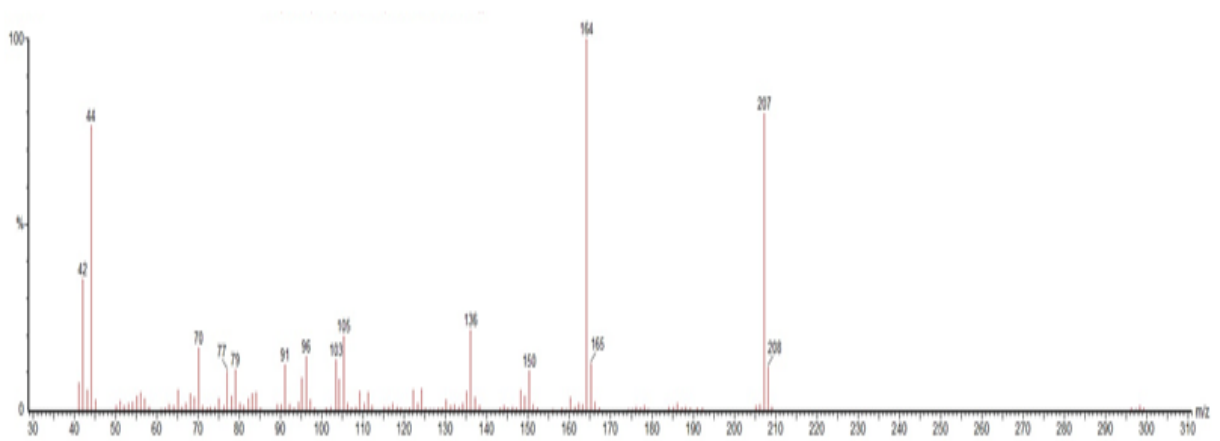


Figure 6: GC-EI MS spectrum for 10 PPM despropionyl para-fluorofentanyl mass 298.

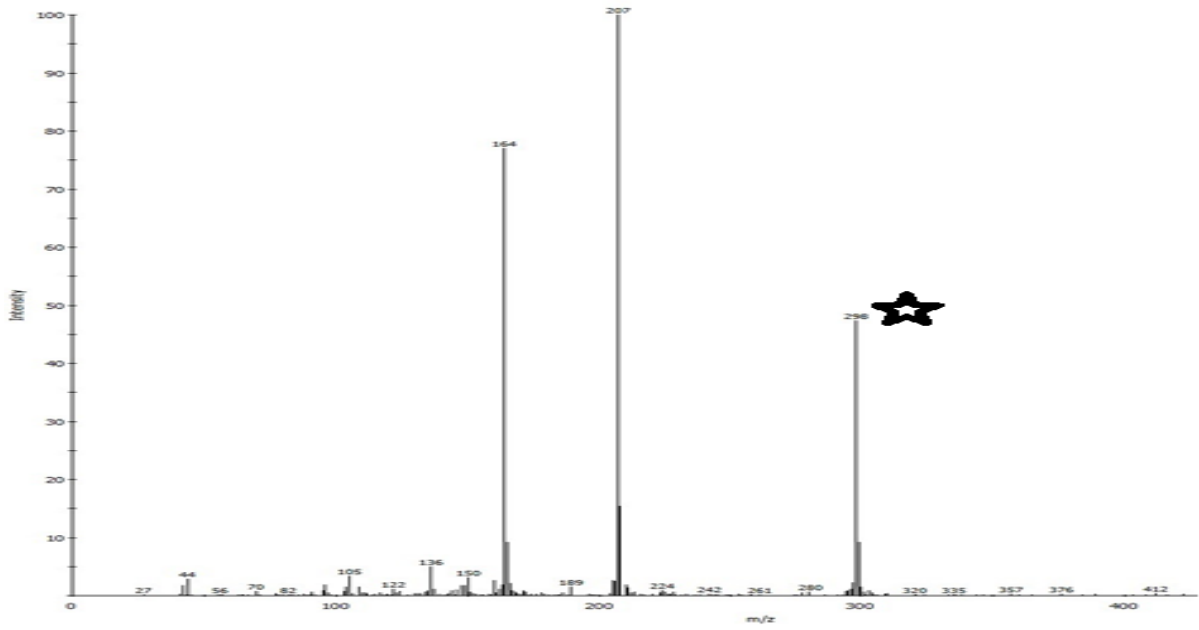


Figure 7: GC-cold EI MS spectrum for 10 PPM despropionyl ortho-fluorofentanyl mass 298.

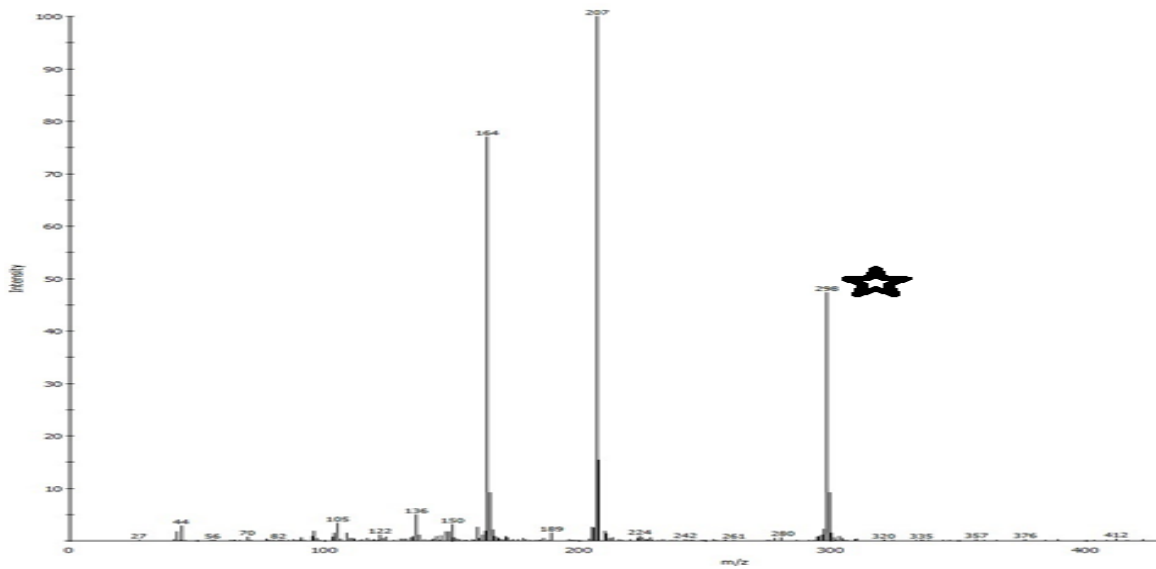


Figure 8: GC-cold EI MS spectrum for 10 PPM despropionyl para-fluorofentanyl mass 298.

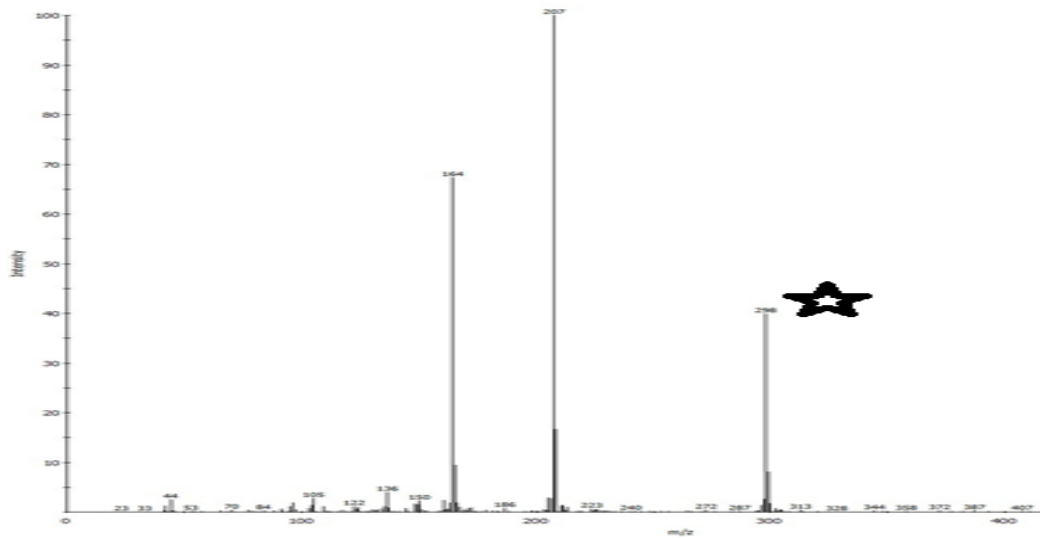


Figure 9: GC-cold EI MS spectrum for 10 PPM despropionyl meta-fluorofentanyl mass 298.

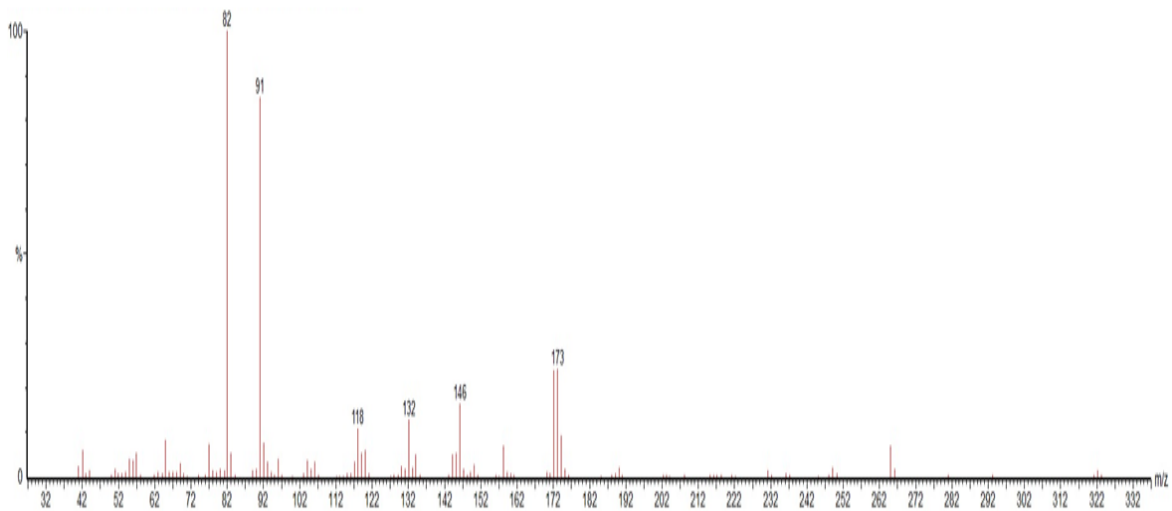


Figure 10: GC-EI MS spectrum for 10 PPM benzyl fentanyl mass 322.

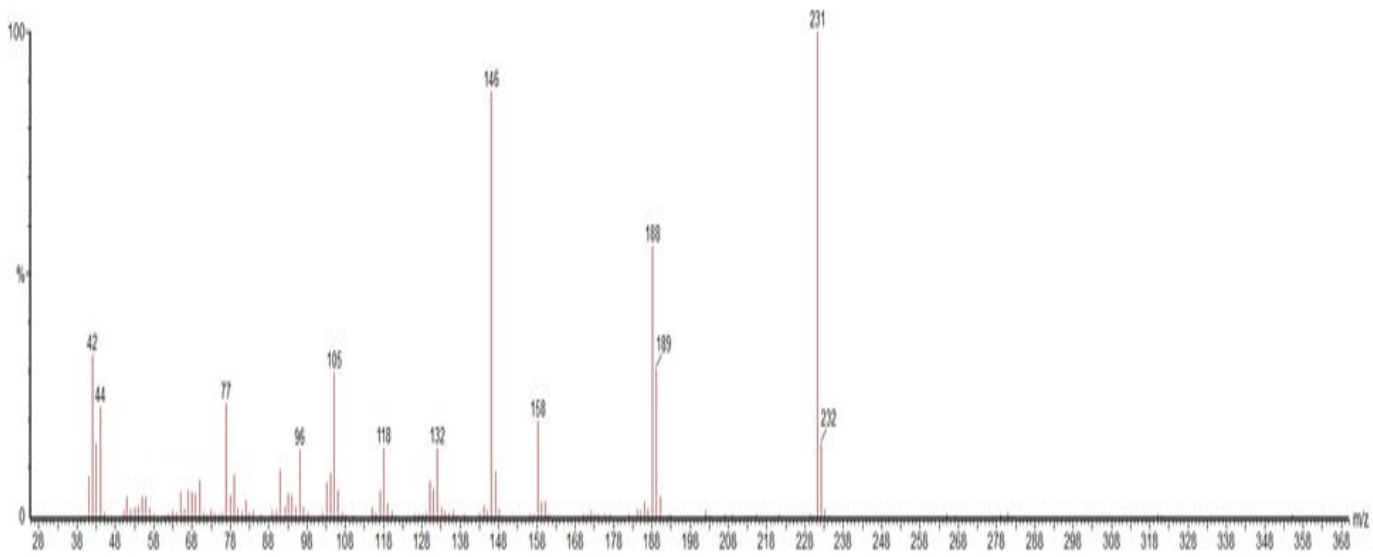


Figure 11: GC-EI MS spectrum for 10 PPM acetyl fentanyl mass 322.

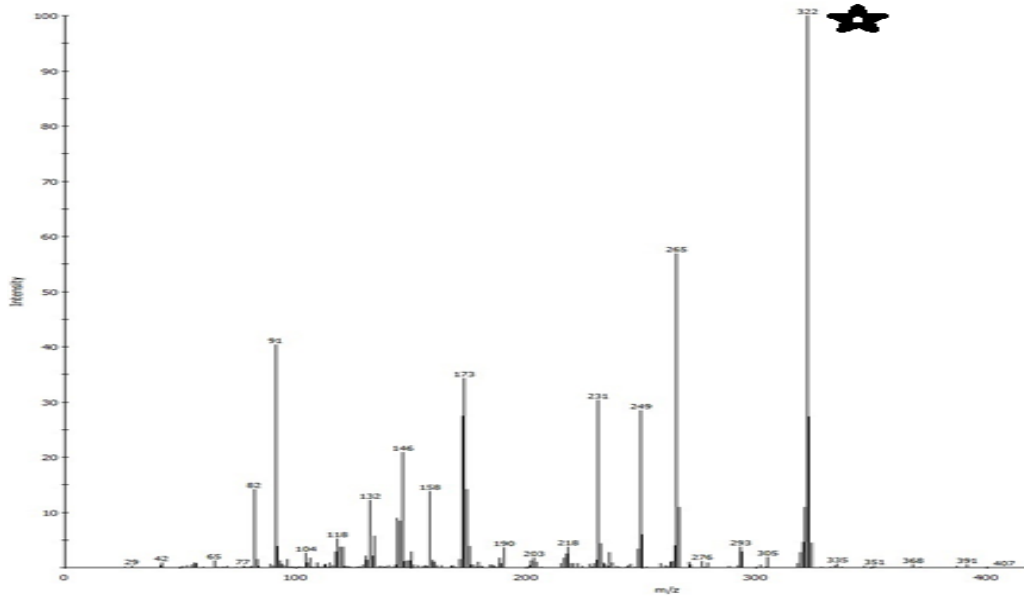


Figure 12: GC-cold EI MS spectrum for 10 PPM benzyl fentanyl mass 322.

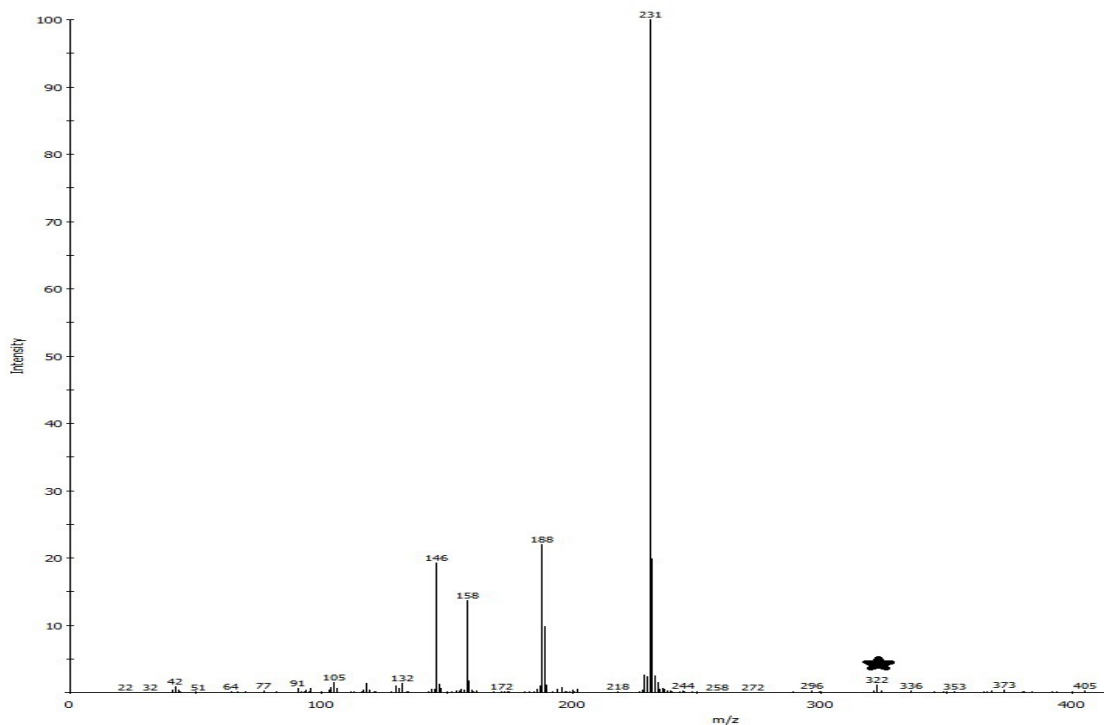


Figure 13: GC-cold EI MS spectrum for 10 PPM acetyl fentanyl mass 322.

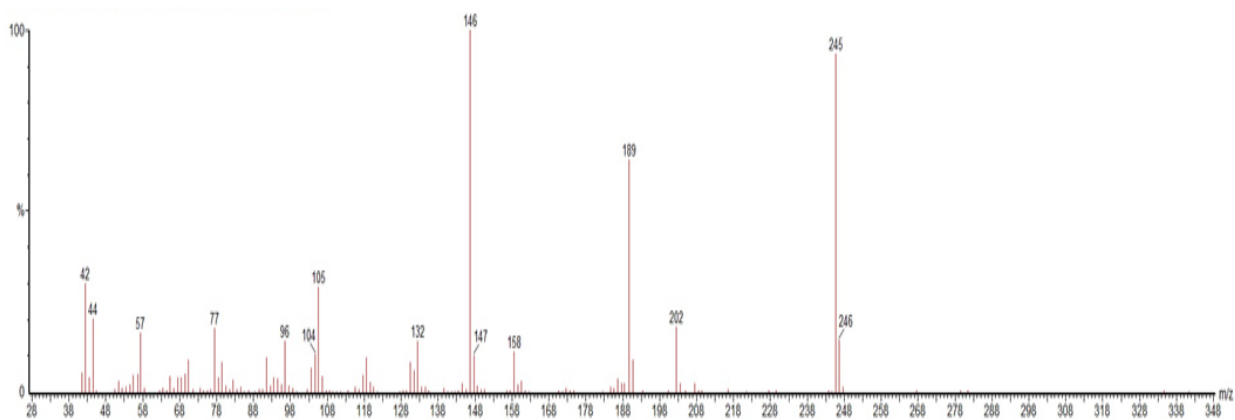


Figure 14: GC-EI MS spectrum for 10 PPM fentanyl mass 336.

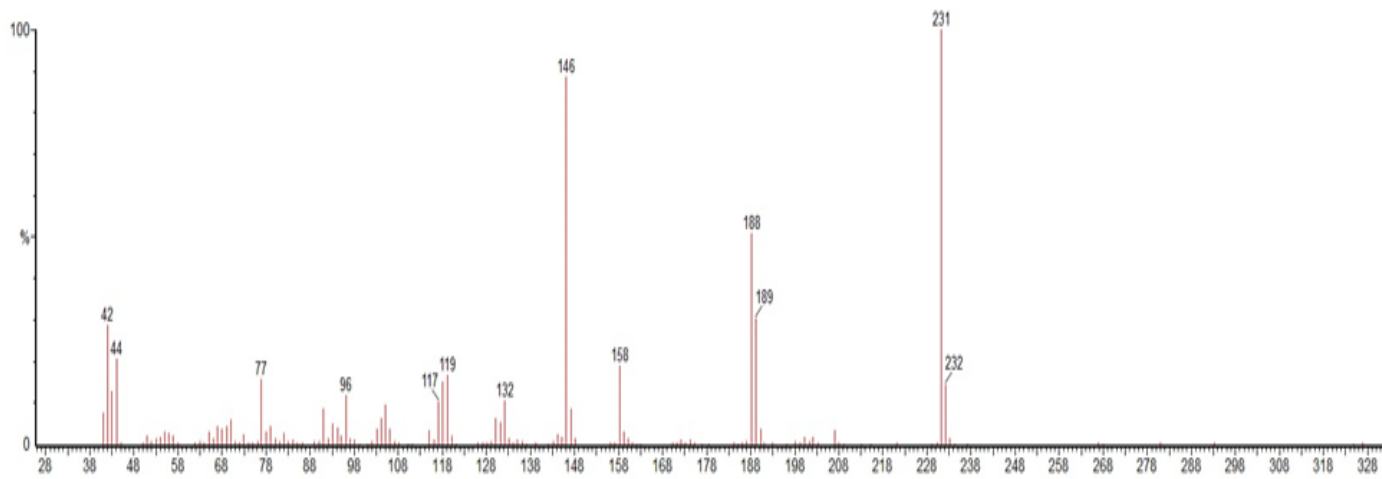


Figure 15: GC-EI MS spectrum for 10 PPM acetyl fentanyl 4-methylphenethyl analogue mass 336.

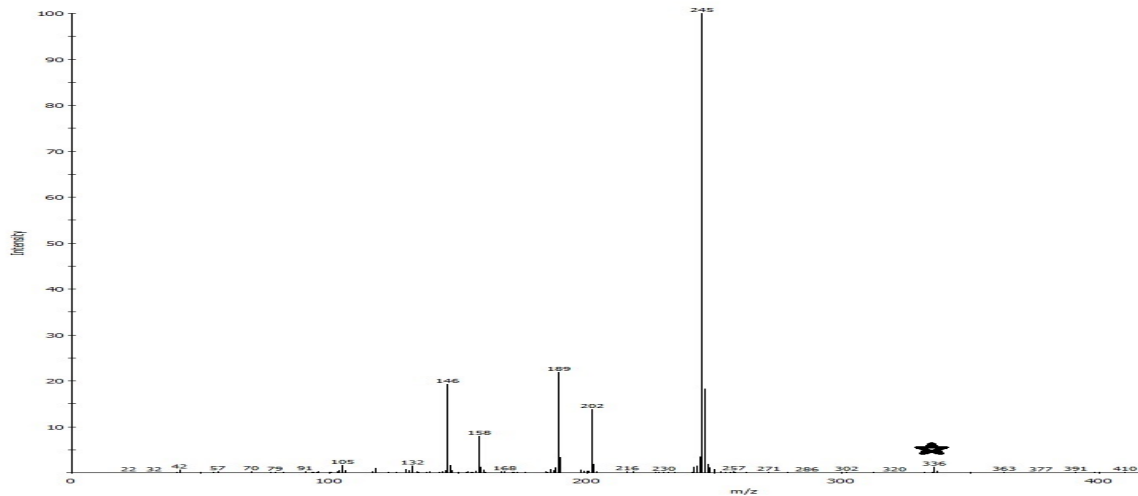


Figure 16: GC-cold EI MS spectrum for 10 PPM fentanyl mass 336.

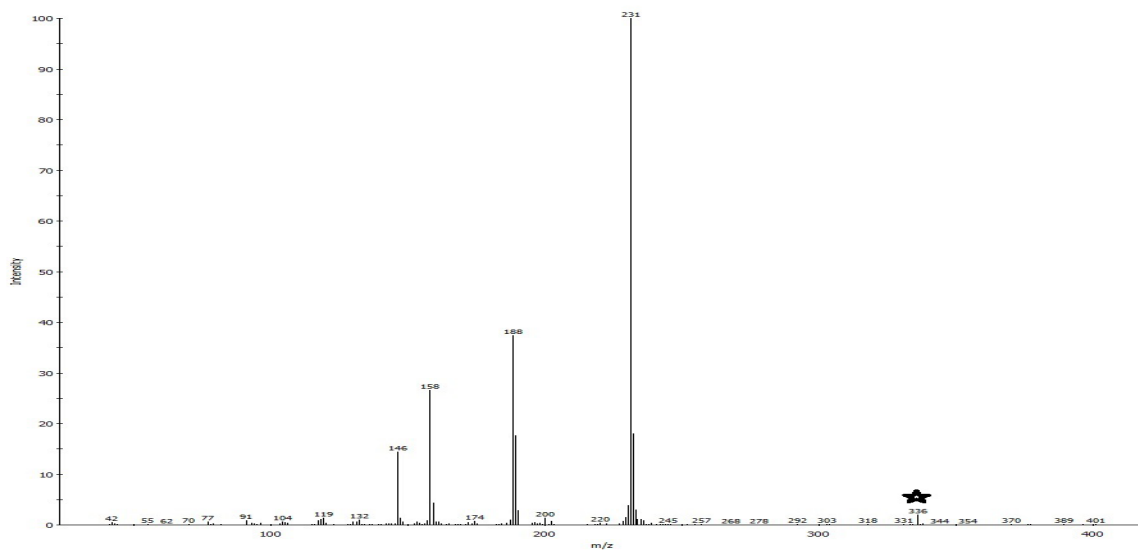


Figure 17: GC-cold EI MS spectrum for 10 PPM acetyl fentanyl 4-methylphenethyl analogue mass 336.

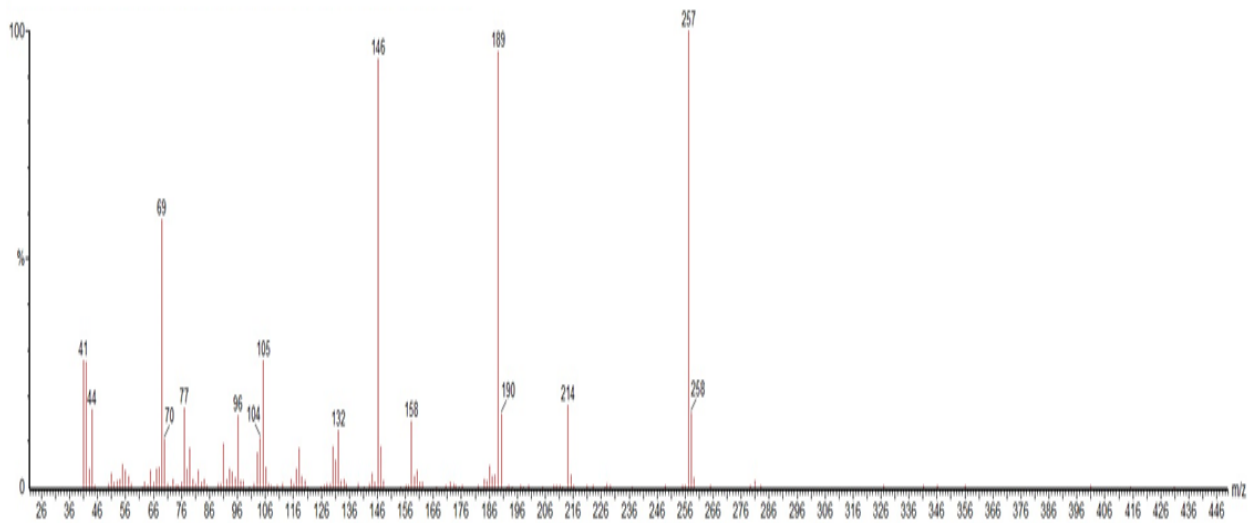


Figure 18: GC-EI MS spectrum for 10 PPM cyclopropyl fentanyl mass 348.

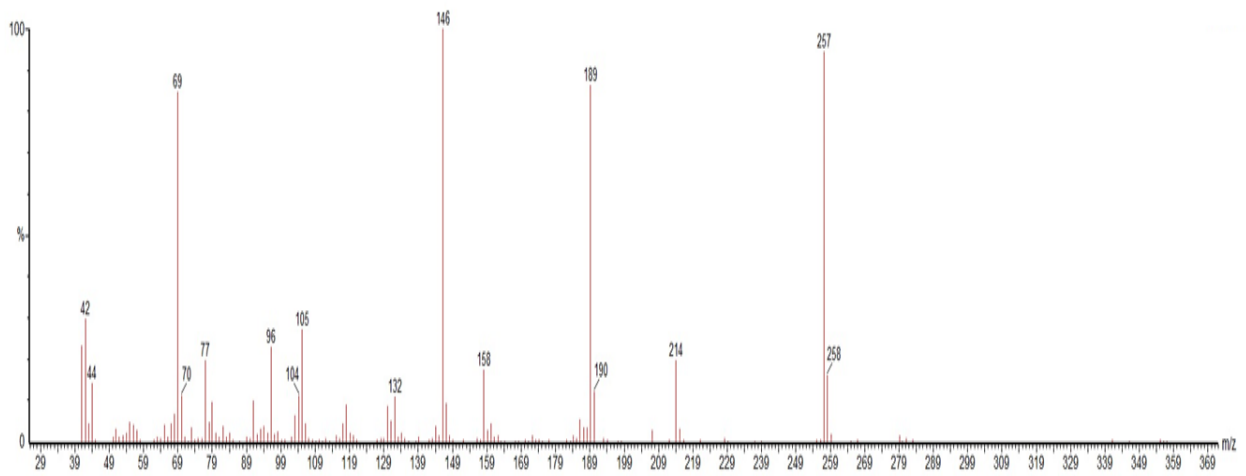


Figure 19: GC-EI MS spectrum for 10 PPM crotonyl fentanyl mass 348.

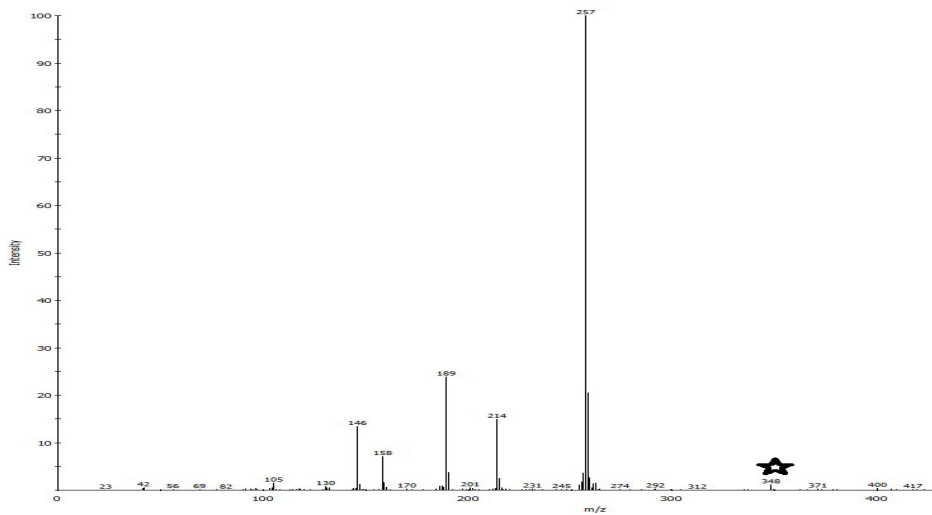


Figure 20: GC-cold EI MS spectrum for 10 PPM cyclopropyl fentanyl mass 348.

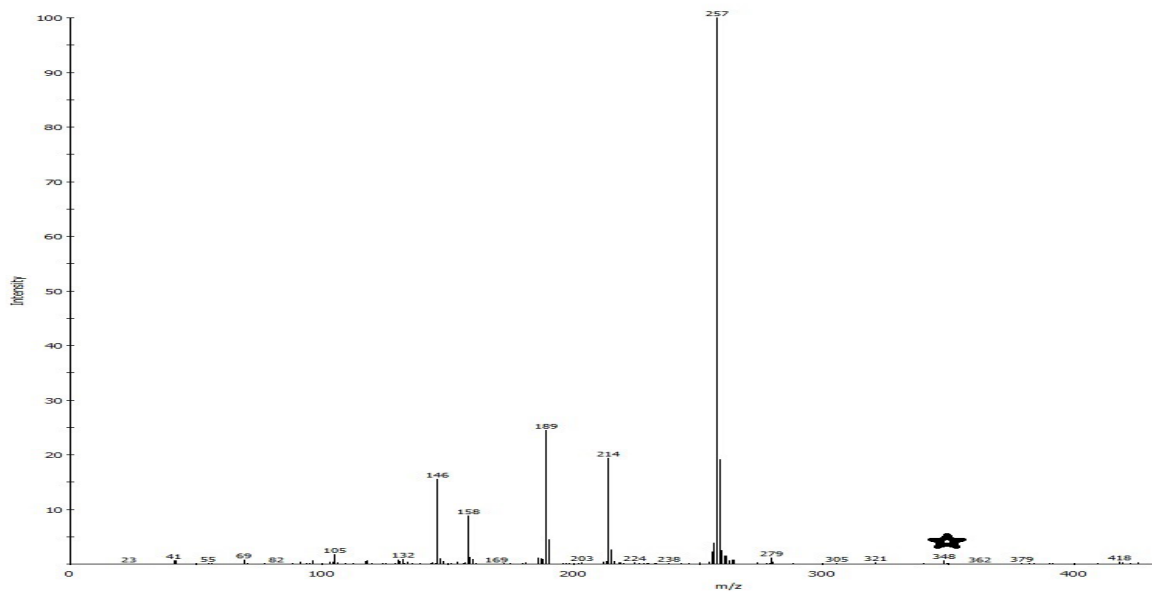


Figure 21: GC-cold EI MS spectrum for 10 PPM crotonyl fentanyl mass 348.

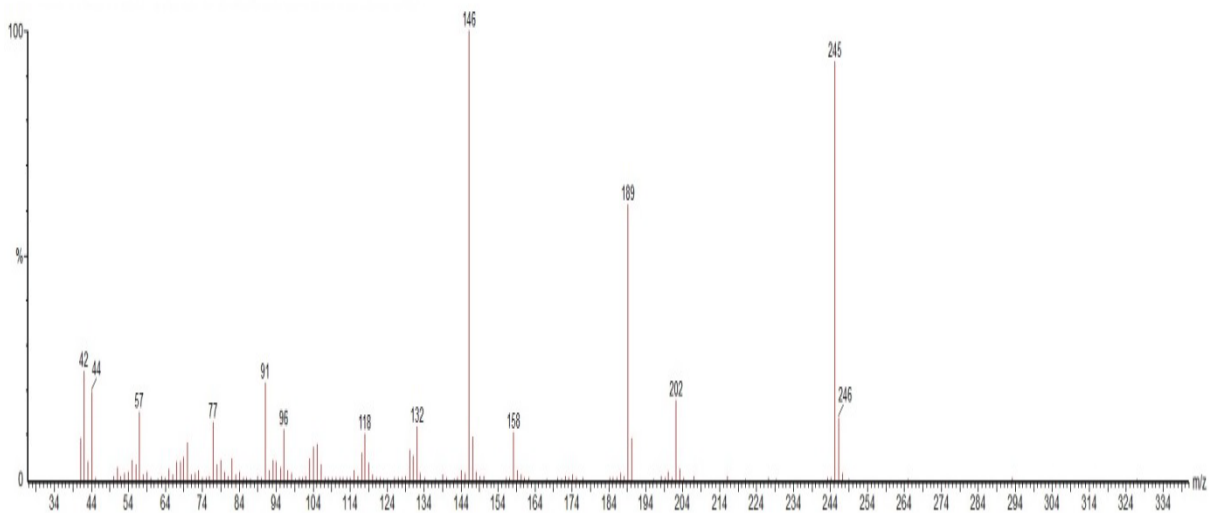


Figure 22: GC-EI MS spectrum for 10 PPM beta-methyl fentanyl mass 350.

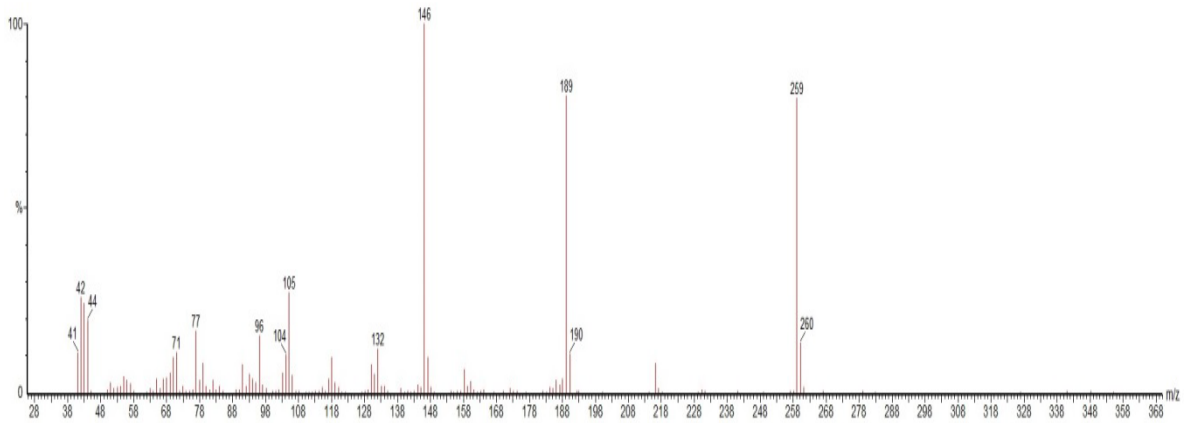


Figure 23: GC-EI MS spectrum for 10 PPM butyryl fentanyl mass 350.

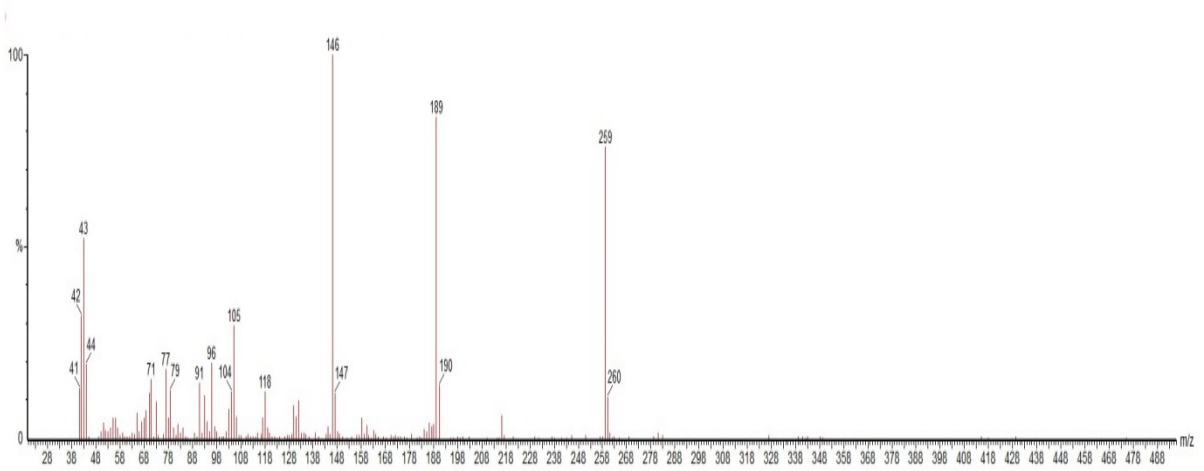


Figure 24: GC-EI MS spectrum for 10 PPM isobutyryl fentanyl mass 350.

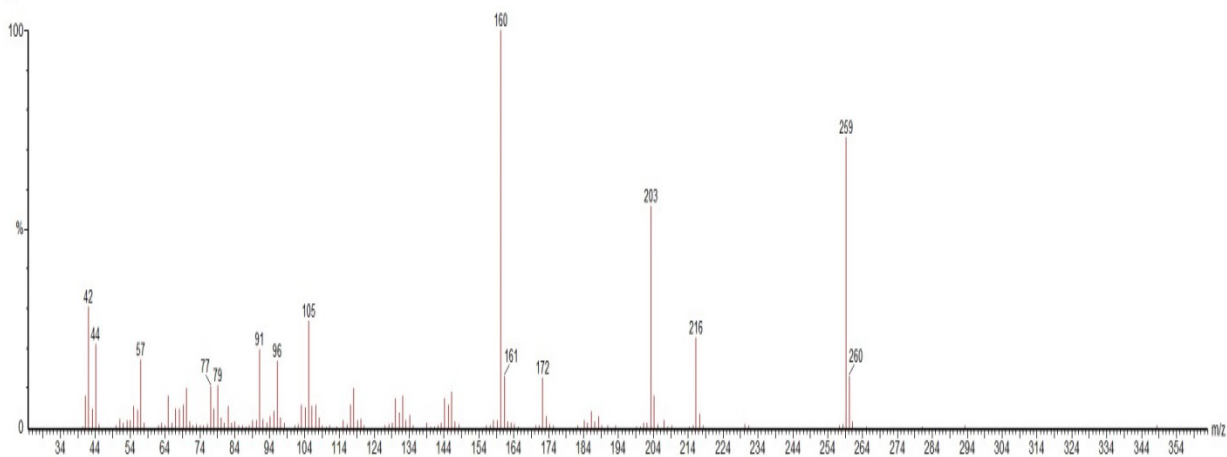


Figure 25: GC-EI MS spectrum for 10 PPM ortho-methylfentanyl mass 350.

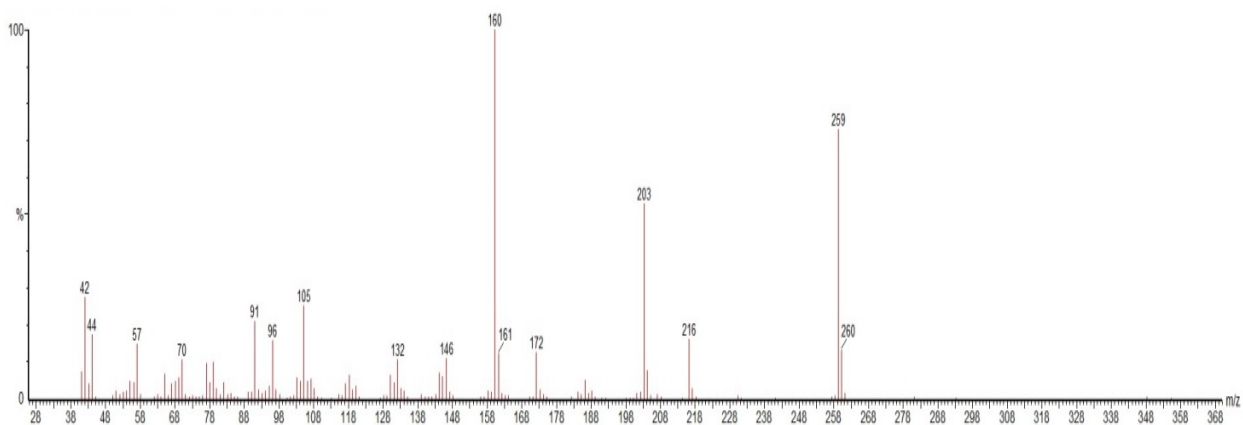


Figure 26: GC-EI MS spectrum for 10 PPM meta-methylfentanyl mass 350.

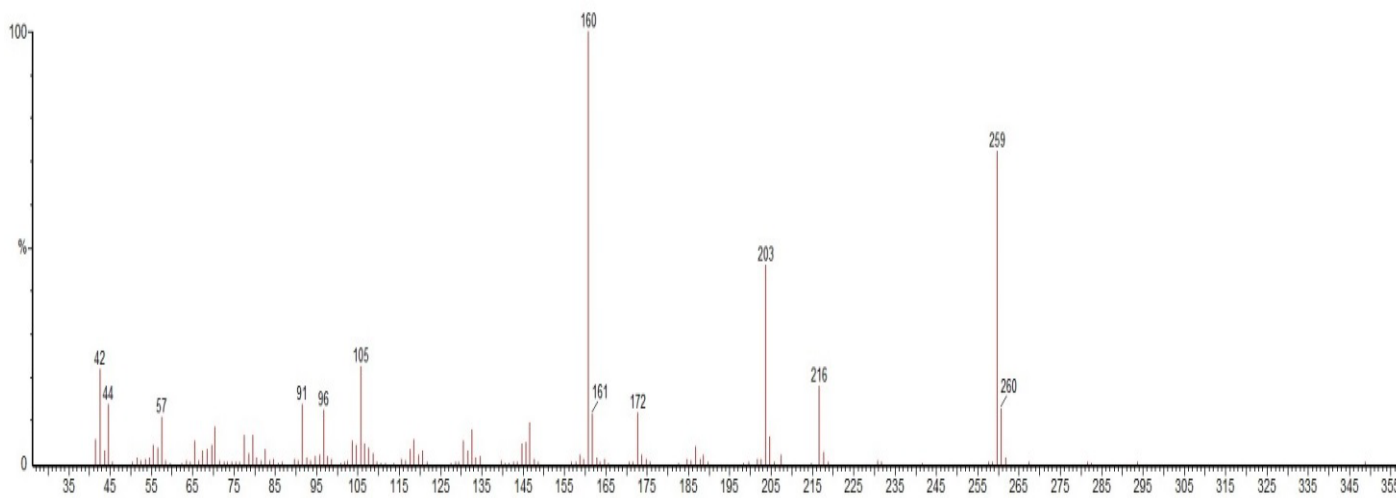


Figure 27: GC-EI MS spectrum for 10 PPM para-methylfentanyl mass 350.

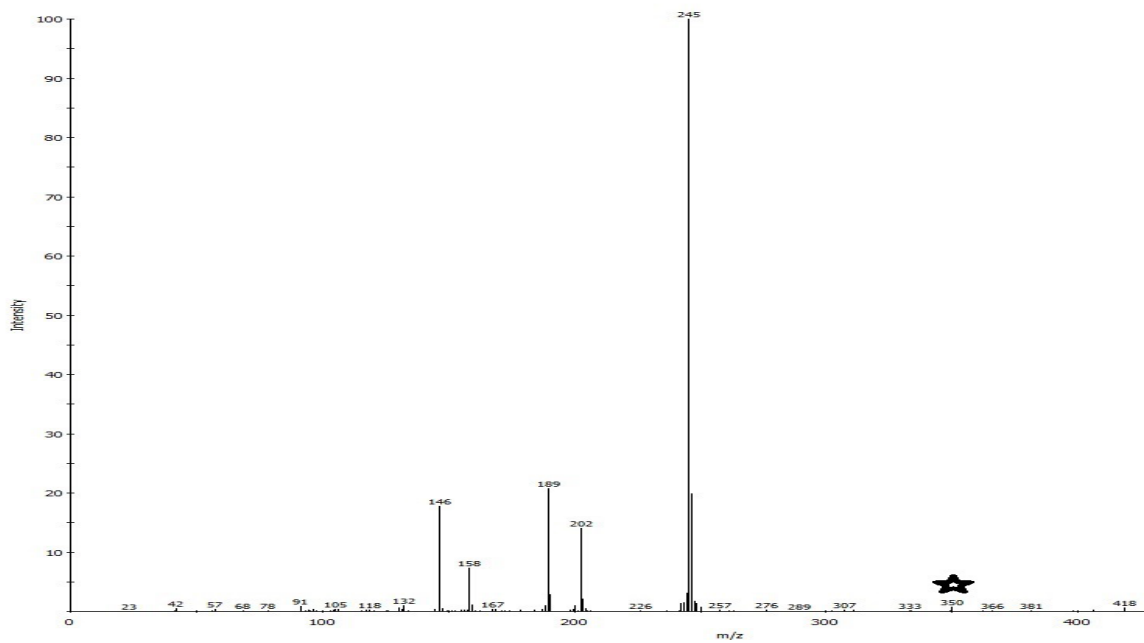


Figure 28: GC-cold EI MS spectrum for 10 PPM beta-methyl fentanyl mass 350.

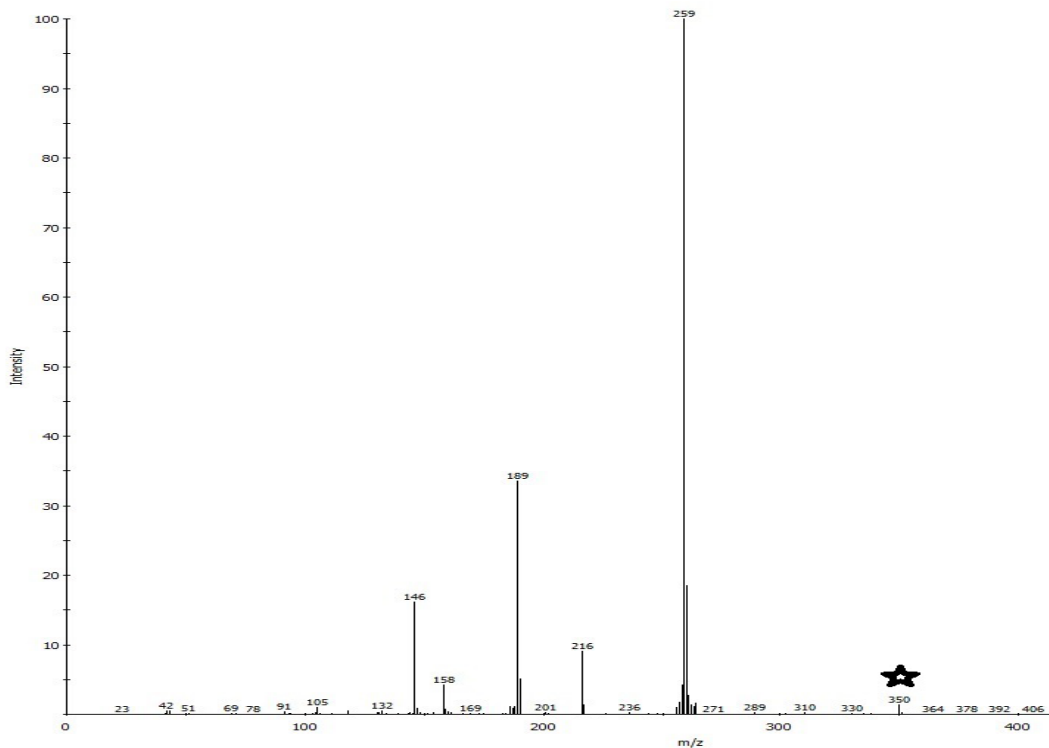


Figure 29: GC-cold EI MS spectrum for 10 PPM butyryl fentanyl mass 350.

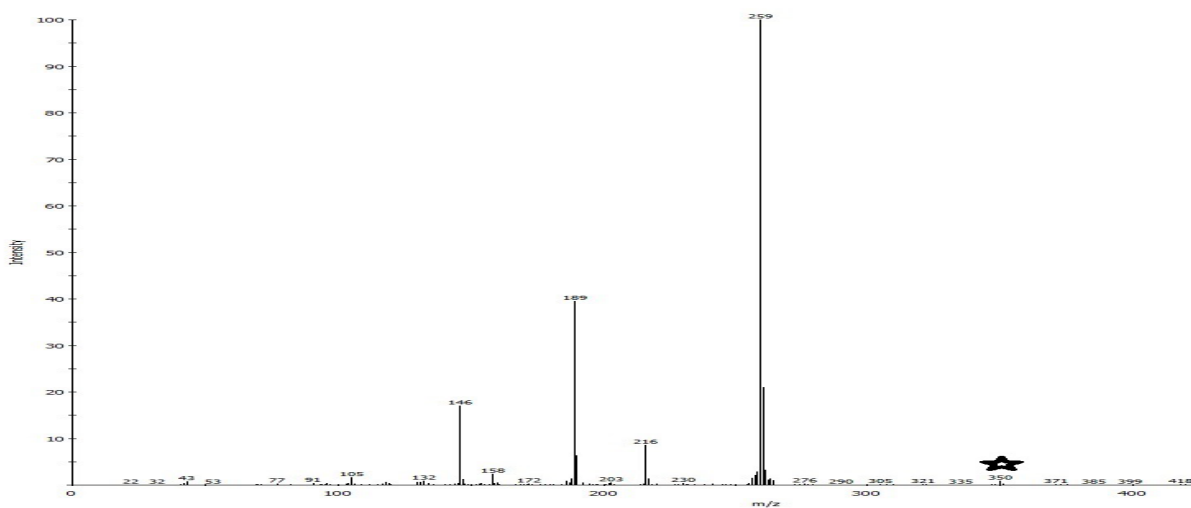


Figure 30: GC-cold EI MS spectrum for 10 PPM isobutyryl fentanyl mass 350.

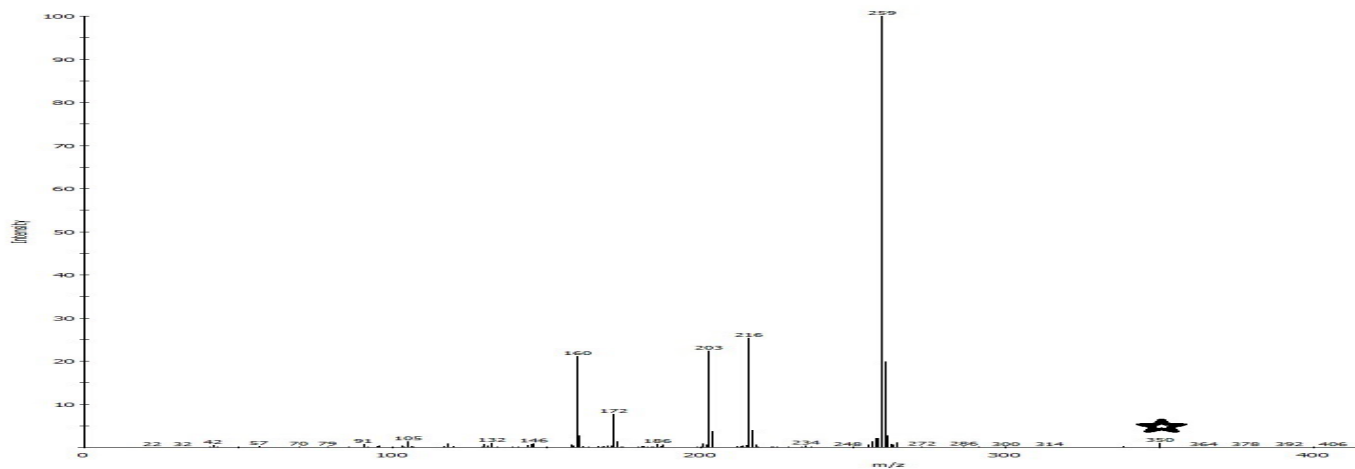


Figure 31: GC-cold EI MS spectrum for 10 PPM ortho-methylfentanyl mass 350.

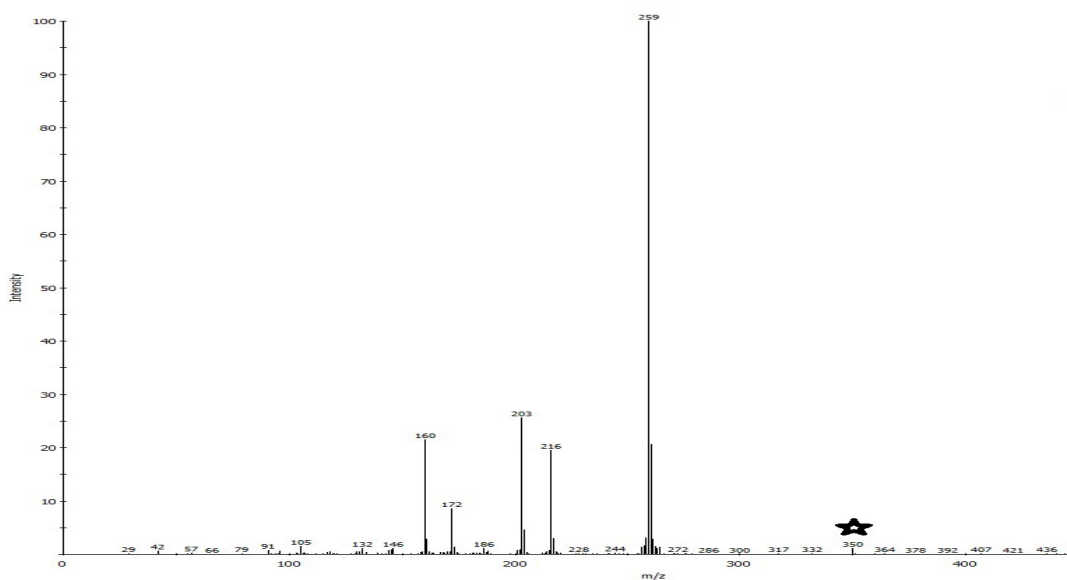


Figure 32: Cold EI MS spectrum for 10 PPM meta-methylfentanyl mass 350.

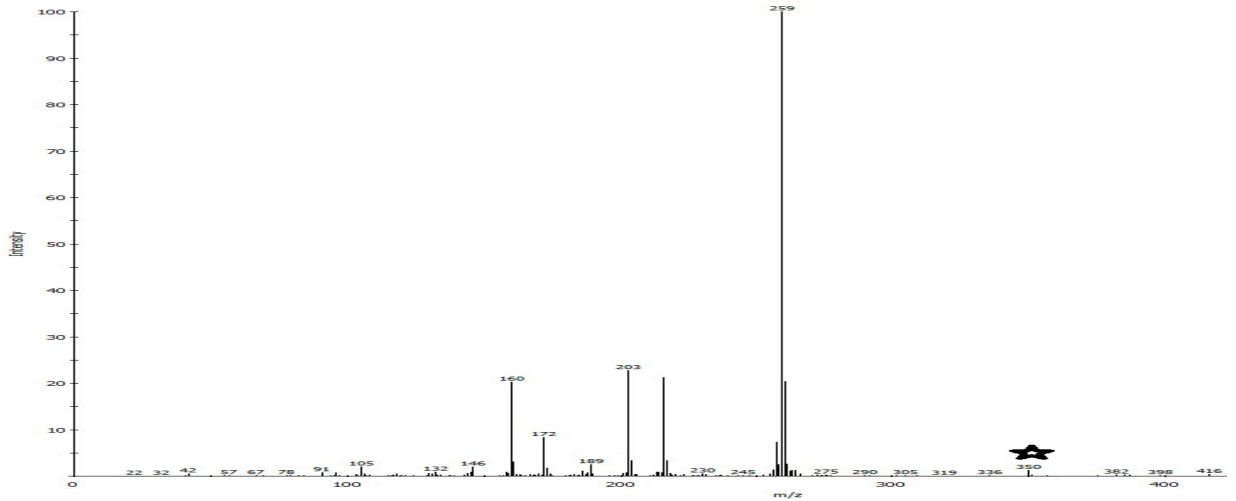


Figure 33: GC-cold EI MS spectrum 10 PPM for para-methylfentanyl mass 350.

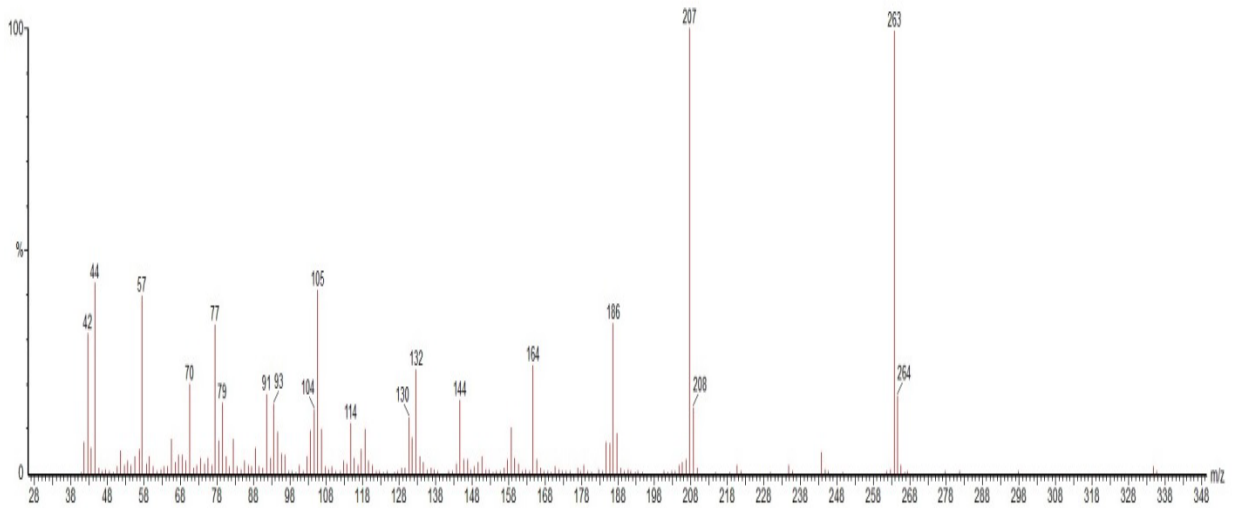


Figure 34: GC-EI MS spectrum for 10 PPM 3-fluorofentanyl mass 354.

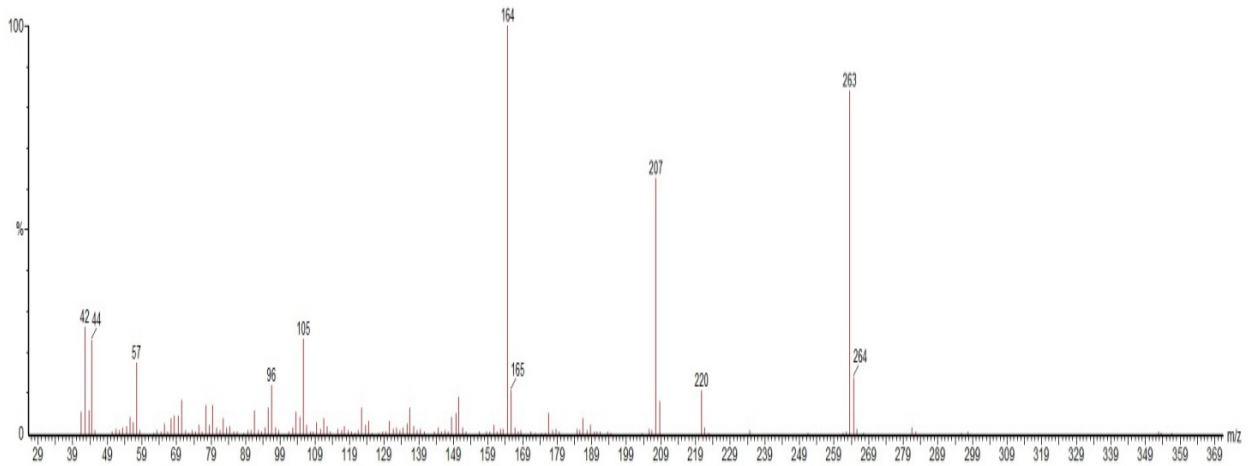


Figure 35: GC-EI MS spectrum for 10 PPM ortho-fluorofentanyl mass 354.

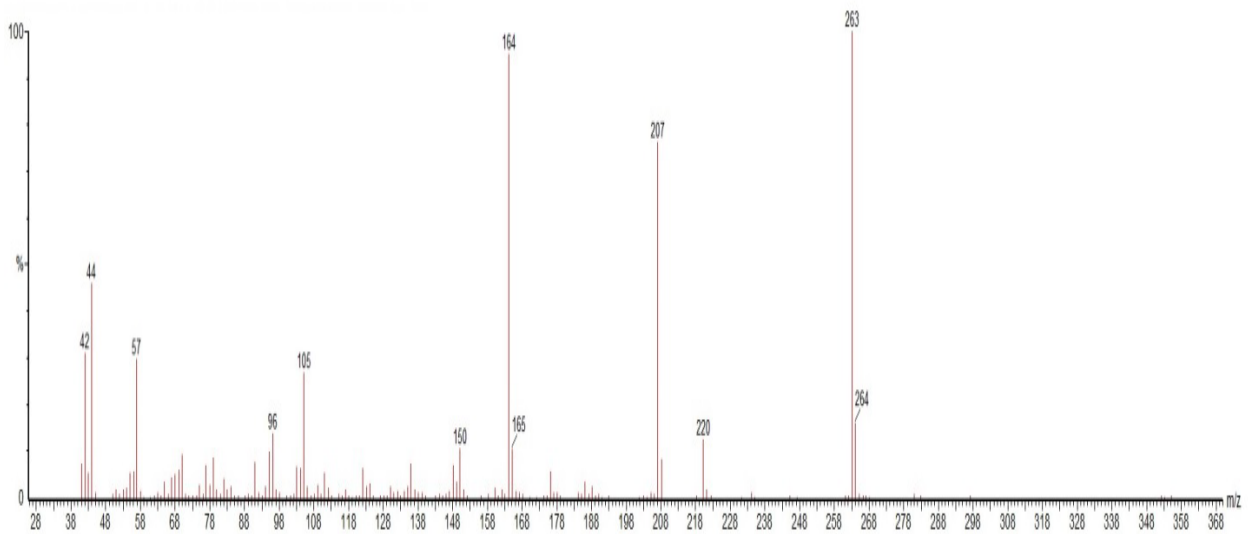


Figure 36: GC-EI MS spectrum for 10 PPM meta-fluorofentanyl mass 354.

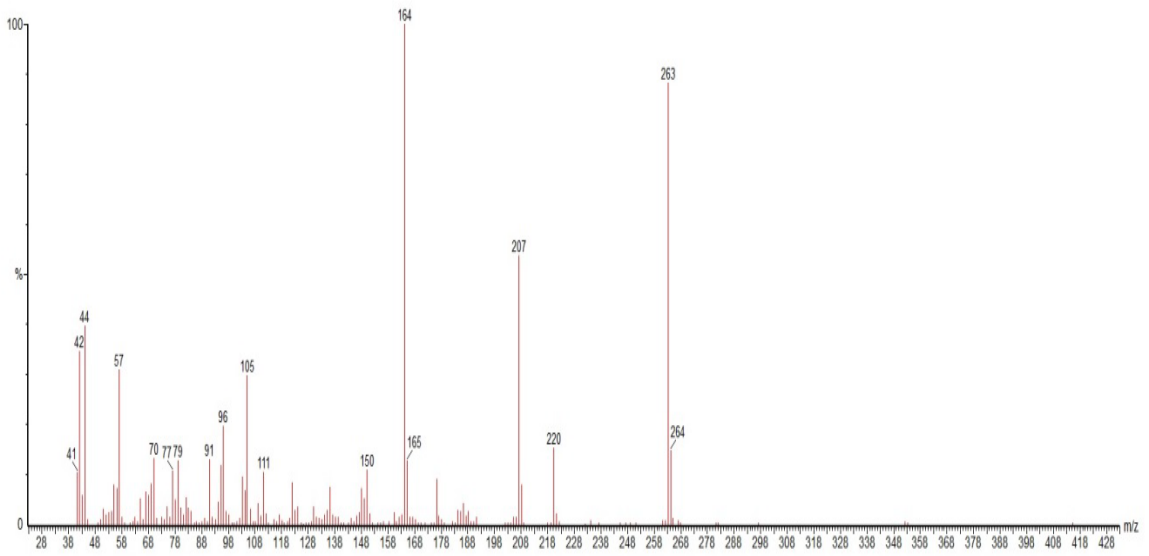


Figure 37: GC-EI MS spectrum for 10 PPM para-fluorofentanyl mass 354.

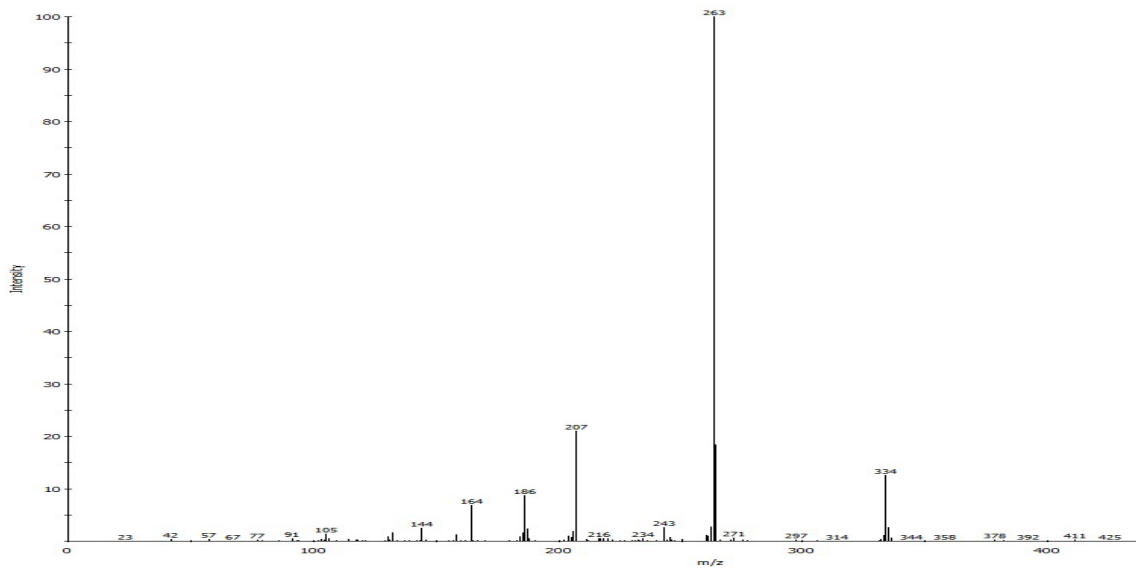


Figure 38: GC-cold EI MS spectrum for 10 PPM 3-fluorofentanyl mass 354.

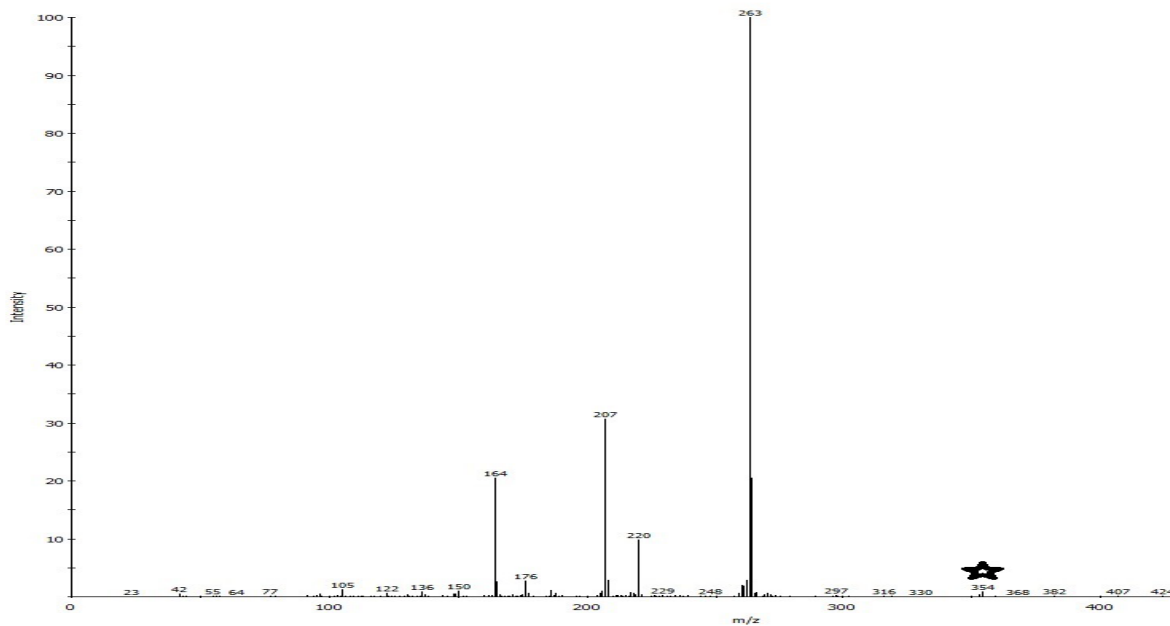


Figure 39: GC-cold EI MS spectrum for 10 PPM ortho-fluorofentanyl mass 354.

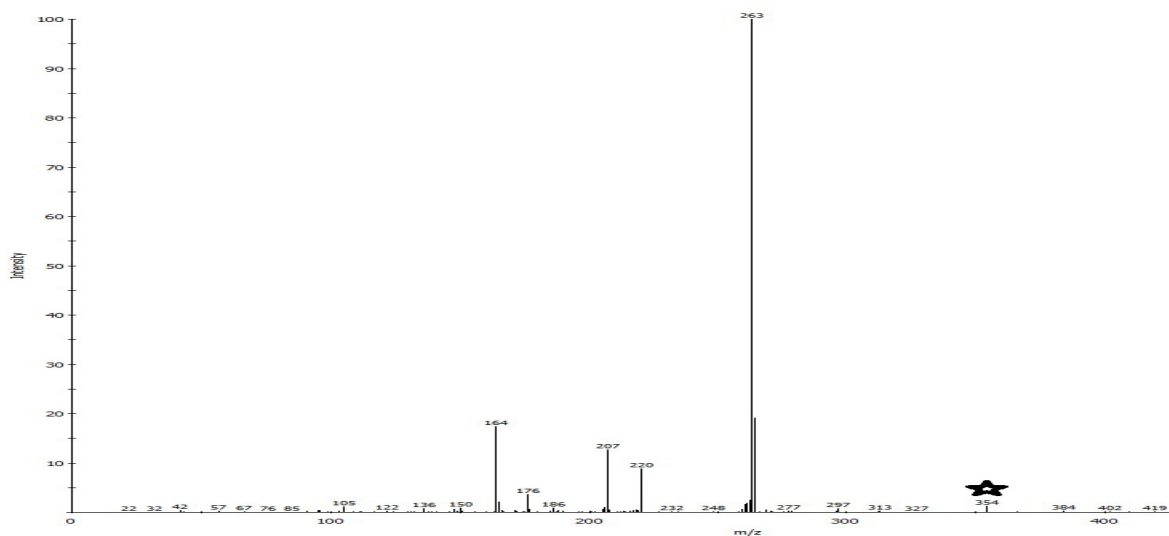


Figure 40: GC-cold EI MS spectrum for 10 PPM meta-fluorofentanyl mass 354.

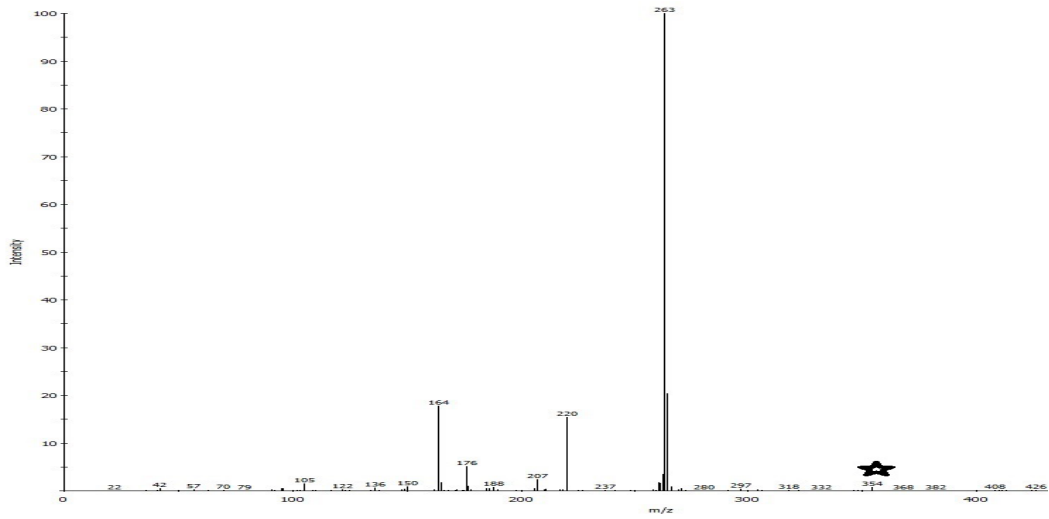


Figure 41: GC-cold EI MS spectrum for 10 PPM para--fluorofentanyl mass 354.

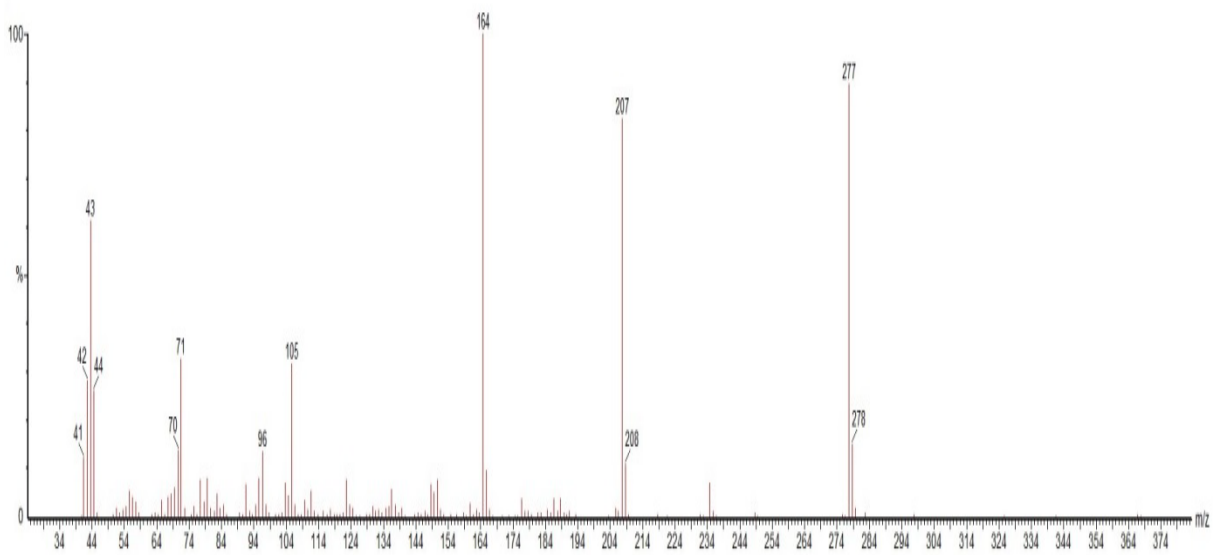


Figure 42: GC-EI MS spectrum for 10 PPM 4-fluoroisobutyryl fentanyl mass 368.

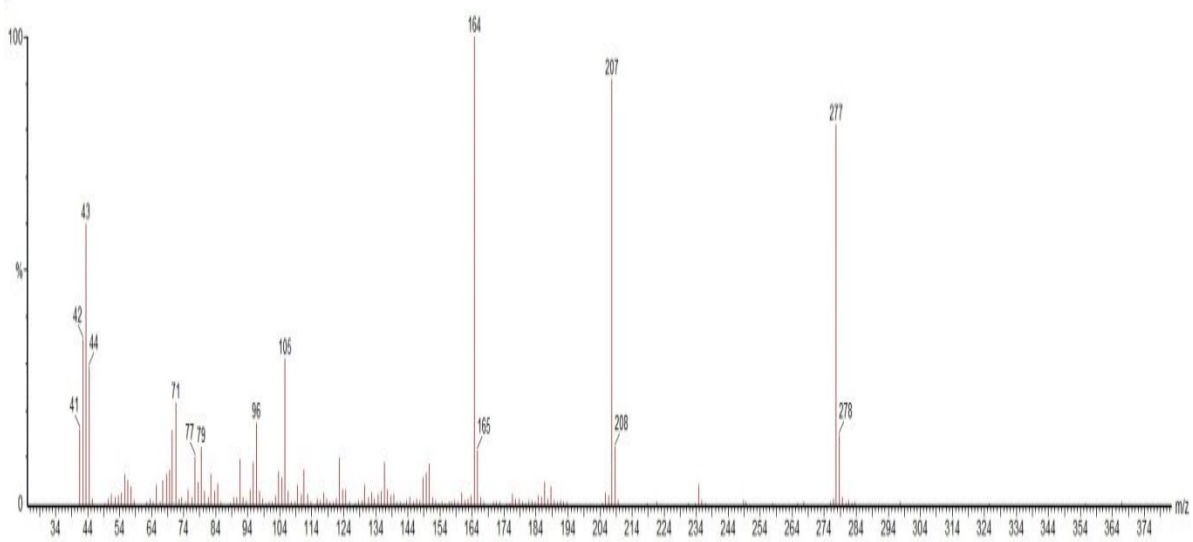


Figure 43: GC-EI MS spectrum for 10 PPM ortho-fluoroisobutyryl fentanyl mass 368.

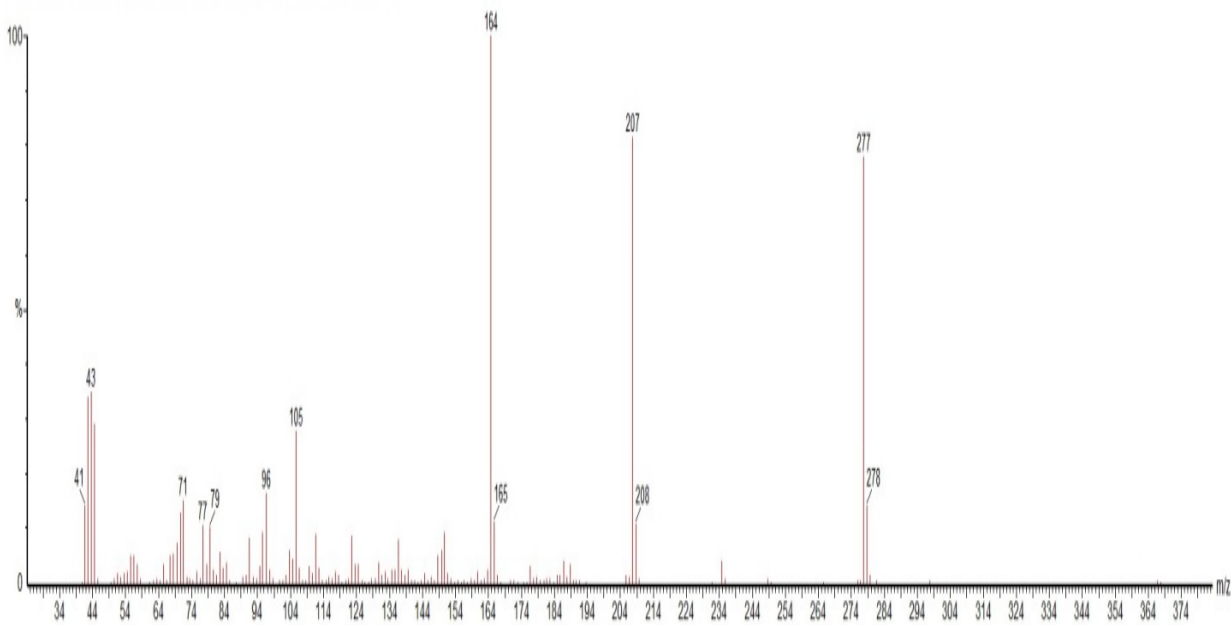


Figure 44: GC-EI MS spectrum for 10 PPM ortho-fluorobutyryl fentanyl mass 368.

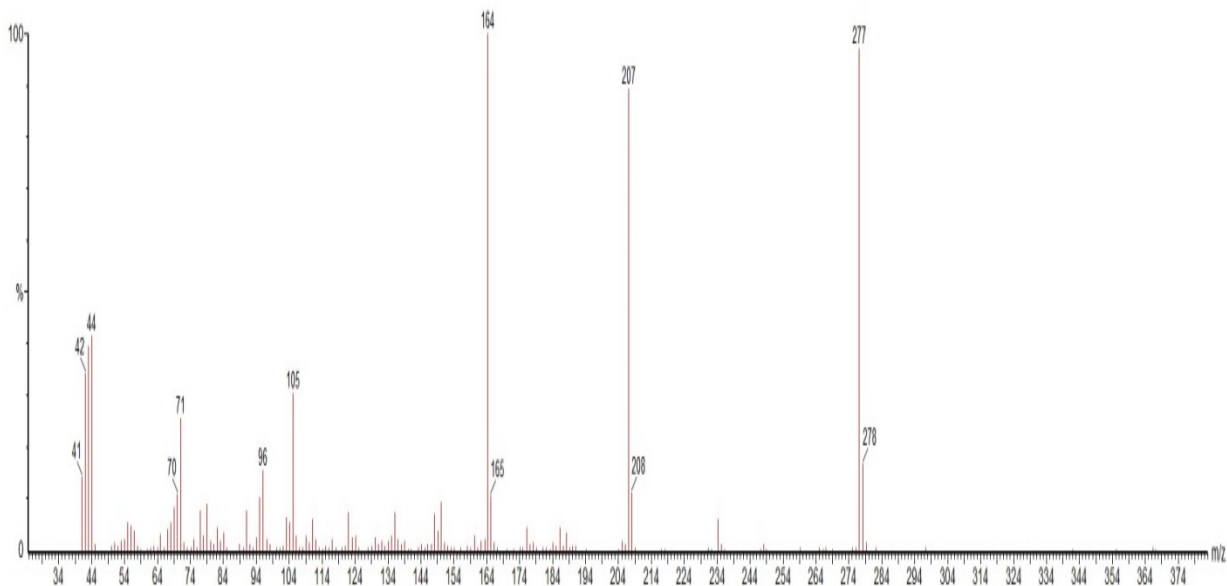


Figure 45: GC-EI MS spectrum for 10 PPM meta-fluorobutyryl fentanyl mass 368.

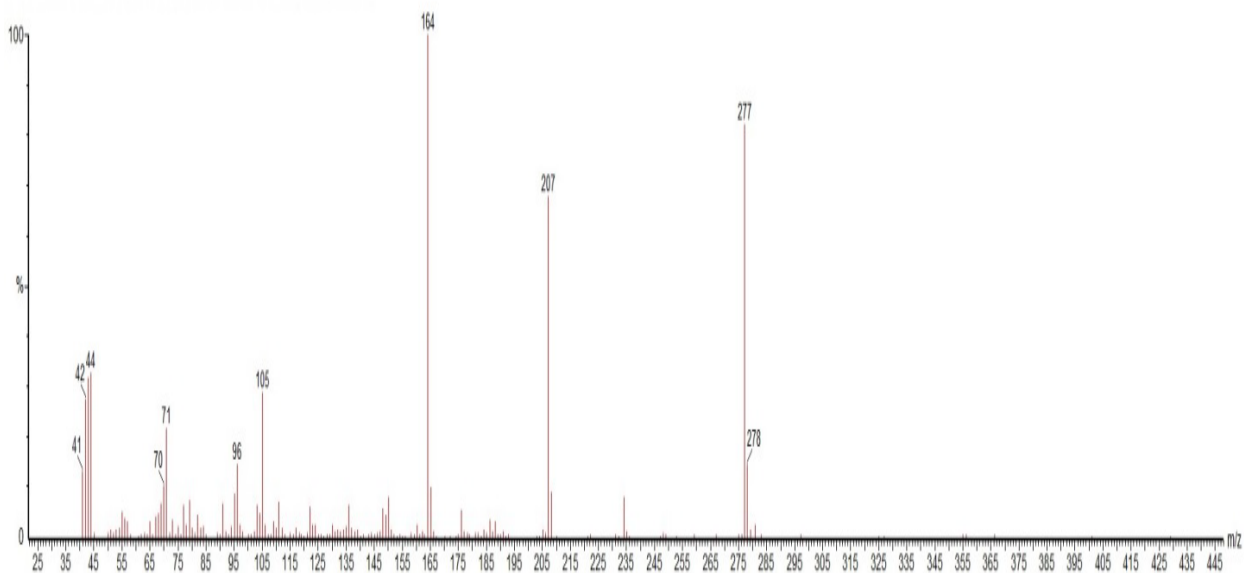


Figure 46: GC-EI MS spectrum for 10 PPM meta-fluorobutyryl fentanyl mass 368.

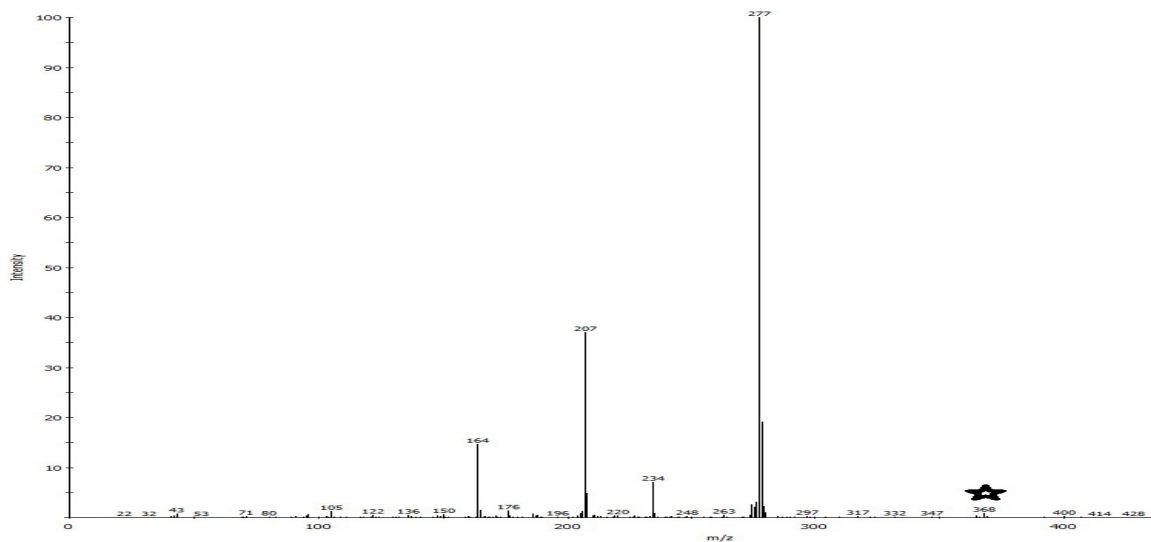


Figure 47: GC-cold EI MS spectrum for 10 PPM 4-fluoroisobutyryl fentanyl mass 368.

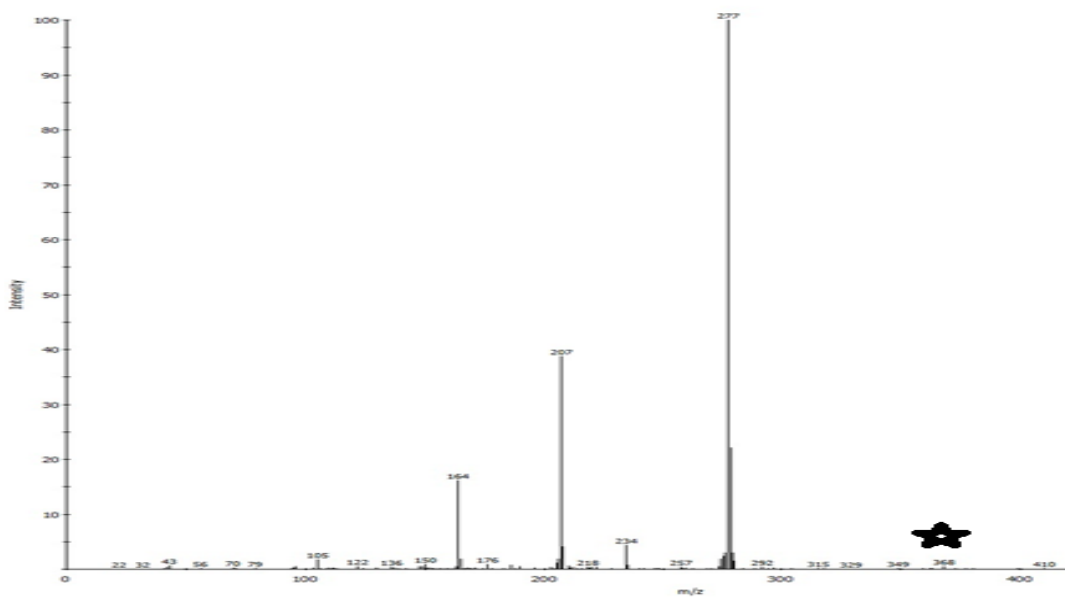


Figure 48: GC-cold EI MS spectrum for 10 PPM ortho-fluoroisobutyryl fentanyl mass 368.

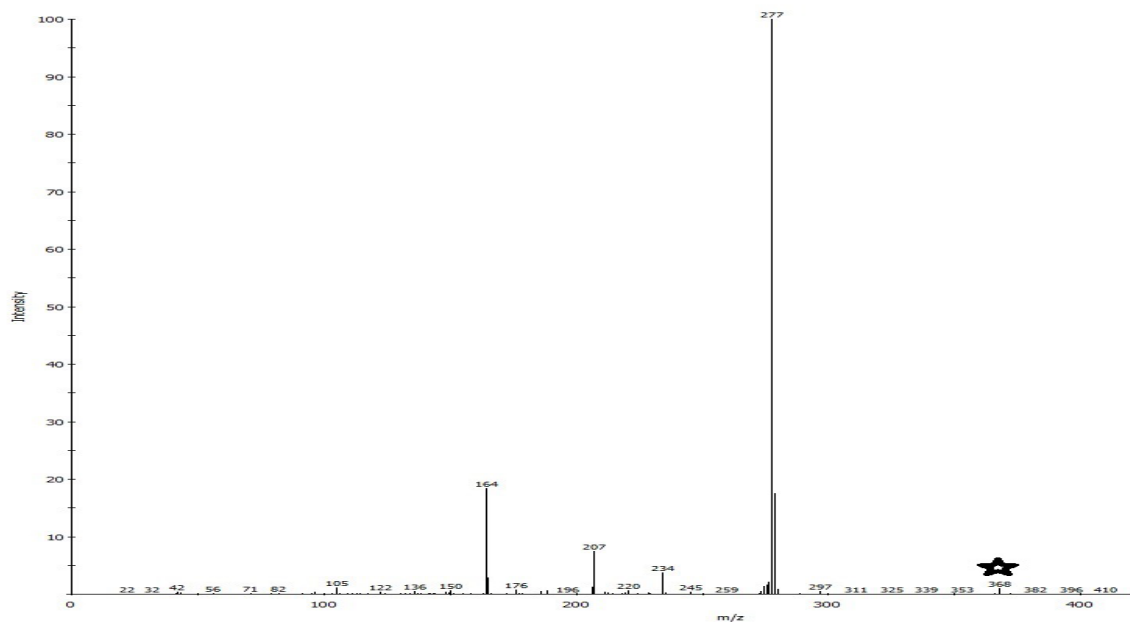


Figure 49: GC-cold EI MS spectrum for 10 PPM ortho-fluorobutyryl fentanyl mass 368.

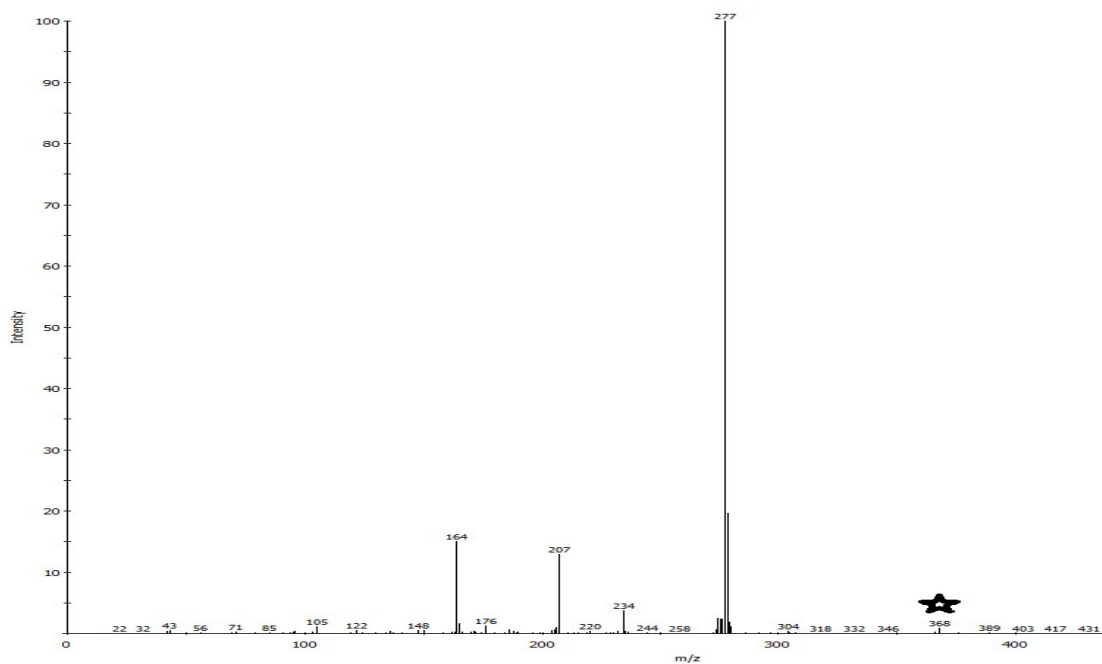


Figure 50: GC-cold EI MS spectrum for 10 PPM meta-fluorobutyryl fentanyl mass 368.

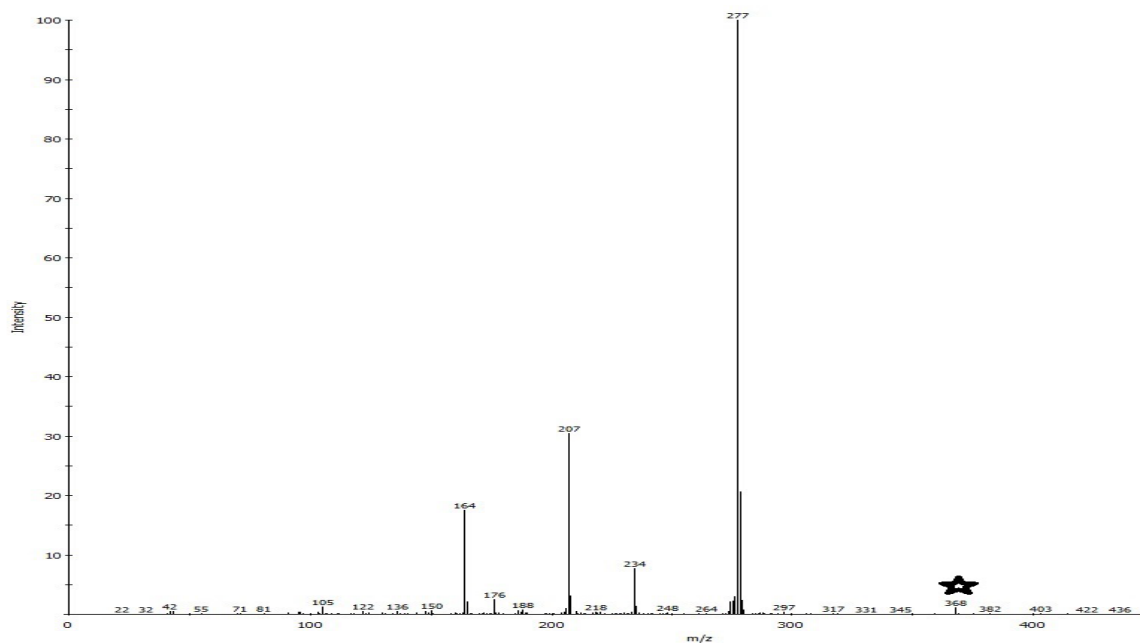


Figure 51: GC-cold EI MS spectrum for 10 PPM para-fluorobutyryl fentanyl mass 368.

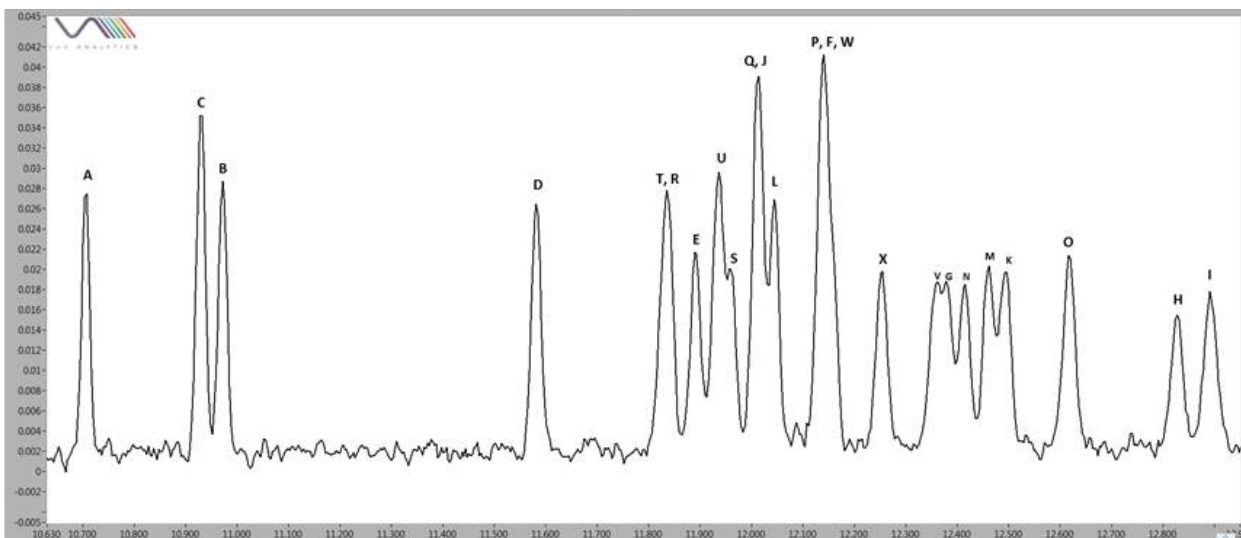


Figure 52: GC-VUV chromatogram of all fentanyl analogues. 10 PPM each compound. See Table 1 for compound identification.

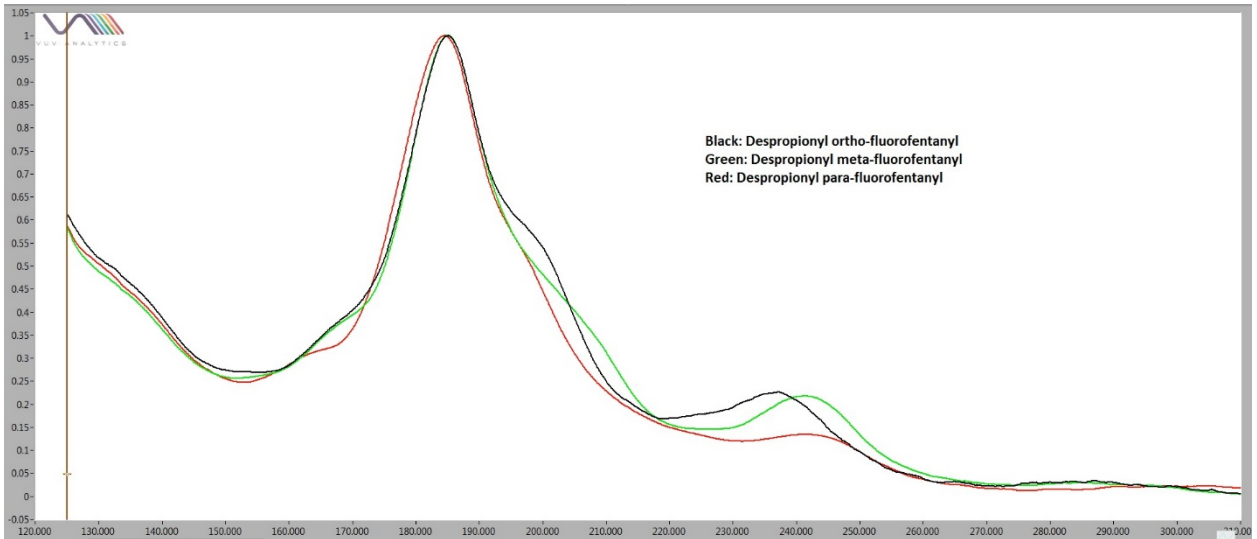


Figure 53: Overlay of GC-VUV spectra for mass 298 positional isomers. 50 PPM each compound.

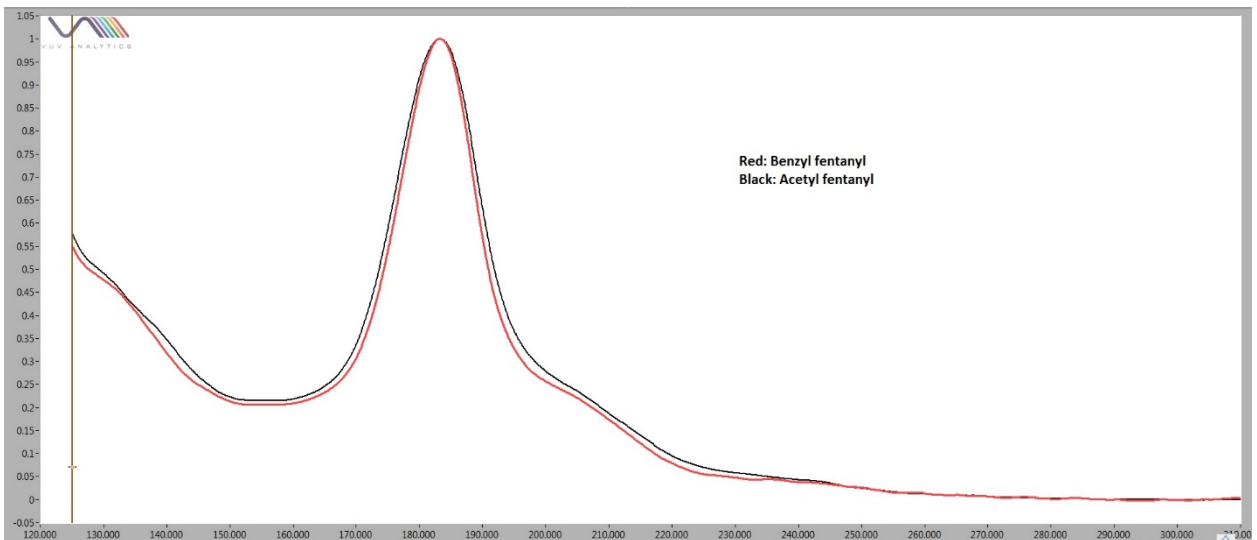


Figure 54: Overlay of GC-VUV spectra for mass 322 positional isomers. 50 PPM each compound.

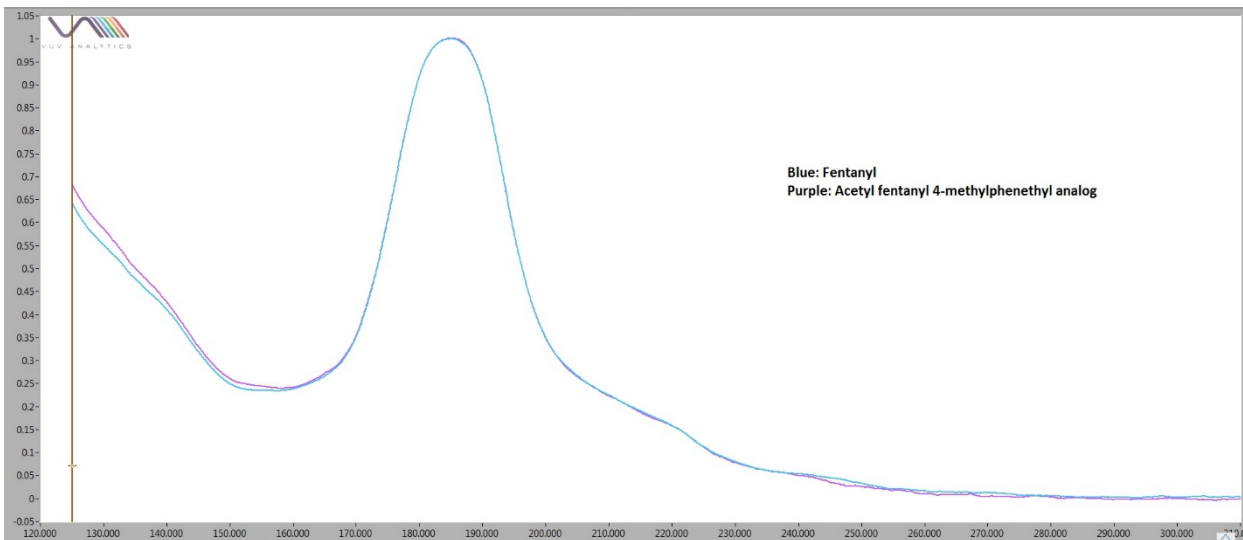


Figure 55: Overlay of GC-VUV spectra for mass 336 positional isomers. 50 PPM each compound.

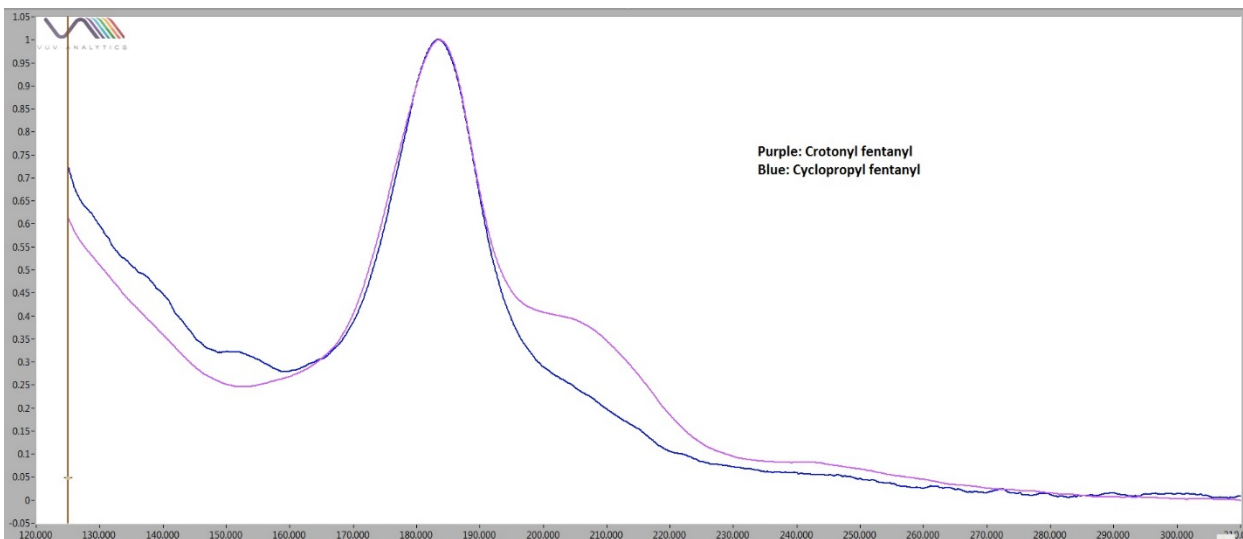


Figure 56: Overlay of GC-VUV spectra for mass 348 positional isomers. 50 PPM each compound.

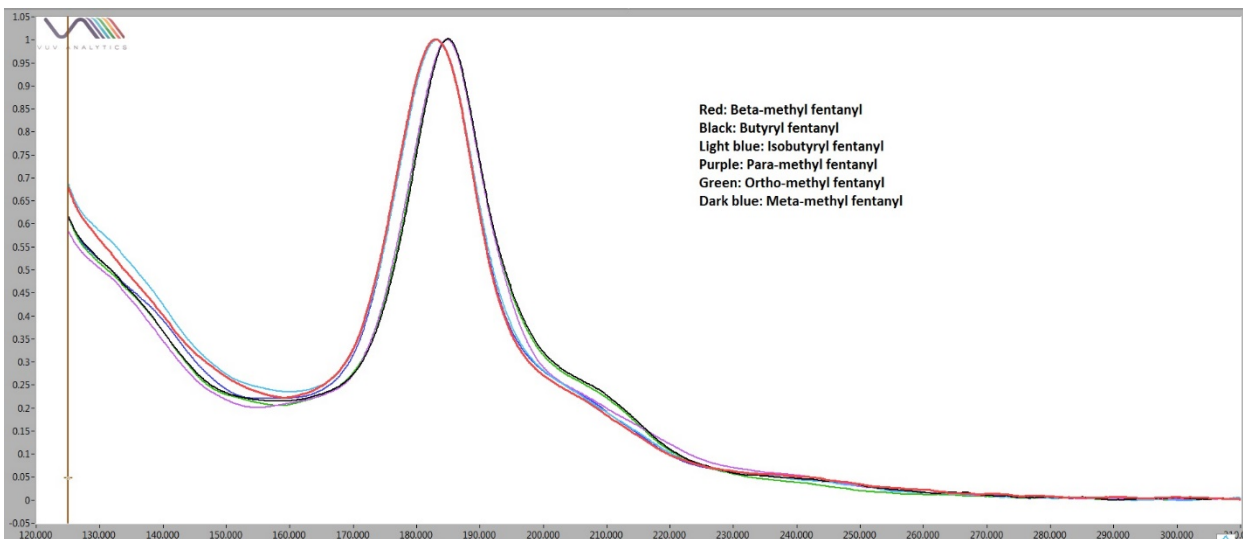


Figure 57: Overlay of GC-VUV spectra for mass 350 positional isomers. 50 PPM each compound.

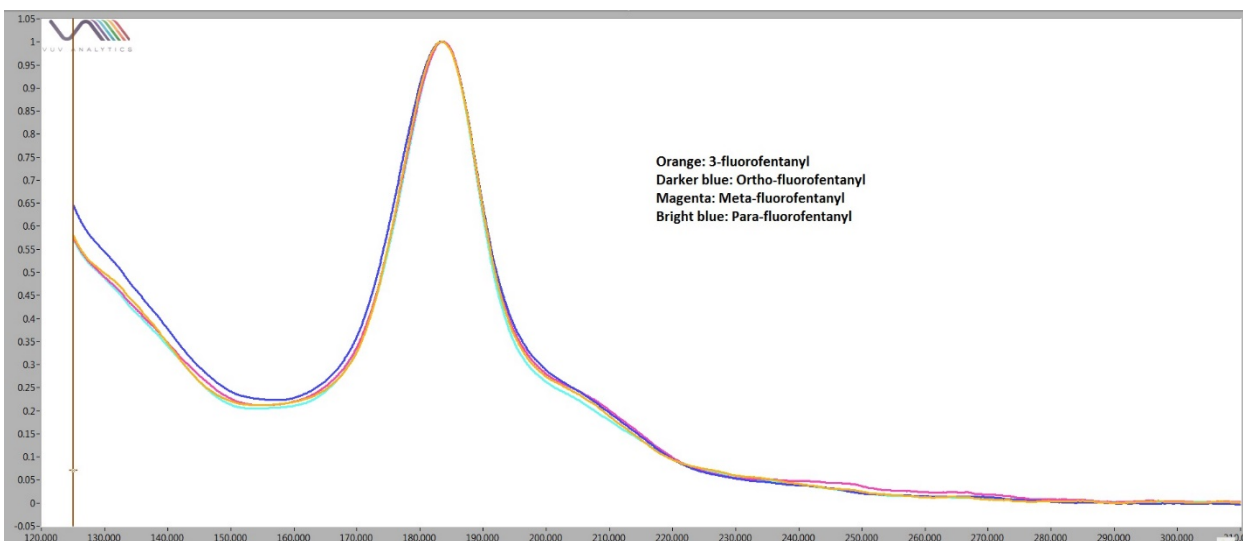


Figure 58: Overlay of GC-VUV spectra for mass 354 positional isomers. 50 PPM each compound.

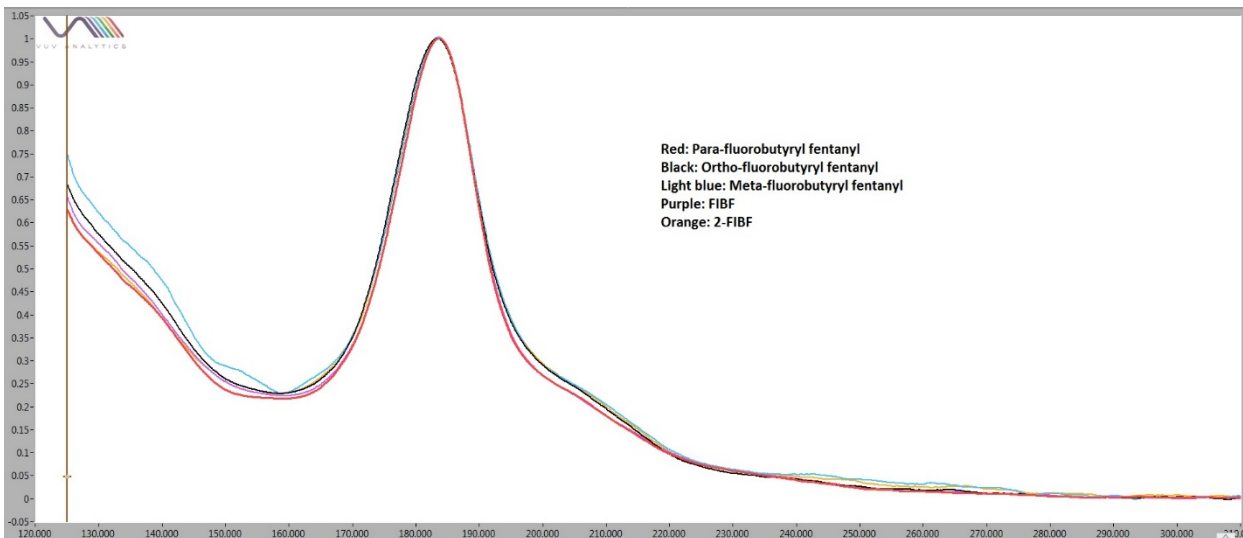


Figure 59: Overlay of GC-VUV spectra for mass 368 positional isomers. 50 PPM each compound.

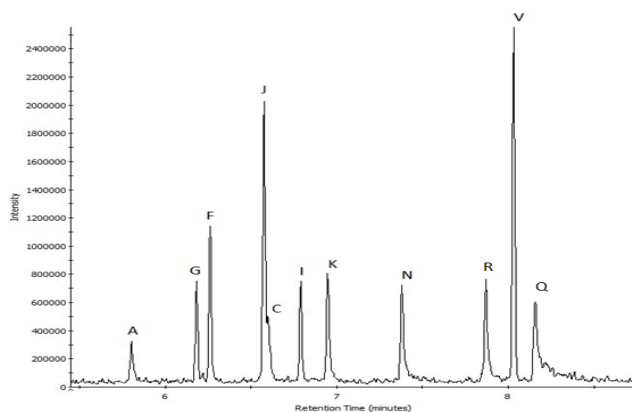


Figure 60: Cold GC-cold EI MS for a mixture of ten controlled synthetic cathinones and one non-controlled isomer. 100 ppm each compound, see Table 2 for analyte identification.

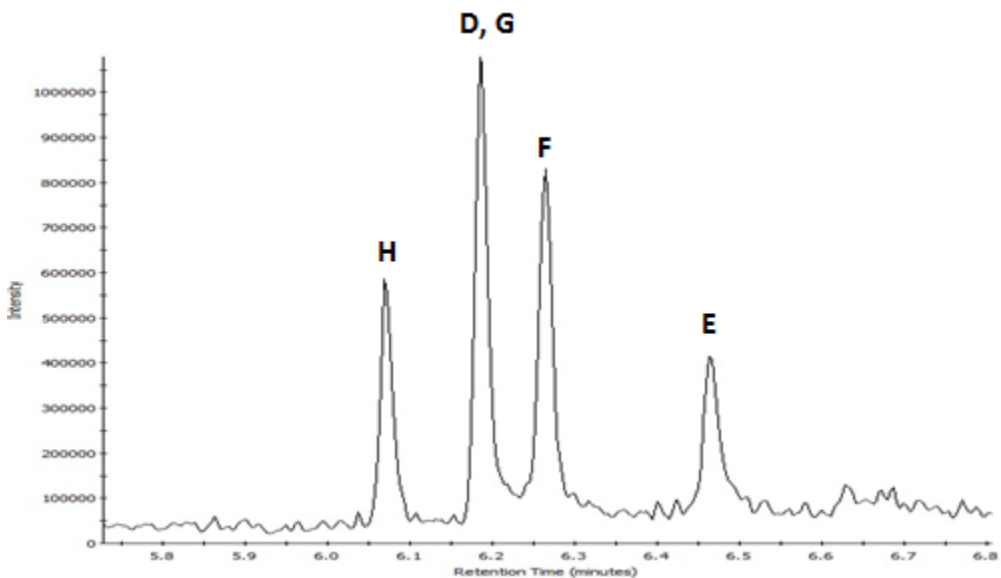


Figure 61: GC-cold EI MS chromatogram for a mixture of mass 177 positional isomers. 100 ppm each compound, see Table 2 for analyte identification.

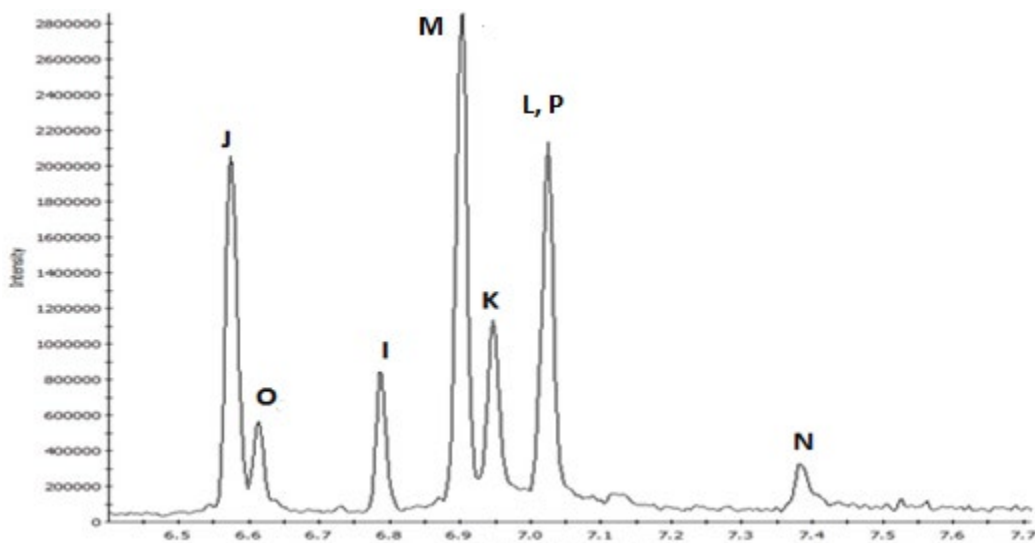


Figure 62: GC-cold EI MS chromatogram for a mixture of mass 191 positional isomers. 100 ppm each compound, see Table 2 for analyte identification.

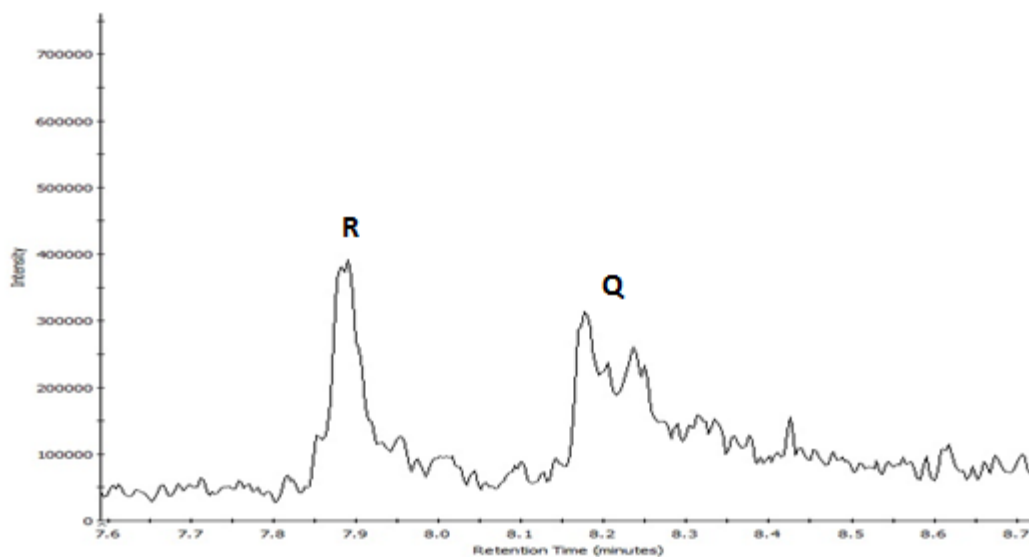


Figure 63: GC-cold EI MS chromatogram for a mixture of mass 207 positional isomers. 100 ppm each compound, see Table 2 for analyte identification.

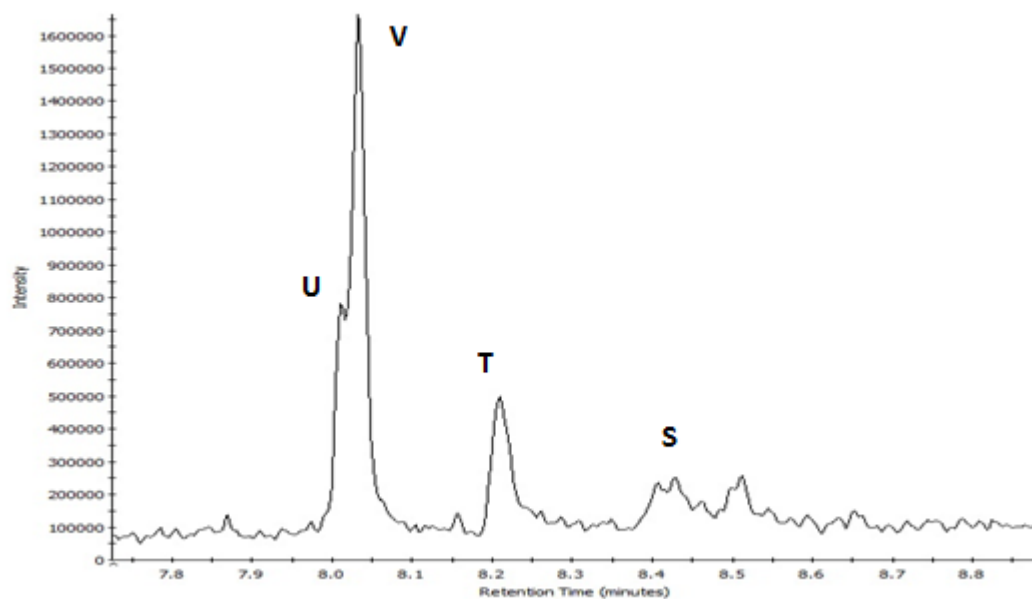


Figure 64: GC-cold EI MS chromatogram for a mixture of mass 217 positional isomers. 100 ppm each compound, see Table 2 for analyte identification.

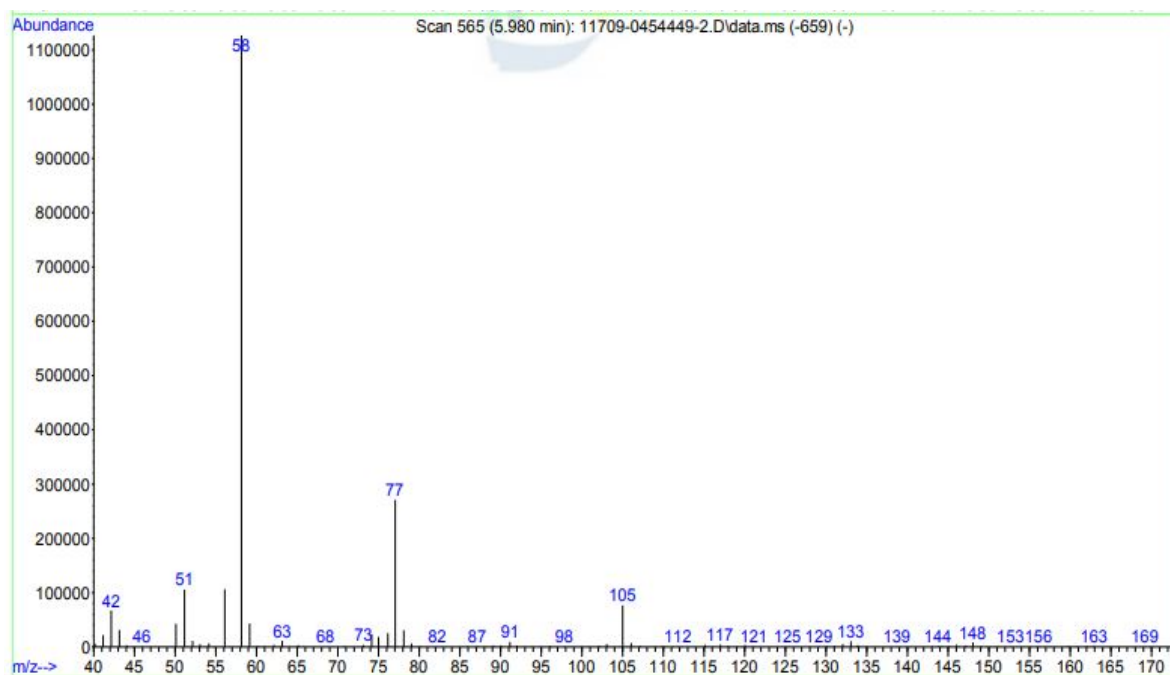


Figure 65: GC-EI MS spectrum for methcathinone mass 163.

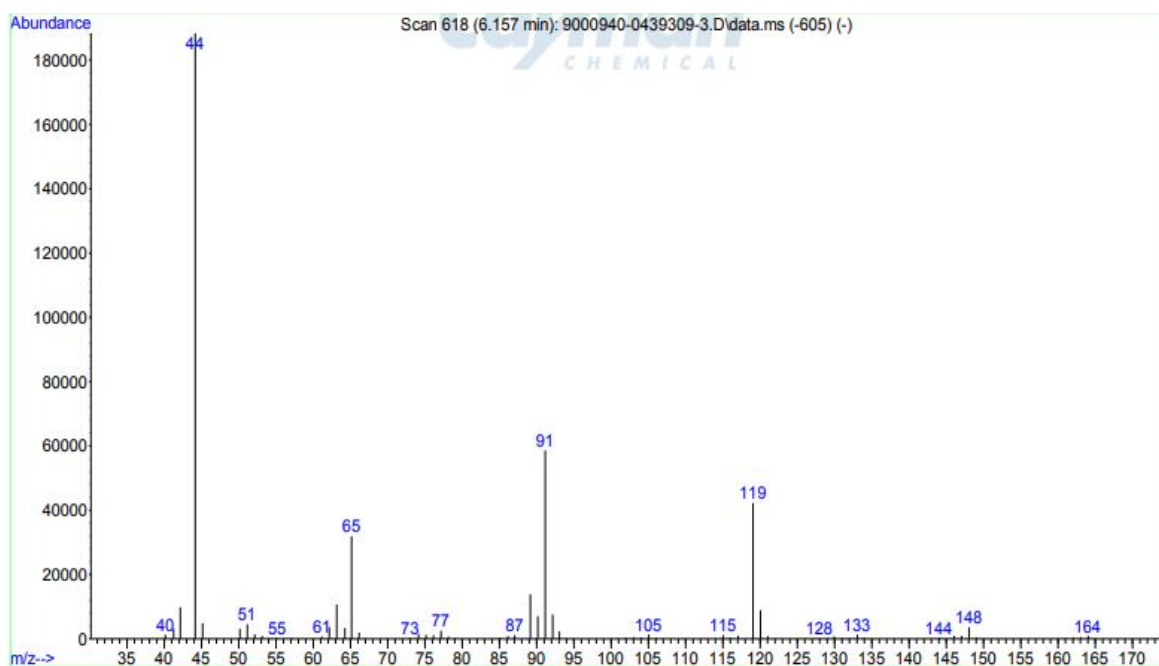


Figure 66: GC-EI MS spectrum for nor-mephedrone mass 163.

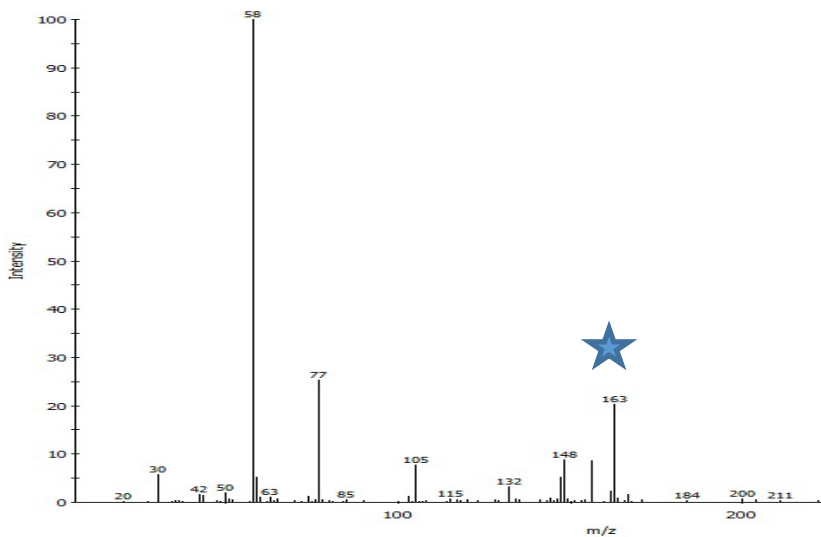


Figure 67: GC-cold EI MS spectrum for 100 PPM methcathinone mass 163.

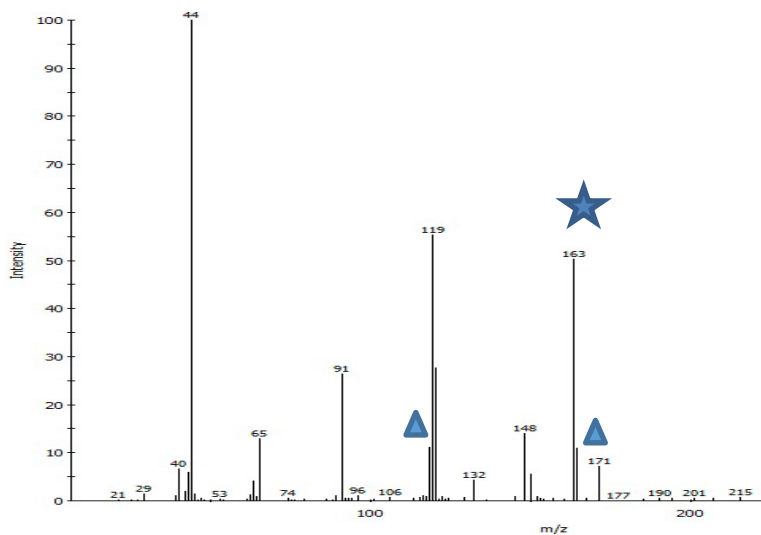


Figure 68: GC-cold EI MS spectrum for 100 PPM nor-mephedrone mass 163. The triangle indicates a fragment found in the background that could not be subtracted.

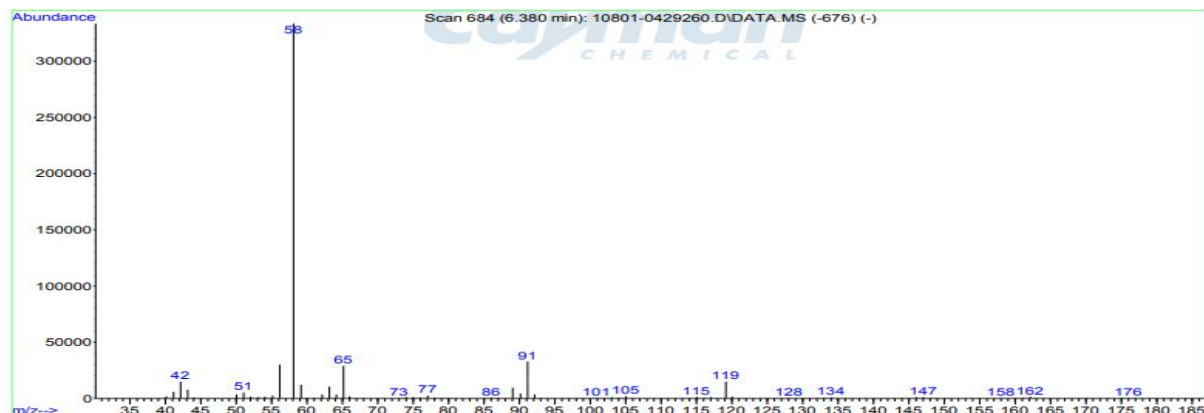


Figure 69: GC-EI MS spectrum for mephedrone mass 177.

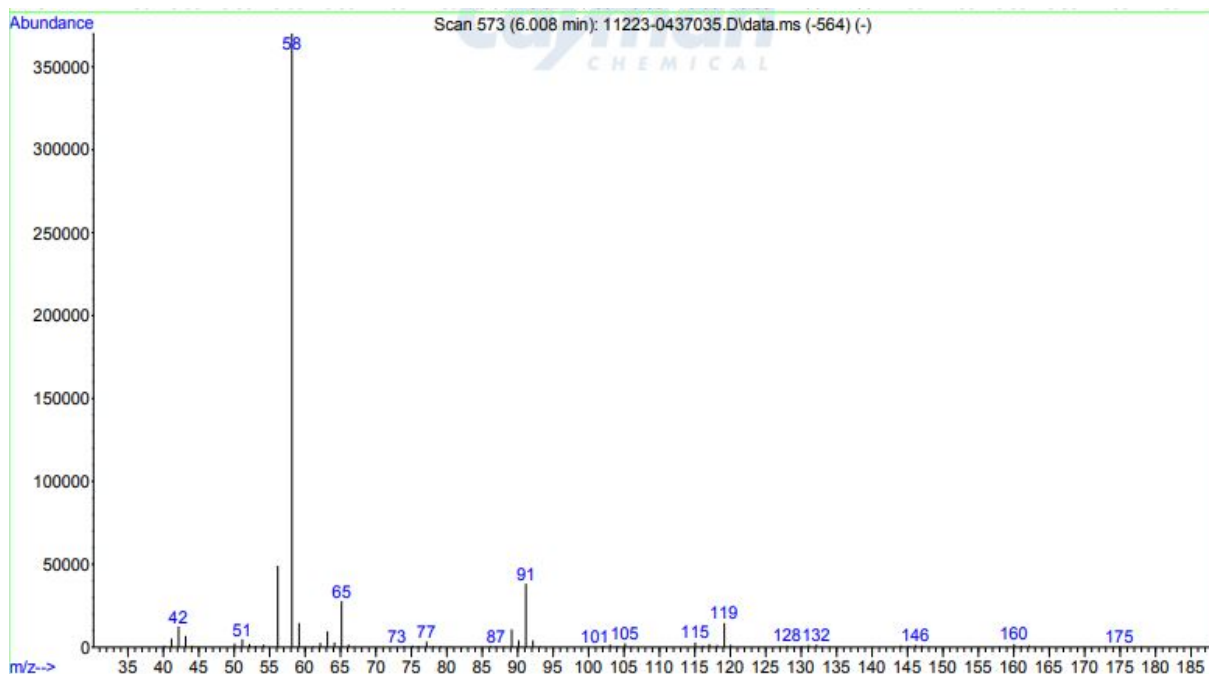


Figure 70: GC-EI MS spectrum for 2-methylmethcathinone mass 177.

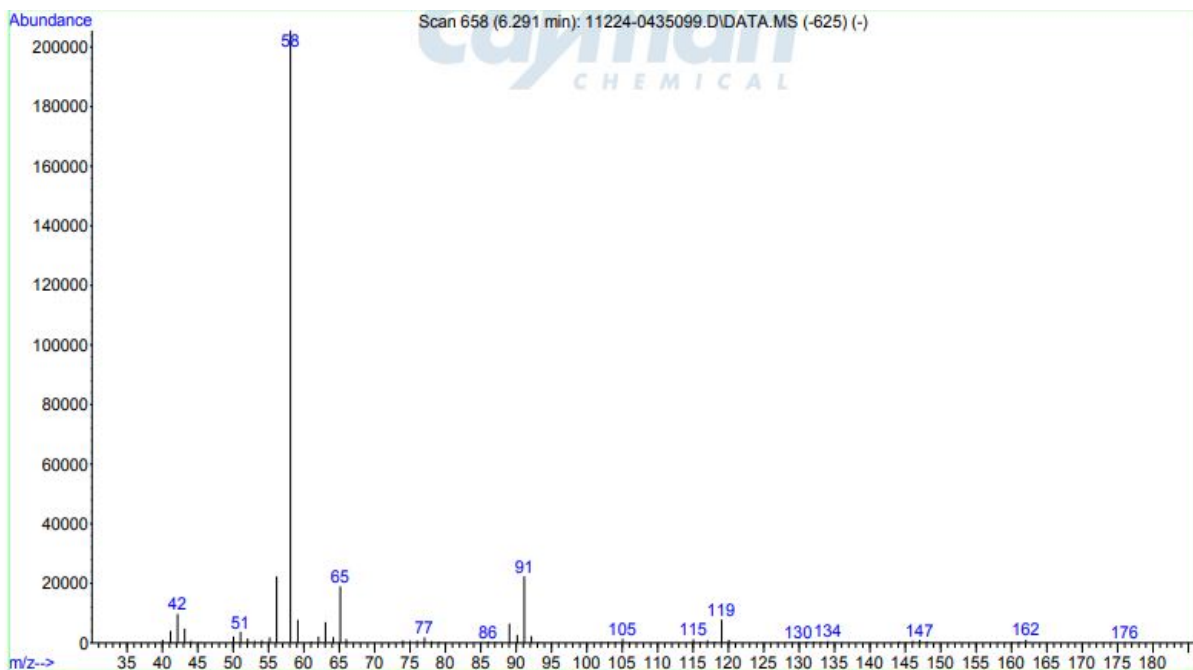


Figure 71: GC-EI MS spectrum for 3-methylmethcathinone mass 177.

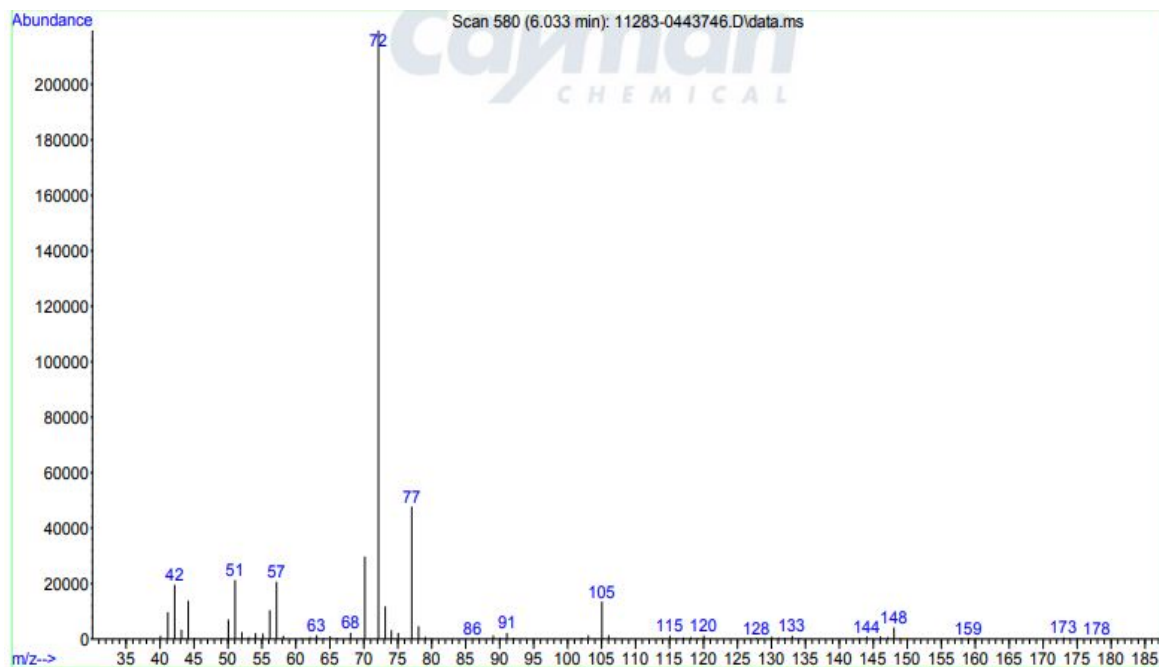


Figure 72: GC-EI MS spectrum for buphedrone mass 177.

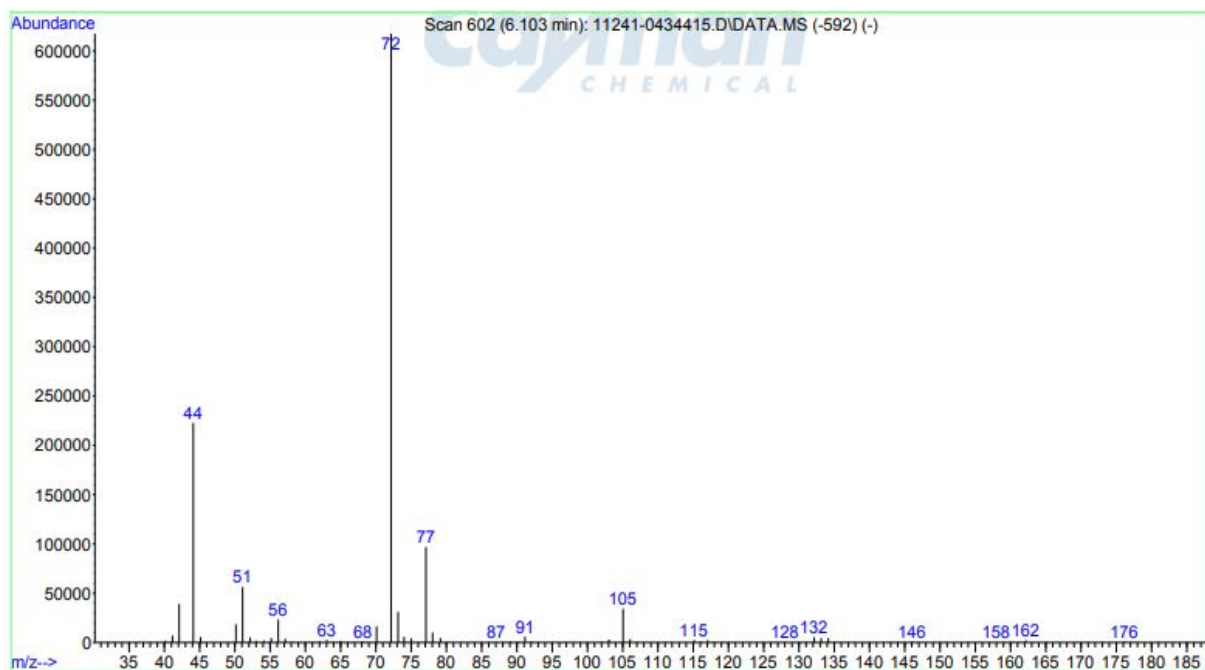


Figure 73: GC-EI MS spectrum for ethcathinone mass 177.

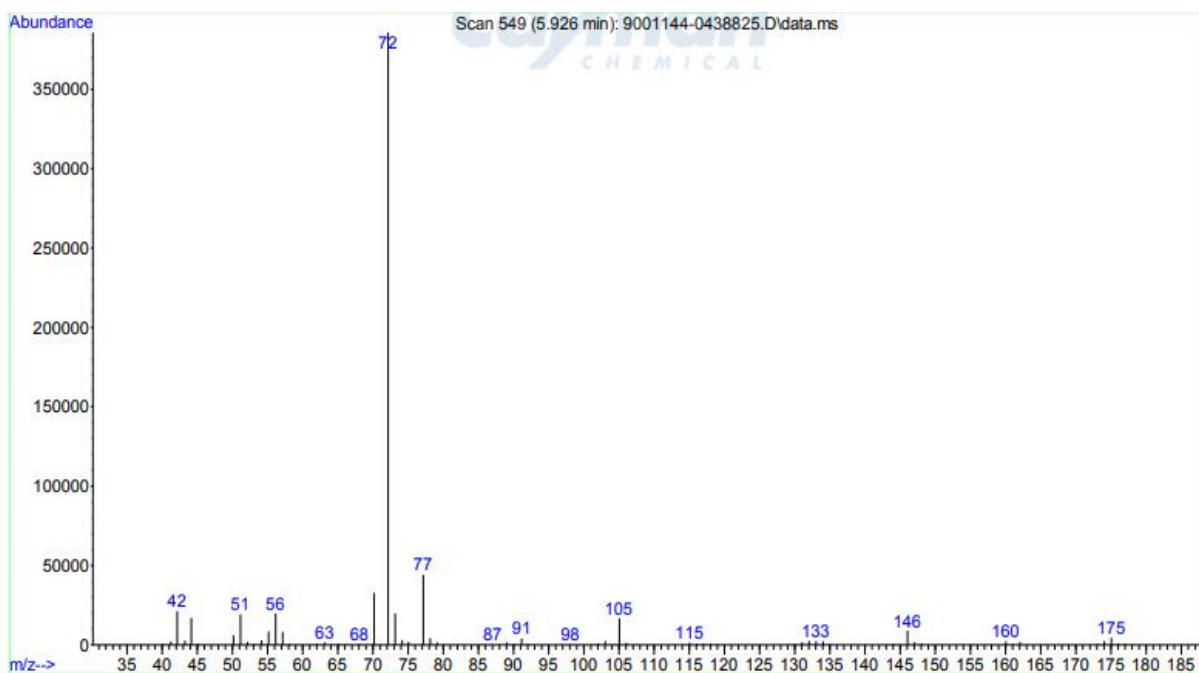


Figure 74: GC-EI MS spectrum for N,N-dimethylmethcathinone mass 177.

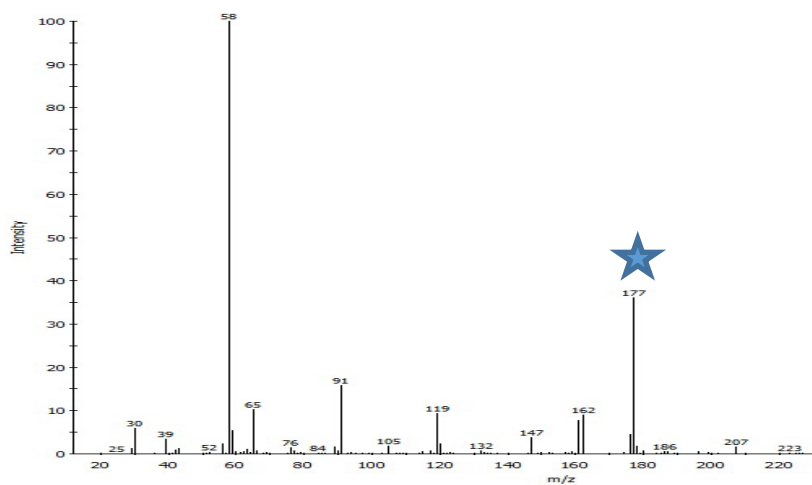


Figure 75: GC-cold EI MS spectrum for 100 PPM mephedrone mass 177.

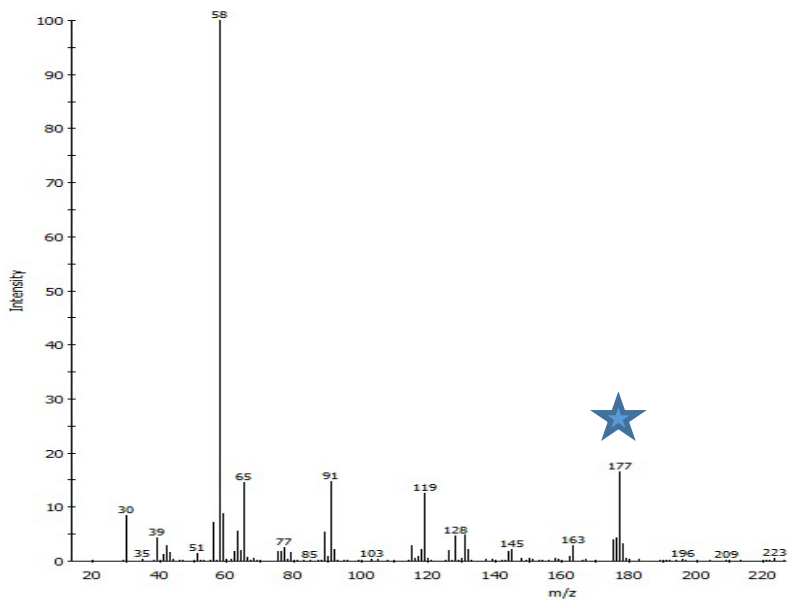


Figure 76: GC-cold EI MS spectrum for 100 PPM 2-methylmethcathinone mass 177.

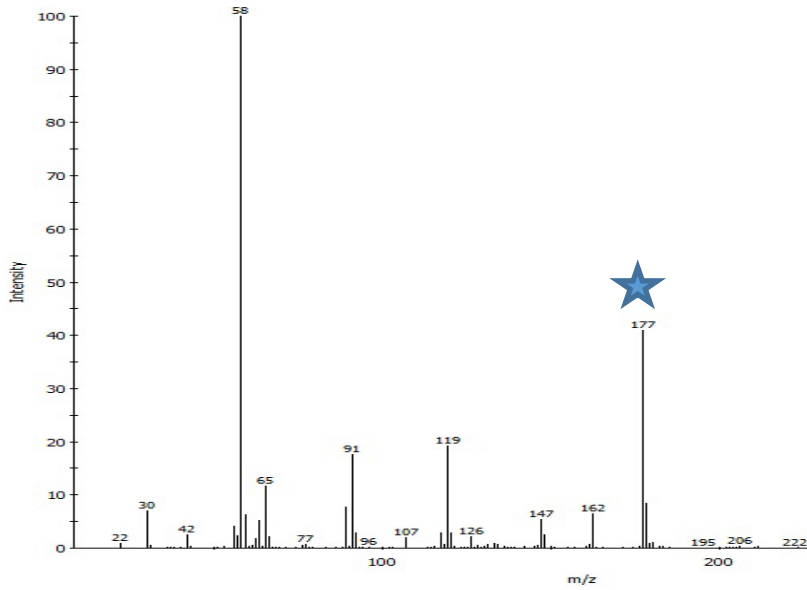


Figure 77: GC-cold EI MS spectrum for 100 PPM 3-methylmethcathinone mass 177.

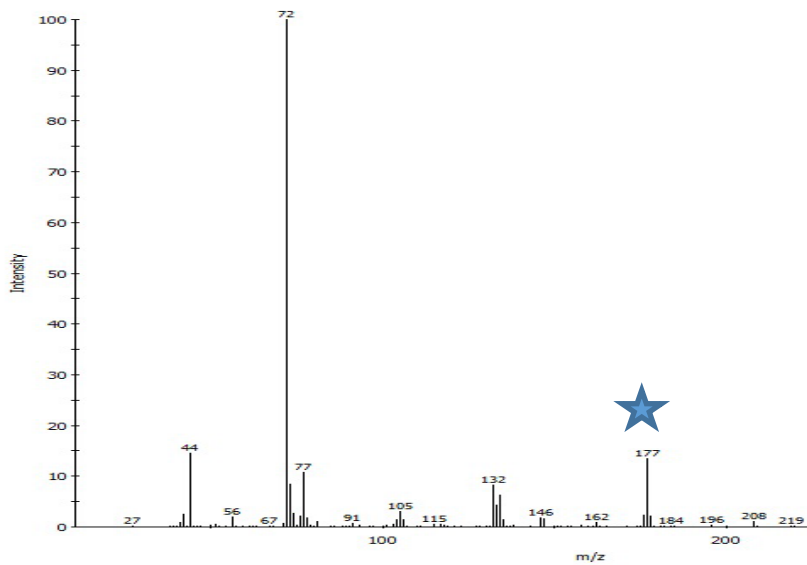


Figure 78: GC-cold EI MS spectrum for 100 PPM buphedrone mass 177.

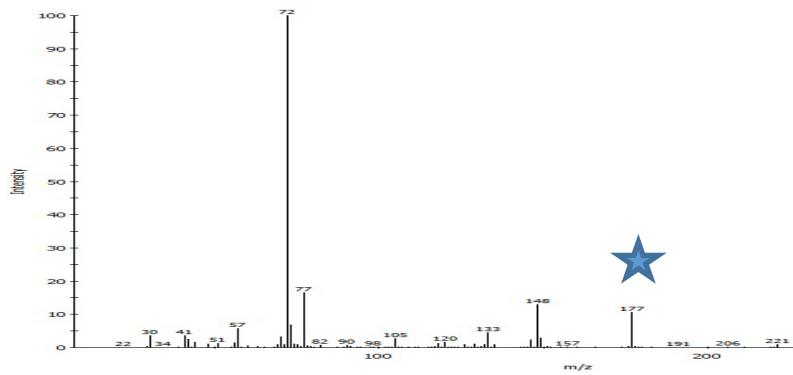


Figure 79: GC-cold EI MS spectrum for 100 PPM ethcathinone mass 177.

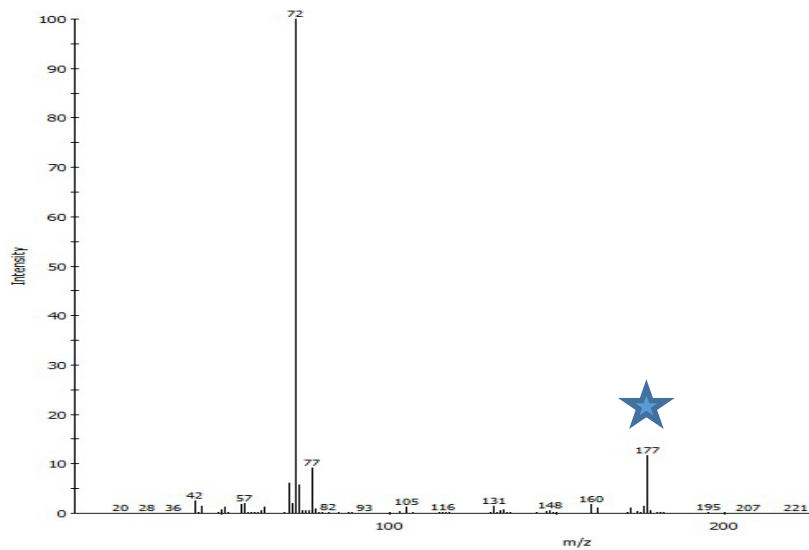


Figure 80: GC-cold EI MS spectrum for 100 PPM N,N-dimethylmethcathinone mass 177.

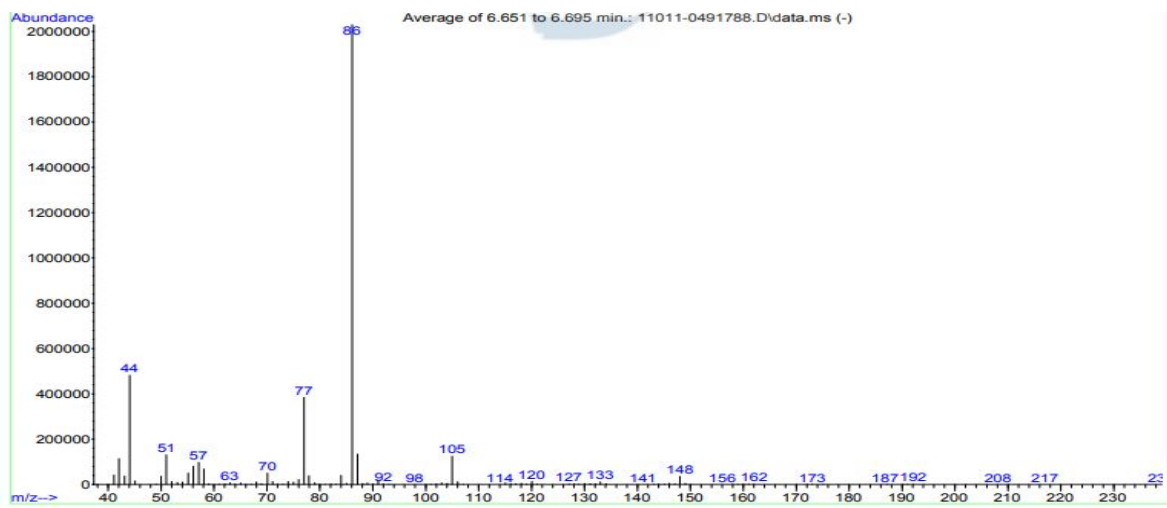


Figure 81: GC-EI MS spectrum for pentedrone mass 191.

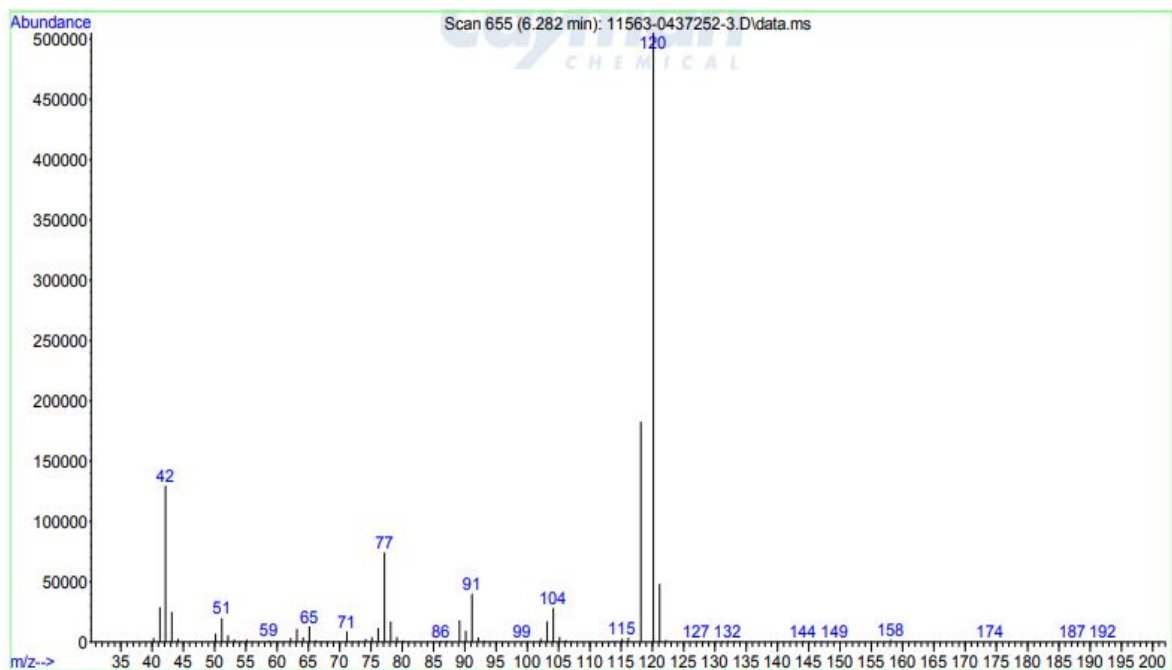


Figure 82: GC-EI MS spectrum for isopentedrone mass 191.

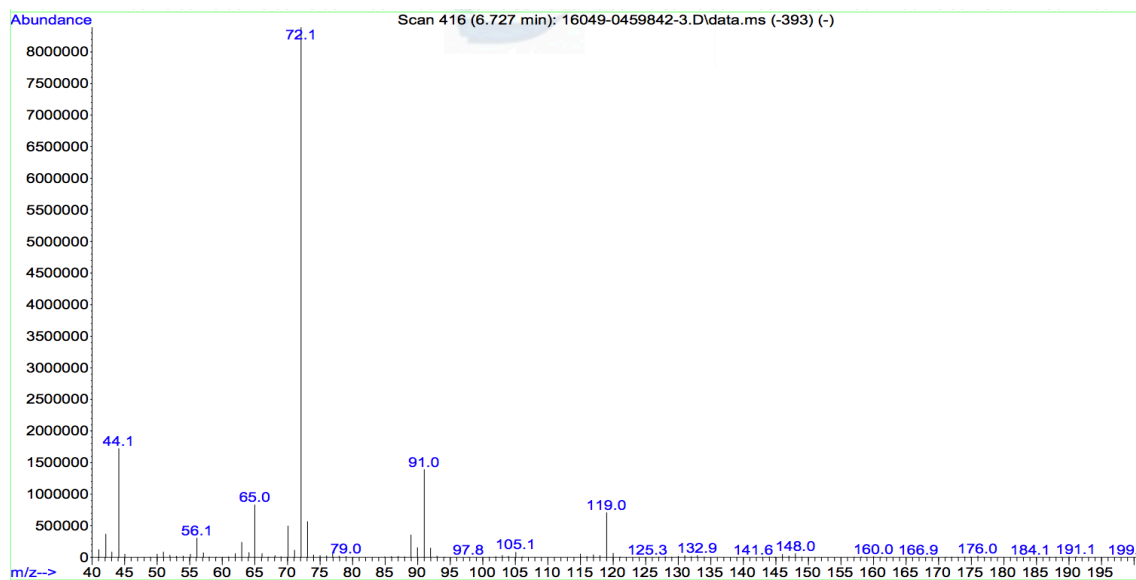


Figure 83: GC-EI MS spectrum for 4-methylethcathinone mass 191.

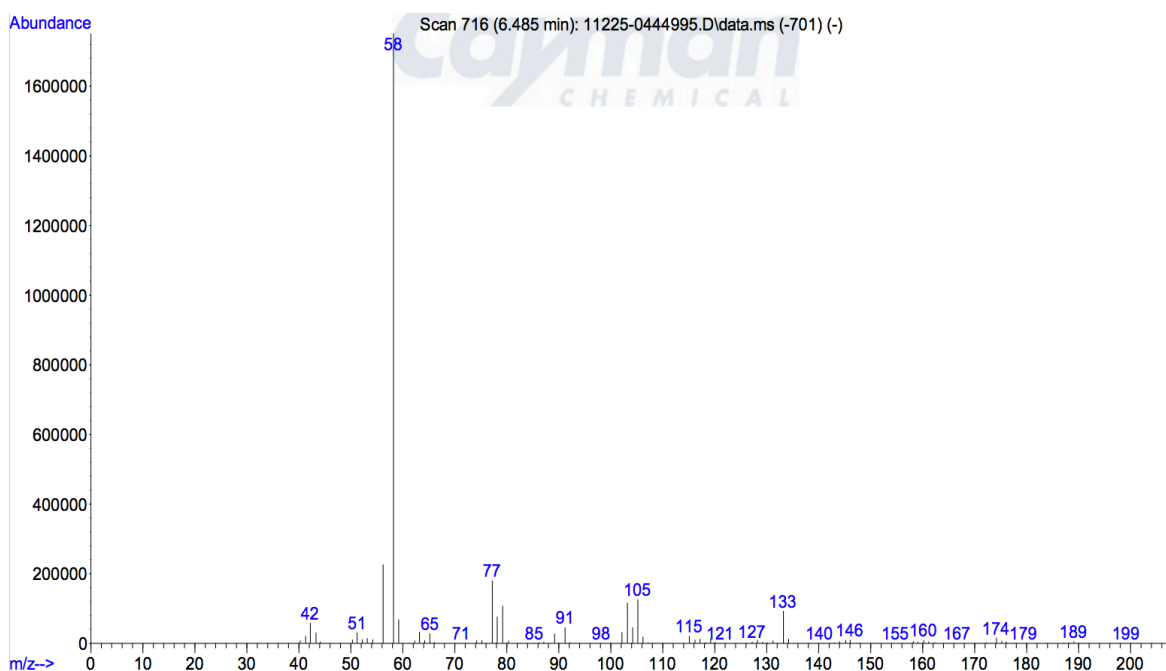


Figure 84: GC-EI MS spectrum for 2,3-dimethylmethcathinone mass 191.

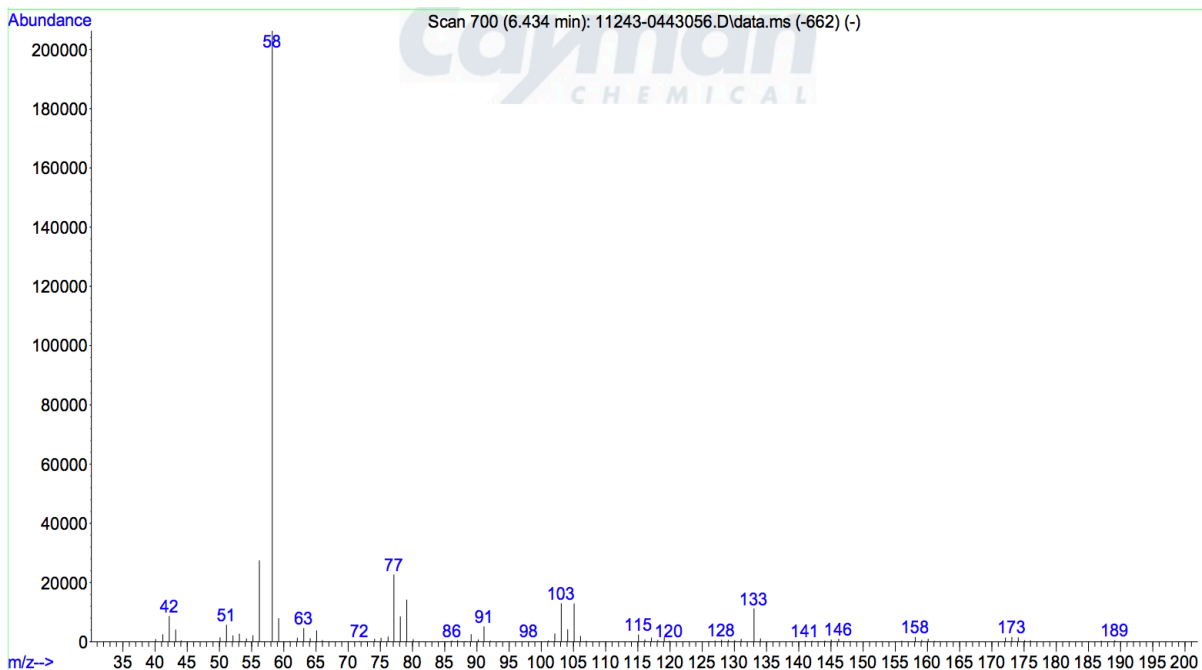


Figure 85: GC-EI MS spectrum for 2,4-dimethylmethcathinone mass 191.

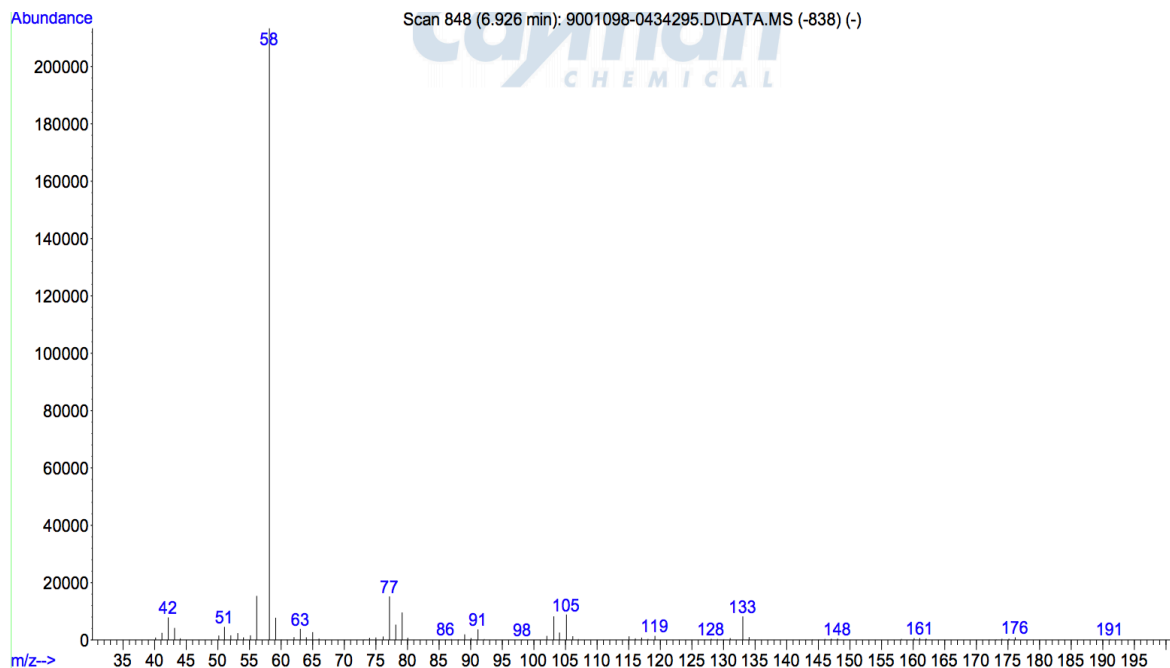


Figure 86: GC-EI MS spectrum for 3,4-dimethylmethcathinone mass 191.

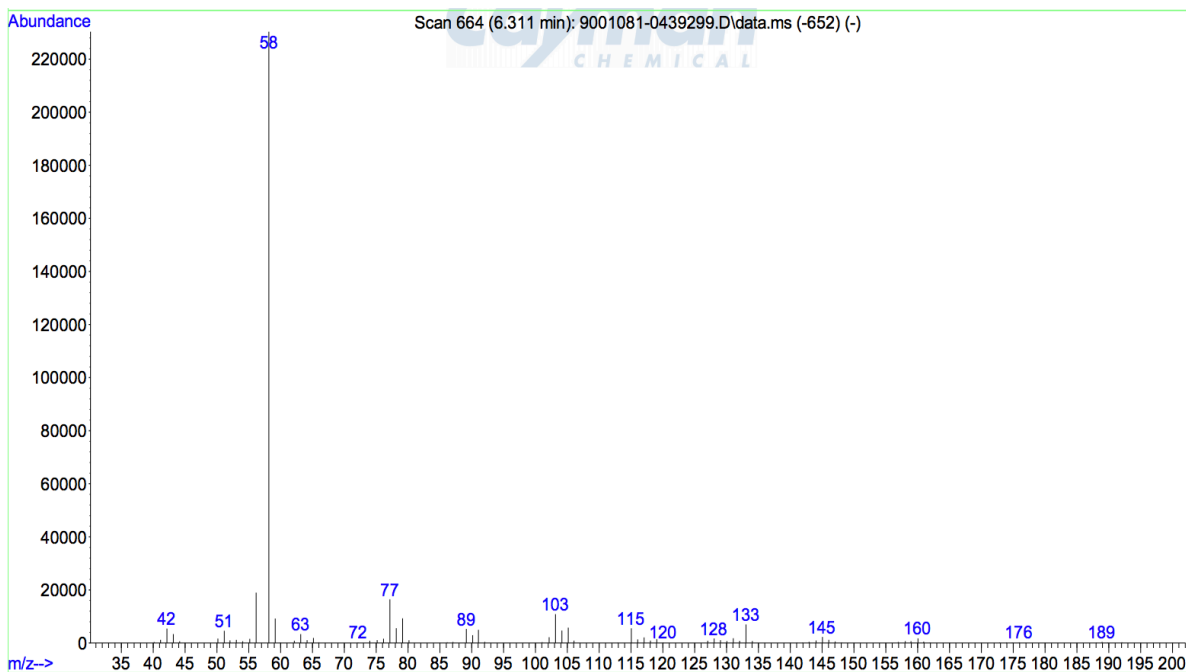


Figure 87: GC-EI MS spectrum for 2-ethylmethcathinone mass 191.

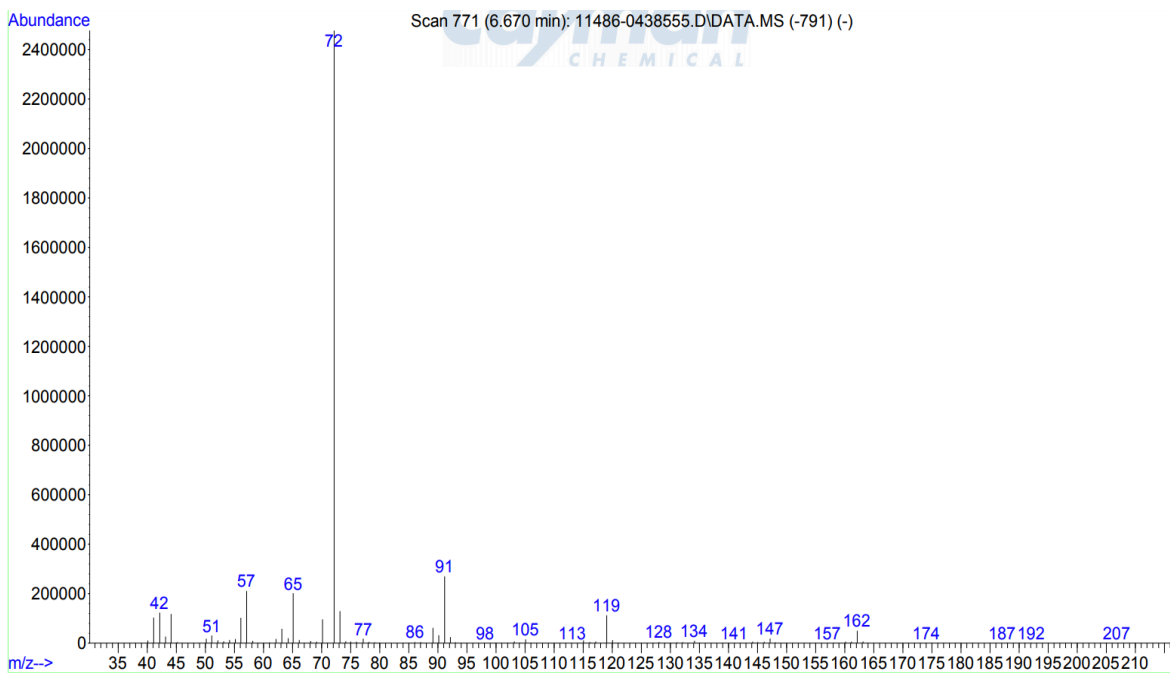


Figure 88: GC-EI MS spectrum for 4-methylbuphedrone mass 191.

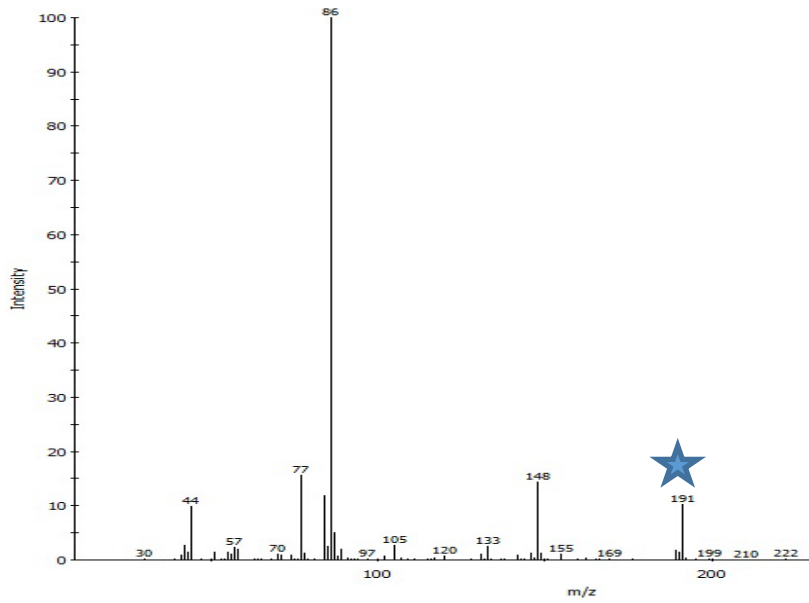


Figure 89: GC-cold EI MS spectrum for 100 PPM pentedrone mass 191.

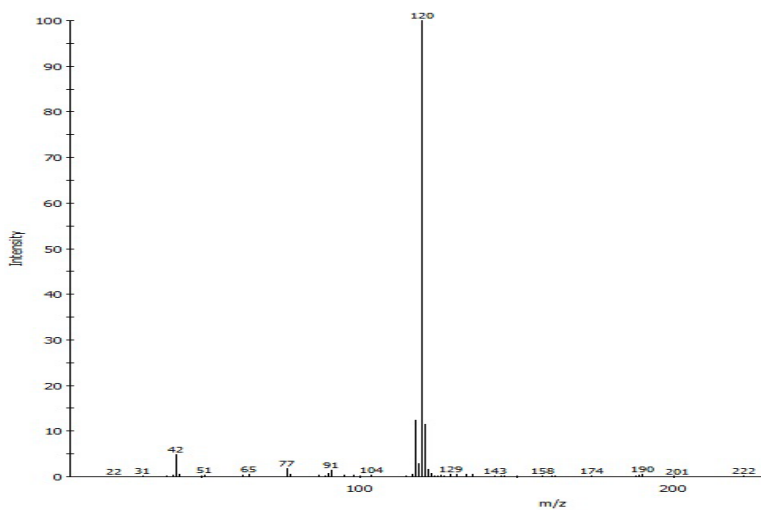


Figure 90: GC-cold EI MS spectrum for 100 PPM isopentedrone mass 191.

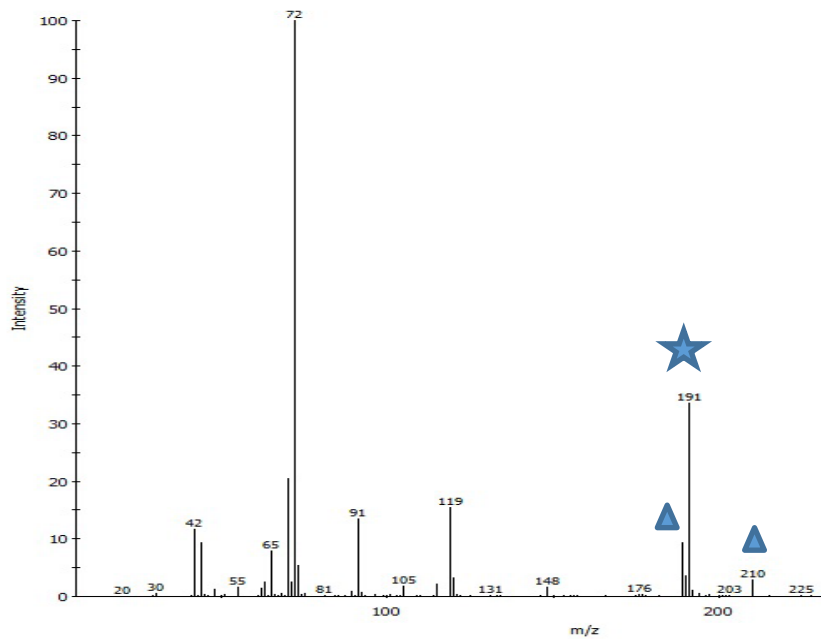


Figure 91: GC-cold EI MS spectrum for 100 PPM 4-methylethcathinone mass 191. The triangle indicates a fragment found in the background that could not be subtracted

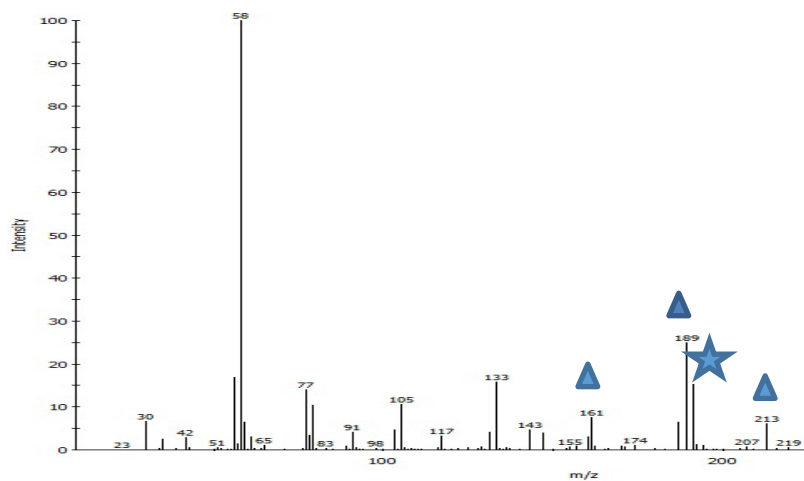


Figure 92: GC-cold EI MS spectrum for 100 PPM 2,3-dimethylmethcathinone mass 191. The triangle indicates a fragment found in the background that could not be subtracted

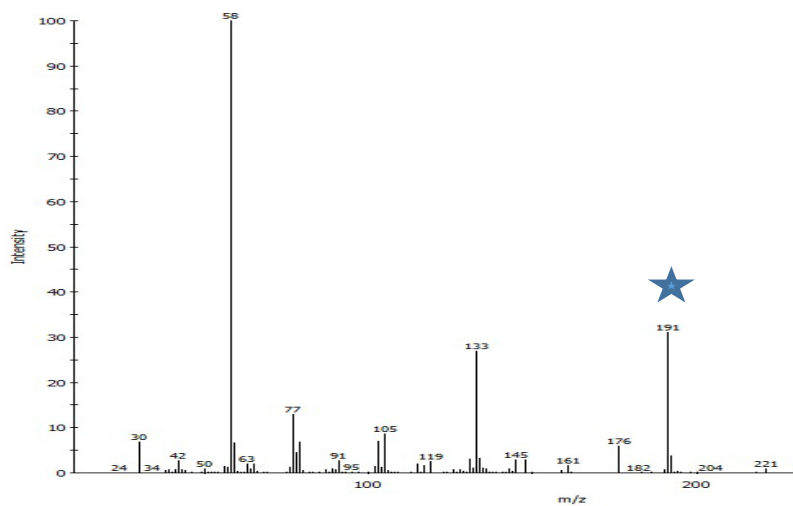


Figure 93: GC-cold EI MS spectrum for 100 PPM 2,4-dimethylmethcathinone mass 191.

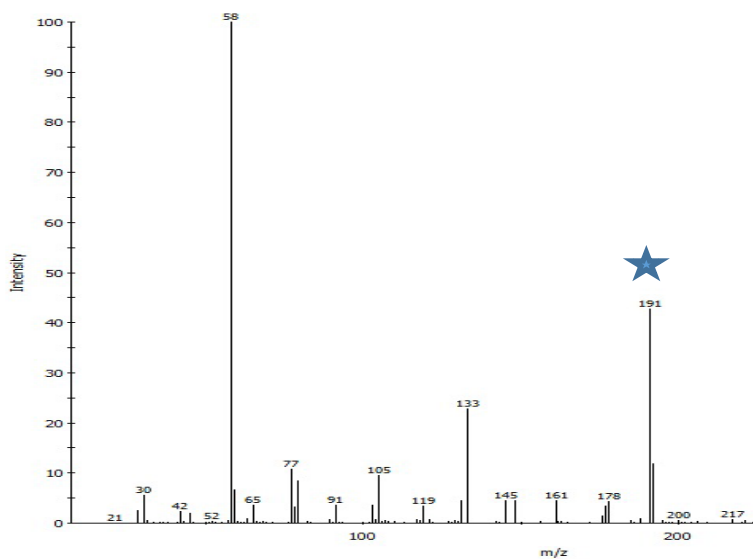


Figure 94: GC-cold EI MS spectrum for 100 PPM 3,4-dimethylmethcathinone mass 191.

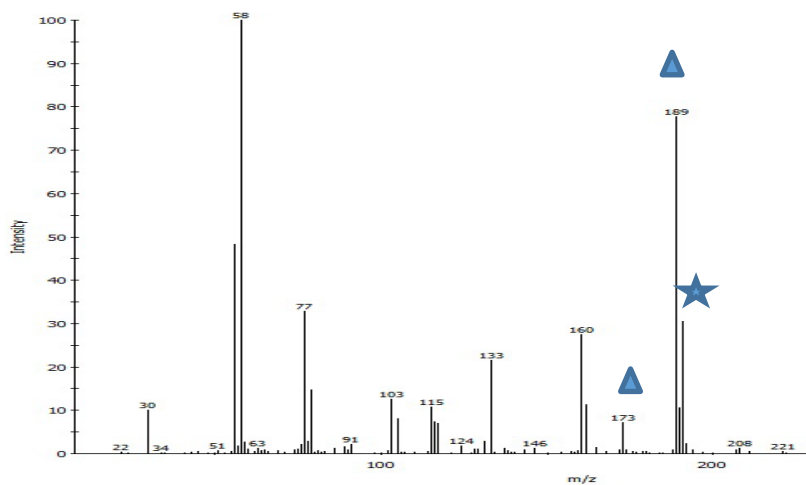


Figure 95: GC-cold EI MS spectrum for 100 PPM 2-ethylmethcathinone mass 191. The triangle indicates a fragment found in the background that could not be subtracted

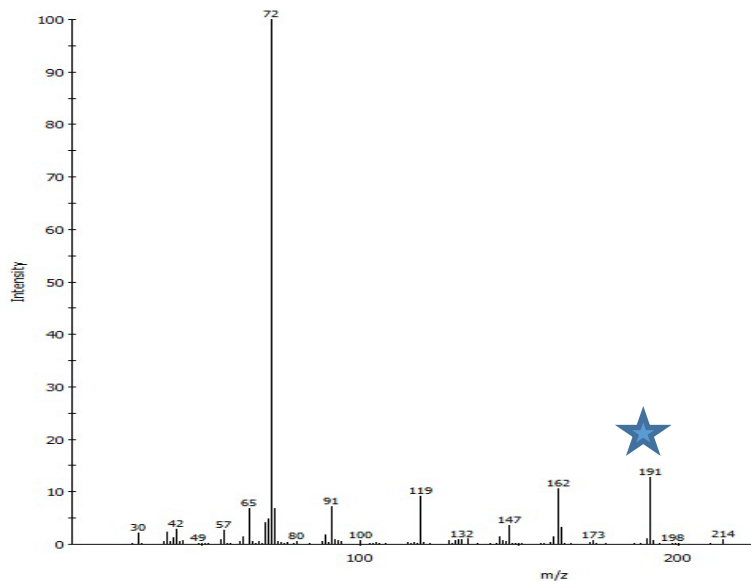


Figure 96: GC-cold EI MS spectrum for 100 PPM 4-methylbuphedrone mass 191.

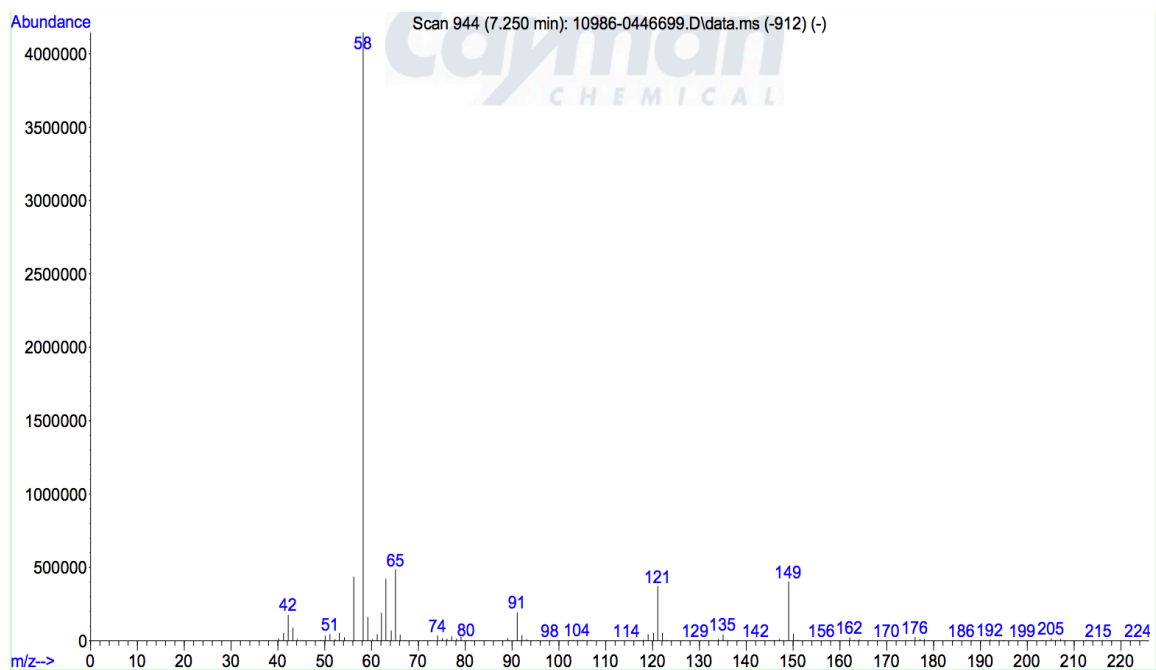


Figure 97: GC-EI MS spectrum for methylone mass 207.

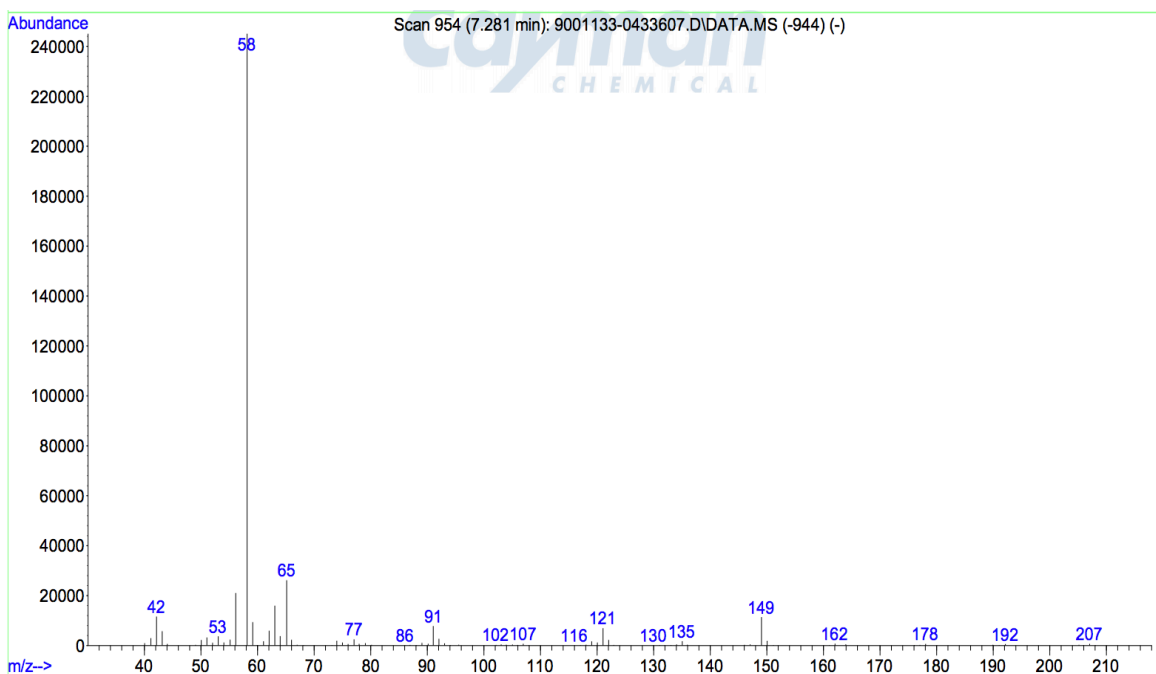


Figure 98: GC-EI MS spectrum for 2,3-methylenedioxy methcathinone mass 207.

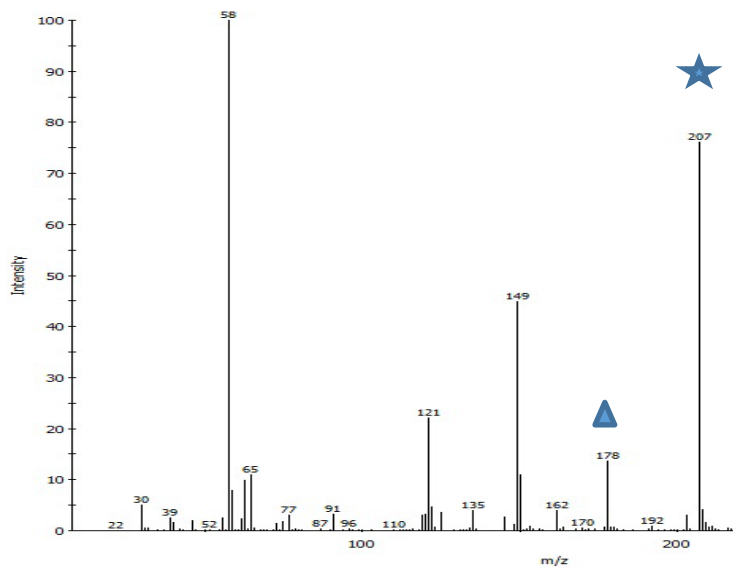


Figure 99: GC-cold EI MS spectrum for 100 PPM methylone mass 207. The triangle indicates a fragment found in the background that could not be subtracted.

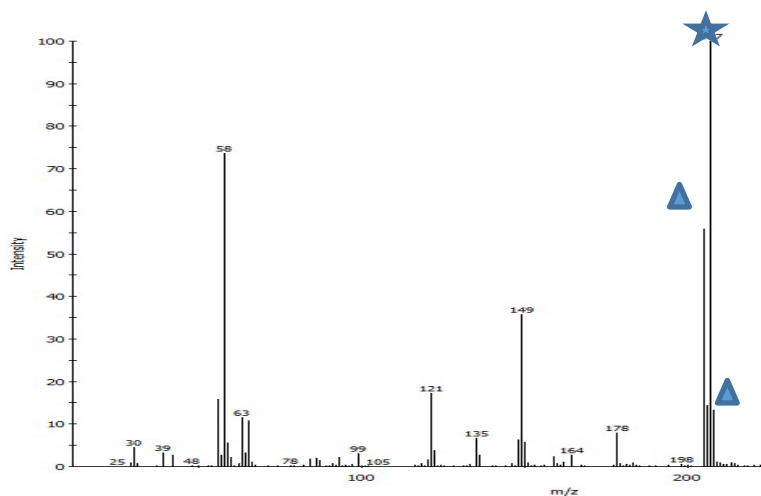


Figure 100: GC-cold EI MS spectrum for 100 PPM 2,3-methylenedioxymethcathinone mass 207. The triangle indicates a fragment found in the background that could not be subtracted.

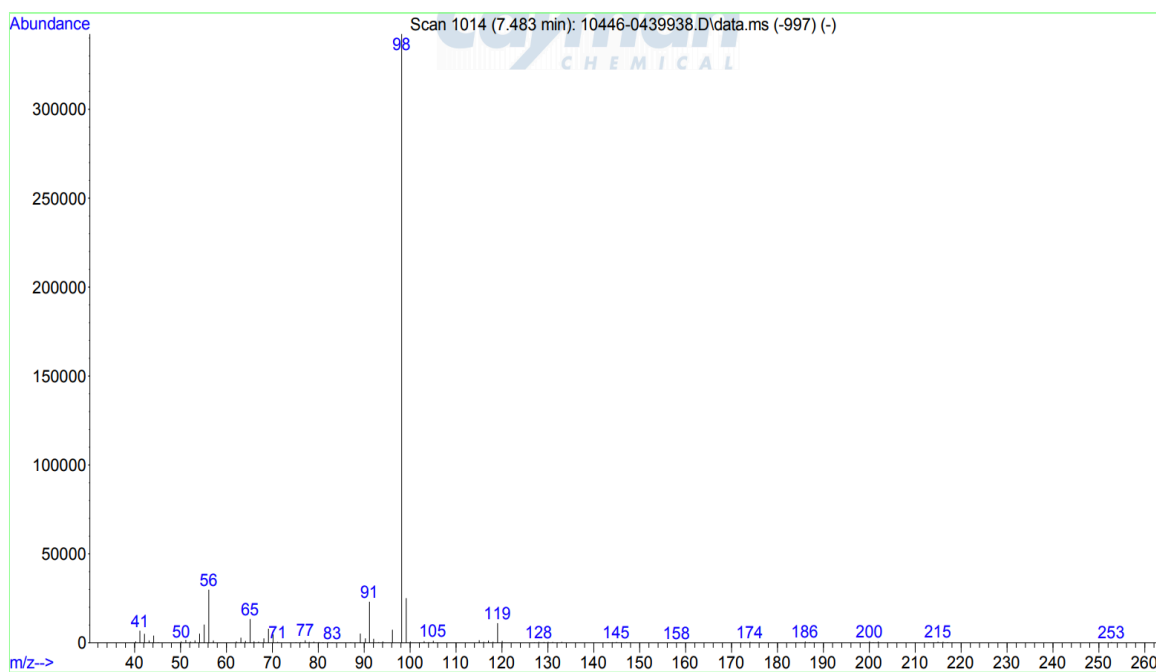


Figure 101: GC-EI MS spectrum for 4-MePPP mass 217.

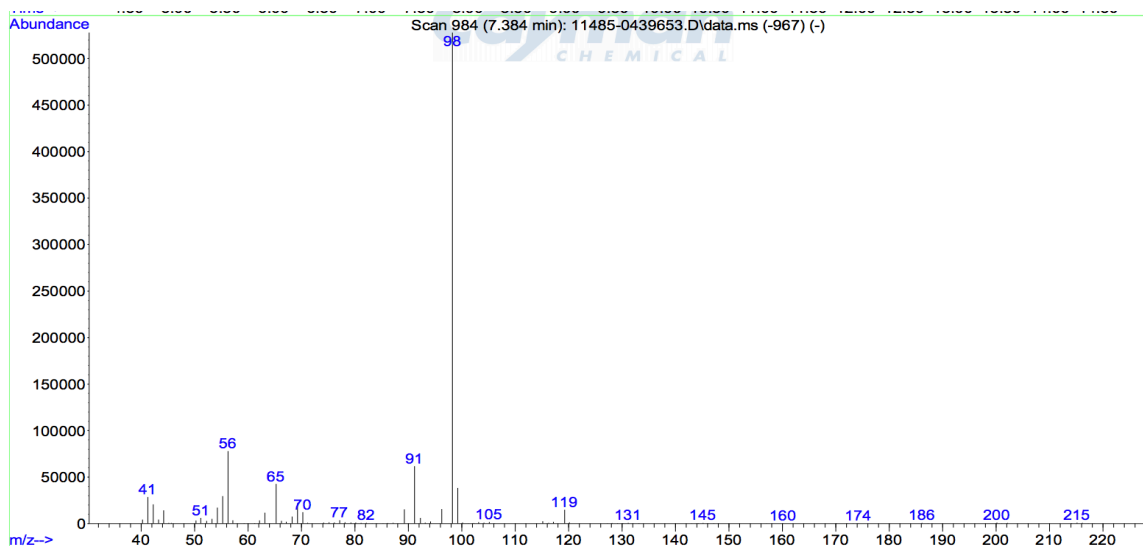


Figure 102: GC-EI MS spectrum for 3-MePPP mass 217.

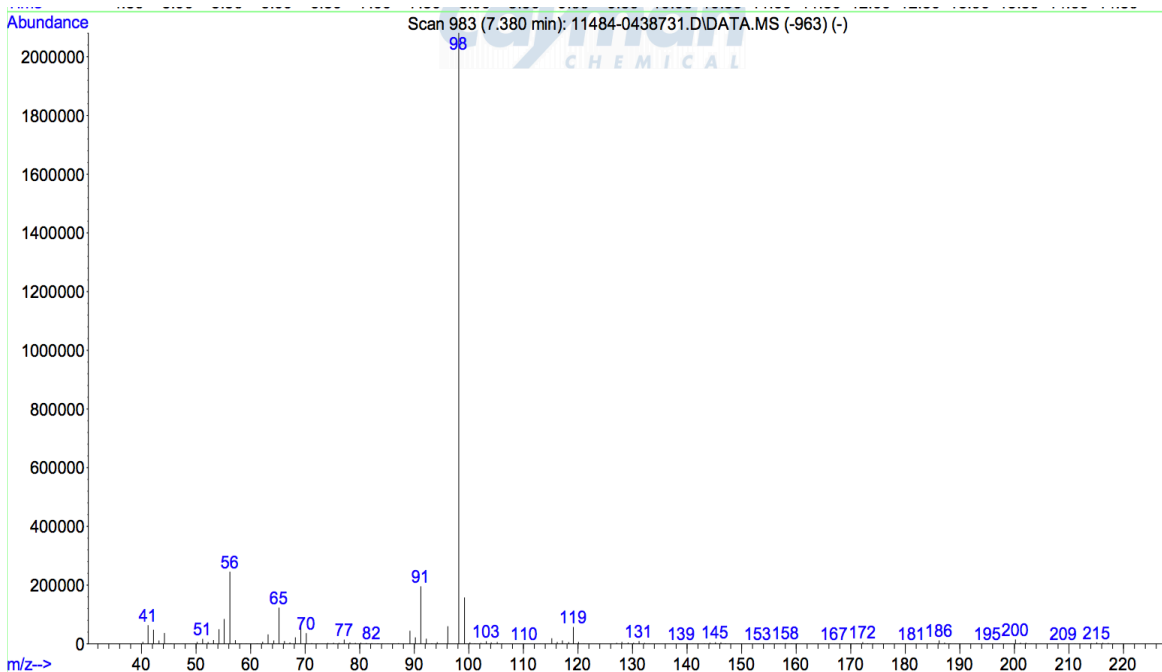


Figure 103: GC-EI MS spectrum for 2-MePPP mass 217.

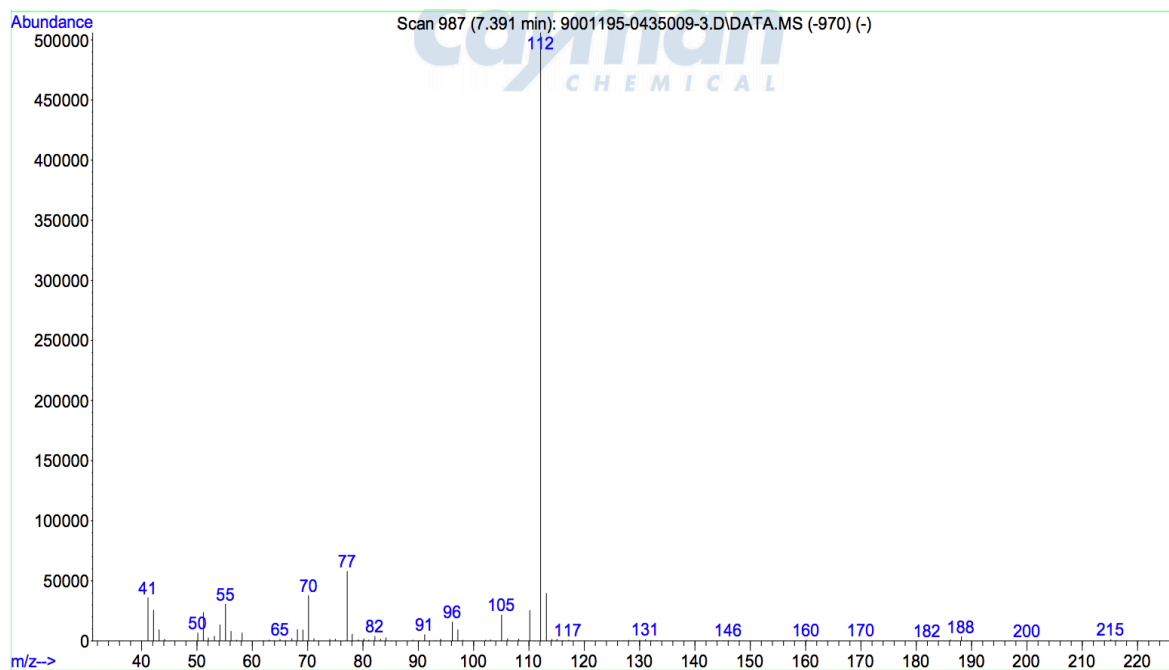


Figure 104: GC-EI MS spectrum for  $\alpha$ -PBP mass 217.

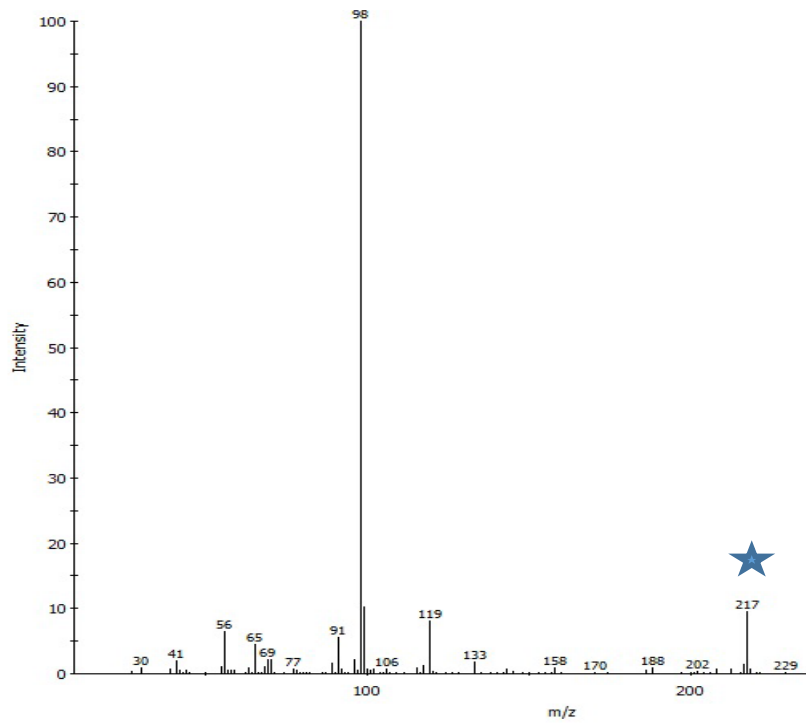


Figure 105: GC-cold EI MS spectrum for 100 PPM 4-MePPP mass 217.

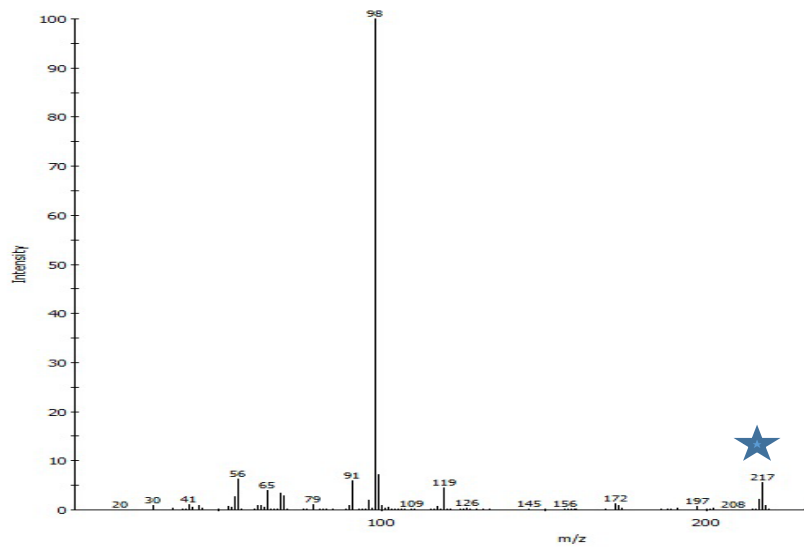


Figure 106: GC-cold EI MS spectrum for 100 PPM 3-MePPP mass 217.

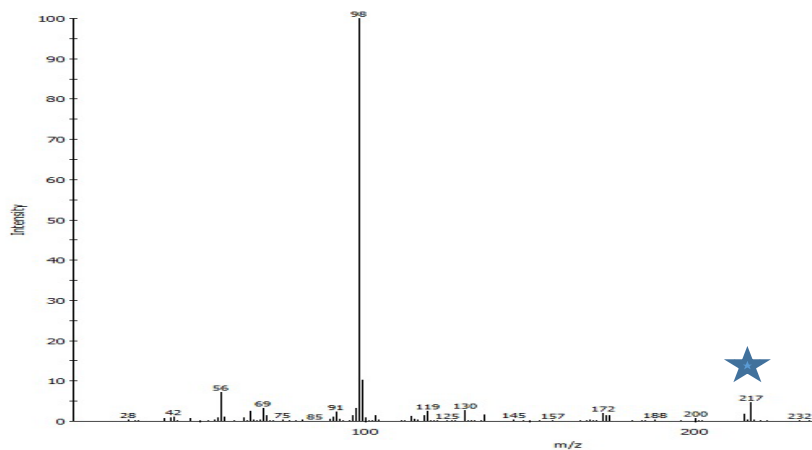


Figure 107: GC-cold EI MS spectrum for 100 PPM 2-MePPP mass 217.

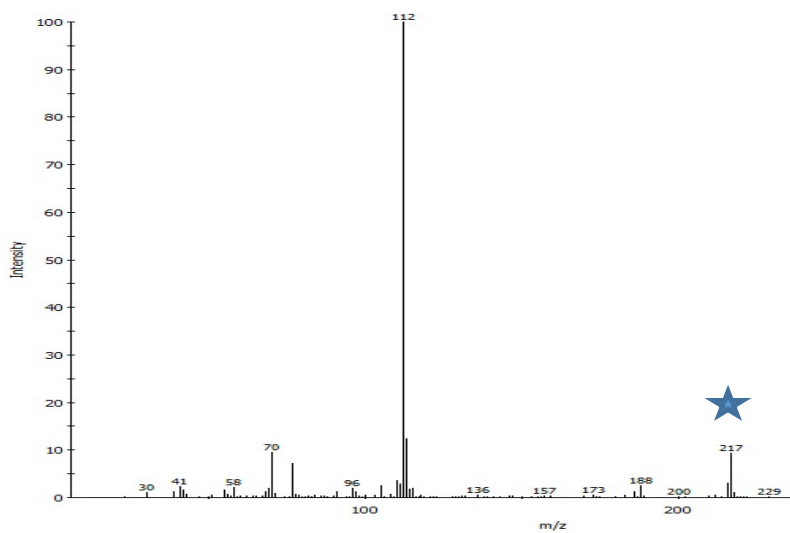


Figure 108: GC-cold EI MS spectrum for 100 PPM  $\alpha$ -PBP mass 217.

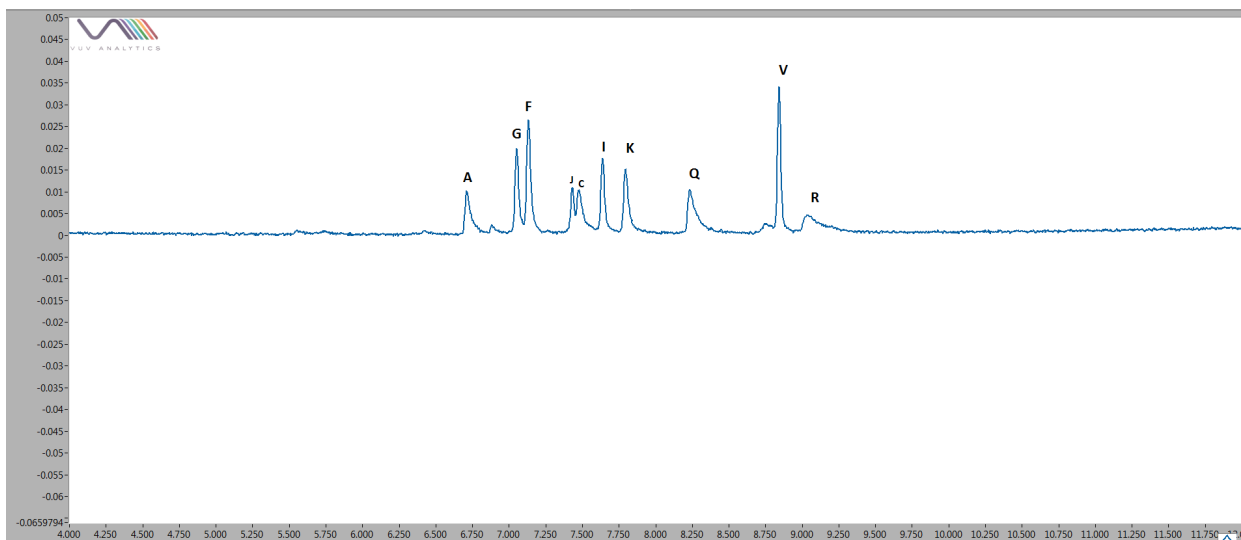


Figure 109: GC-VUV chromatogram of a synthetic cathinone mixture containing ten controlled isomers and one non-controlled isomer. Each isomer has a concentration of 100 ppm. See Table 2 for peak identification and figure 92 for GC parameters.

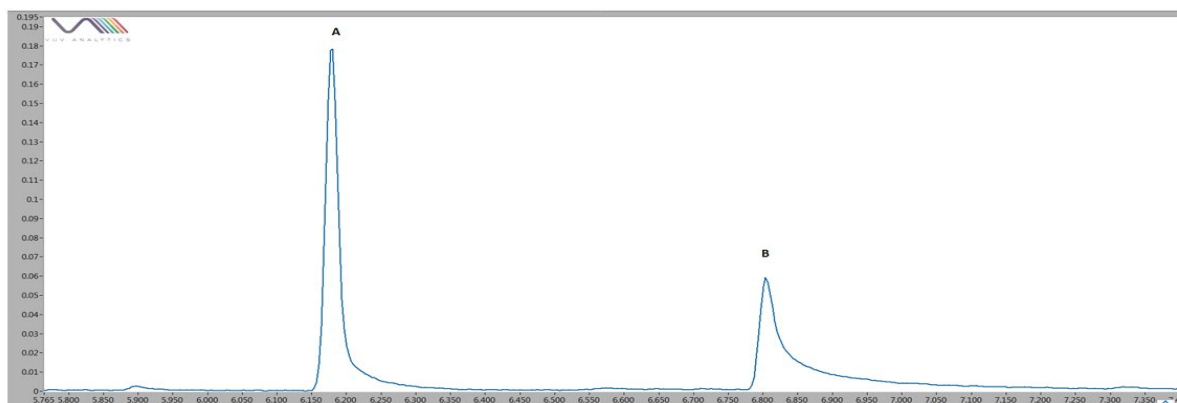


Figure 110: GC-VUV chromatogram of 150 PPM mass 163 isomer set extracted into methylene chloride. See Table 2 for peak identification.

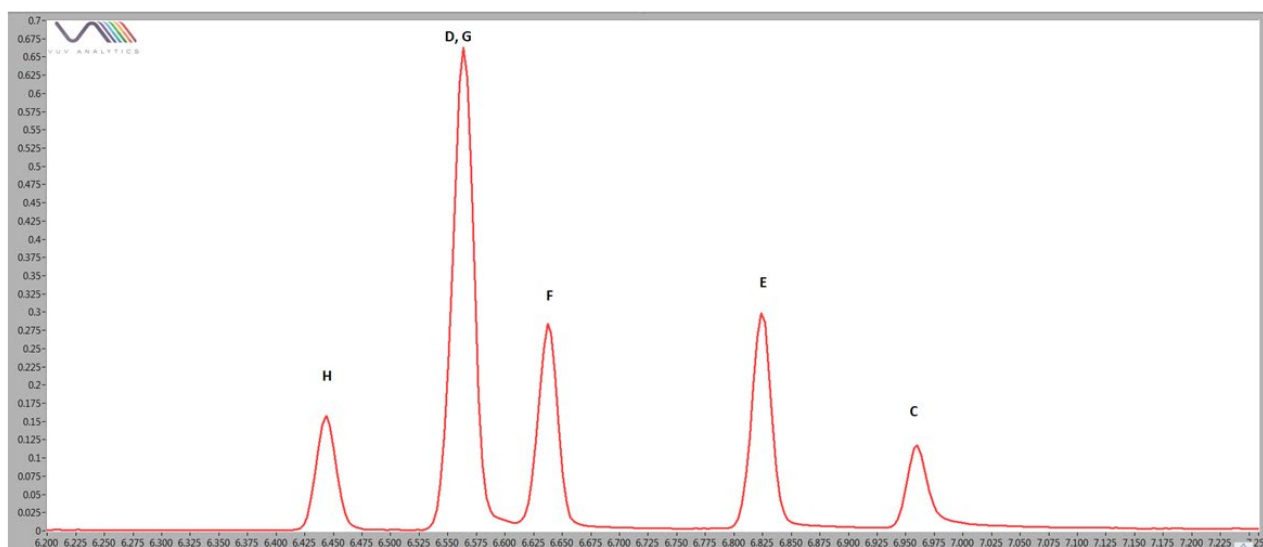


Figure 111: GC-VUV chromatogram of 150 PPM mass 177 isomer set extracted into methylene chloride. See Table 2 for peak identification.

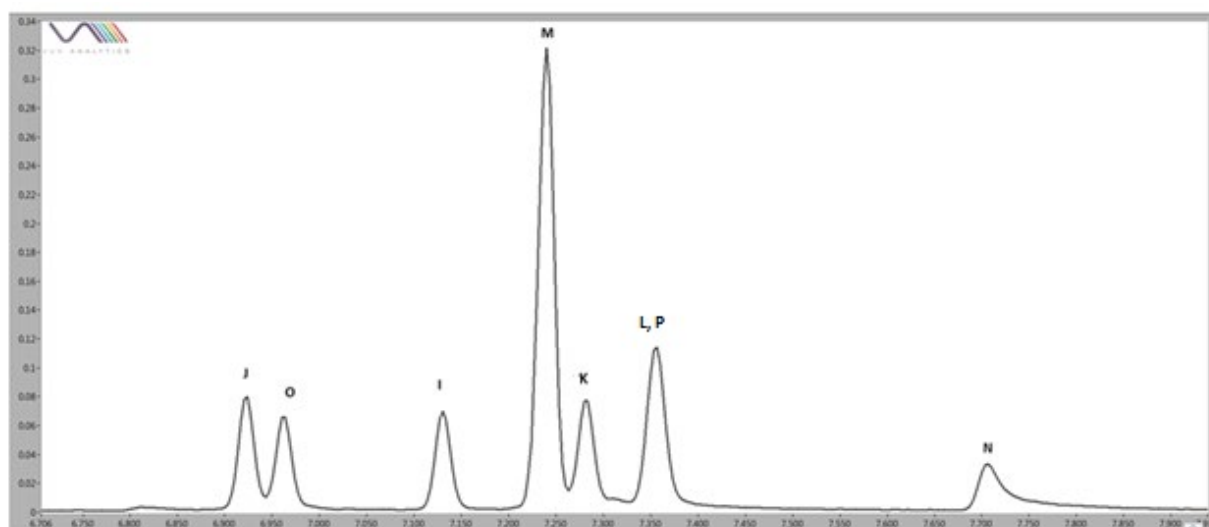


Figure 112: GC-VUV chromatogram of 150 PPM mass 191 isomer set extracted into methylene chloride. See Table 2 for peak identification.

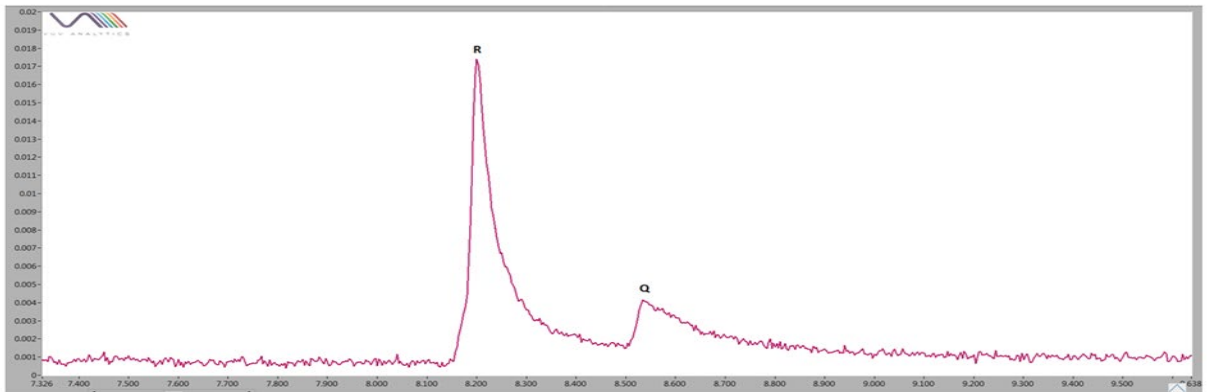


Figure 113: GC-VUV chromatogram of 150 PPM mass 207 isomer set extracted into methylene chloride. See Table 2 for peak identification.

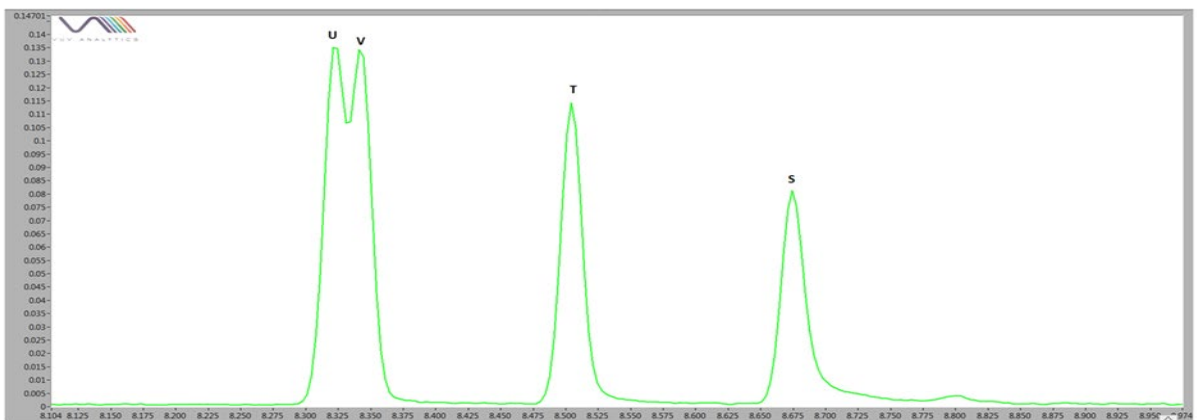


Figure 114: GC-VUV chromatogram of 150 PPM mass 217 isomer set extracted into methylene chloride. See Table 2 for peak identification.

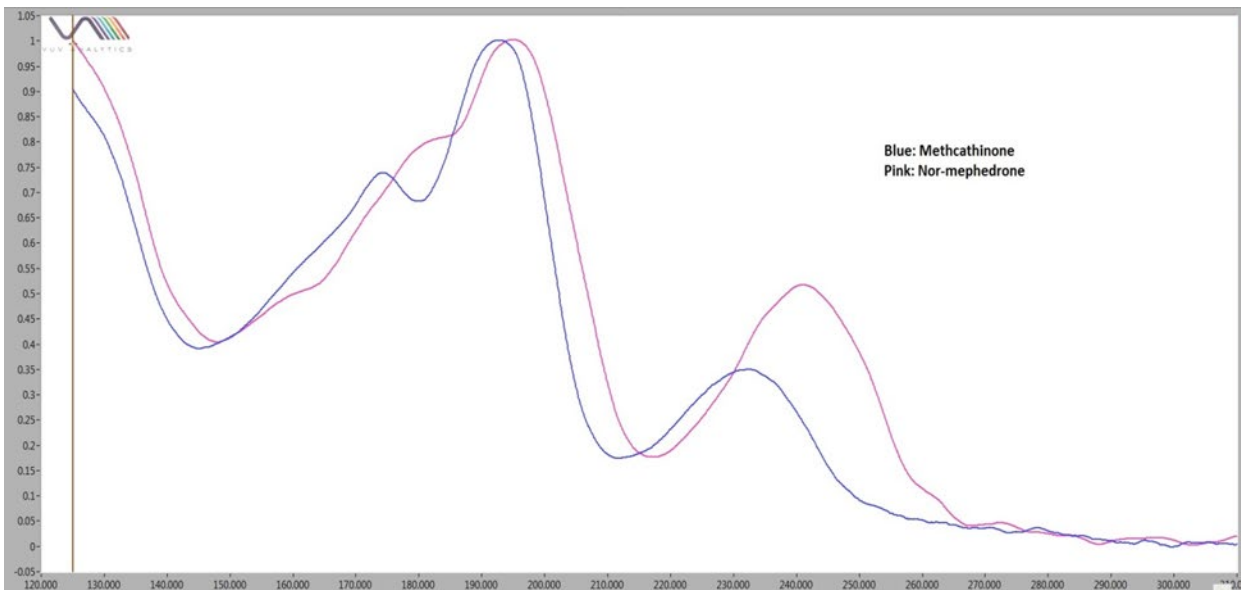


Figure 115: GC-VUV spectra overlay of mass 163 positional isomers extracted into methylene chloride. 150 PPM each compound.

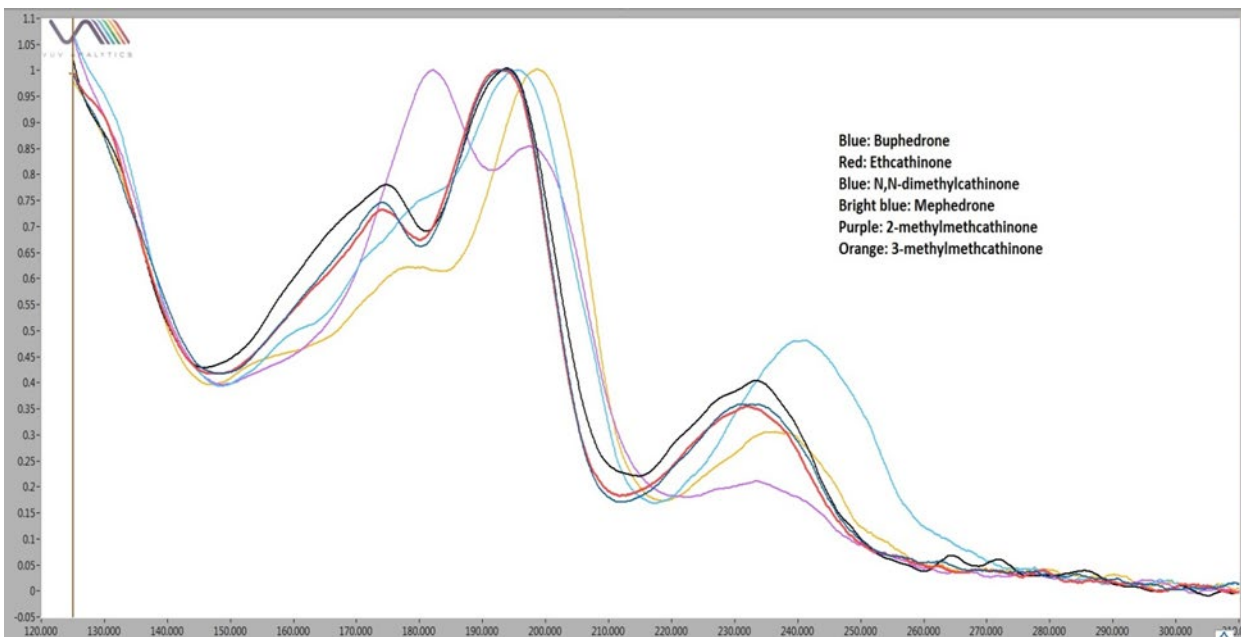


Figure 116: GC-VUV spectra overlay of mass 177 positional isomers extracted into methylene chloride. 150 PPM each compound.

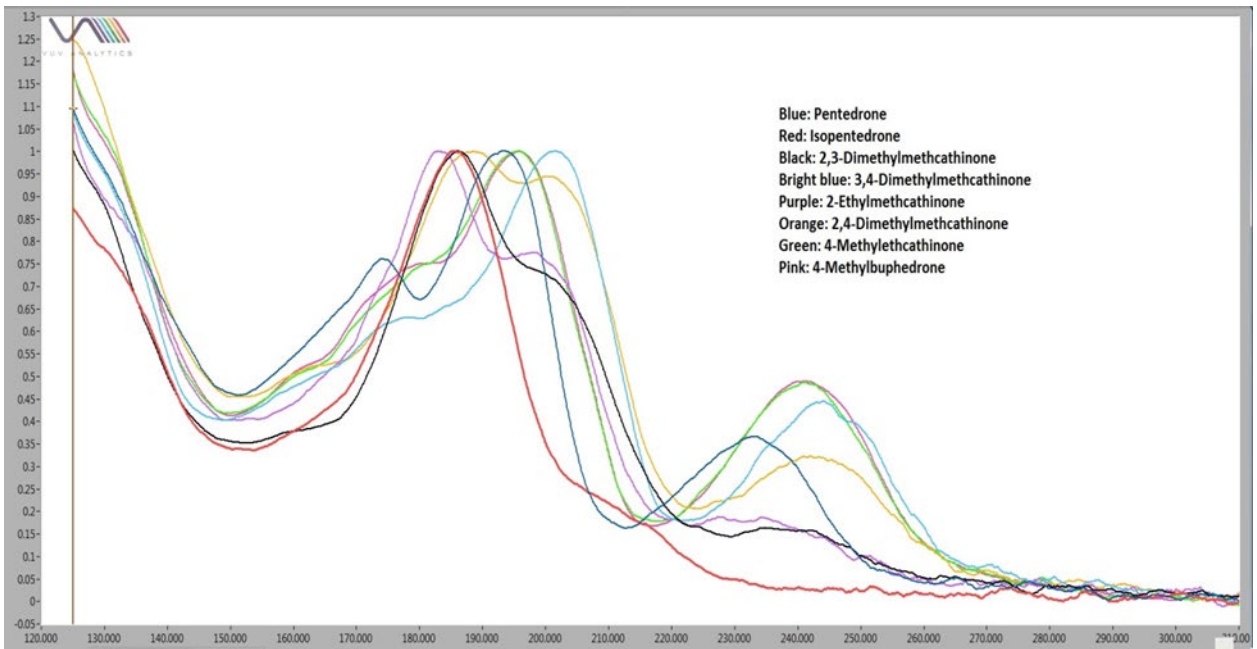


Figure 117: GC-VUV spectra overlay of mass 191 positional isomers extracted into methylene chloride. 150 PPM each compound.

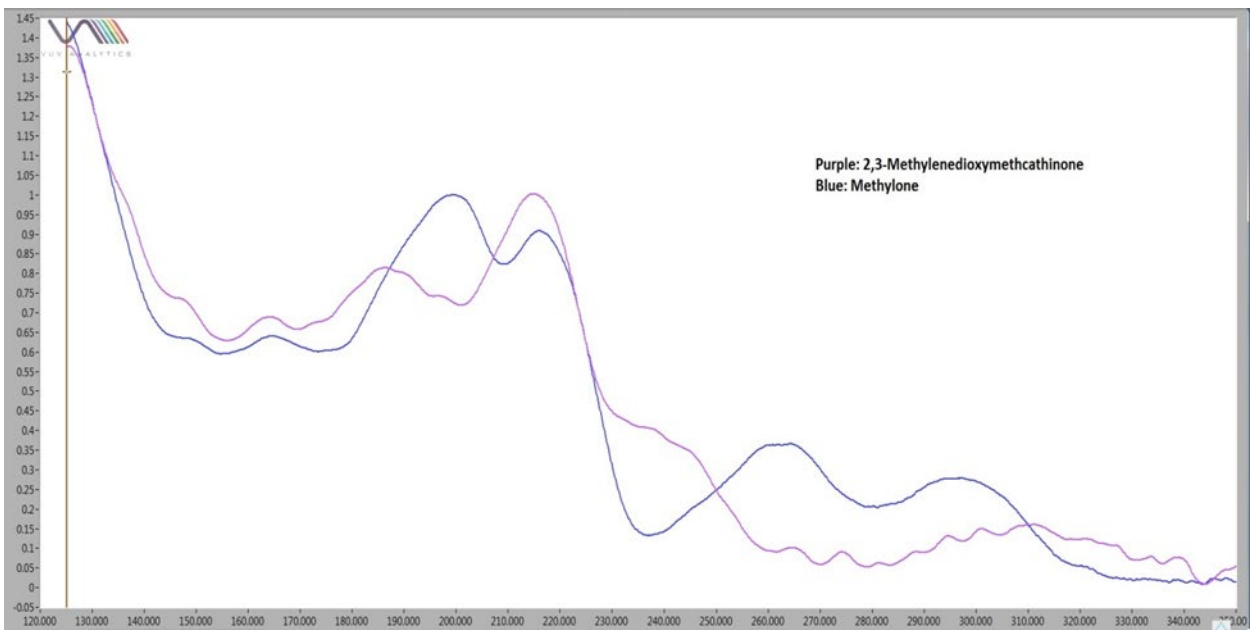


Figure 118: GC-VUV spectra overlay of mass 207 positional isomers extracted into methylene chloride. 150 PPM each compound.

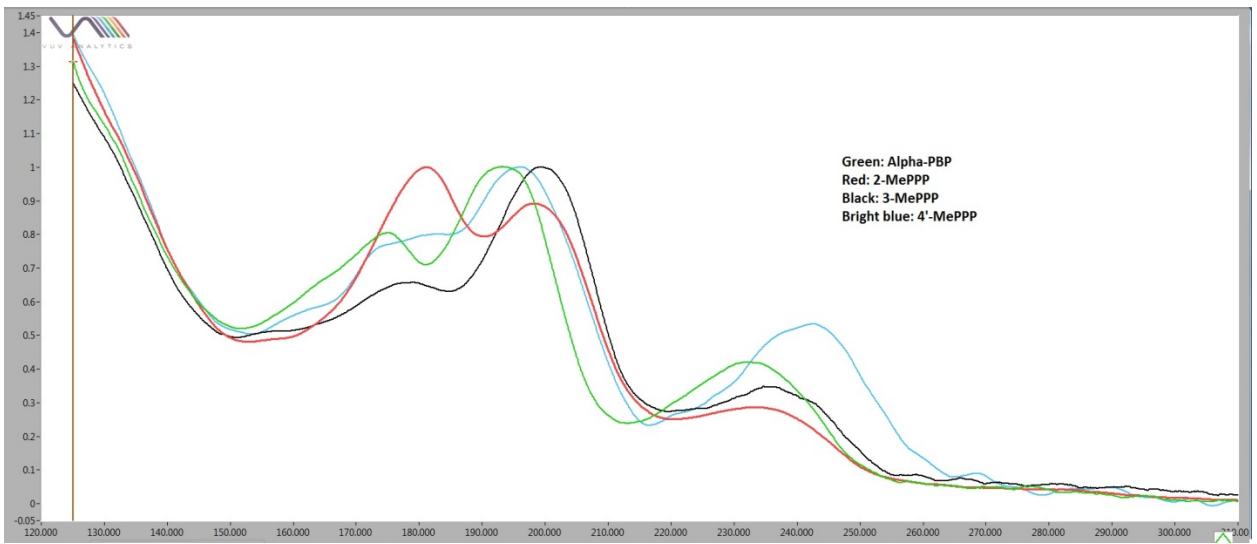


Figure 119: GC-VUV spectra overlay of mass 217 positional isomers extracted into methylene chloride. 150 PPM each compound.

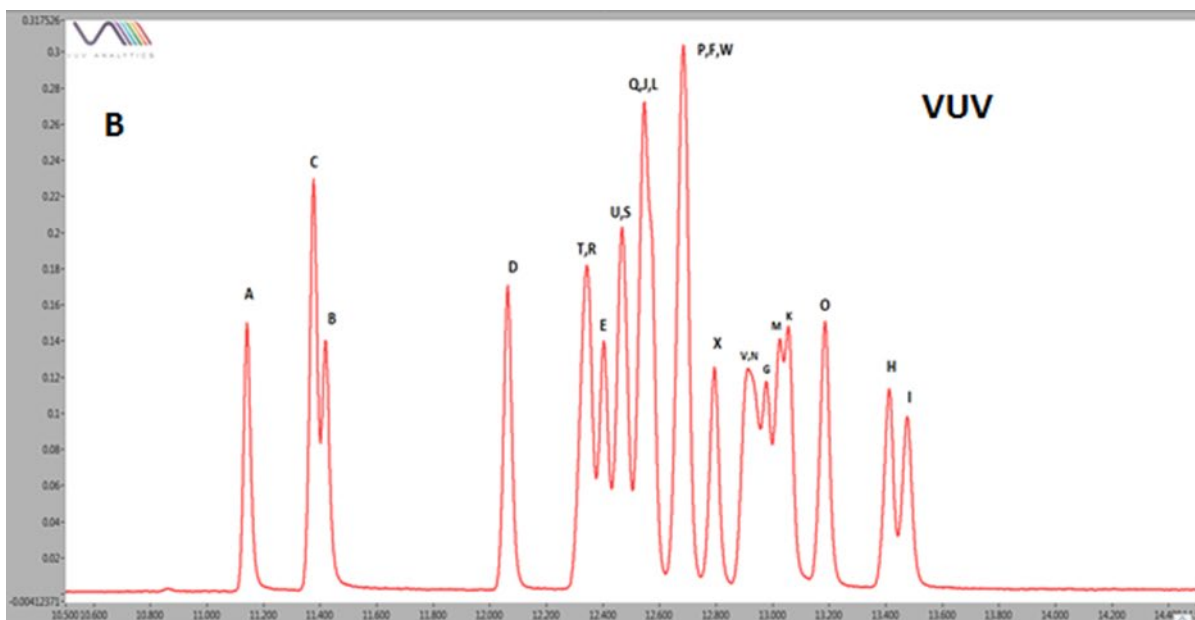
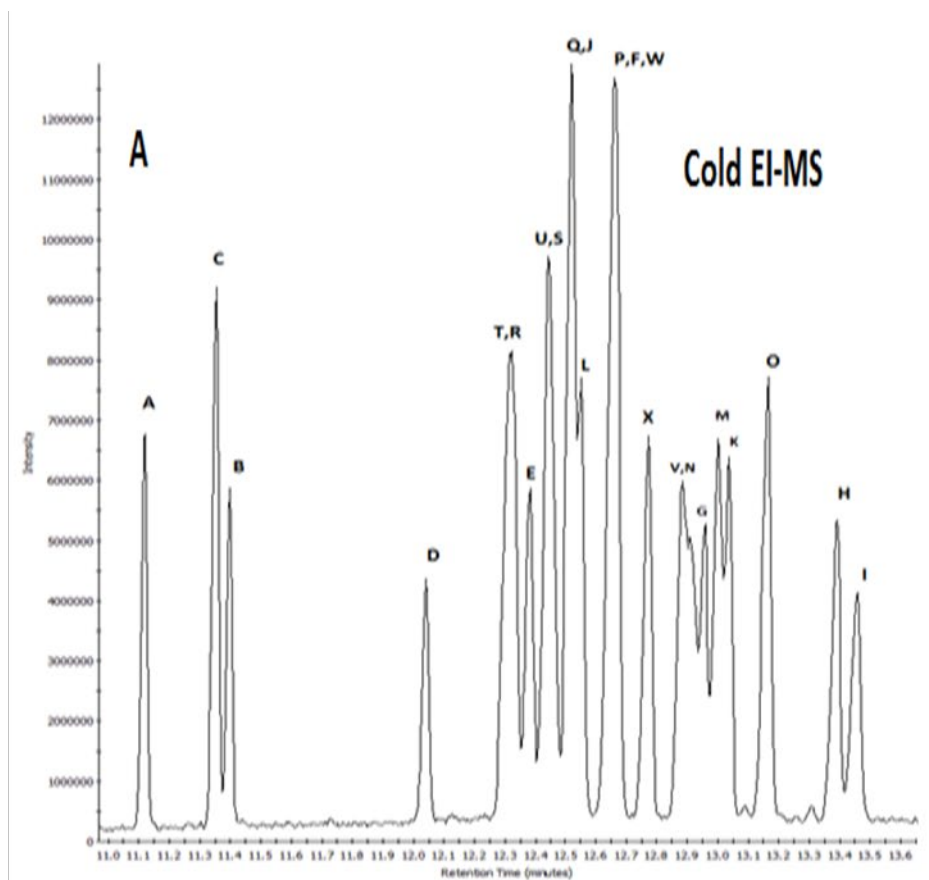


Figure 120: Simultaneous Cold E-MS (A) and VUV detection (B) for a mixture 50 ppm each of 24 fentanyl analogues. See Table 1 for peak identification

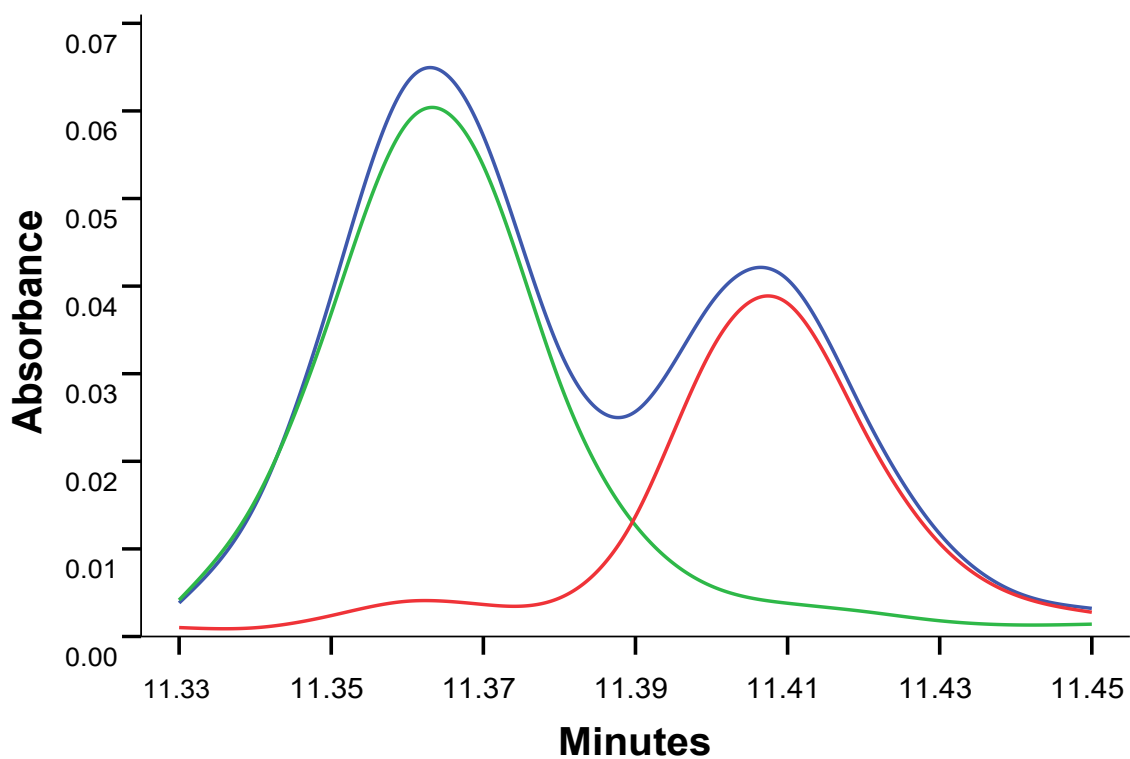
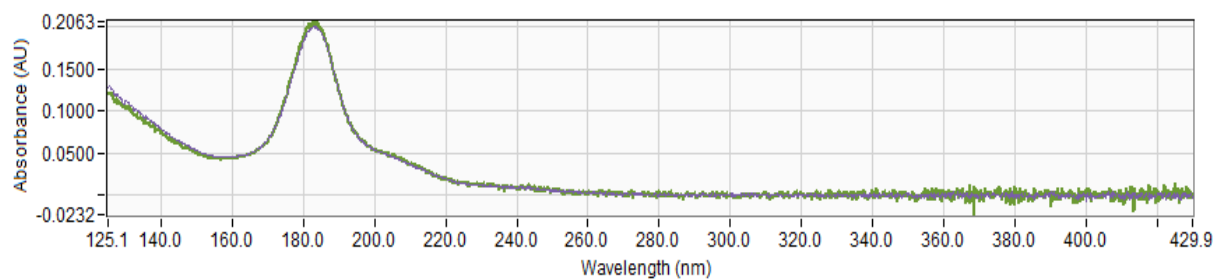


Figure 121: Deconvolution of peaks B and C corresponding to the coelution of 50 ppm despropionyl para-fluorofentanyl (green) and 50 ppm despropionyl meta-fluorofentanyl (red).



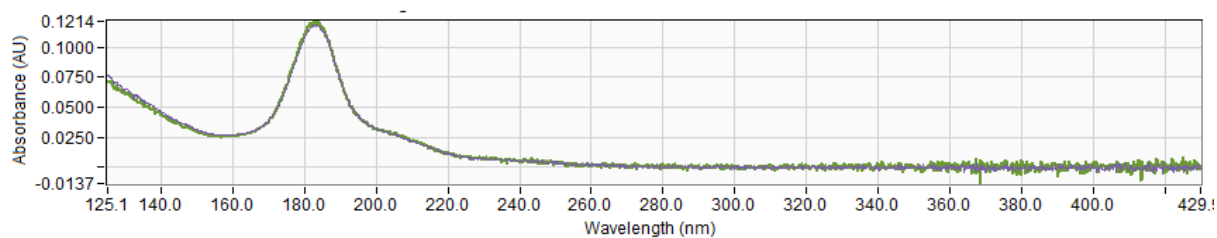
100 ppm  $R^2 = .9987$



Combined Ret. Reg. Spectra



Beta-methyl fentanyl SRB



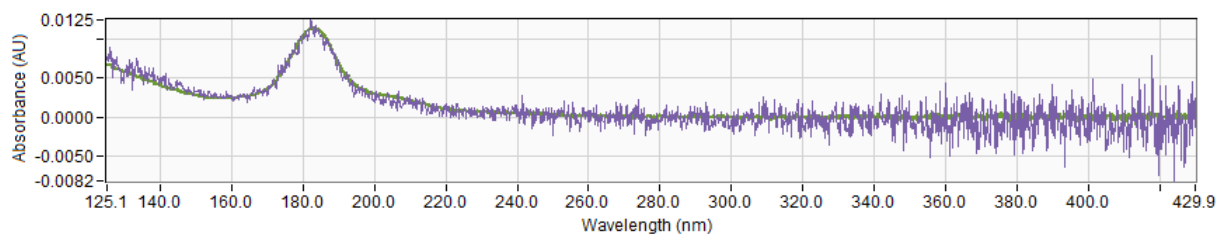
50 ppm  $R^2 = .9992$



Combined Ret. Reg. Spectra



Beta-methyl fentanyl SRB



3.12 PPM  $R^2 = .9665$



Combined Ret. Reg. Spectra



Beta-methyl fentanyl SRB

Figure 122: GC-VUV spectrum of beta-methyl fentanyl at various concentrations including library matches.

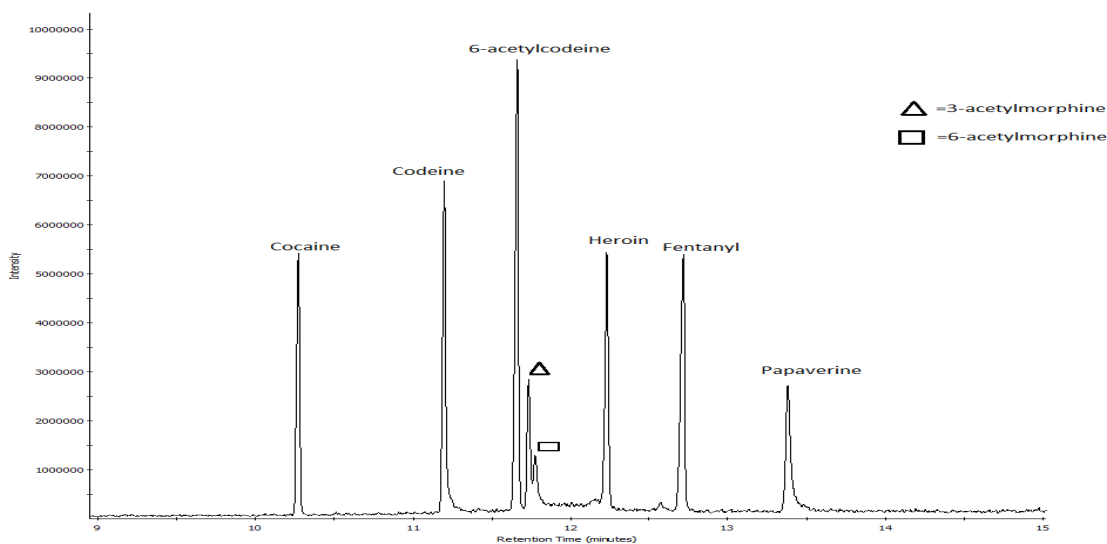


Figure 123: GC-cold EI MS chromatogram of selected adulterants, heroin by-products and heroin impurities. (50 PPM each compound). Column-Perkin Elmer Elite-5MS (30m x 0.25mm x 0.25  $\mu$ m df); 3  $\mu$ L splitless injection, injector temperature 280°C; oven temperature profile- 1 min @ 100°C, 20°C/min to 300°C, Hold 8 min.; helium flow 3.0 mL/min.

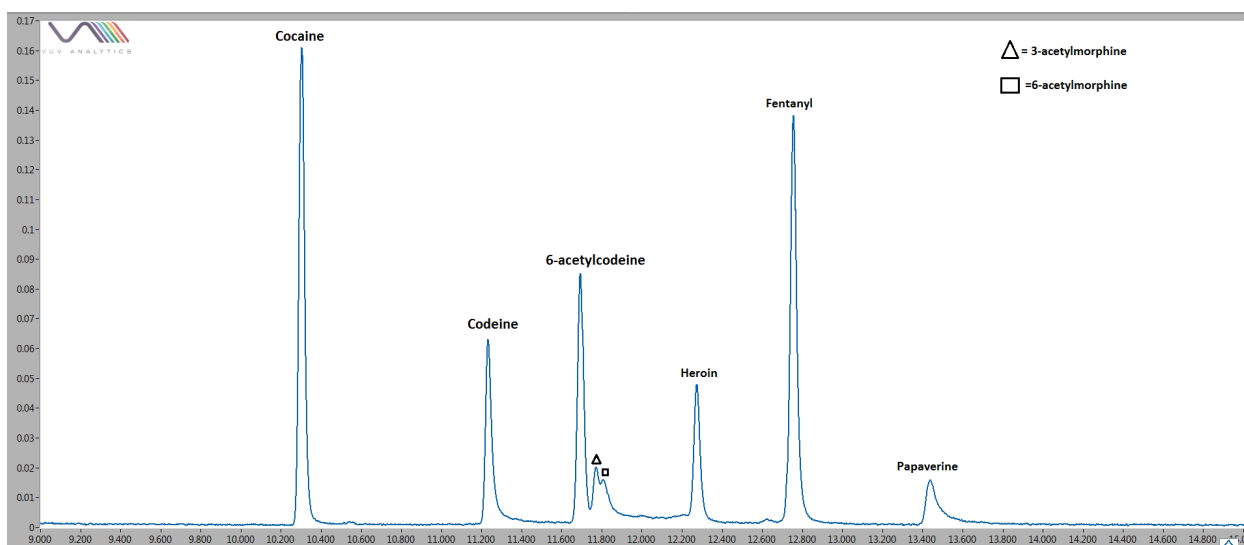


Figure 124: GC-VUV chromatogram of selected adulterants, heroin by-products and heroin impurities (50 PPM each compound); see Figure 1 for GC conditions.

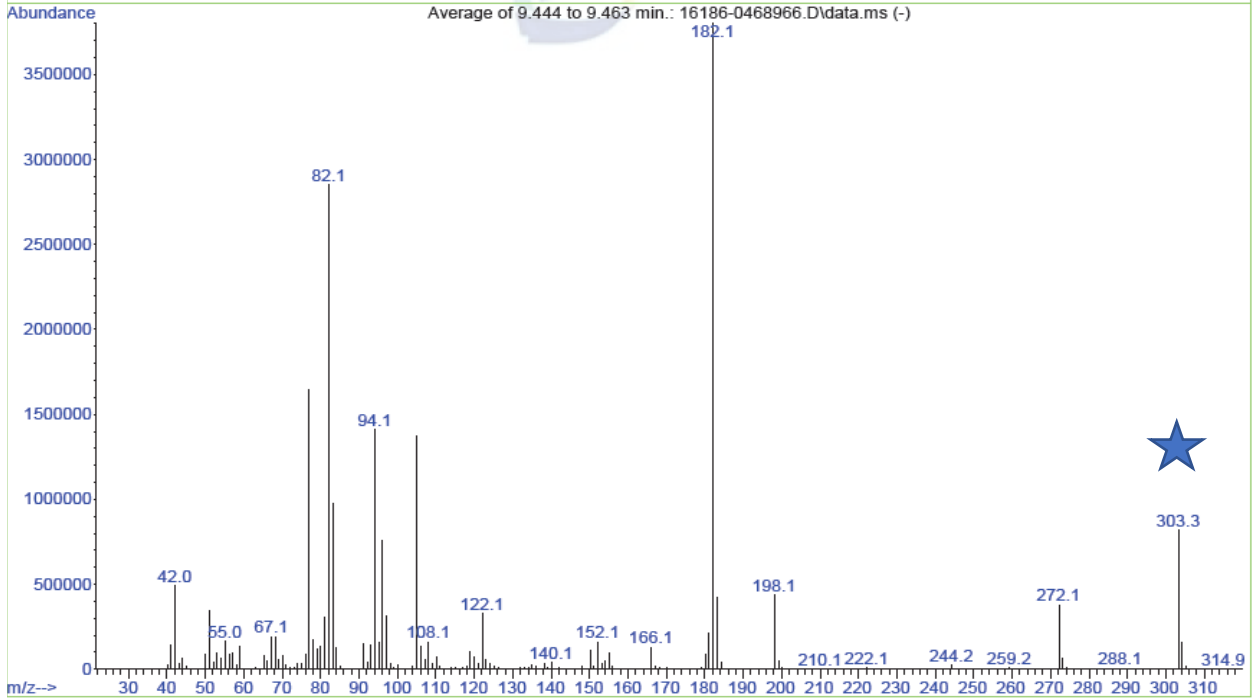


Figure 125: GC-classical EI MS cocaine spectrum (mass 303) (Cayman Chemical)

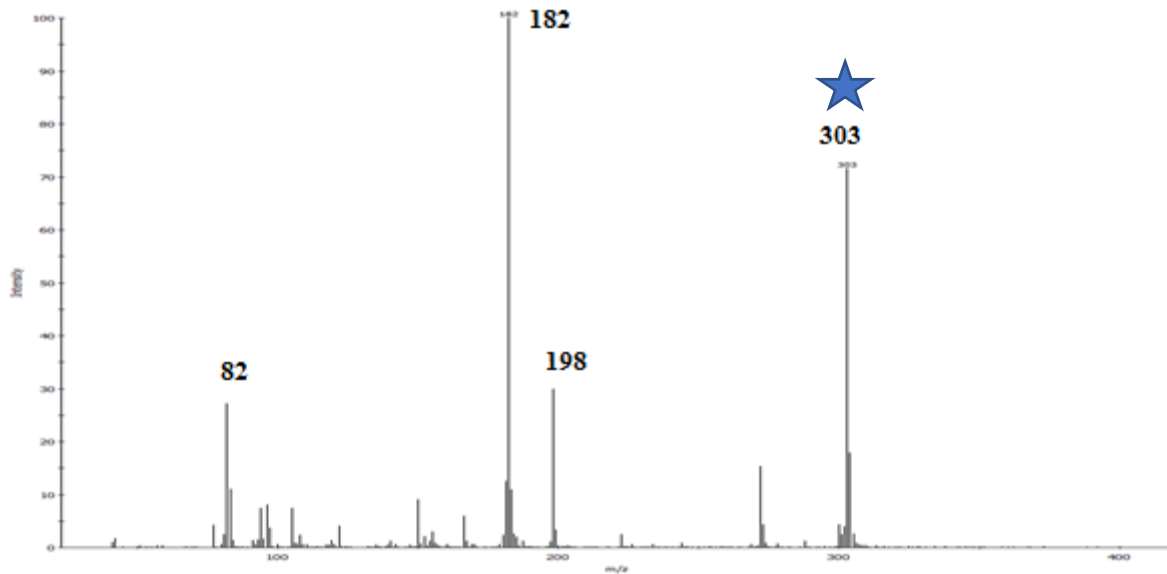


Figure 126: GC-cold EI MS cocaine spectrum (mass 303) spectrum.

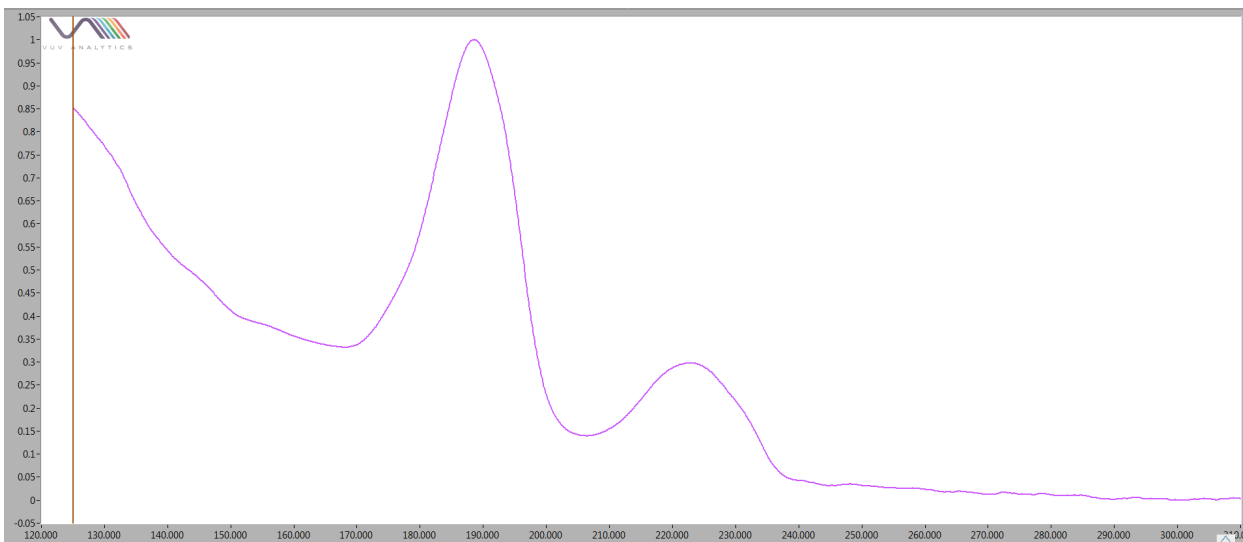


Figure 127: GC-VUV cocaine spectrum

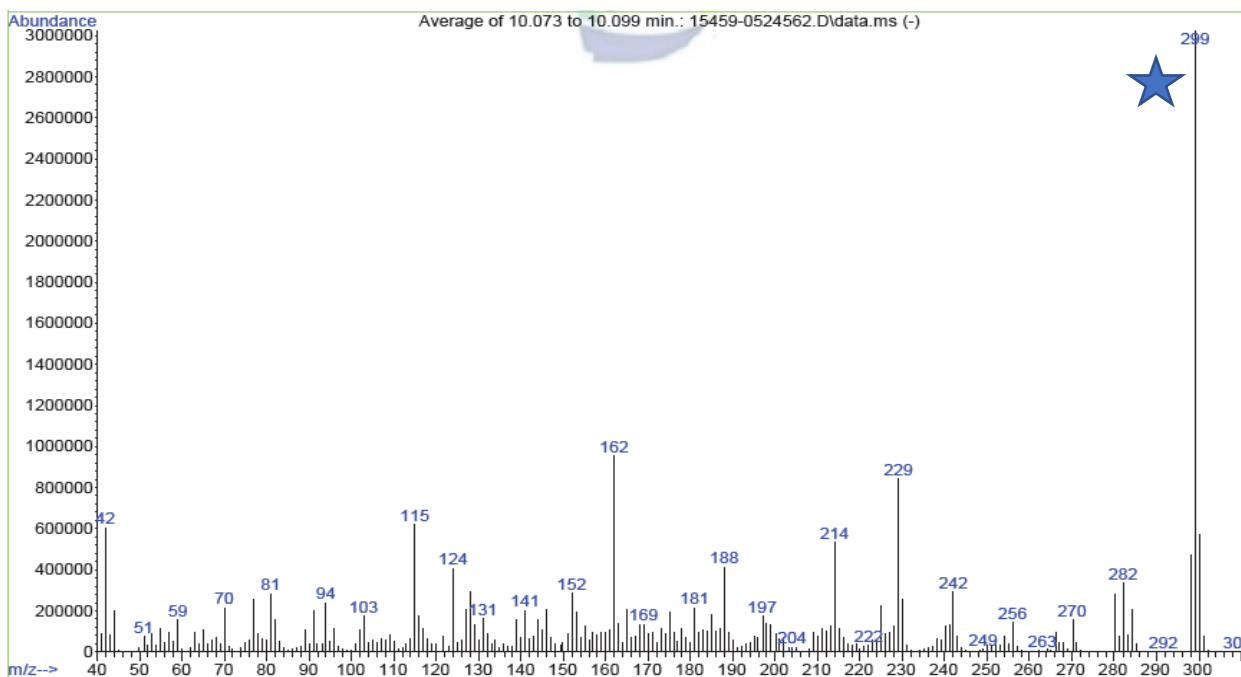


Figure 128: GC-classical EI MS codeine spectrum (mass 299) (Cayman Chemical)

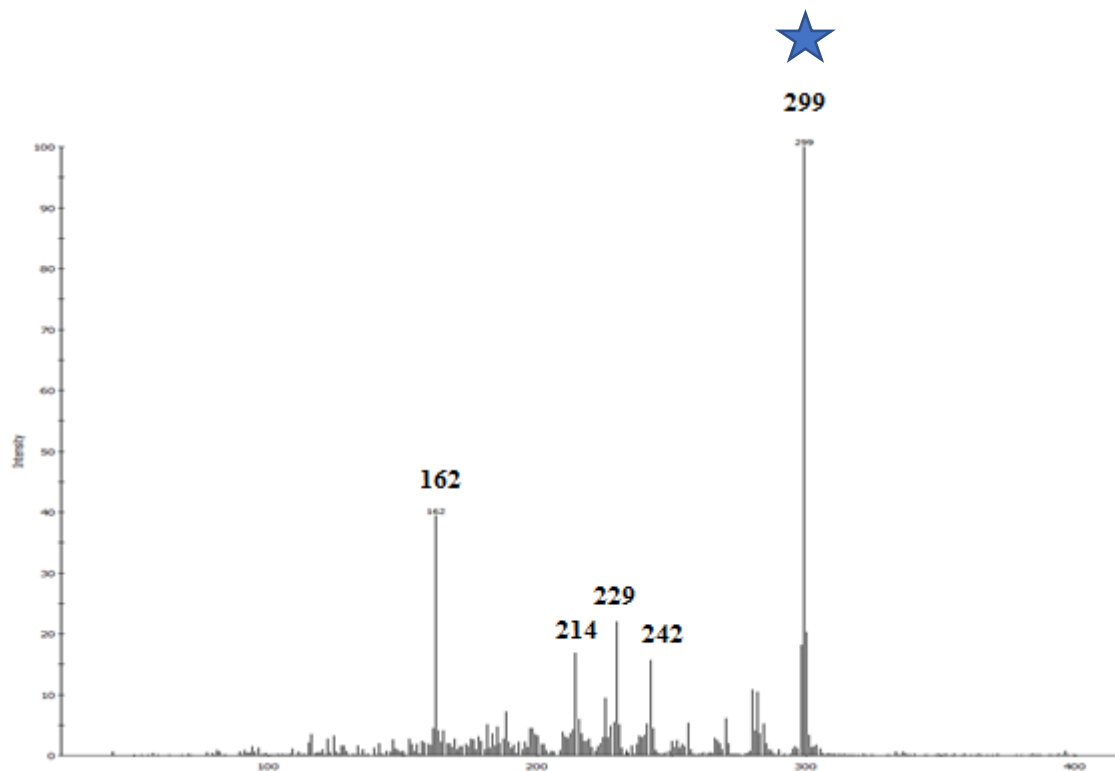


Figure 129: GC-cold EI MS codeine spectrum (mass 299).

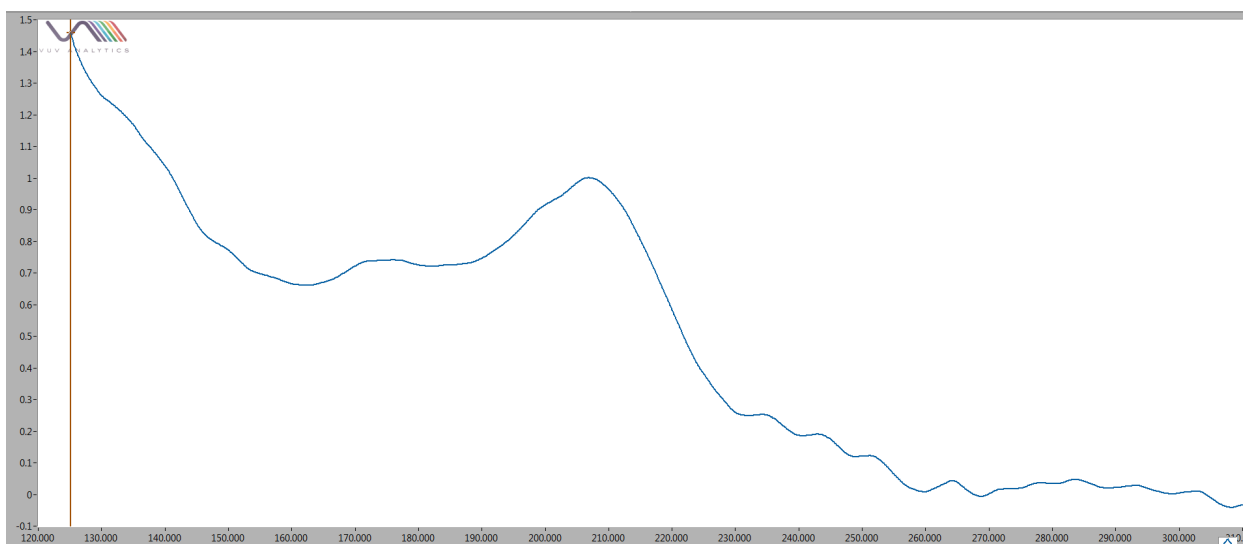


Figure 130: GC-VUV codeine spectrum.

Morphinan-6-ol, 7,8-didehydro-4,5-epoxy-3-methoxy-17-methyl-, acetate (ester), (5.alpha.,6.alpha.)-

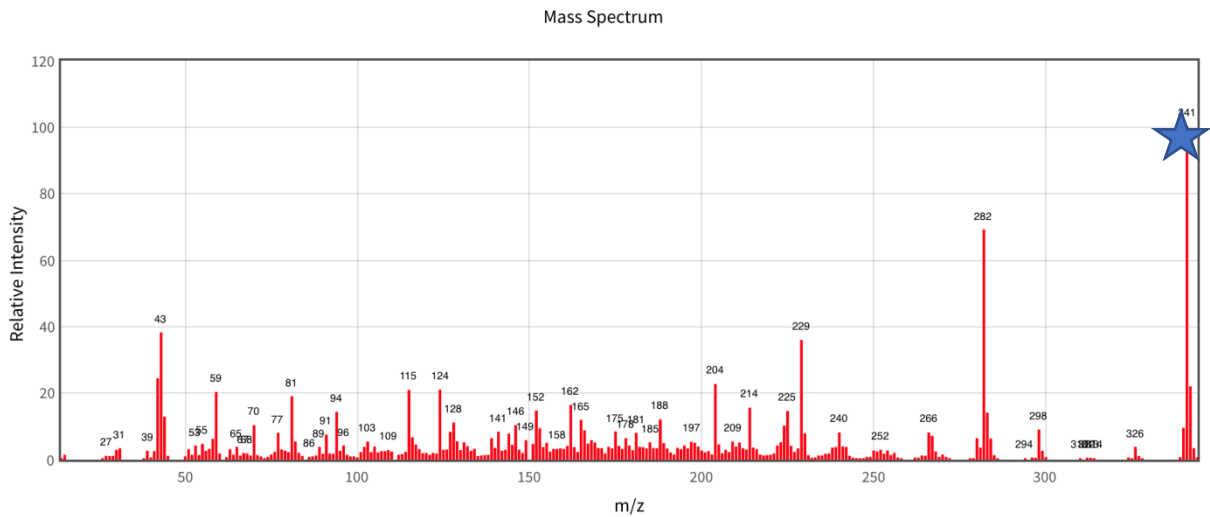


Figure 131: GC-classical EI MS acetyl codeine (mass 341) (NIST).

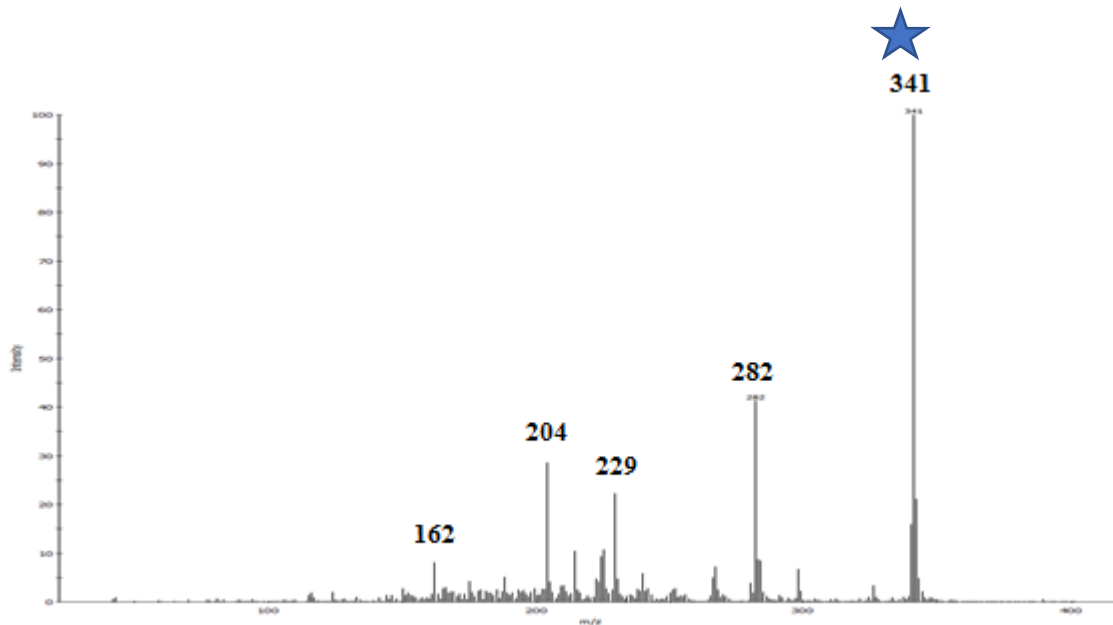


Figure 132: GC-cold EI acetyl codeine (mass 341).

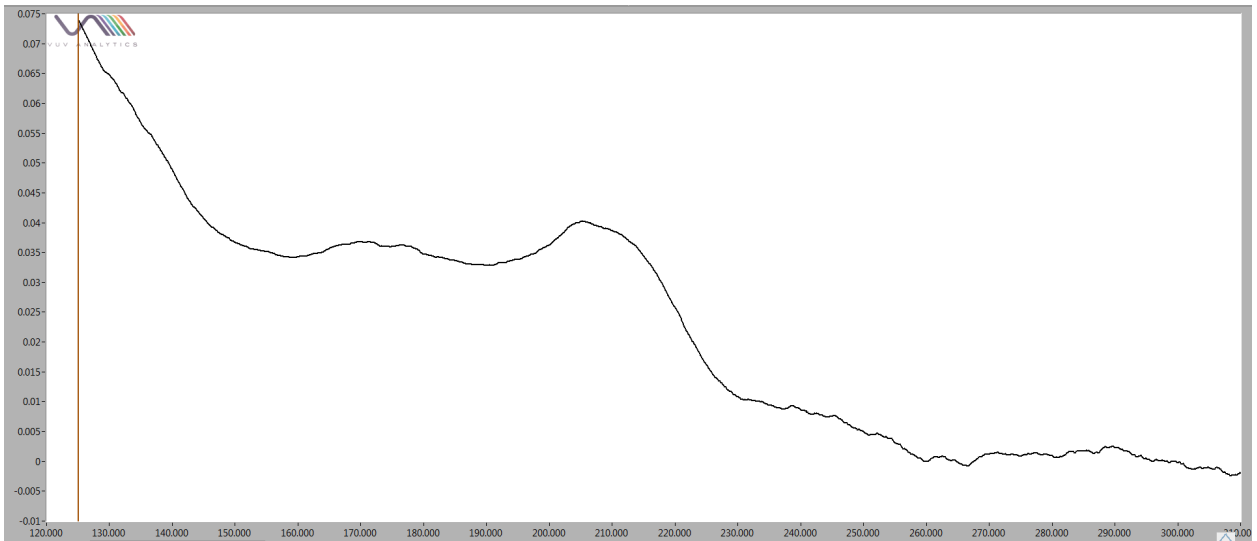


Figure 133: GC-VUV acetyl codeine spectrum.

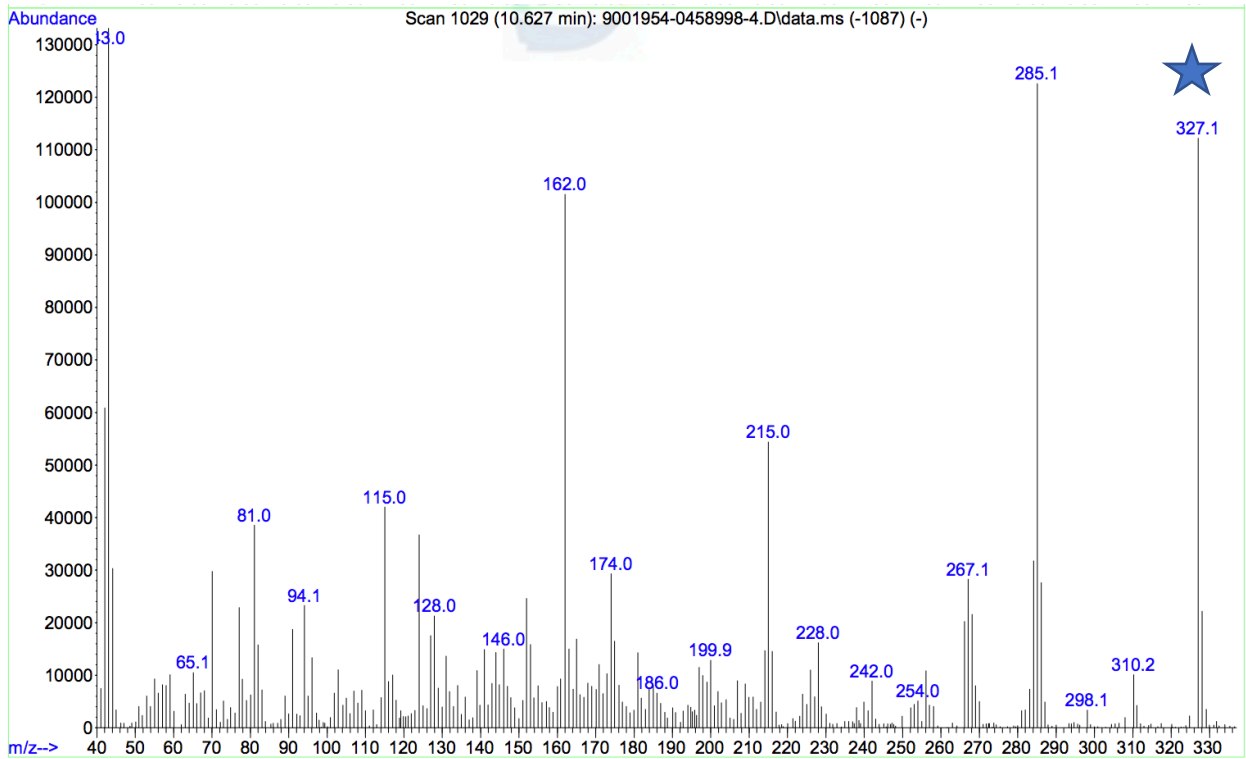


Figure 134: GC-classical EI MS O3-monoacetylmorphine (mass 327) (Cayman).

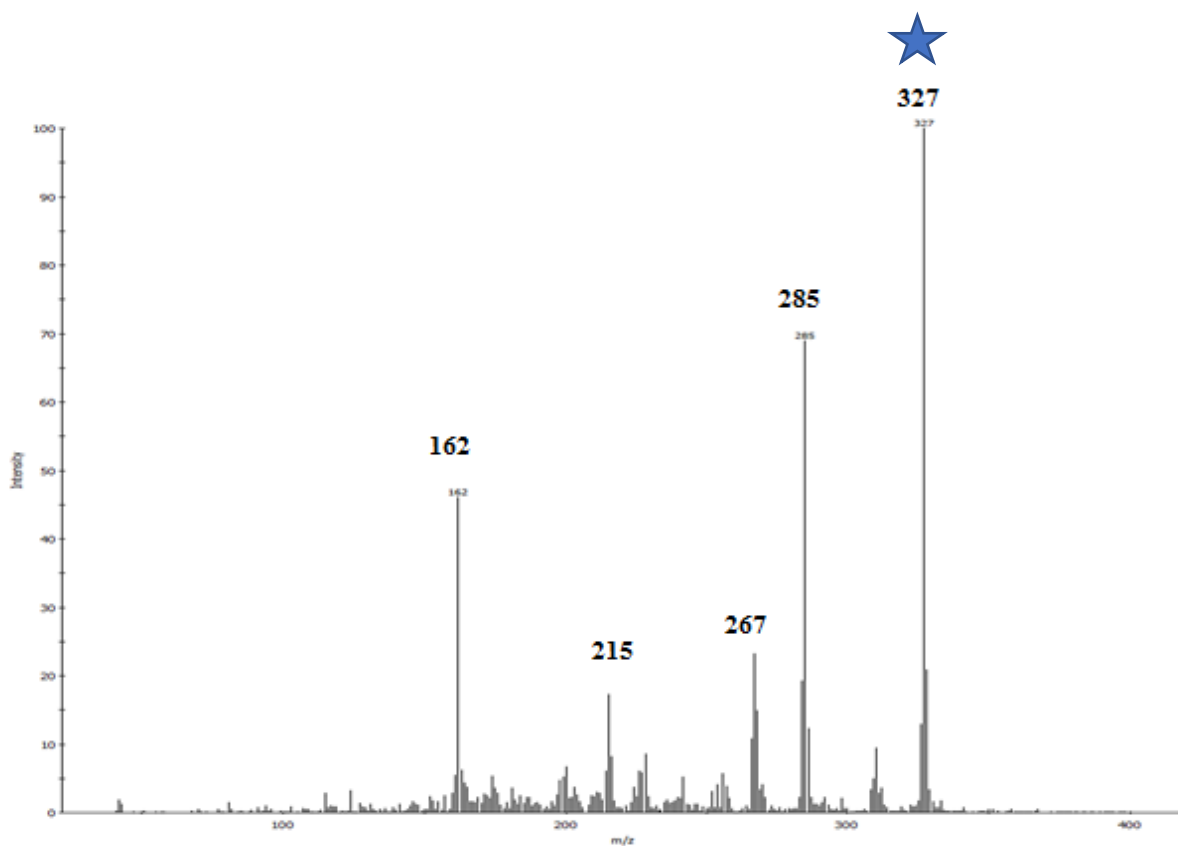


Figure 135: GC-cold EI MS O3-monoacetylmorphine (mass 327).

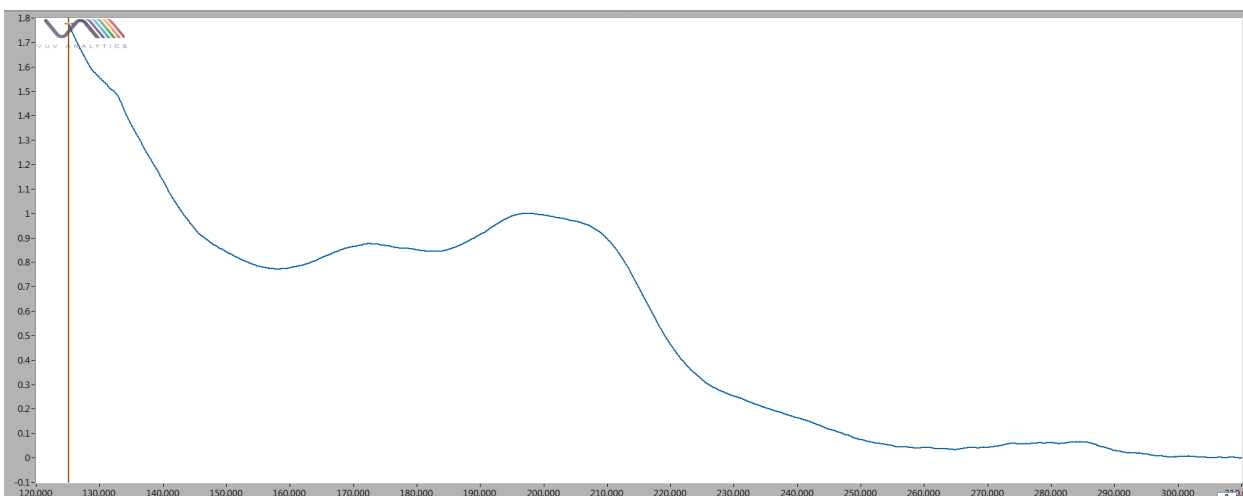


Figure 136: GC-VUV O3-monoacetylmorphine spectrum.

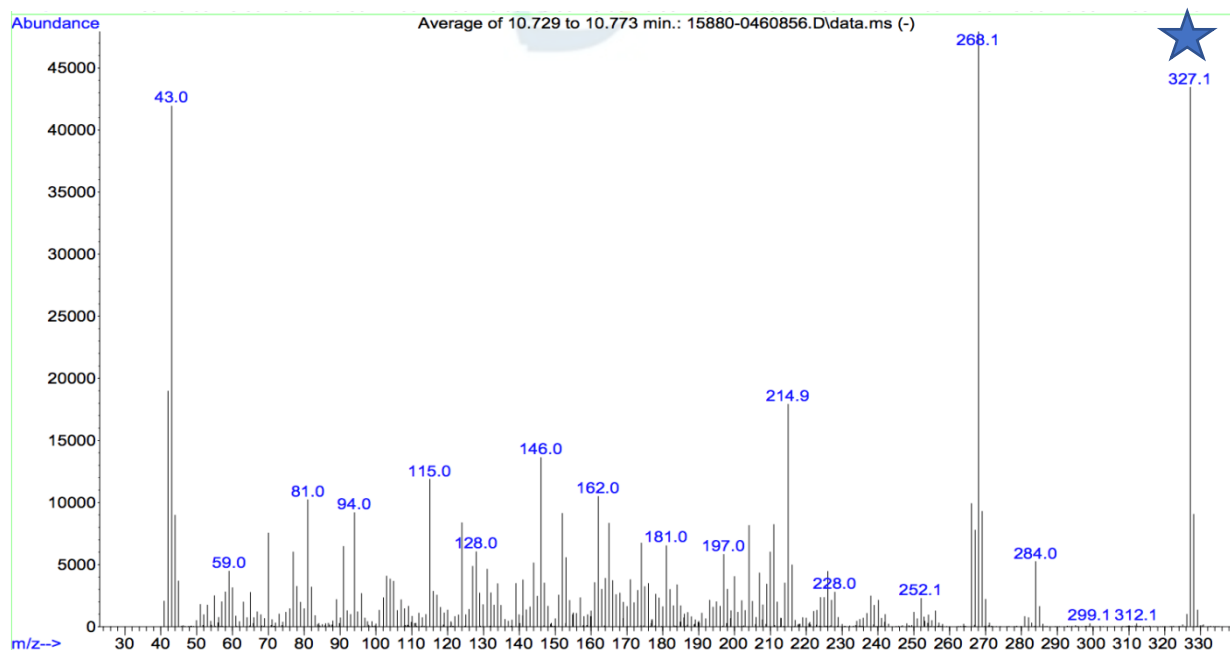


Figure 137: GC-classical EI MS O6-monoacetylmorphine (mass 327) (Cayman).

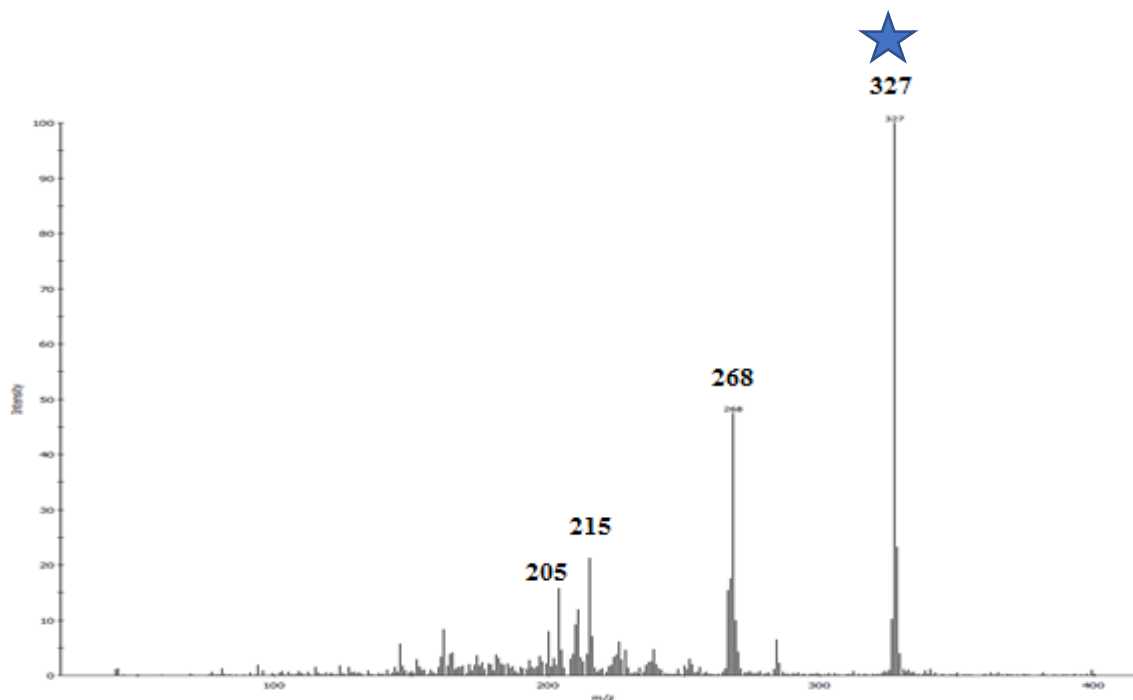


Figure 138: GC-cold EI MS O6-monoacetylmorphine (mass 327) (Cayman).

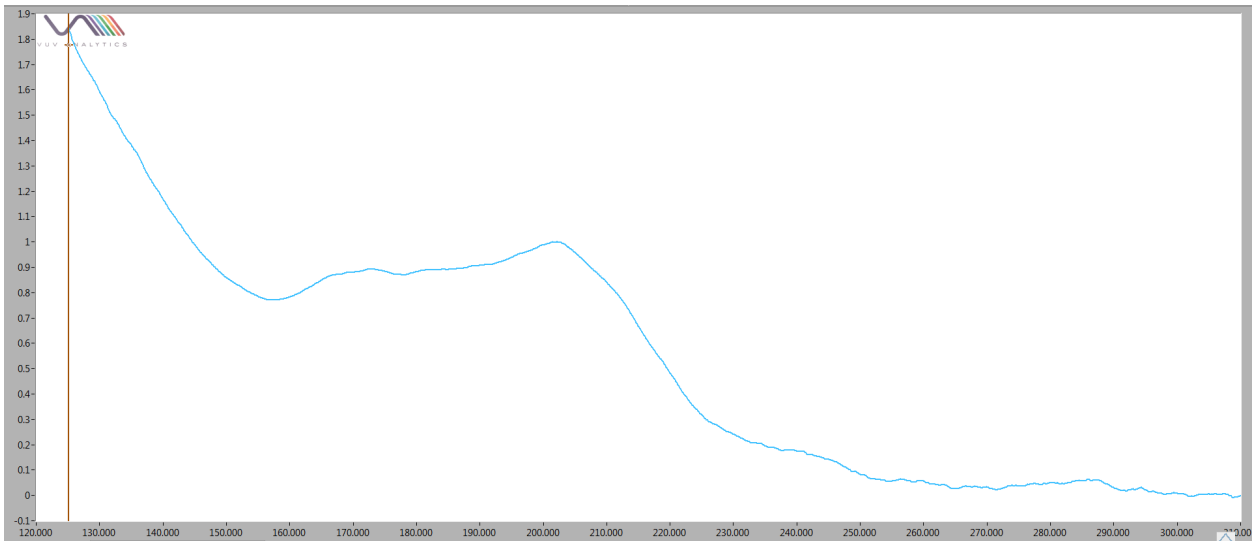


Figure 139: GC-VUV O6-monoacetylmorphine spectrum.

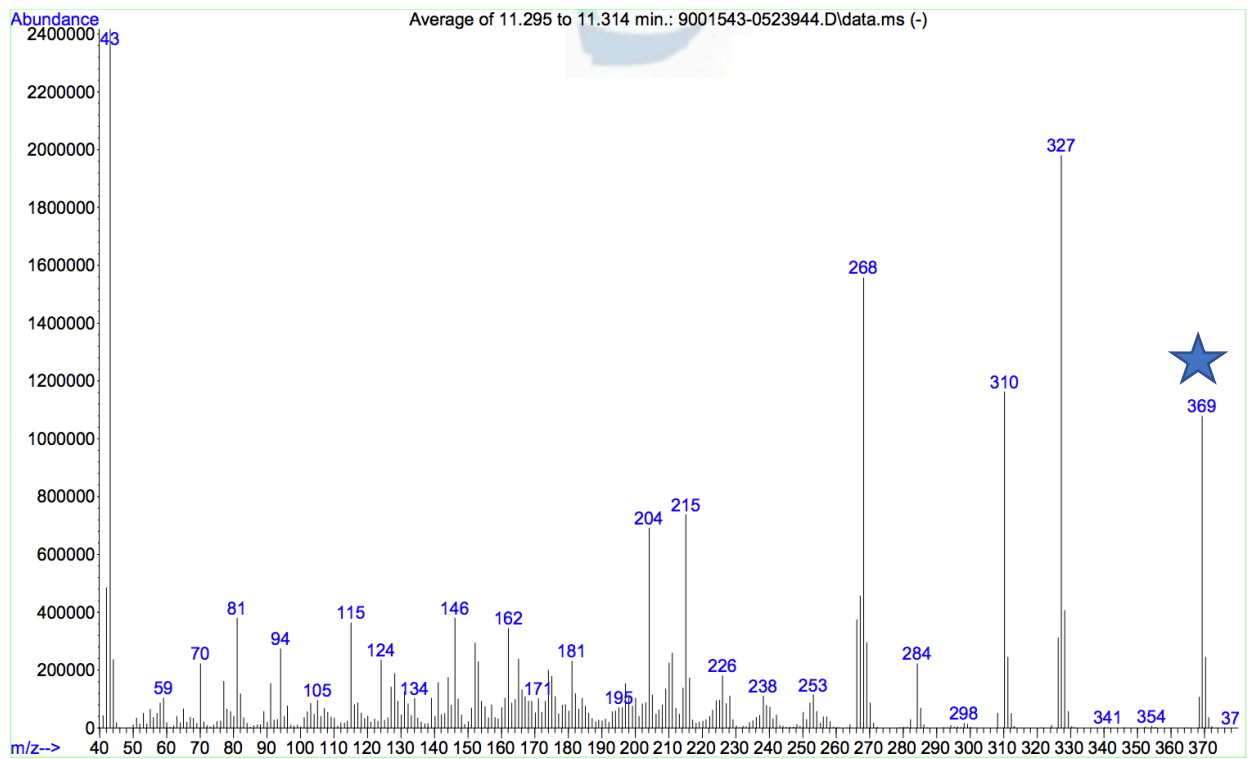


Figure 140: GC-classical EI MS heroin (mass 369) (Cayman).

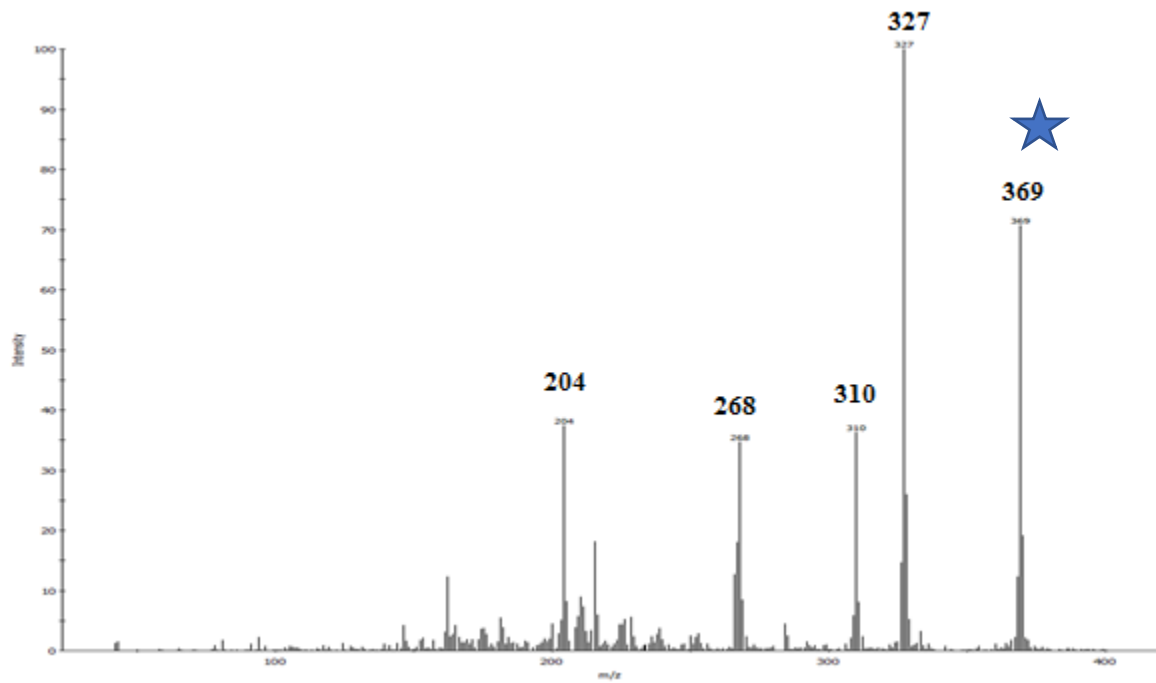


Figure 141: GC-cold EI MS heroin (mass 369).

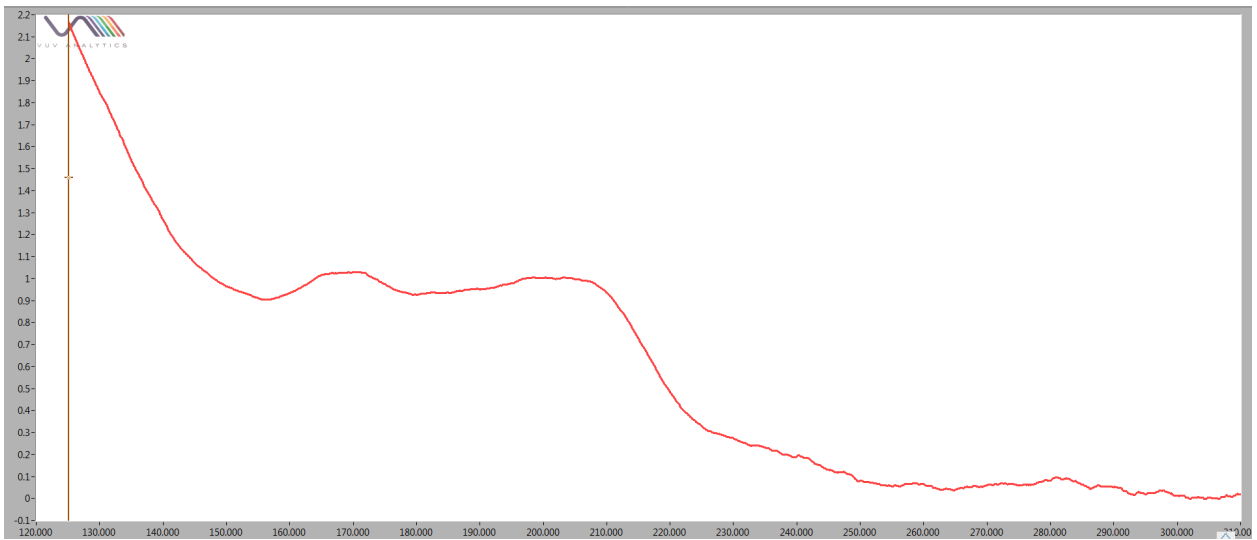


Figure 142: GC-VUV heroin spectrum.

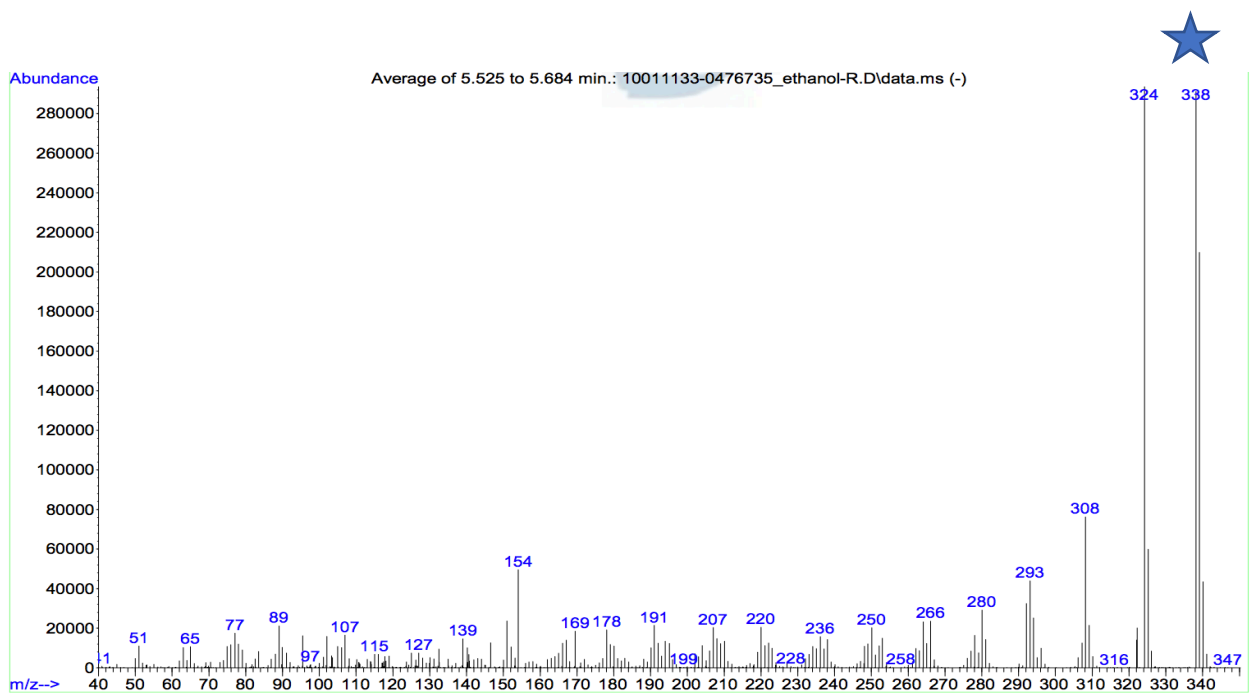


Figure 143: GC-classical EI MS papaverine (mass 338) (Cayman).

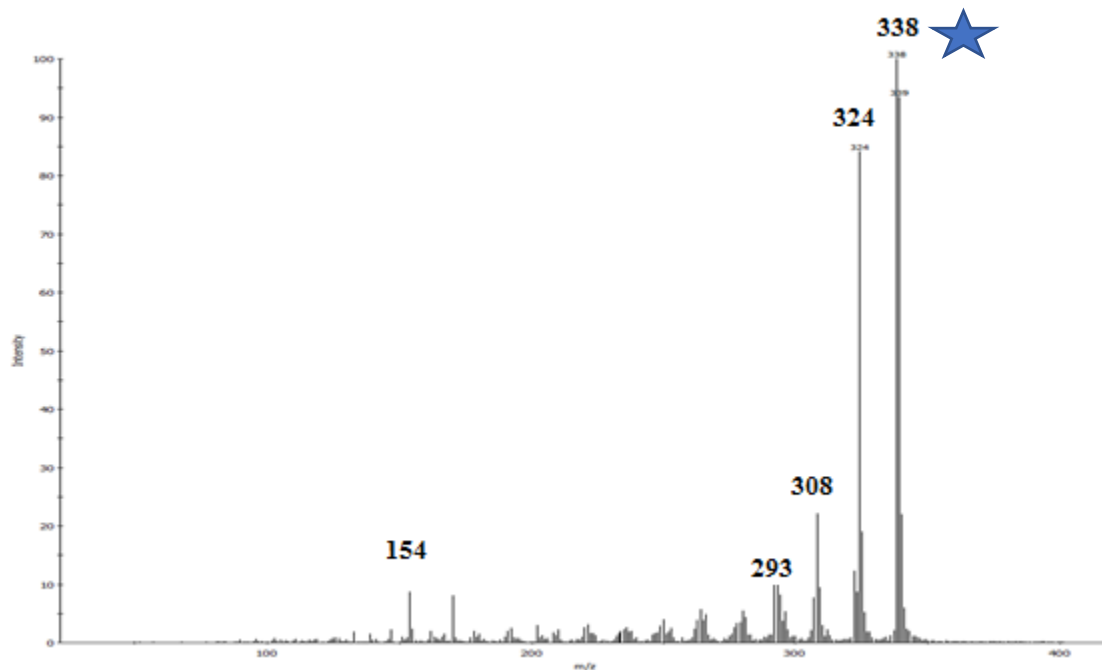


Figure 144: GC-cold EI MS papaverine (mass 338).

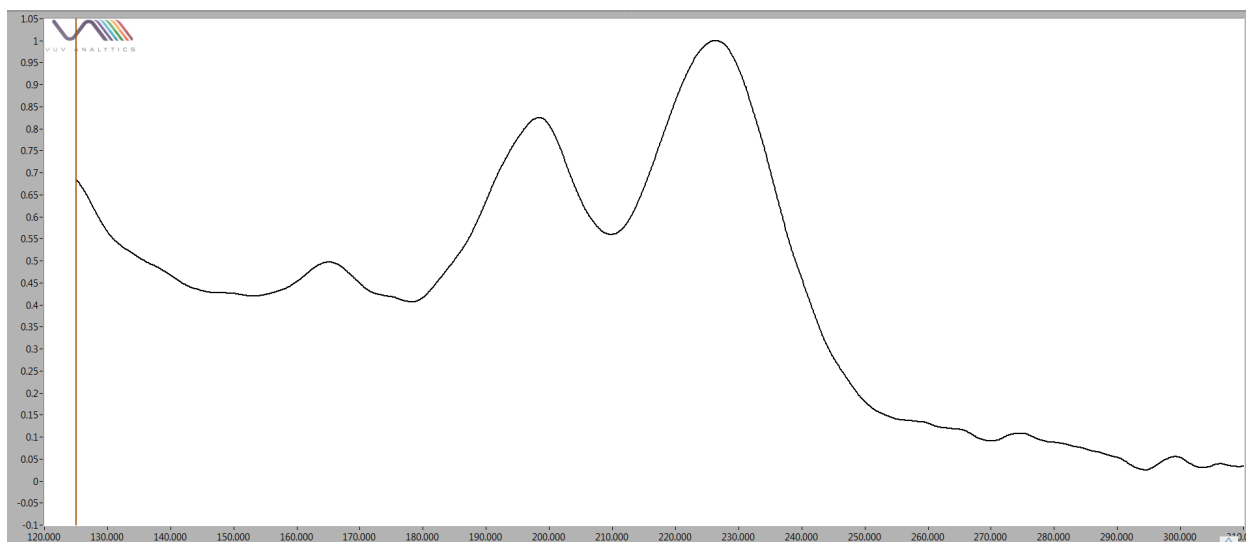


Figure 145: GC-VUV papaverine spectrum.

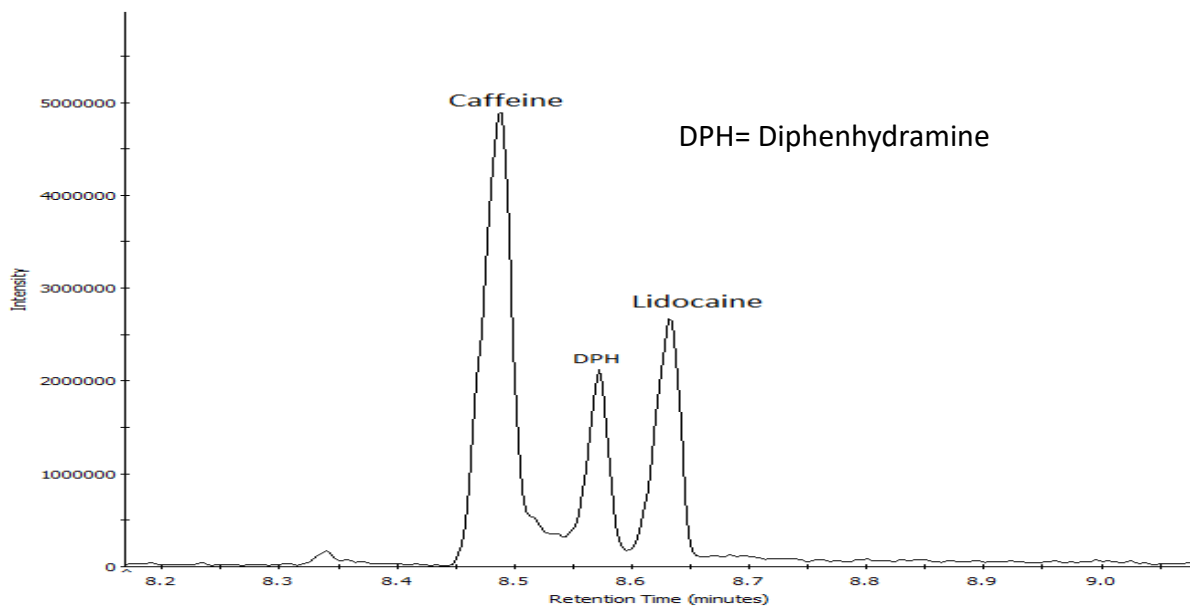


Figure 146: Cold EI MS chromatogram of selected adulterants (50 PPM each compound); see Figure 1 for GC conditions.

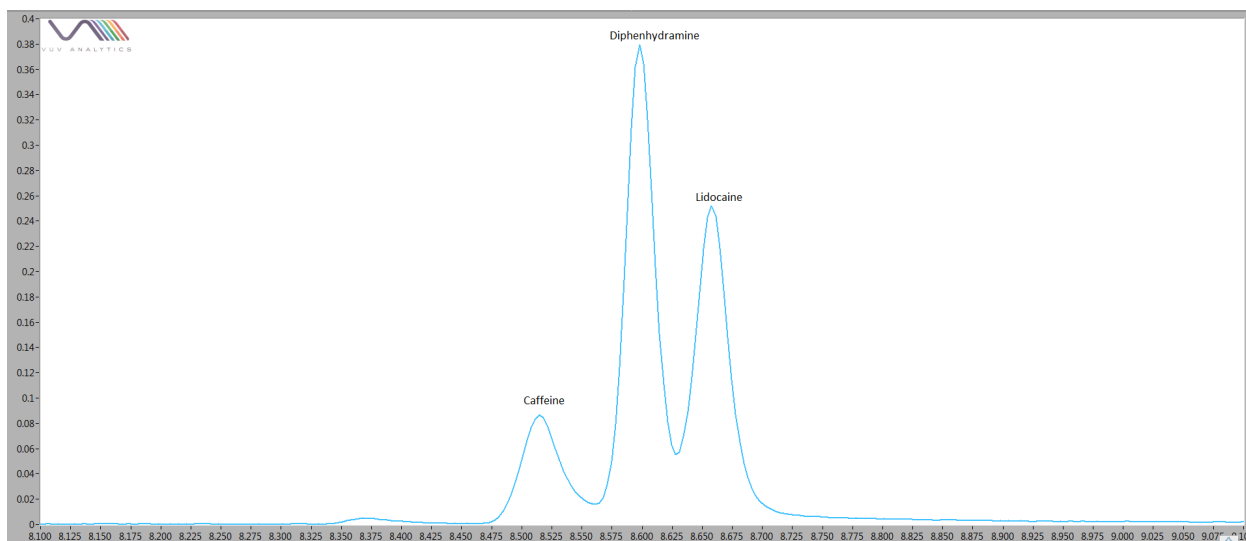


Figure 147: GC-VUV chromatogram of selected adulterants (50 PPM each compound); see Figure 1 for GC conditions.

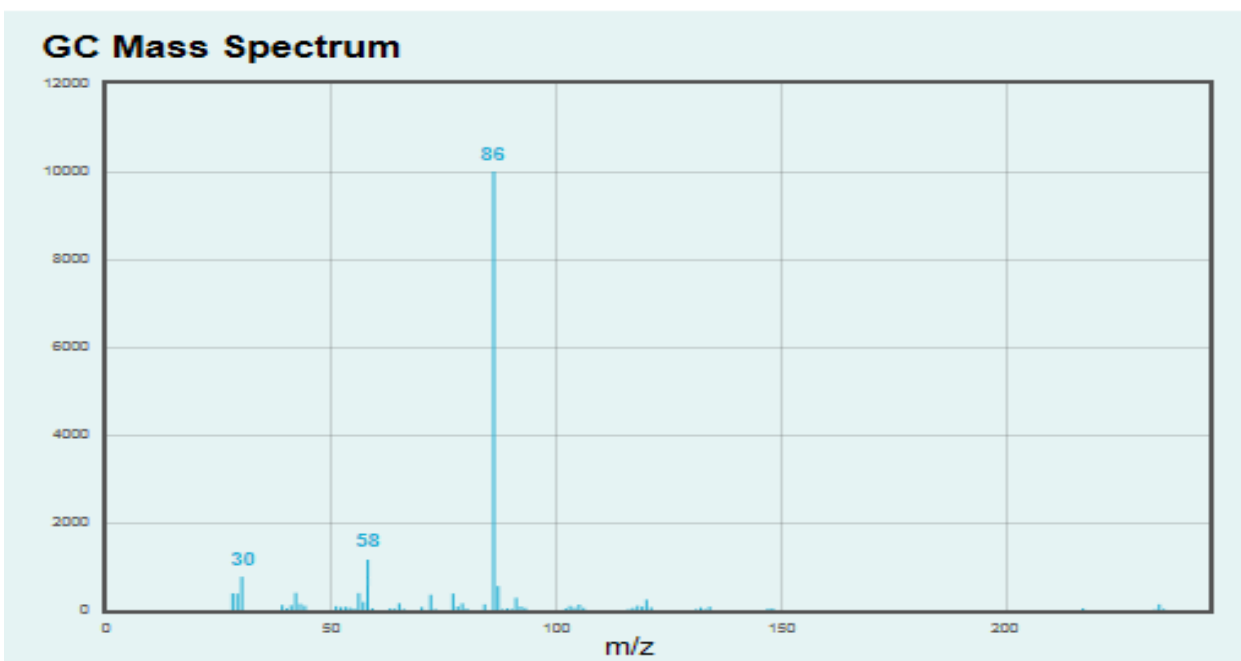


Figure 148: GC-classical EI MS lidocaine (mass 234) (Restek).

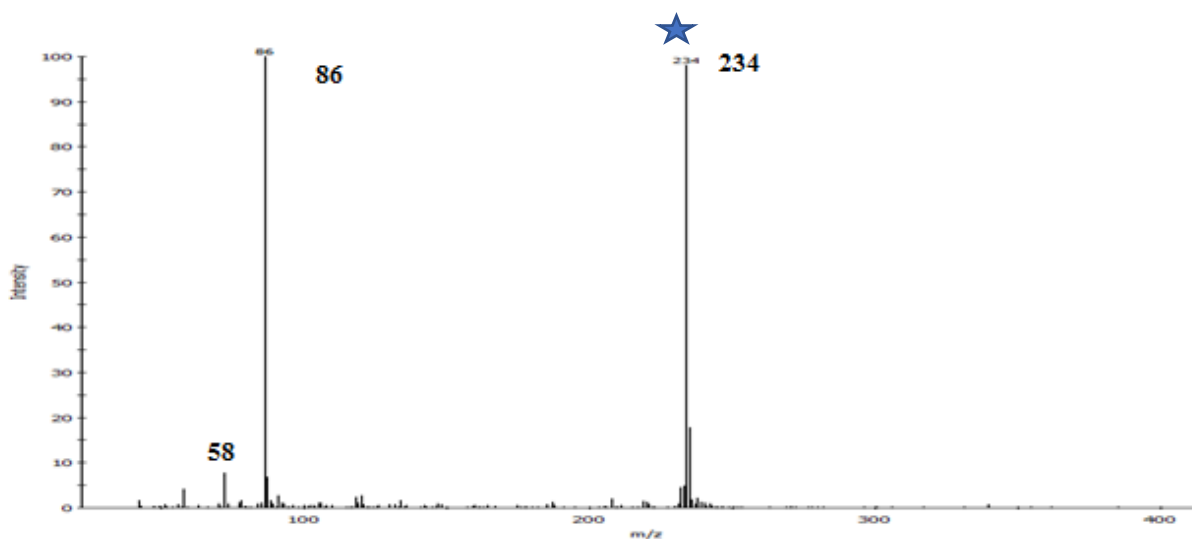


Figure 149: GC-cold EI MS lidocaine (mass 234).

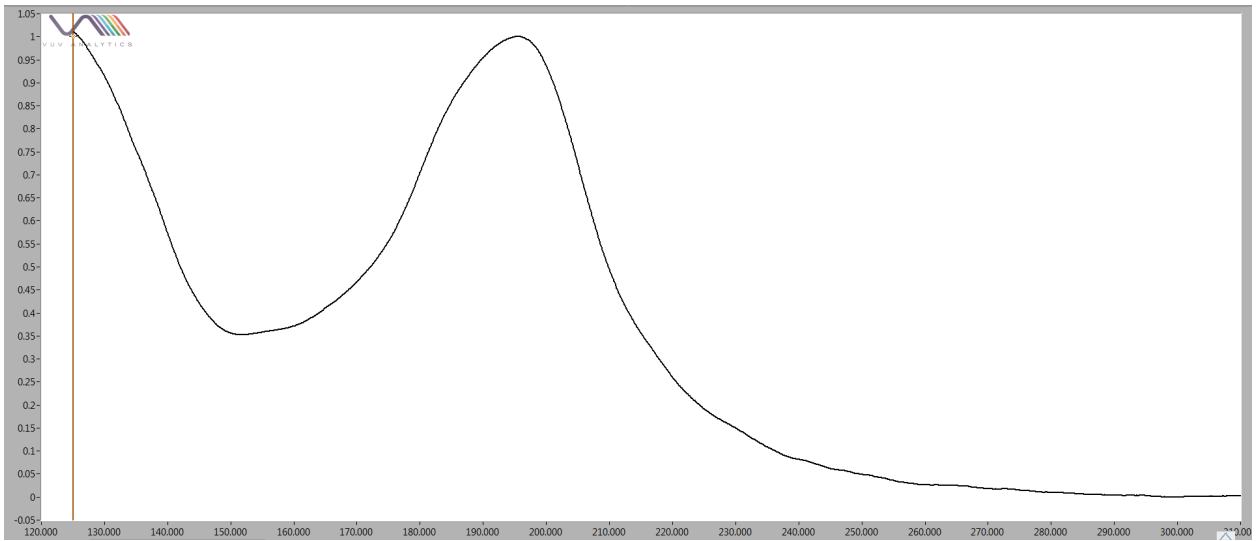


Figure 150: GC-VUV lidocaine spectrum.

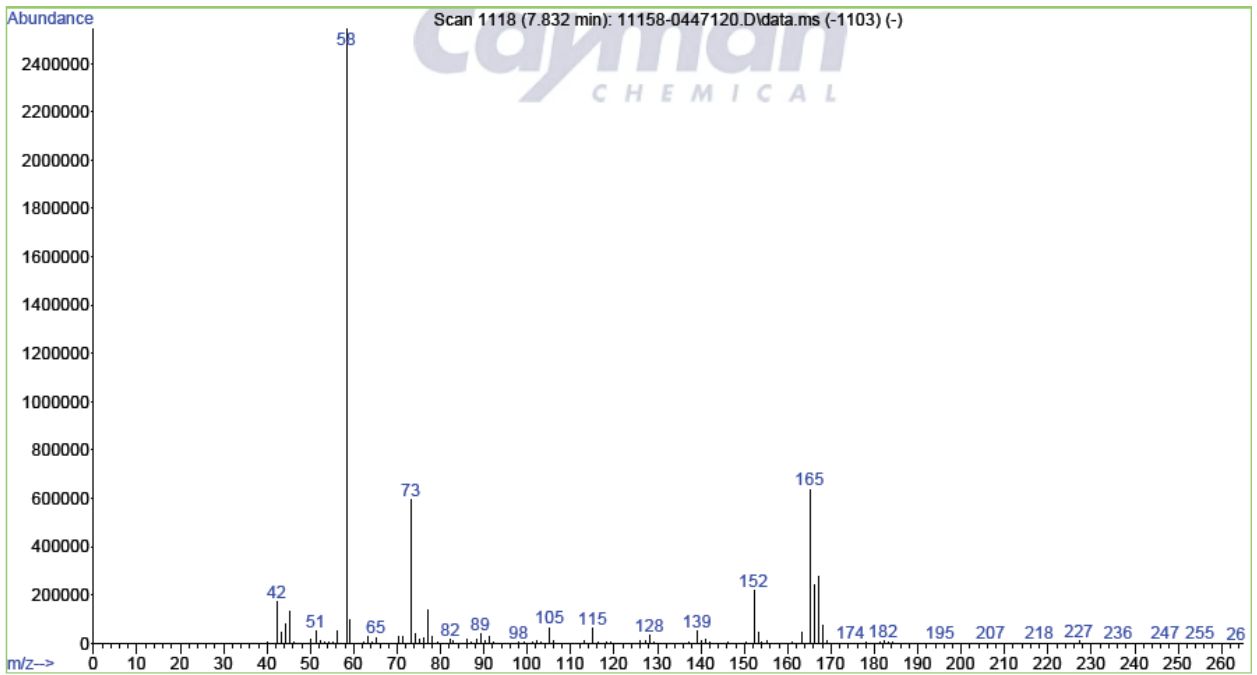


Figure 151: GC-classical EI MS diphenhydramine (mass 291) (Cayman).

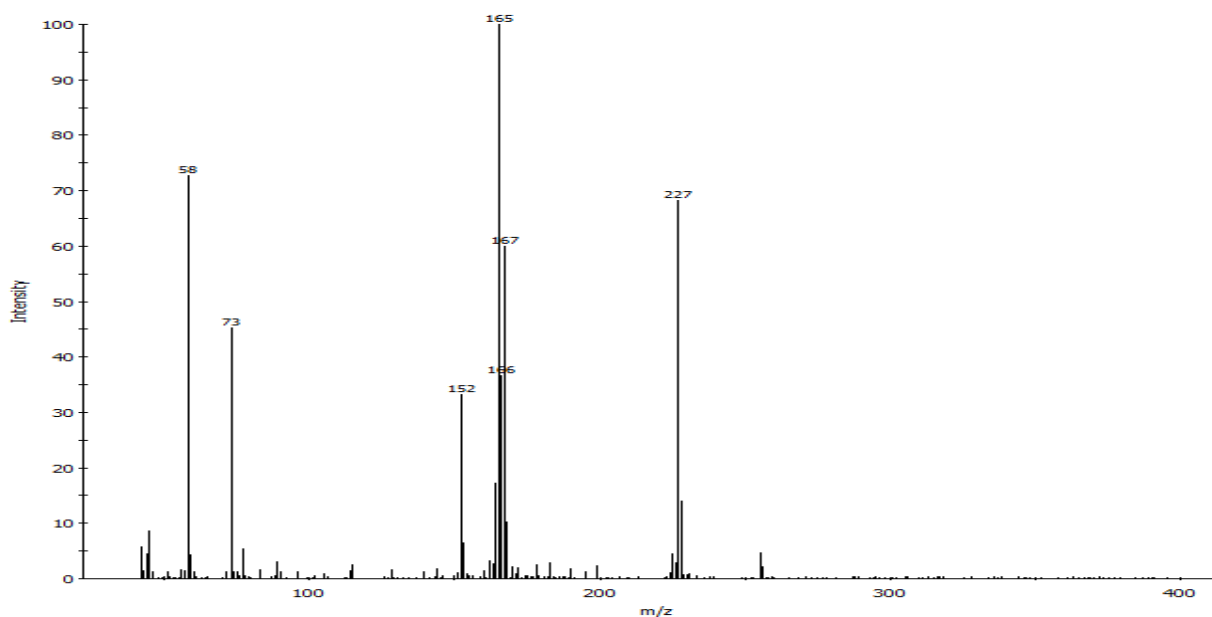


Figure 152: GC-cold EI MS diphenhydramine (mass 291) (Cayman).

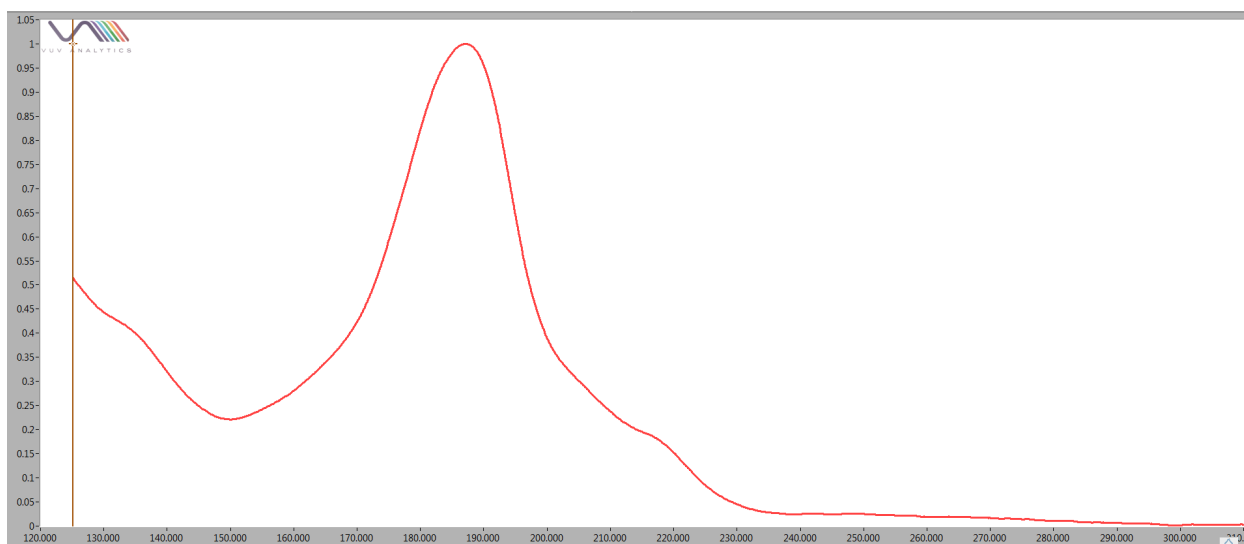


Figure 153: GC-VUV diphenhydramine spectrum.

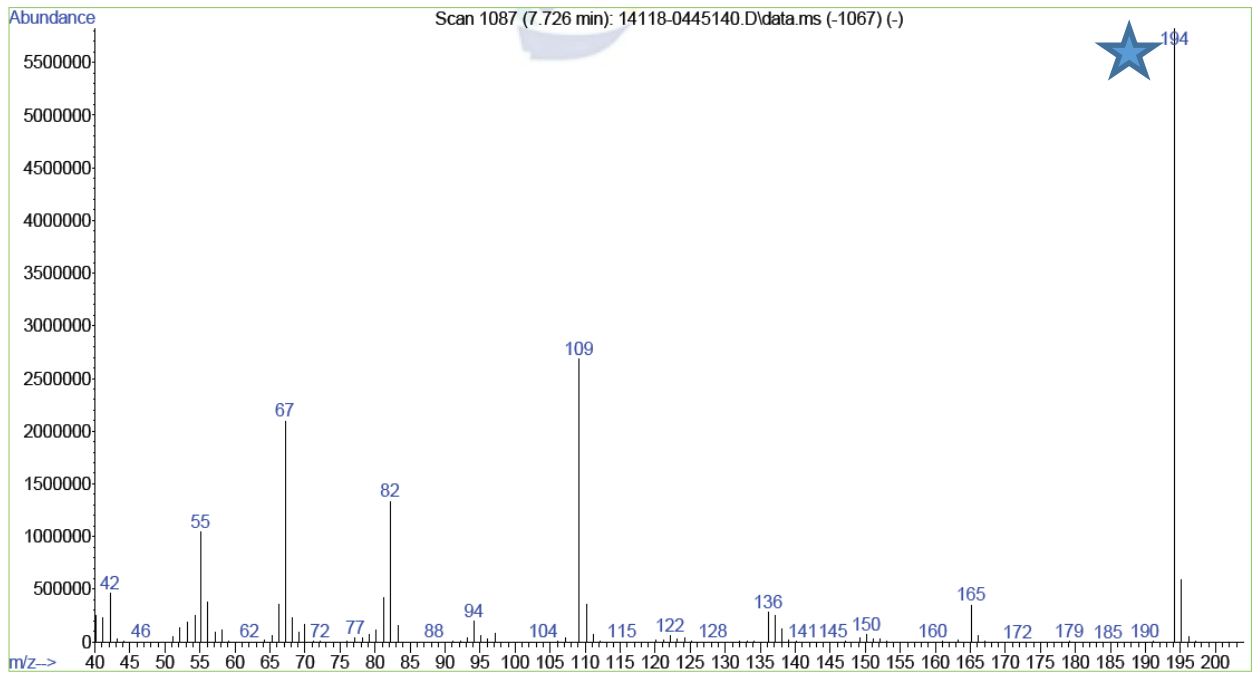


Figure 154: GC-classical EI MS caffeine (mass 194) (Cayman).

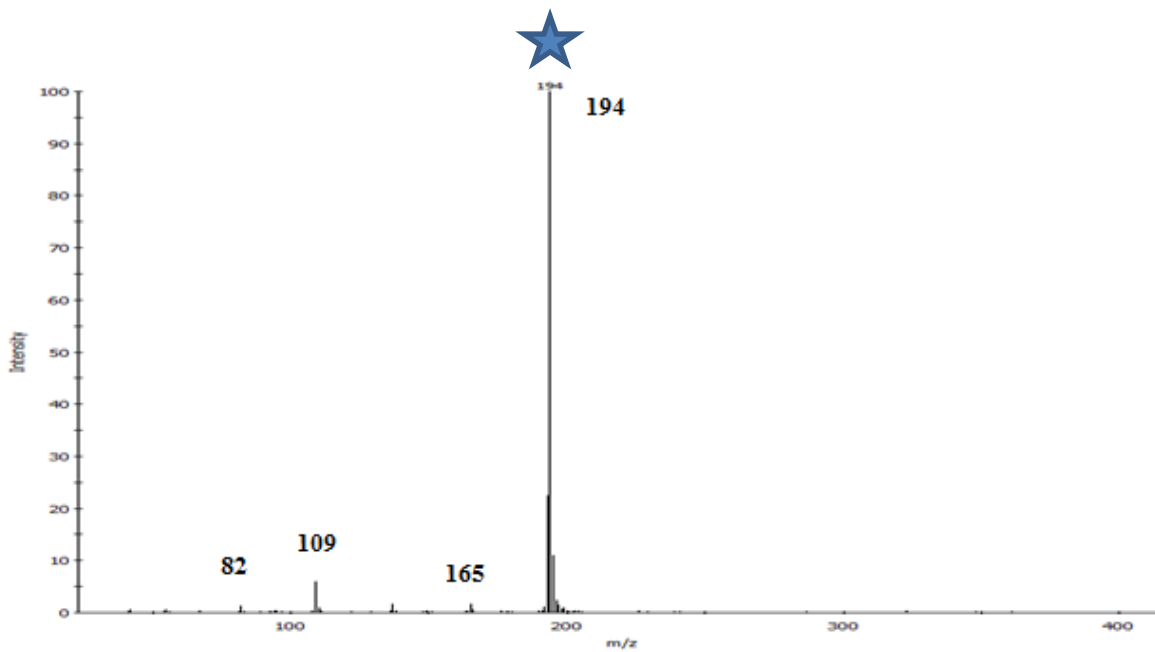


Figure 155: GC-cold EI MS caffeine (mass 194).

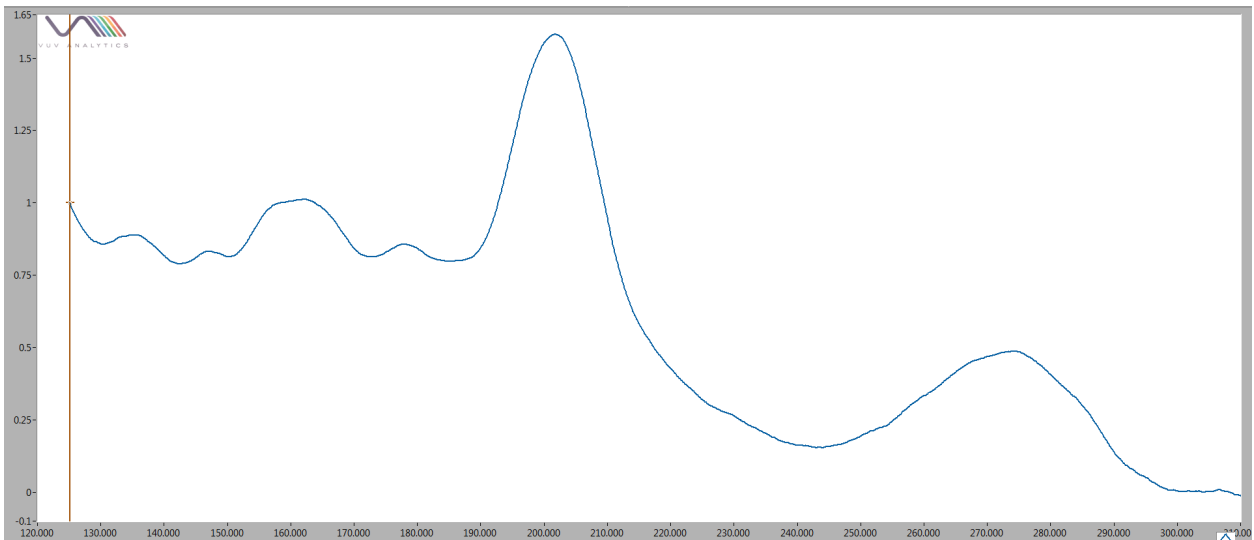


Figure 156: GC-VUV caffeine spectrum.

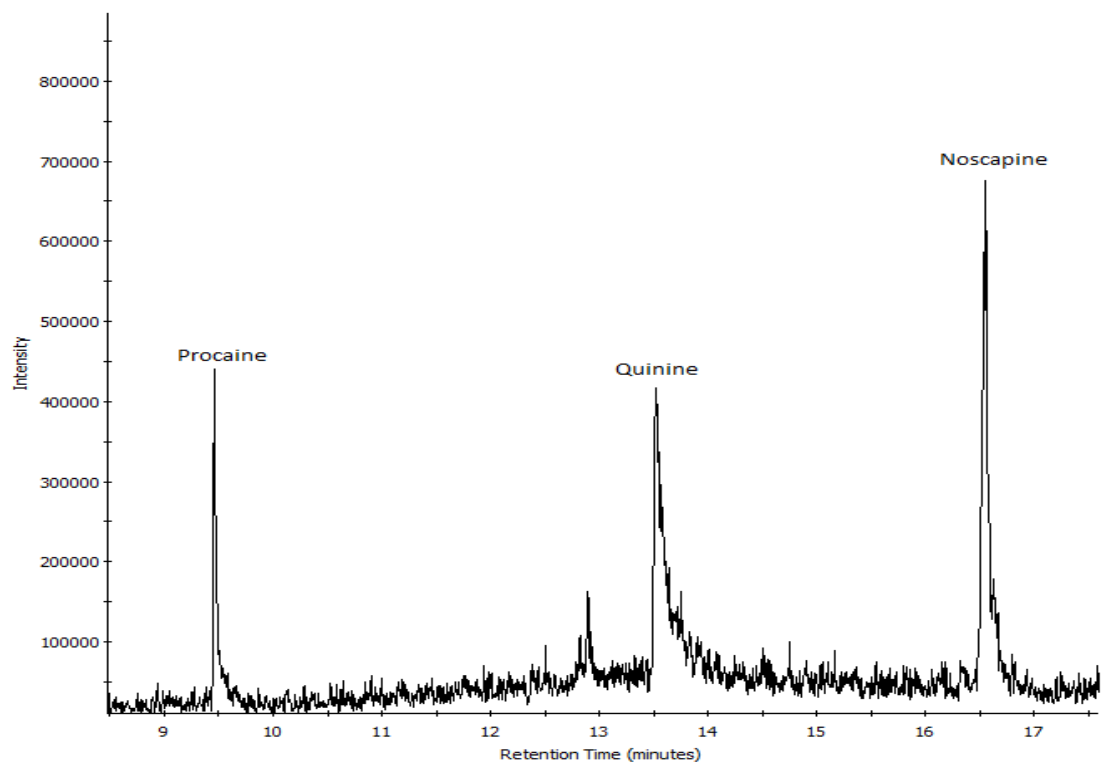


Figure 157: GC-cold EI MS chromatogram of selected adulterants (500 PPM each compound); see Figure 1 for GC conditions.

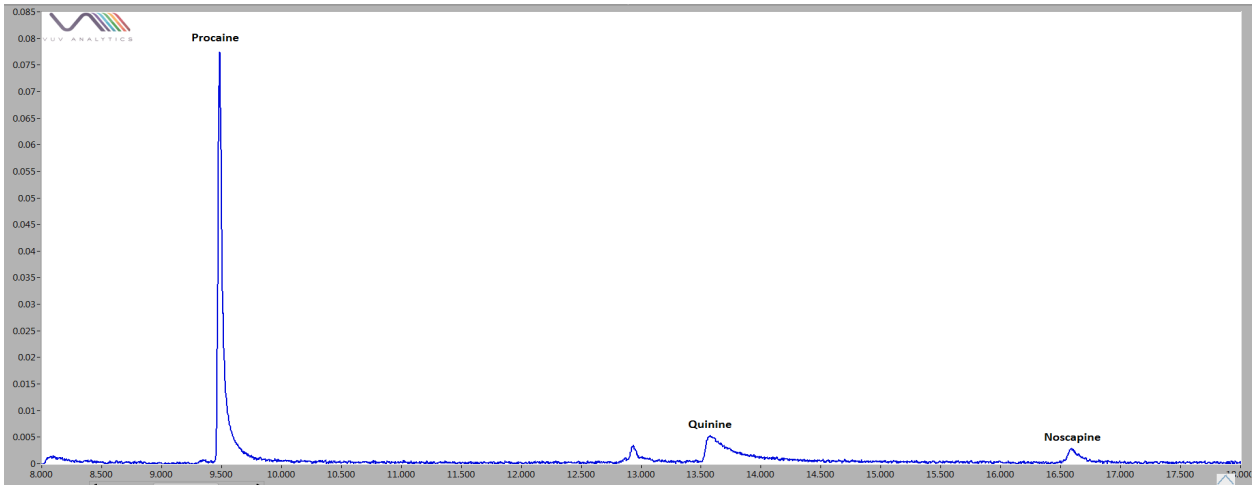


Figure 158: GC-VUV chromatogram of selected adulterants (500 PPM each compound); see Figure 1 for GC conditions.

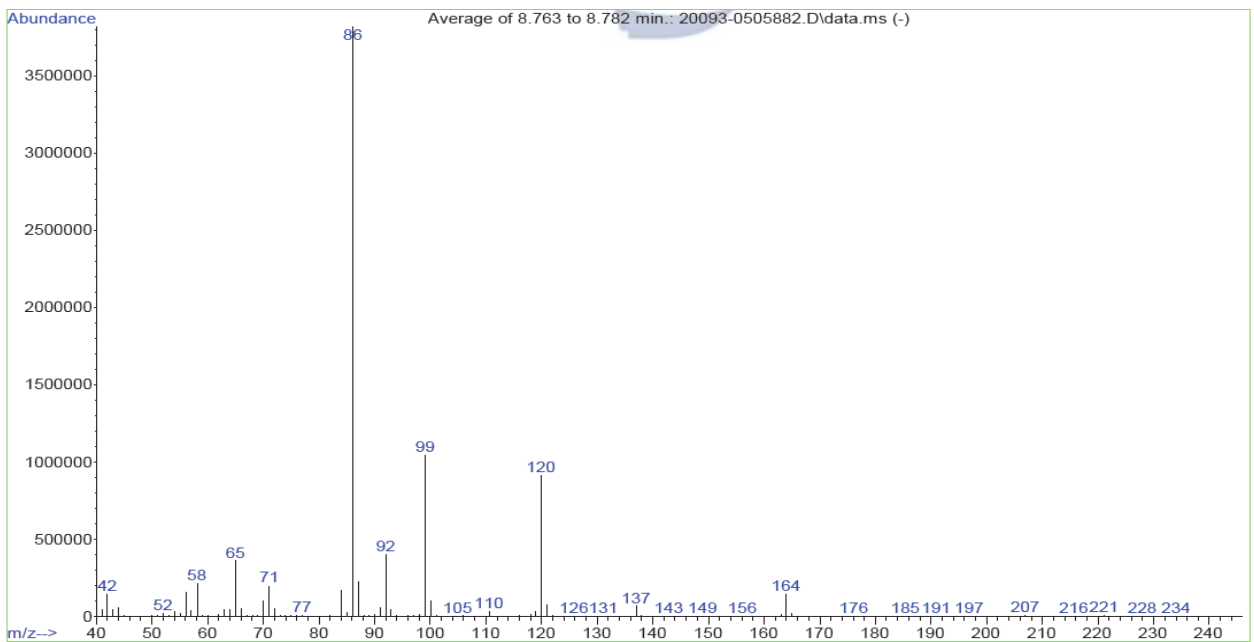


Figure 159: GC-classical EI MS procaine (mass 236) (Cayman).

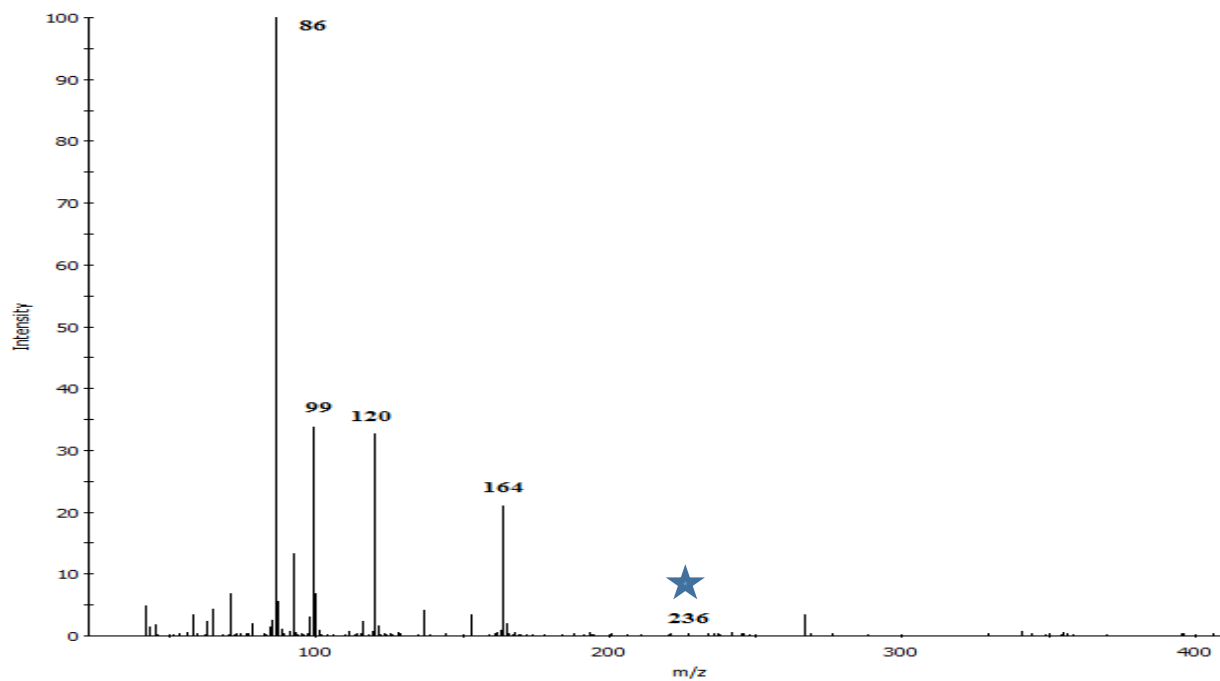


Figure 160: GC-cold EI MS procaine (mass 236).

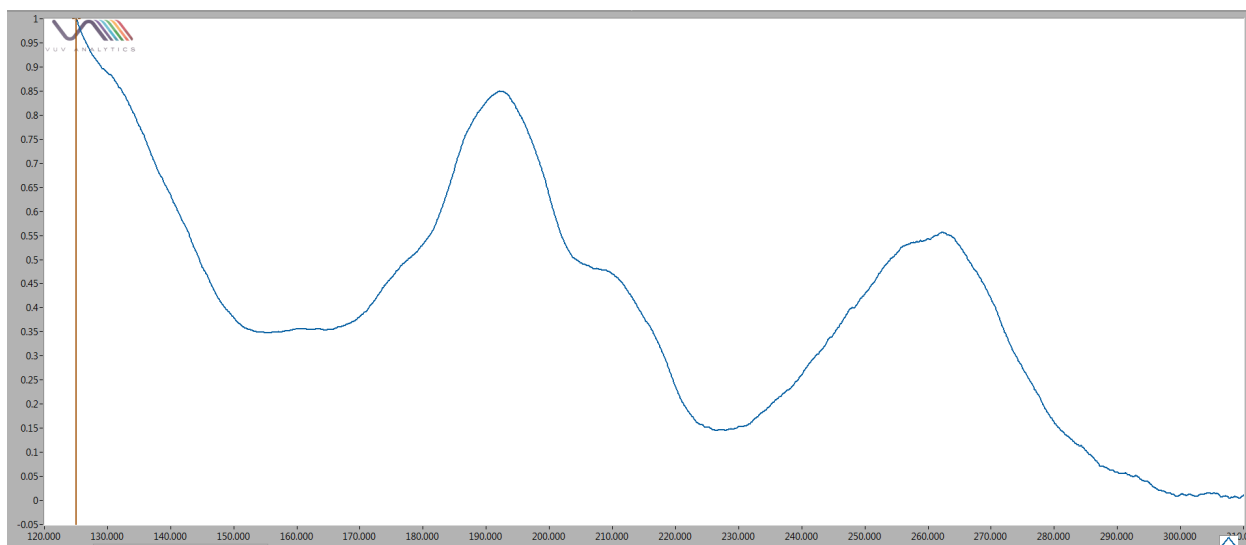


Figure 161: GC-VUV procaine spectrum.

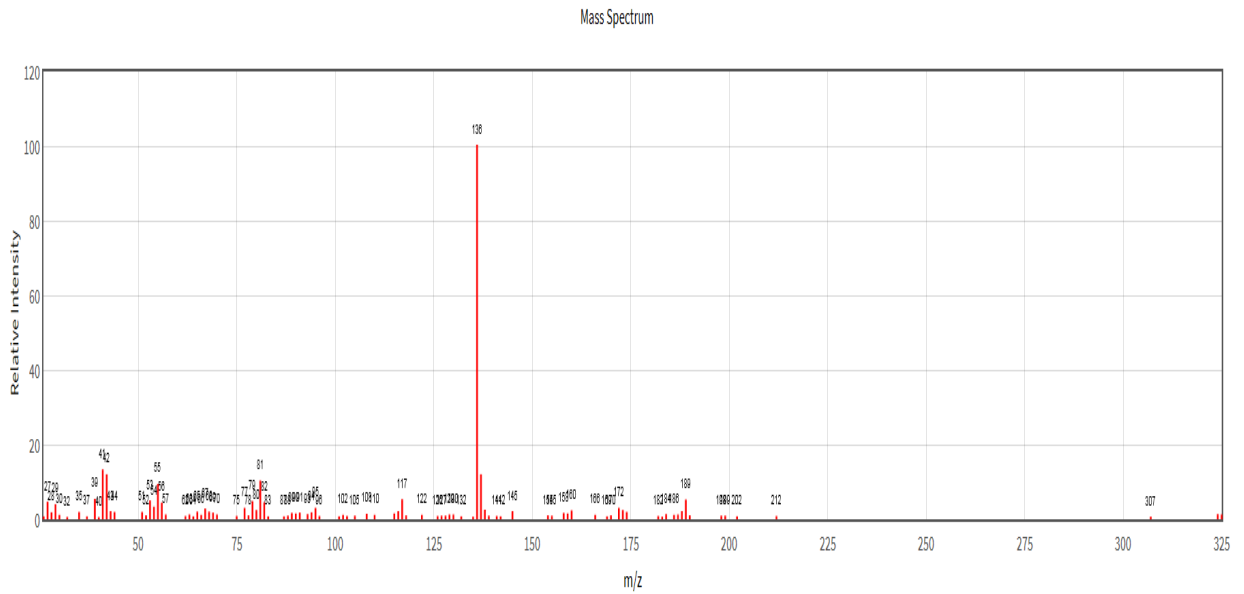


Figure 162: GC-classical EI MS quinine (mass 324) (NIST).

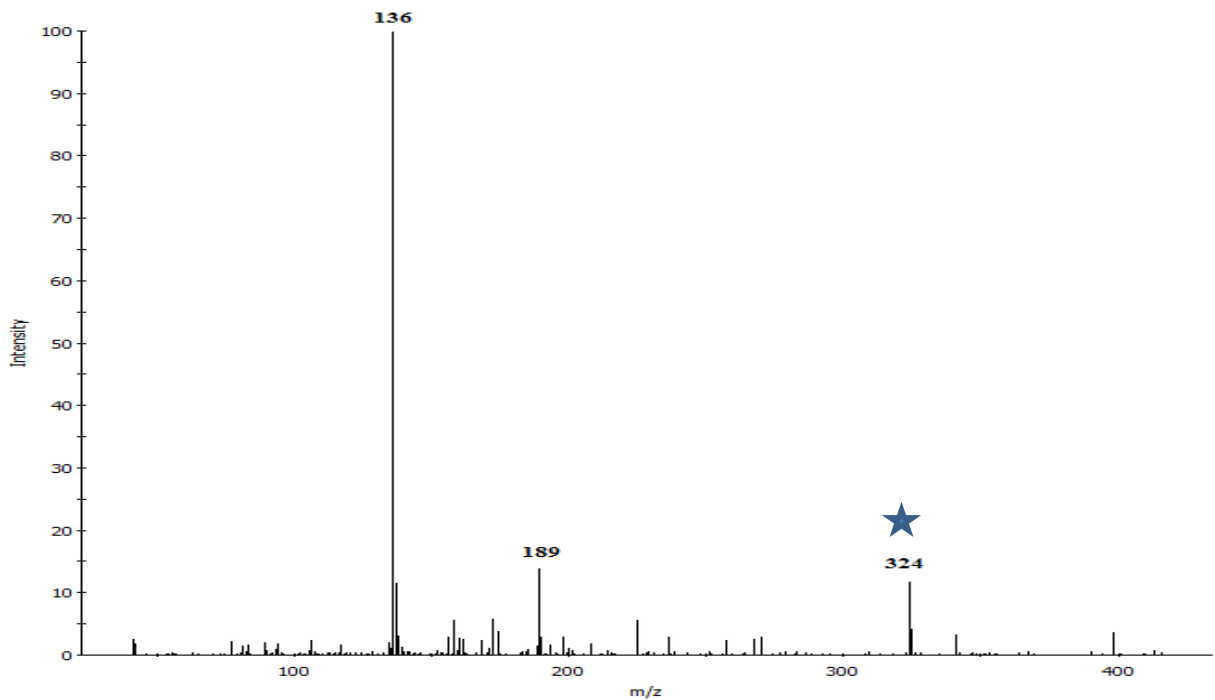


Figure 163: GC-cold EI MS quinine (mass 324).

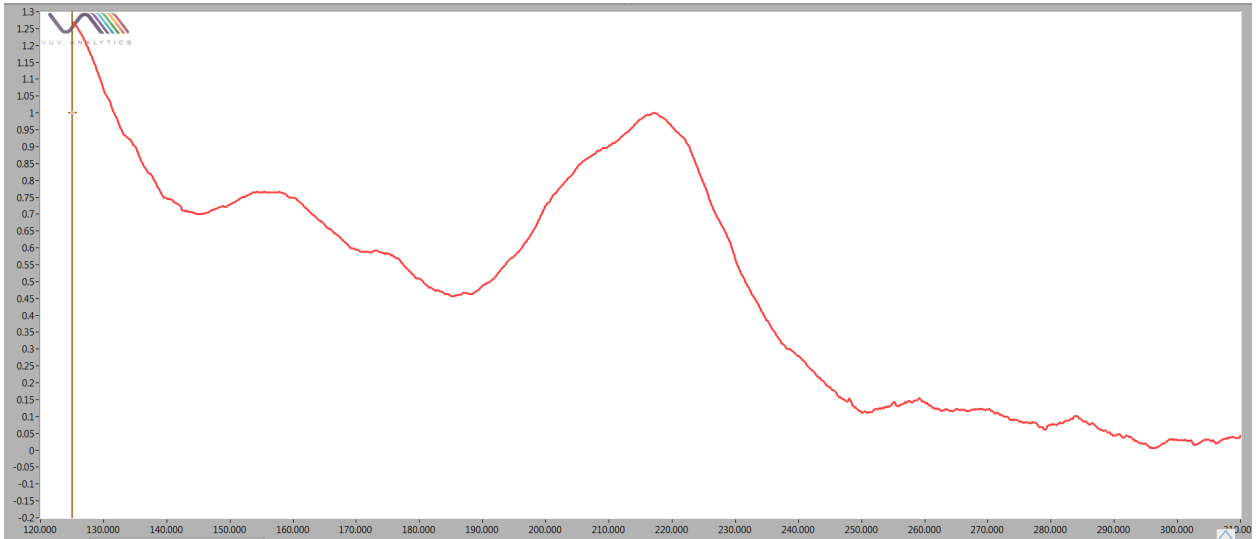


Figure 164: GC-VUV quinine spectrum.

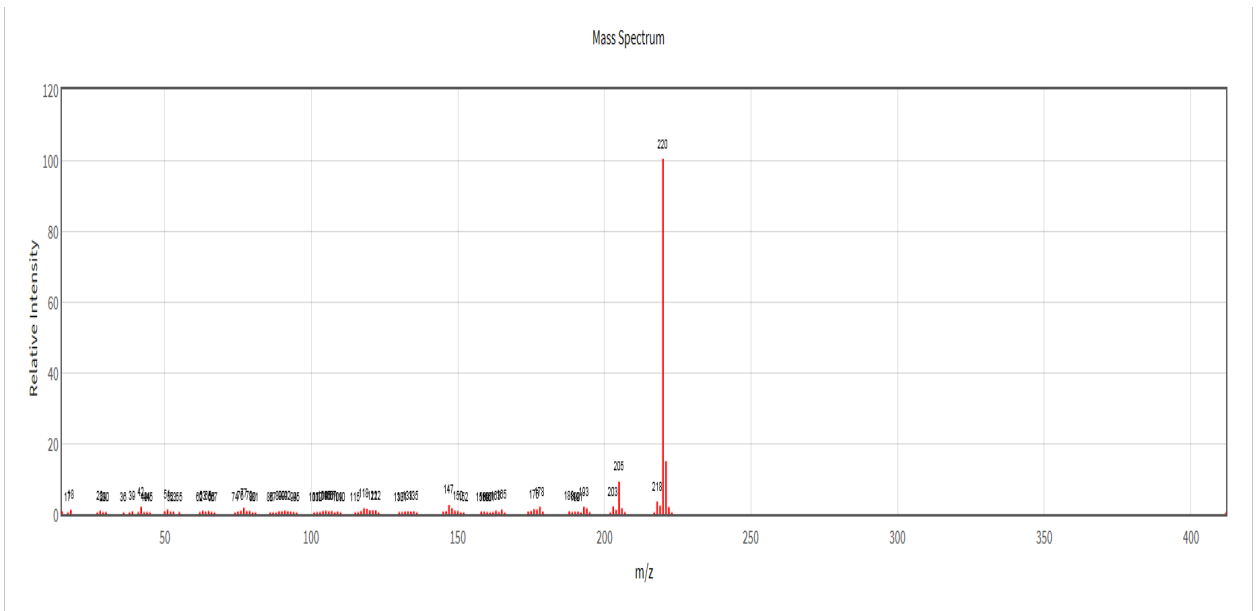


Figure 165: GC-classical EI MS noscapine (mass 324) (NIST).

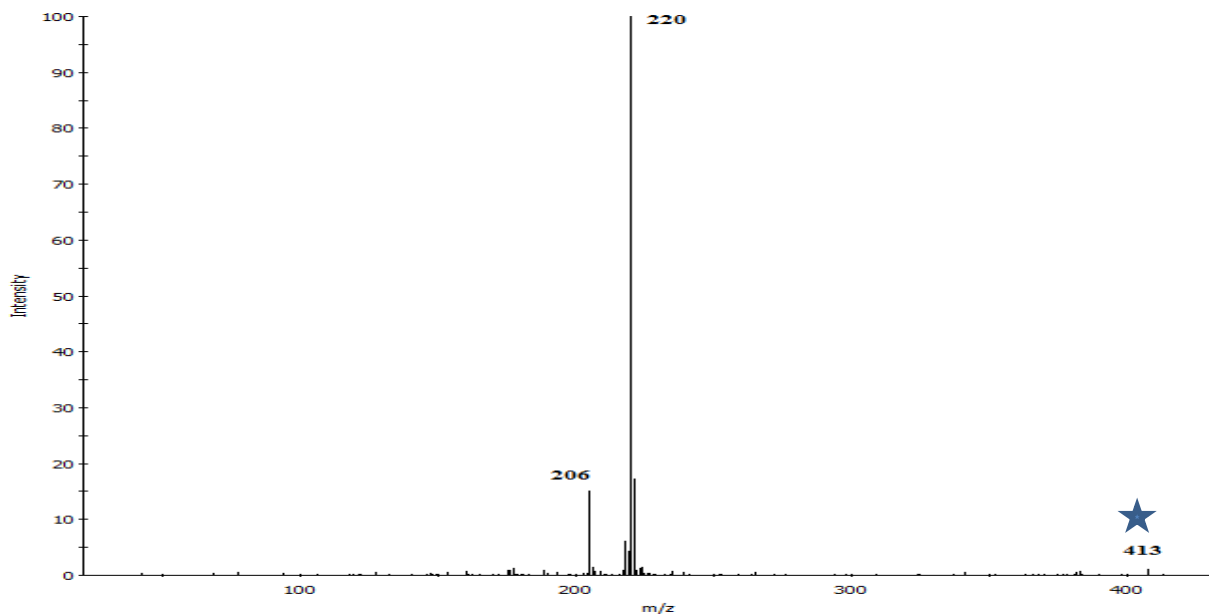


Figure 166: GC-cold EI MS noscapine (mass 324).

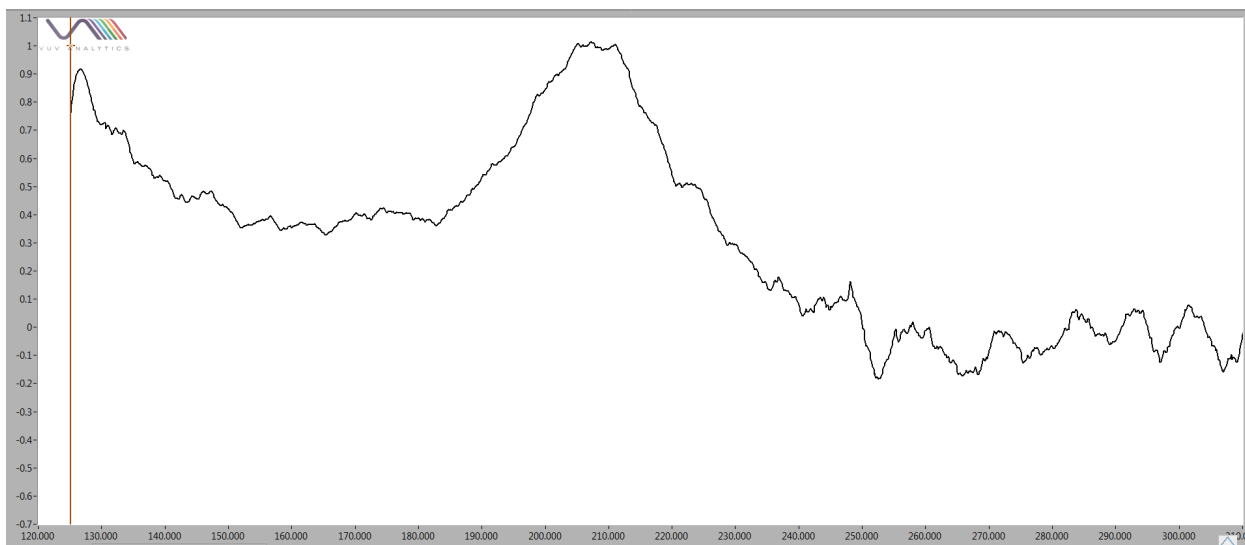


Figure 167: GC-VUV noscapine spectrum.

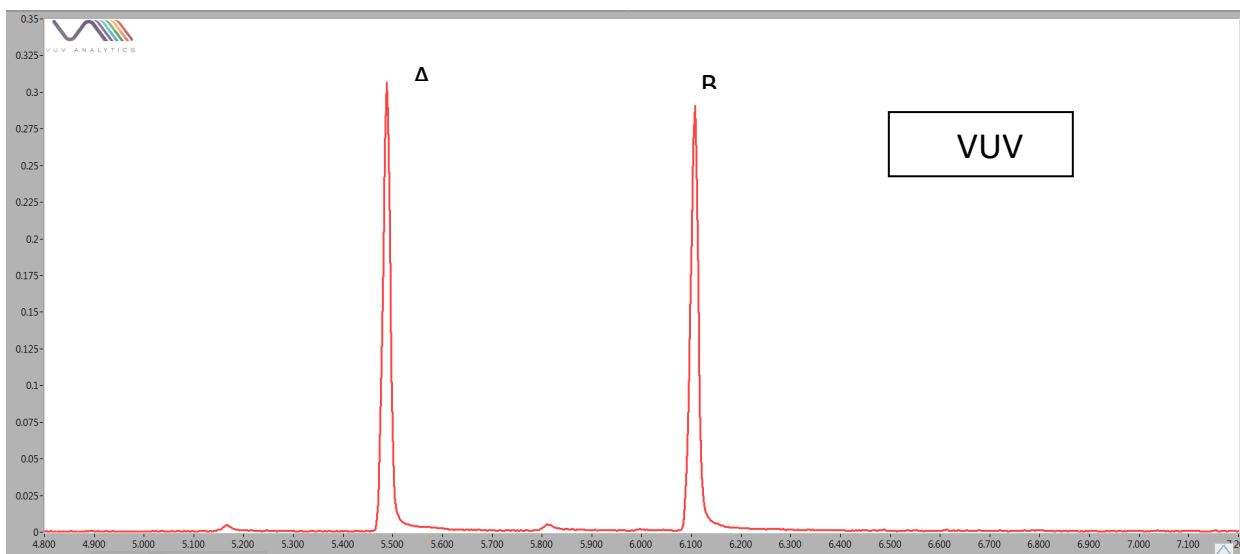
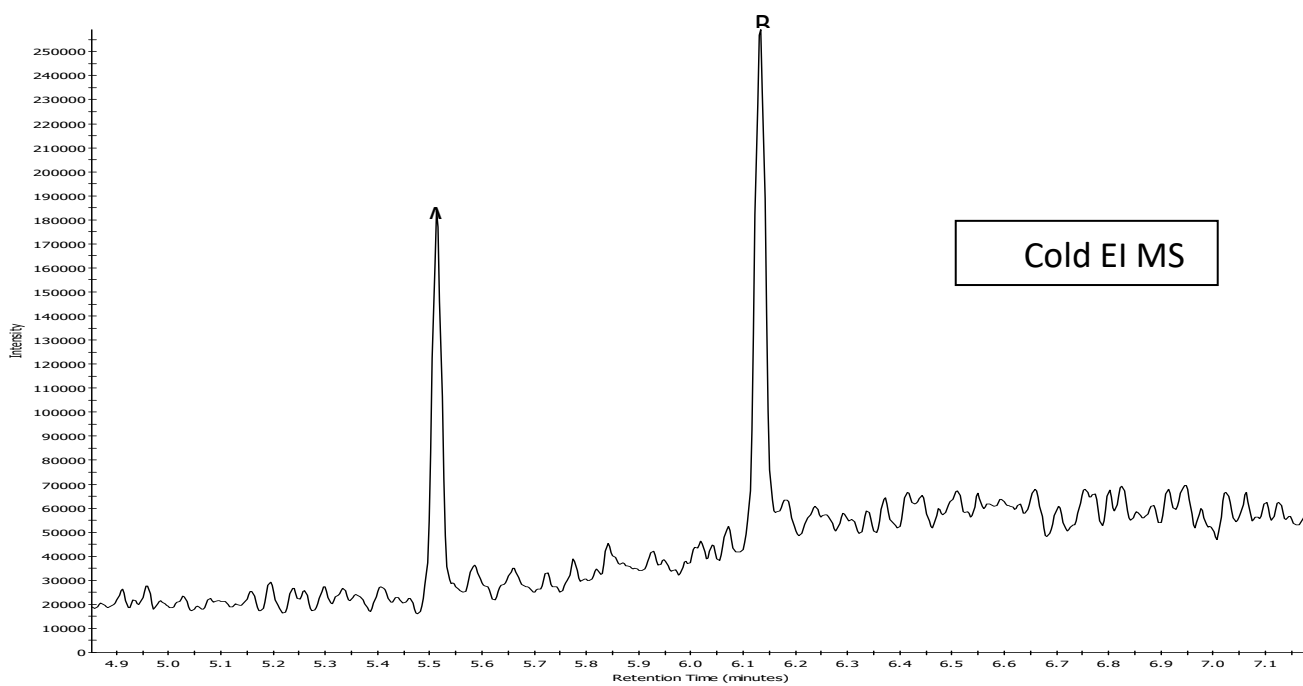
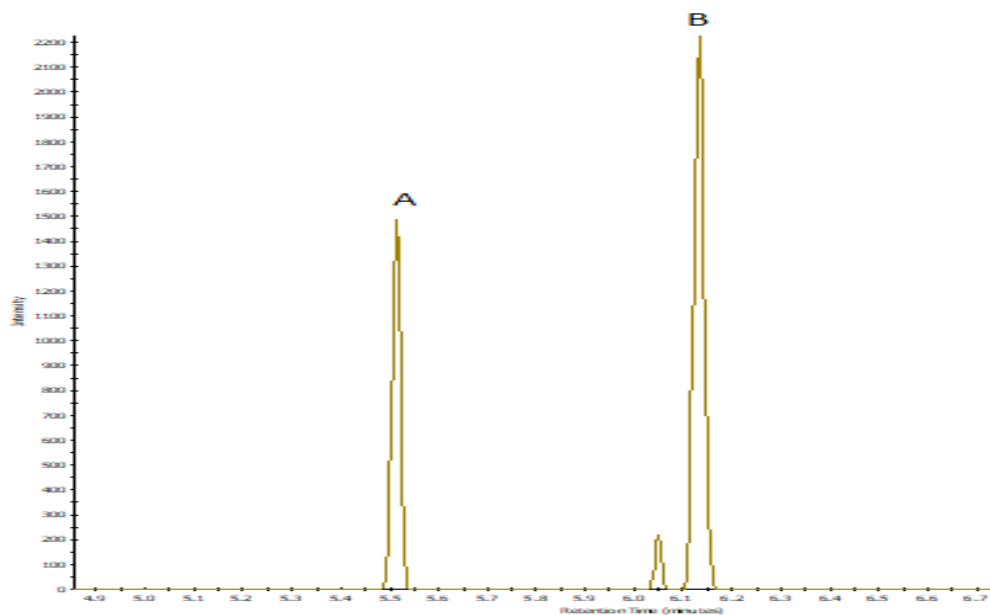
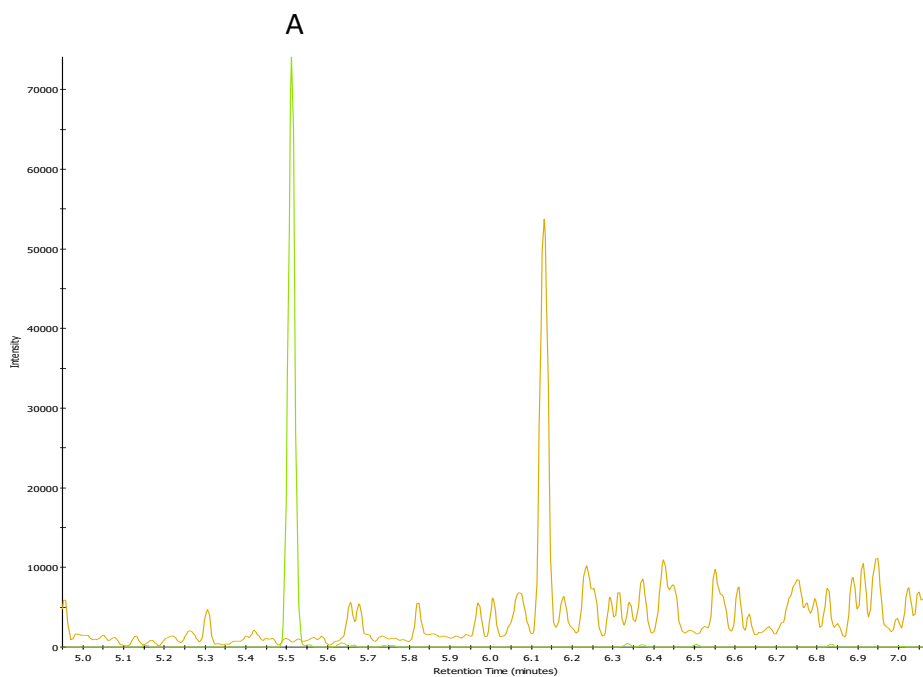


Figure 168: Simultaneous Cold EI MS and VUV detection for a mixture 300 ppm each of mass 163 positional isomers of synthetic cathinones. See Table 2 for peak identity.



m/z 163 (molecular ion)



**(A) Green= m/z 58, (B) Orange= m/z 44 (base peaks)**

Figure 169: Extracted ion chromatograms for a mixture 300 ppm each of mass 163 positional isomers of synthetic cathinones. See Table 2 for peak identity.

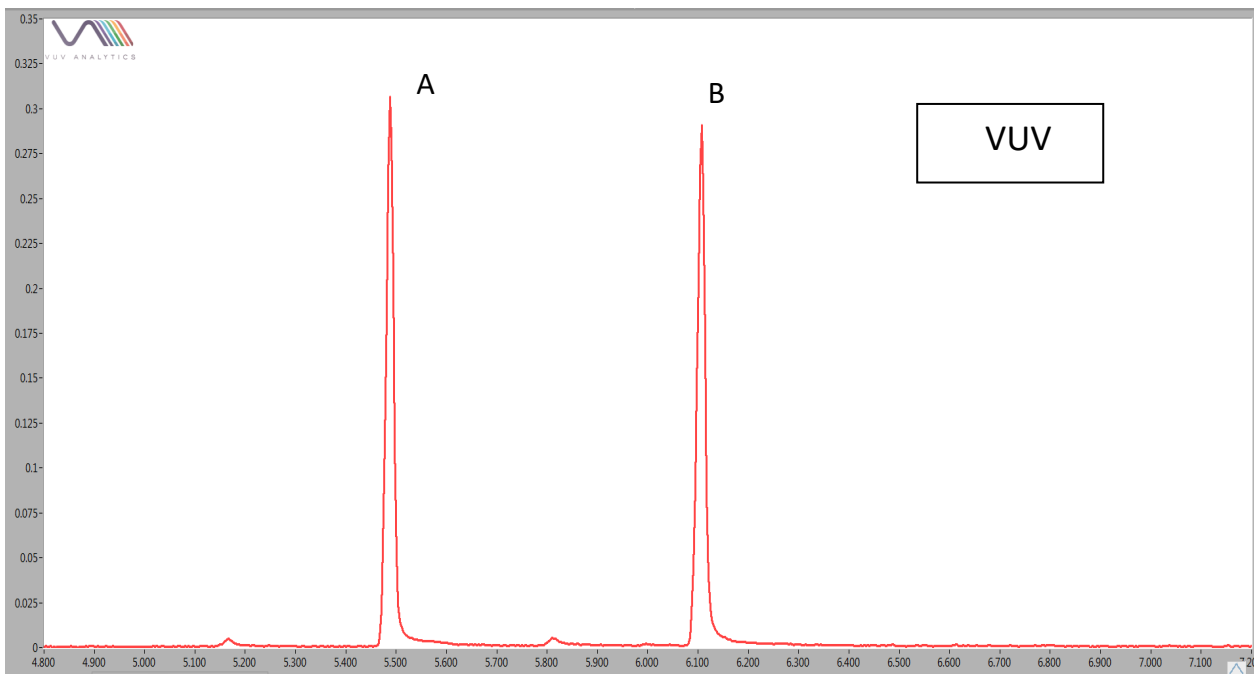
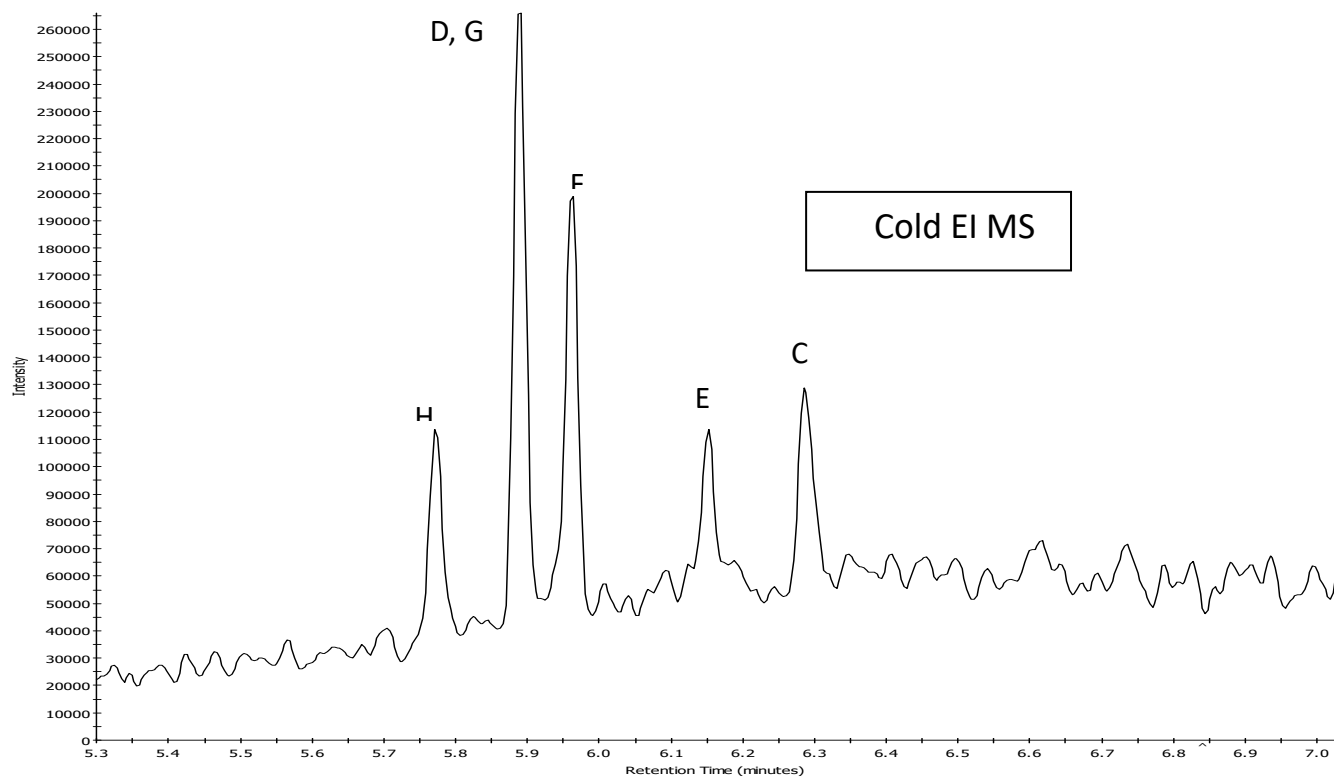
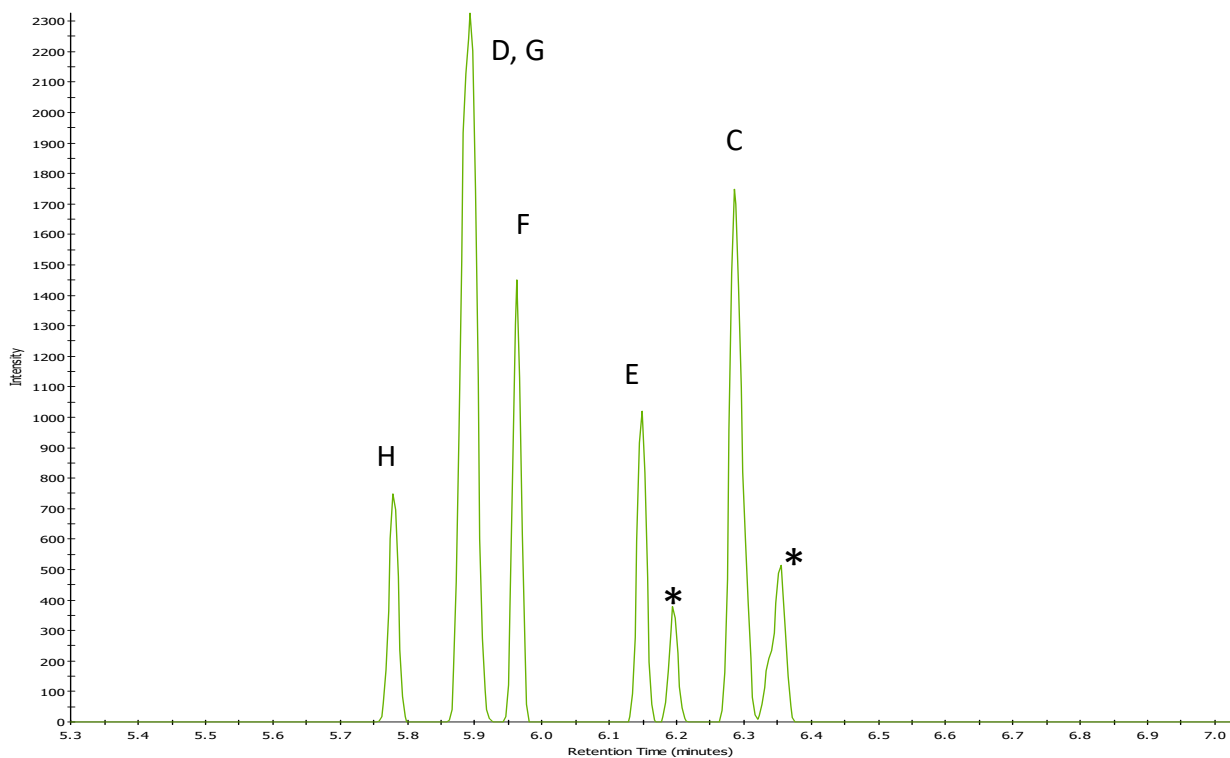
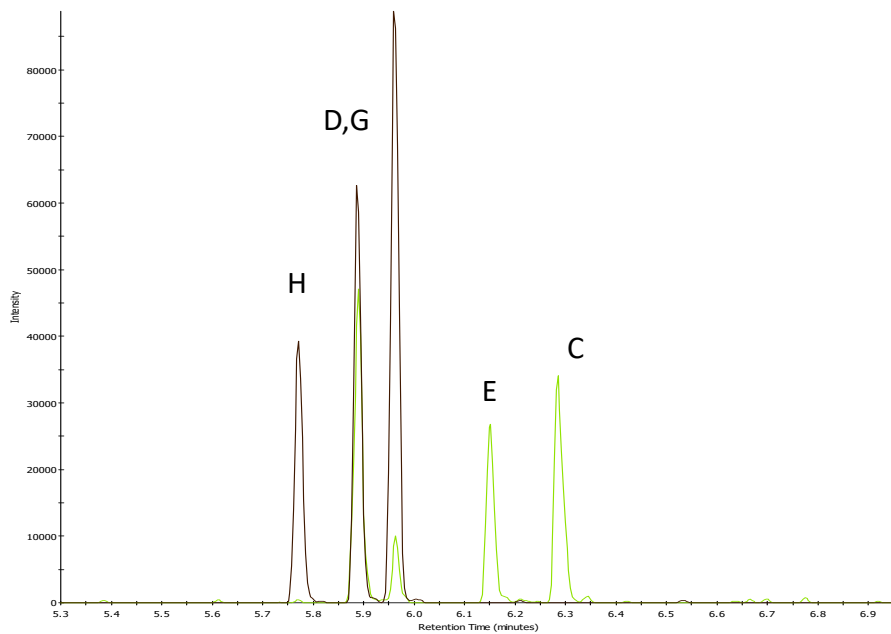


Figure 170: Simultaneous Cold EI MS and VUV detection for a mixture 300 ppm each of mass 177 positional isomers of synthetic cathinones. See Table 2 for peak identity.



m/z 177 (molecular ion)



(H, D, G, F) Black= m/z 72, (E, C) Green= m/z 58

Figure 171: Extracted ion chromatograms for a mixture 300 ppm each of mass 177 positional isomers of synthetic cathinones. See Table 2 for peak identity.

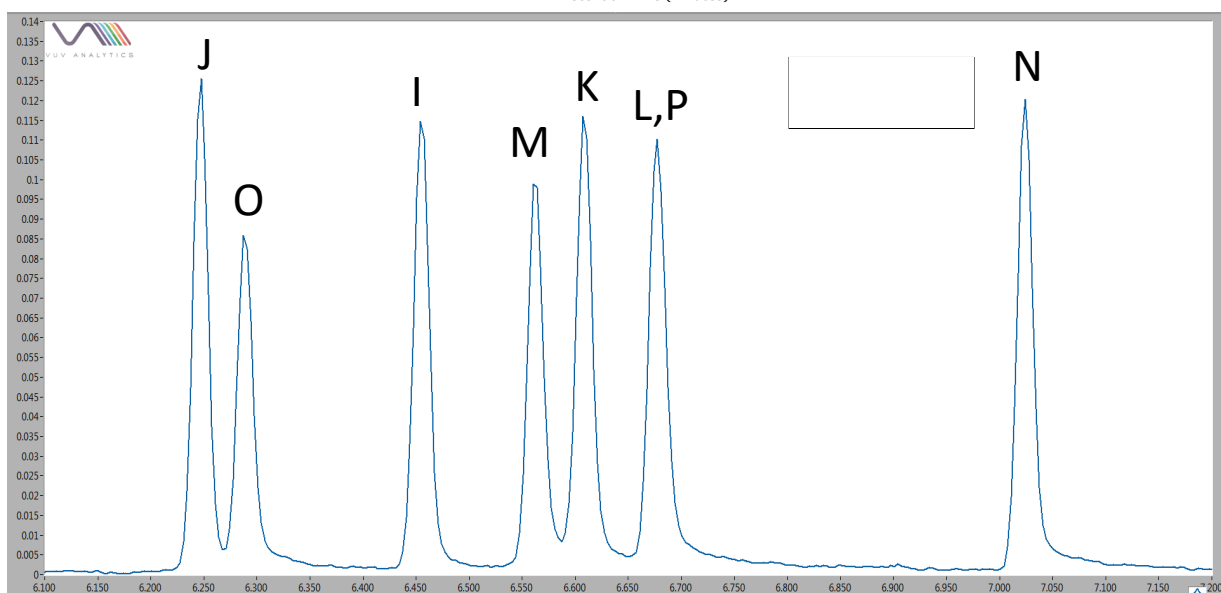
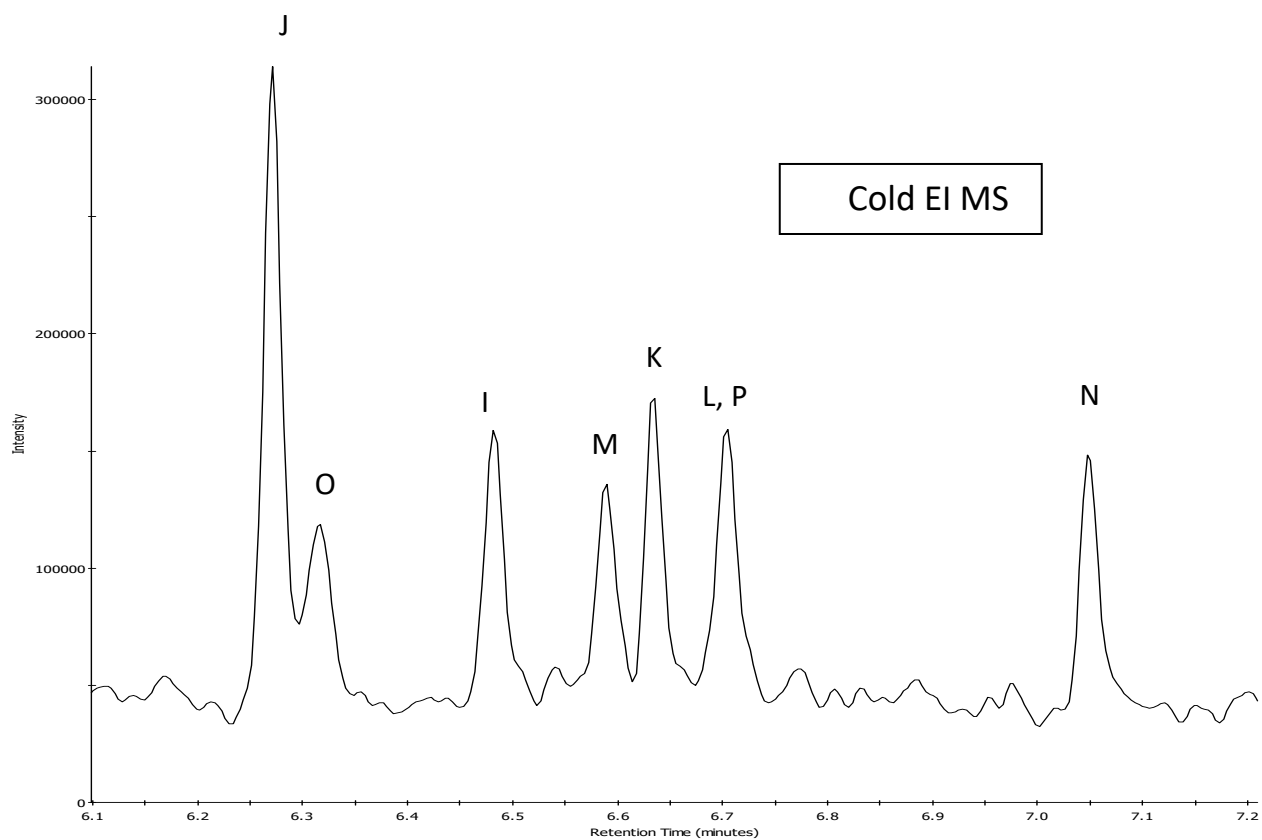
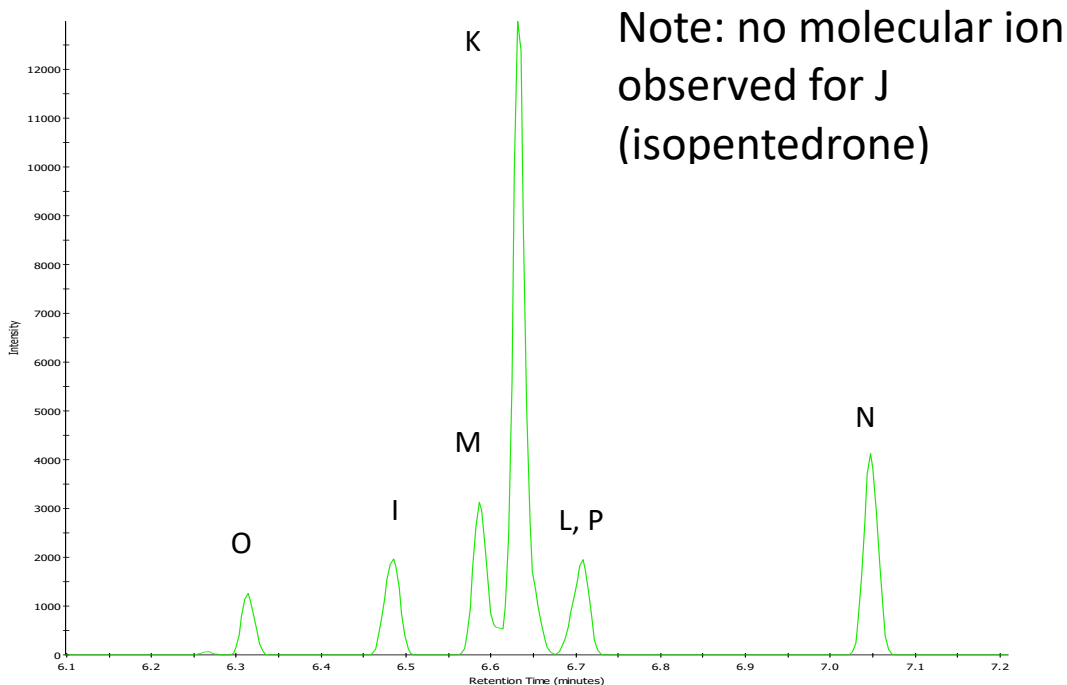
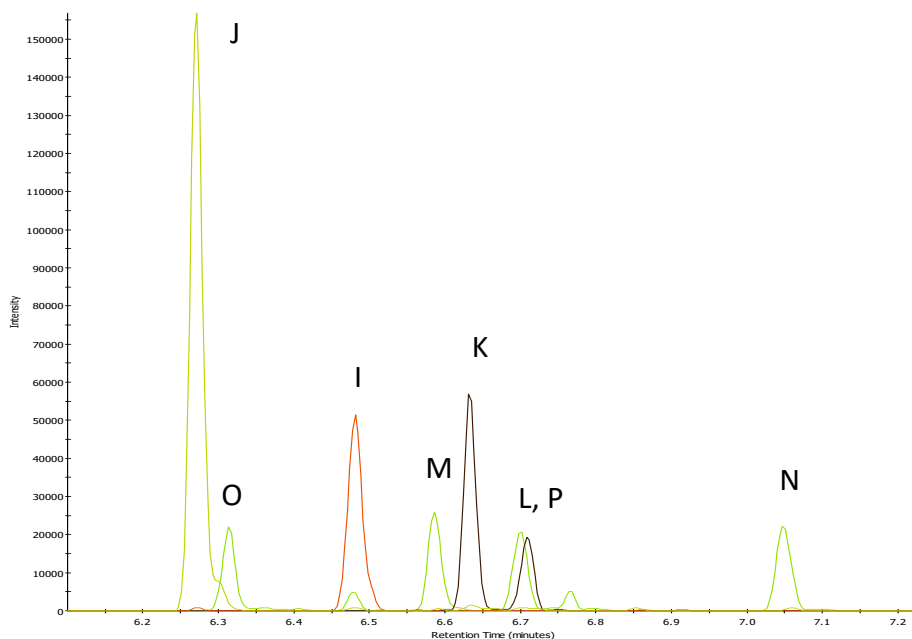


Figure 172: Simultaneous Cold EI MS and VUV detection for a mixture 300 ppm each of mass 191 positional isomers of synthetic cathinones. See Table 2 for peak identity.



**m/z 191 (molecular ion)**



(J) Darker Green= m/z 86, (O, M, N, L) Bright Green= m/z 58  
 (I) Red= m/z 120 (K,P) Black= m/z 72 (base peaks)

Figure 173: Extracted ion chromatograms for a mixture 300 ppm each of mass 191 positional isomers of synthetic cathinones. See Table 2 for peak identity.

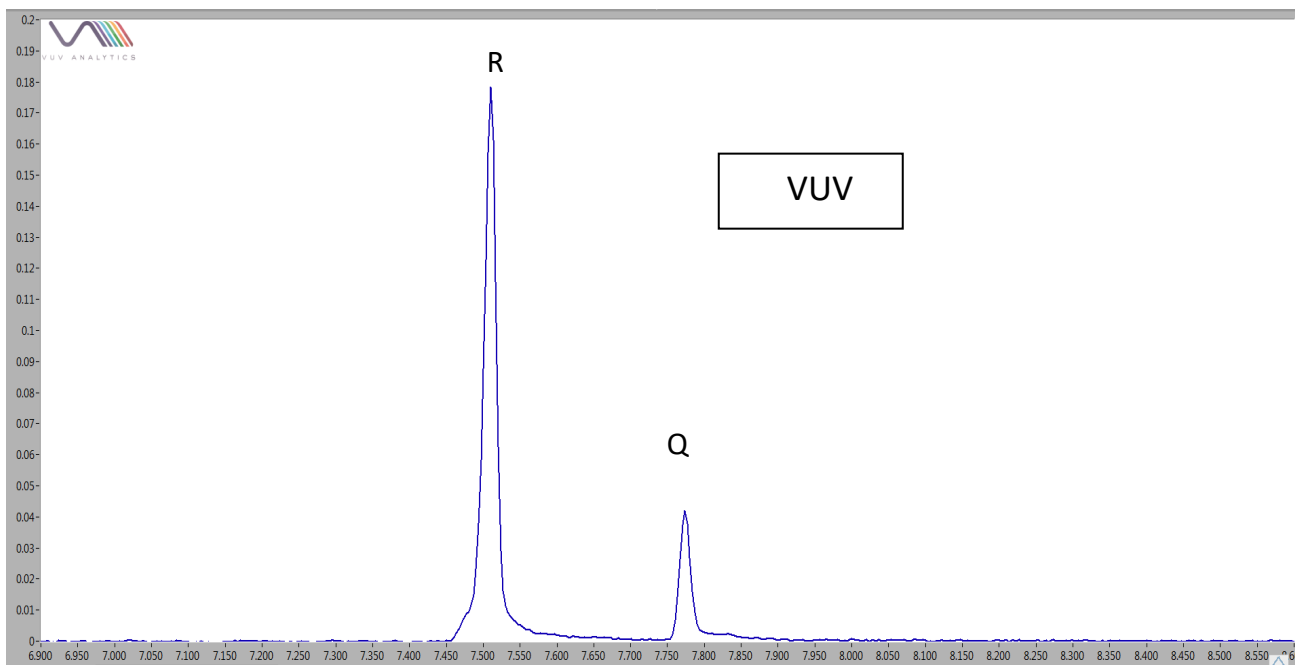
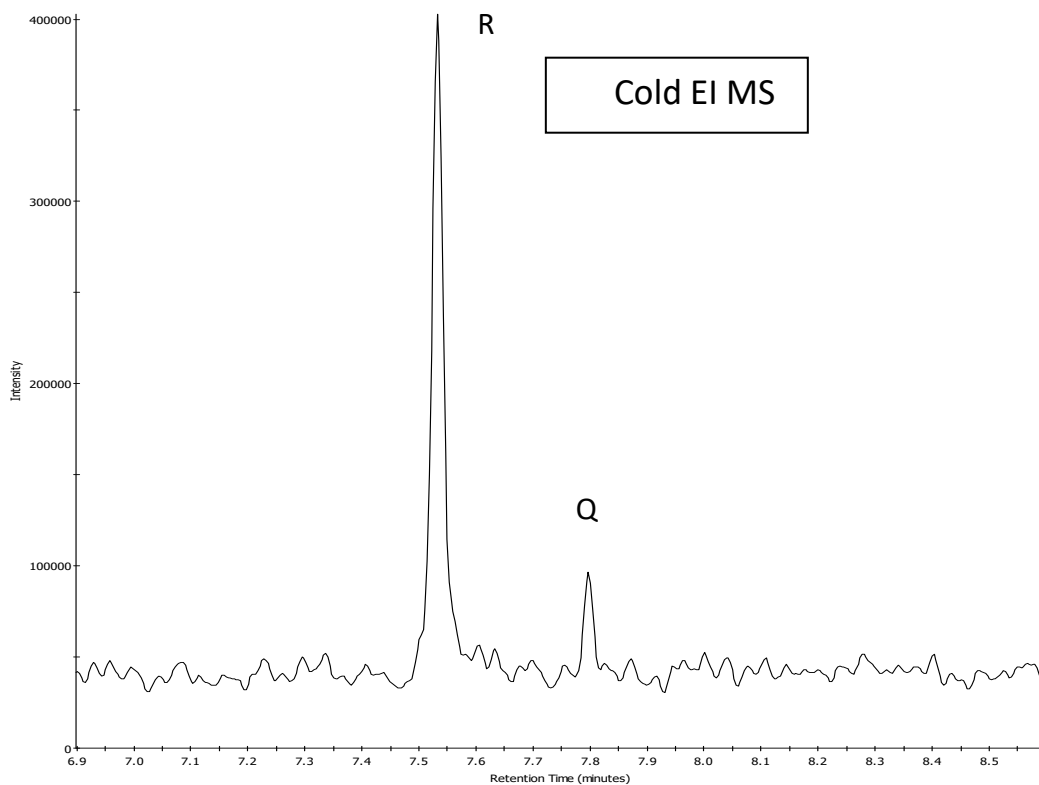
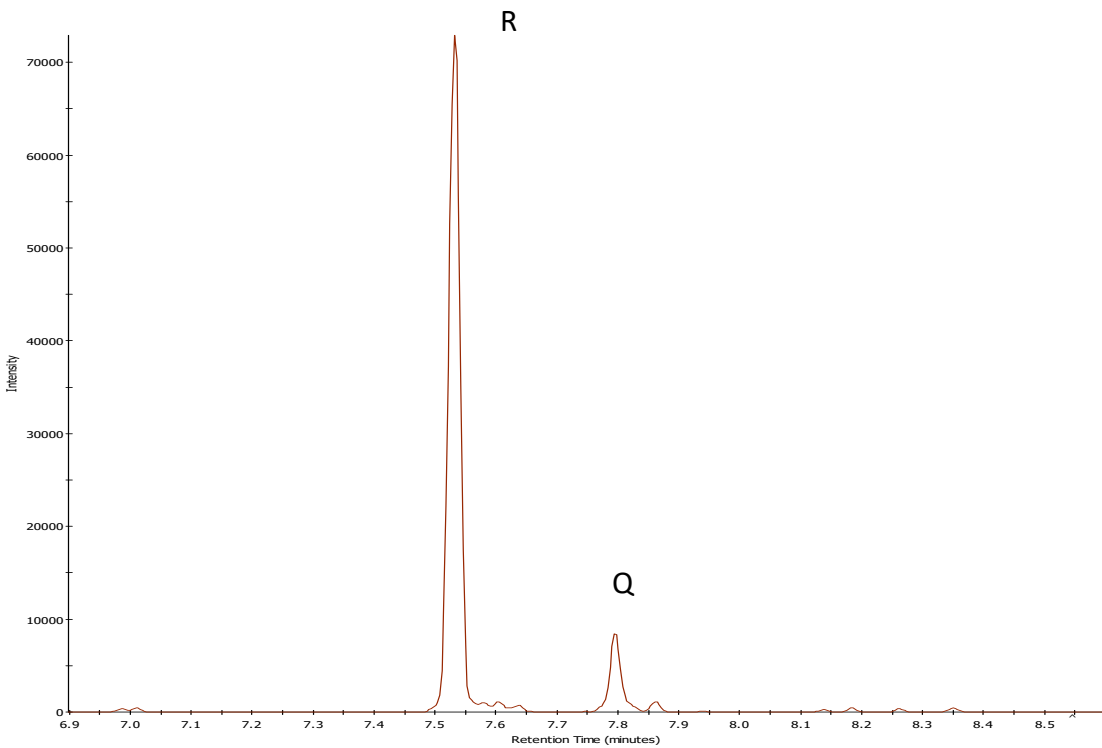
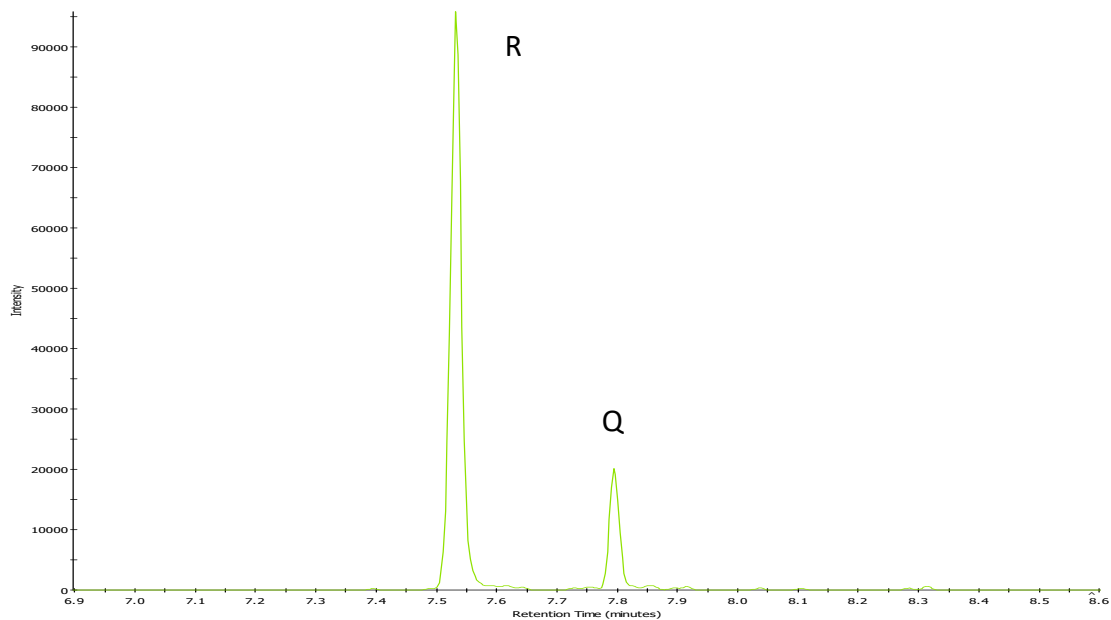


Figure 174: Simultaneous Cold EI MS and VUV detection for a mixture 300 ppm each of mass 207 positional isomers of synthetic cathinones. See Table 2 for peak identity.



m/z 207 (molecular ion)



m/z 58 (base peak)

Figure 175: Extracted ion chromatograms for a mixture 300 ppm each of mass 207 positional isomers of synthetic cathinones. See Table 2 for peak identity.

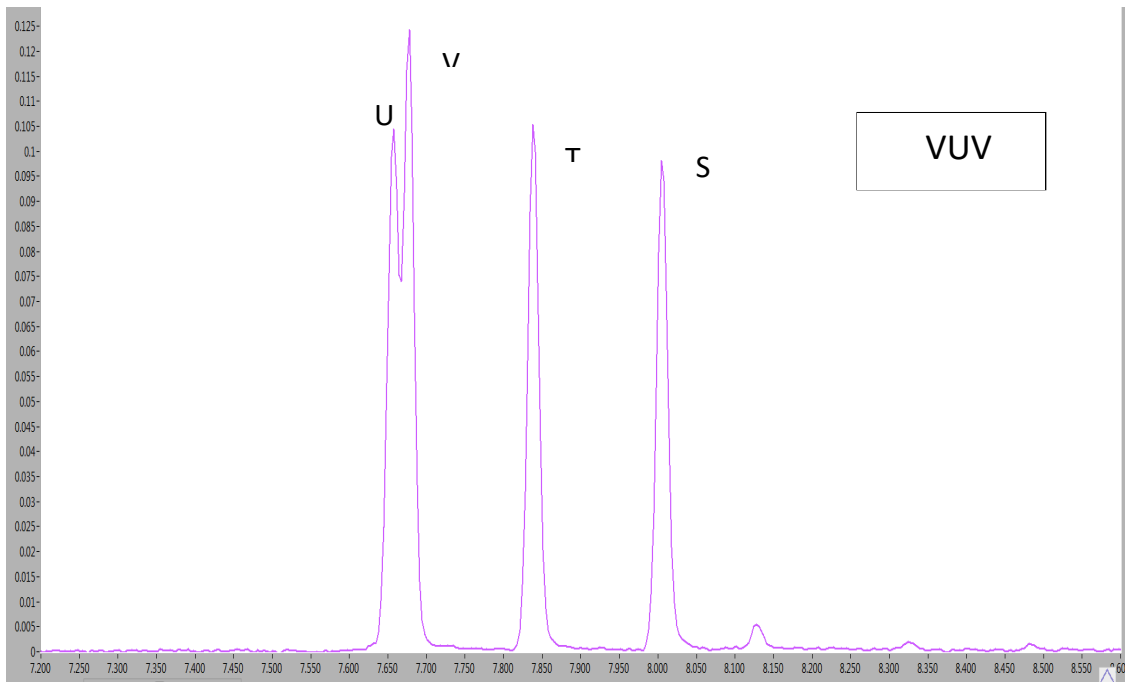
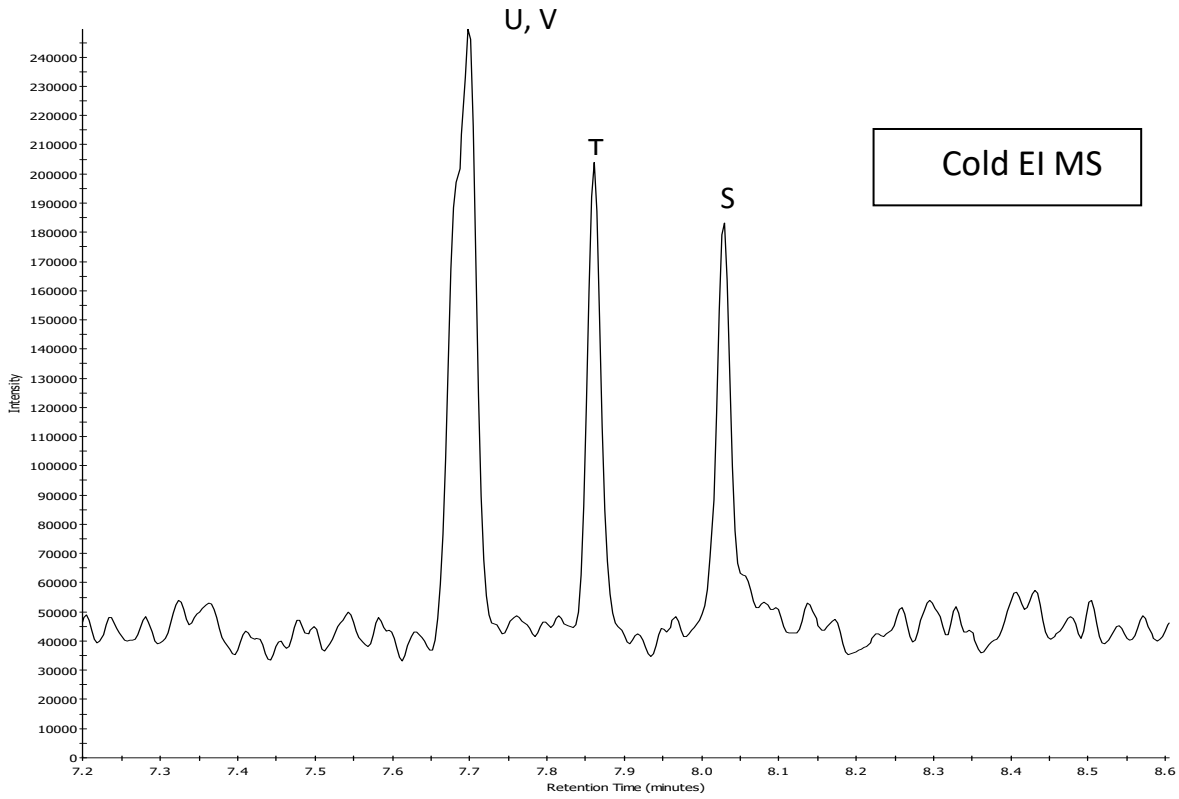
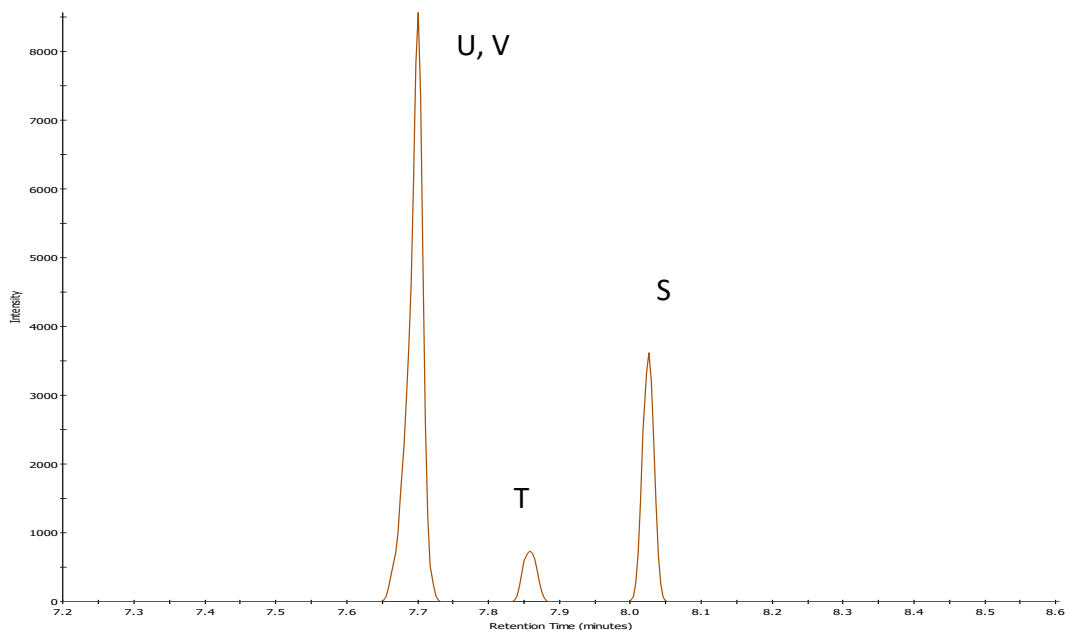
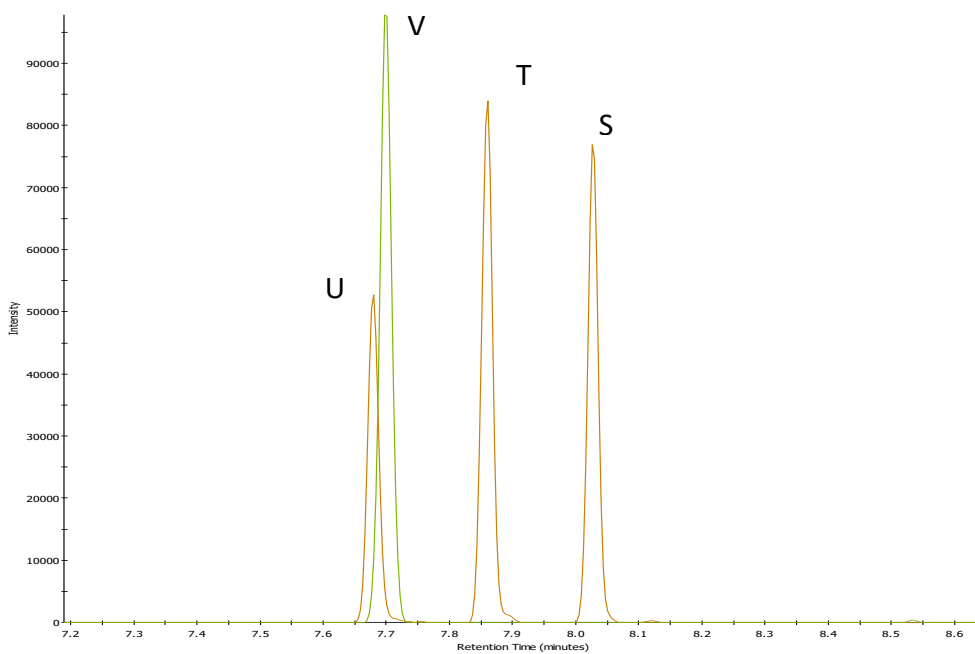


Figure 176: Simultaneous Cold EI MS and VUV detection for a mixture 300 ppm each of mass 217 positional isomers of synthetic cathinones. See Table 2 for peak identity.



m/z 217 (molecular ion)



(V) Green = m/z 112, (U, T, S) Red= m/z 98  
(base peaks)

Figure 177: Extracted ion chromatograms for a mixture 300 ppm each of mass 217 positional isomers of synthetic cathinones. See Table 2 for peak identity.

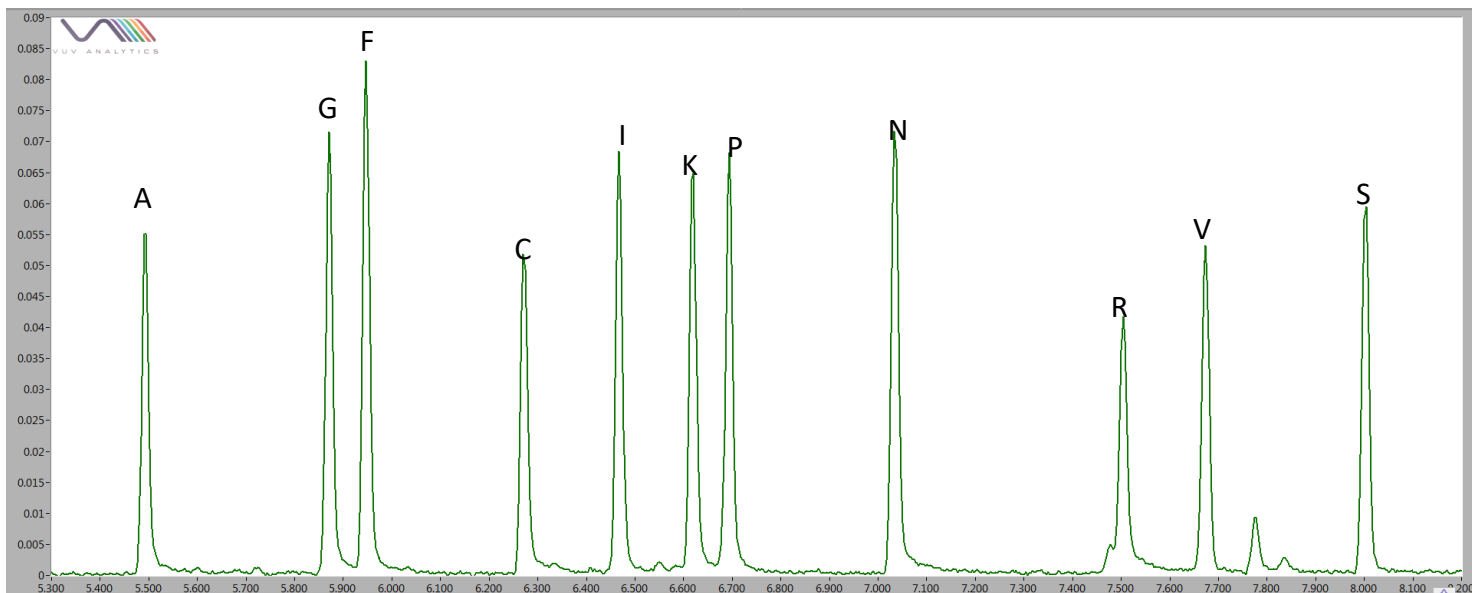
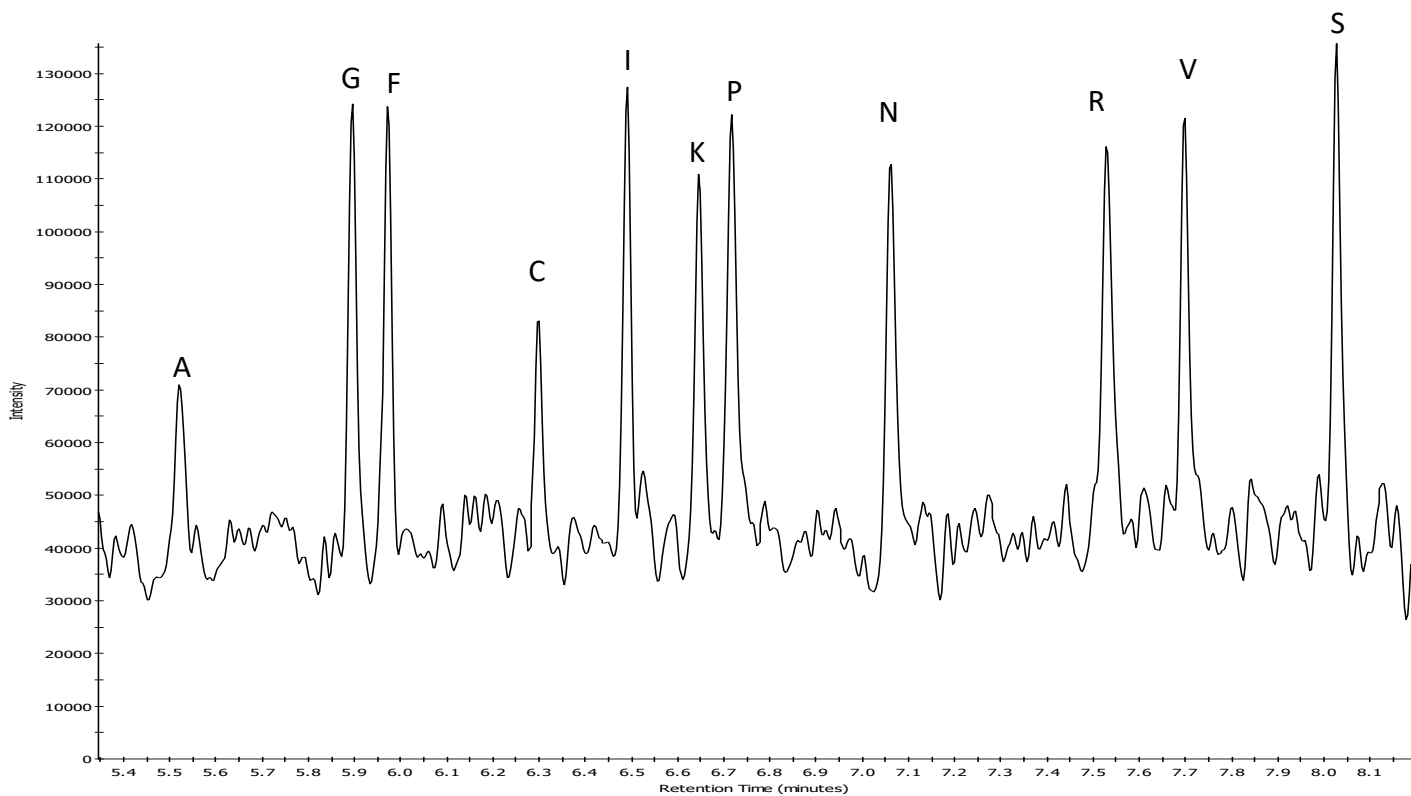


Figure 178: Simultaneous Cold E-MS (A) and VUV detection (B) for a mixture 300 ppm each of 12 synthetic cathinones. See Table 2 for peak identity.